Cooperative Research Centre for Viticulture

Australian Government
Grape and Wine Research and Development Corporation

Early detection of phylloxera in grapevines (*Vitis vinifera*) a test-bed for spectro-optical and chemical fingerprinting of pest-induced grapevine stress



FINAL REPORT to

COOPERATIVE RESEARCH CENTRE FOR VITICULTURE

Project Number: **S2.2.5**

Principal Investigators: **Kevin Powell, David Lamb and Damien Barret**

Research Organisation: Cooperative Research Centre for Viticulture

Date: **April, 2006**

Project Title: Early detection of phylloxera in grapevines (*Vitis vinifera*) a test-bed for spectro-optical and chemical fingerprinting of pest-induced grapevine stress

CRCV Project Number: S2.2.5

Period Report Covers: 1/8/2002 – 31/12/2005
(spectral reflectance)

1/10/2003 – 31/12/2005
(chemical fingerprinting)

Author Details: Name: David Lamb
Agency/Organisation Name: UNE
Postal address: School of BBMS
University of New England
Armidale, NSW, 2350.
Phone: 02 67733565
Fax: 02 67732844
Mobile: 0428 886088
Email: dlamb@pobox.une.edu.au

Date report completed: April, 2006

Publisher: Cooperative Research Centre for Viticulture
ISBN OR ISSN:

Copyright:

© Copyright in the content of this report is owned by the Cooperative Research Centre for Viticulture.

Disclaimer:
The information contained in this report is a guide only. It is not intended to be comprehensive, nor does it constitute advice. The Cooperative Research Centre for Viticulture accepts no responsibility for the consequences of the use of this information. You should seek expert advice in order to determine whether application of any of the information provided in this guide would be useful in your circumstances.

The Cooperative Research Centre for Viticulture is a joint venture between the following core participants, working with a wide range of supporting participants.

FINAL PROJECT REPORT

Early detection of phylloxera in grapevines (*Vitis vinifera*) — a test-bed for spectro-optical and chemical fingerprinting of pest-induced grapevine stress

Project Investigators

Kevin Powell (Victoria Department of Primary Industries)
David Lamb (University of New England)
Damien Barret (CSIRO Land & Water)
Annette Blanchfield (Victoria Department of Primary Industries)
Alex Held (CSIRO Earth Observation Centre)
Luigi Renzullo (CSIRO Land & Water)
David Tucker (University of New England)
Ian Brereton (University of Queensland)
Robert Murison (University of New England)

Table of Contents

Abstract 6

Executive Summary 7

1. Introduction and Scope of Research 8
   1.1 Leaf pigments as stress indicators 9
   1.2 Remote sensing for phylloxera detection- the need for spectral fingerprinting 10
   1.3 Chemical fingerprinting using nuclear magnetic resonance techniques 12

2. Instrumentation and Protocols 14
   2.1 High-performance liquid chromatography (HPLC) for pigment determination 14
      2.1.1 Statistical Analysis of HPLC data 14
   2.2 Spectral reflectance measurements 15
      2.2.1 Statistical Analysis of Spectral Reflectance Profiles 16
   2.3 Nuclear magnetic resonance (NMR) spectroscopy 16
      2.3.1 Preparation of extracts 16
      2.3.2 NMR Spectroscopy 16
      2.3.3 Principal Component Analysis 17

3. Glasshouse Infestation Level Trial (Trial 1) 18
   3.1 Plant Material 18
   3.2 Trial Design and Infestation Method 18
   3.3 Data collection for HPLC analysis and leaf reflectance 19
   3.4 Phylloxera population counts 19
   3.5 Results & Discussion (Trial 1) 20
      3.5.1 Phylloxera infestation levels 20
      3.5.2 Spectral measurements 20
      3.5.3 HPLC analysis 21
   3.6 Key Recommendations 22

4. Fieldwork (Trial 2) 23
   4.1 Site details 25
   4.2 Sampling strategy 26
   4.3 Results & Discussion - Pigments 27
      4.3.1 Pigment Results - Upton 27
         4.3.1.1 Total chlorophyll content 27
         4.3.1.2 Total carotenoid content 27
         4.3.1.3 Total carotenoid to total chlorophyll ratio 27
         4.3.1.4 Total xanthophyll cycle pigments to total chlorophyll ratio (VAZ/Tchlorophyll) 28
         4.3.1.5 Xanthophyll cycle pigment ratio (AZ/VAZ) 28
         4.3.1.6 β-carotene to total chlorophyll ratio 28
      4.3.2 Pigment Results - Buckland Valley 31
         4.3.2.1 Total chlorophyll 31
         4.3.2.2 Total carotenoid content 31
         4.3.2.3 Total carotenoid to total chlorophyll ratio 31
         4.3.2.4 Total xanthophyll cycle pigments to total chlorophyll ratio (VAZ/Tchlorophyll) 31
         4.3.2.5 Xanthophyll cycle pigment ratio (AZ/VAZ) 32
         4.3.2.6 β-carotene to total chlorophyll ratio 32
      4.3.3 Discussion - Pigments 35
      4.3.4 Conclusion - Pigments 36
   4.4 Results & Discussion - Spectral Reflectance 36
   4.5 Results & Discussion - NMR and Chemical Fingerprinting 42
      4.5.1 NMR Results - Introduction 42
      4.5.2 NMR Results - Upton 44
         4.5.2.1 November 2003 44
         4.5.2.2 January 2004 50
         4.5.2.3 March 2004 57
         4.5.2.4 Variation in extracts during growing season 59
         4.5.2.5 January 2005 61
         4.5.2.6 Variation in extracts between growing seasons 62

4.5.3 NMR Results - Buckland Valley 63
4.5.3.1 January and February 2004 63
4.5.3.2 November 2004 66
4.5.3.3 January 2005 67
4.5.3.4 March 2005 67
4.5.3.5 Variation in extracts during growing season 70
5. Glasshouse Grapevine Stress Detection Trial (Trial 3) 71
5.1 Plant material 71
5.2 Trial design 71
5.3 Infestation method 72
5.4 Trial conditions 72
5.5 Pigment Analysis 73
5.6 Spectral reflectance measurements 73
5.7 NMR measurements 73
5.8 Nitrogen content and phylloxera populations 74
5.9 Results & Discussion (Trial 3) 74
5.9.1 Phylloxera populations 74
5.9.2 Vigour Assessment 75
5.9.3 Leaf nitrogen content 77
5.9.4 Pigment analysis 77
5.9.4.1 Total chlorophyll 77
5.9.4.2 Total carotenoid content 79
5.9.4.3 Total carotenoids to total chlorophyll ratio 80
5.9.4.4 Xanthophyll cycle pigment ratio (AZ/VAZ) 80
5.9.4.5 Total xanthophyll cycle pigments to total chlorophyll ratio (VAZ/Tchlorophyll) 80
5.9.4.6 β-carotene to total chlorophyll ratio 81
5.9.5 Spectral reflectance measurements 83
5.9.6 NMR measurements 89
6. Global Conclusions and Recommendations 96
6.1 Phylloxera infestation 96
6.2 Treatment assessment 96
6.3 Leaf Pigment content 97
6.4 Spectral Reflectance Profiles 99
6.5 NMR Fingerprinting 100
6.6 An integrated approach to phylloxera detection 102
Appendix 1: Communication 103
Scientific Publications (refereed) 103
Research Conference, Seminars, Workshop Presentations and Technical Reports (non-refereed) 103
Seminars 104
Posters & Conference Proceedings 104
Workshops 105
Technical Reports and Industry Journal articles (non-refereed) 106
Reprints of Publications 107
Appendix 2: Intellectual Property 145
Appendix 3: References 146
Appendix 4: Staff 151
Appendix 5: Sampling strategy for leaves used for reflectance spectra and HPLC in the field trial. 152
Appendix 6: Budget reconciliation 153

Abstract

The overall aim of this research project was to focus on improved and/or novel detection strategies for grapevine phylloxera to improve the early detection of phylloxera using a targeted approach focusing on grapevine physiological response to infestation. New developments in this project were to highlight the potential for using a spectrochemical response for phylloxera detection which would be an improvement on existing approaches to detection on an area-wide scale. Three key analytical approaches, HPLC, NMR and hyperspectral sensors, were evaluated and the potential for integration into targeted phylloxera detection programs are discussed.

Executive Summary

Grape phylloxera, *Daktulosphaira vitifoliae* Fitch (Hemiptera: Phylloxeridae), is a devastating pest of cultivated grapes, *Vitis vinifera* L., worldwide. In Australia phylloxera management relies on three key areas initially detection and surveillance of the insect, followed by implementation of stringent quarantine protocols and the use of phylloxera-resistant rootstocks to prevent economic losses. Improvement of detection methods for phylloxera is crucial to ensure faster implementation of quarantine protocols to reduce the risk of transfer and ensure improved rootstock management. This report focuses on the key area of phylloxera detection and surveillance. It explores the opportunities available to either (i) improve existing remote sensing detection methods, for wide area detection or (ii) implement novel chemical detection methods for targeted detection. In particular the research presented examines approaches to differentiate phylloxera induced stress symptoms from stresses induced by water and nutrient deficiencies.

Three key analytical approaches for early detection are presented. The first examines the use of hyperspectral imaging techniques and this was validated using ground based spectral reflectance measurements. Linked to this is the use of High Performance Liquid Chromatography (HPLC) to examine the relationship between spectral reflectance observed in stressed grapevines and leaf pigment ratios. The third approach is the use of nuclear magnetic resonance (NMR) spectroscopy to examine if metabolic changes induced by root-feeding phylloxera are expressed as unique chemical signatures in leaves of phylloxera-infested vines.

Phylloxera-infested and non-infested vines could be separated spectrally by using statistical procedures and the selected spectral regions corresponded predominantly to areas related to vine physiology, in particular pigments involved in photosynthesis and photoprotection. HPLC analysis identified that changes in pigment concentration and ratios occurred in phylloxera-infested grapevines and these were detected as early as nine weeks under controlled environment conditions. These changes in pigments were closely related to spectral reflectance observations.

Using NMR spectroscopy, identifiable metabolic changes in the chemical profile of phylloxera-infested vines could be detected including the presence of a number of potential chemical markers. Further investigation is recommended to characterise these compounds and ensure that the response is phylloxera specific.

This research has highlighted that detection methods for phylloxera can be improved. However, several factors could influence expression of pigment, chemical and spectral signatures including grapevine variety, phylloxera genotype and stresses imposed and further investigation is warranted in this area.

1. Introduction and Scope of Research

Grapevine phylloxera (*Daktulosphaira vitifoliae* Fitch) is a root-feeding insect pest, which due to its small size and predominantly subterranean habitat is notoriously difficult to detect until significant economic damage has been inflicted on its primary host plant European grapevine V*itis vinifera* L. It also has a range of genetic strains that differ in their level of virulence on a range of *Vitis* spp. (Powell, 2006, in prep). Despite being present in Australia since 1875, when it was first detected in Geelong, phylloxera still poses a major threat to the sustainability of the Australian viticulture industry, which is predominantly planted to phylloxera susceptible grapevines. The only two long-term options for phylloxera management are quarantine, to restrict movement of the pest and planting on resistant rootstocks to prevent economic decline of grapevines. However the relative success of both management options relies on early detection and surveillance of phylloxera. Early detection is critical in the early enforcement of quarantine boundaries and protocols, to prevent risk of spread from infested to non-infested regions, and the rapid implementation of resistant rootstock planting strategies.

However, currently detection of phylloxera takes several years, post-infestation, as it relies predominantly on observations below-ground by ground surveys to examine potentially infested roots and aerial surveys using multispectral systems which can only detect changes in canopy vigour (ie weak spots). These weak spots can be caused by stress factors other than phylloxera presence and therefore follow-up ground truthing is still required. The issues and potential future directions for improved early detection of phylloxera have been reviewed in Herbert *et al*. (2003). These include molecular approaches (Powell and Herbert, 2005), multispectral imagery systems (Edwards *et al*., 2004, Frasier *et al*., 2004), hyperspectral imagery systems (Renzullo *et al,* 2004) and chemical and pigment fingerprinting (Blanchfield *et al*., 2006; Tucker *et al.,* 2006).

The objective of this research was to investigate whether above-ground symptoms of phylloxera infestation could be detected through analysis of vine leaf pigments using high performance liquid chromatography (HPLC), via leaf and canopy spectral reflectance measurements using a portable spectroradiometer, and through analysis of leaf chemical composition using nuclear magnetic resonance (NMR) techniques. The research was conducted in three separate trials: (1) Glasshouse infestation level trial, (2) Field trial and (3) Glasshouse stress response trial. The Glasshouse infestation level trial was used to refine techniques of vine management and leaf sampling and analysis protocols. The Field trial involved collection of leaves from commercial vineyards in Phylloxera Infested Zones in North Eastern Victoria and the Glasshouse stress response trial involved a comparative investigation of the effects of nitrogen and water stress relative to the symptoms presented by phylloxera-infested grapevines. HPLC and spectral measurements only were conducted during the first

glasshouse infestation trial, whilst all analytical techniques were applied to the second and third trials.

This report commences with a brief introduction to the three key analytical techniques used in the research project: HPLC, canopy and leaf spectral reflectance and NMR analysis, followed by a description of the execution of each of the three trials, with their respective results and some key recommendations where appropriate. The report finishes with a global discussion and conclusion.

1.1 Leaf pigments as stress indicators

Leaf pigments can be divided into two major groups, the chlorophylls and the carotenoids. The chlorophylls, of which there are two, chlorophyll *a* and *b*, absorb light energy and transfer the energy into the photochemical reaction centre, where photosynthesis takes place. The carotenoids, which consist of neoxanthin, lutein, the carotenes and the xanthophyll cycle pigments, also contribute to light harvesting as accessory pigments, but play a more important role in protecting the photosynthetic system from photo-oxidative damage caused by excess light energy (Young and Britton 1990; Suzuki and Shioi 2004). Because of the importance of pigments for leaf and overall plant function, leaf pigment composition can provide valuable information about the physiological performance of a leaf (Sims and Gamon 2002). Chlorophyll concentration can be used to assess nutrient status. By determining both carotenoid and chlorophyll composition much about the phenology and general stress status of a plant can be decided and the photosynthetic efficiency of a leaf can be rated by xanthophyll cycle pigment assessment (Penuelas and Filella 1998).

Non-destructive optical methods of vegetation assessment, based on absorbance and/or reflectance of light by an intact leaf have been developed and might provide a rapid and easy alternative means of assessing plant health with further investigation (Penuelas and Filella 1998; Richardson *et al*. 2002; Sims and Gamon 2002; Gitelson *et al*. 2003). High performance liquid chromatography (HPLC) offers a quantitative analysis of all pigments present in a leaf, which is not possible with other methods, such as spectrophotometric analysis. When linked to reflectance spectra pigment analysis can provide further information to aid the interpretation of the spectral data.

In this project, HPLC was used to analyse the pigment content of leaf samples collected from grapevines in all three trials, and wherever possible, the HPLC data was utilised in the interpretation of leaf reflectance spectra collected from the same leaf samples.

1.2 Remote sensing for phylloxera detection- the need for spectral fingerprinting

Remote sensing technologies have been used in the viticulture industry to map sub-paddock variability in canopy development and maturation. The derived information has been used to support selective harvesting, the quantification of missing grapevines, and broad regional assessment of grape-growing areas. The advantage of this technology is that it can rapidly survey a much greater area of vineyard than is feasible with on-ground methods. Moreover, it has been demonstrated that remotely-sensed observations, such as infrared photography, multispectral and hyperspectral imagery, can successfully identify *weak spots* in vine canopies that are a result of phylloxera infestation (Lobitz *et al.*, 1997; Held, 2001; Edwards, 2003). However, discrimination between phylloxera infestation and other stresses is complex.

Figure 1 shows three examples of remotely-sensed imagery for some vineyards in north-eastern Victoria. Displayed are (a) a true-colour composite from a Compact Airborne Imaging Spectrometer (CASI); (b) false-colour composite of a Digital Multi-Spectral (DMS) Imager image (this is also an airborne imager); and (c) a normalised difference vegetation index image (NDVI) derived from the imagery of a multispectral sensor on the QuickBird satellite. All three of these images show regions of low vigour (i.e. weak spots, identified by white polygons) along the rows of grapevines. Weak spots, however, may be a result of phylloxera infestation just as easily as they may be due to dehydration or nutrient deficiency, which is why there is still a need for ground surveys to accompany remotely sensed surveys for verification of phylloxera presence.

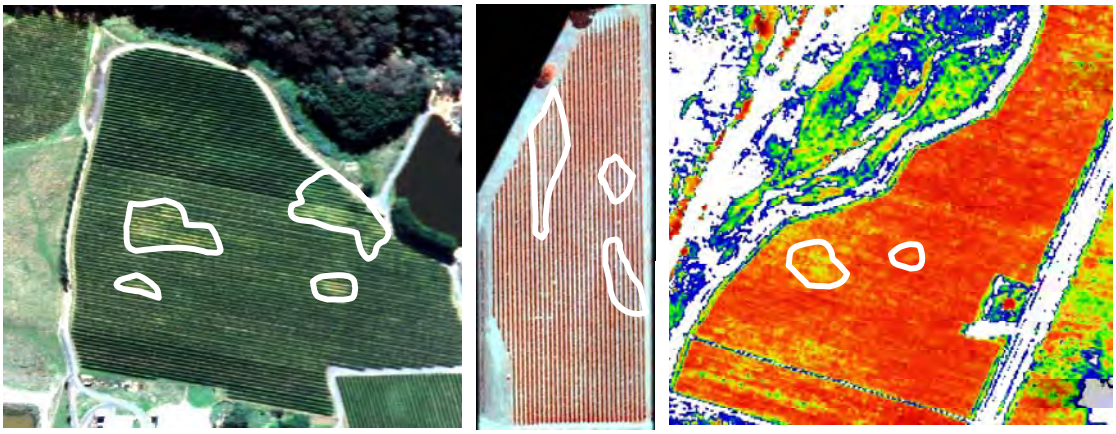


Figure 1: Some examples of remotely-sensed multispectral imagery: (a) true-colour CASI imagery; (b) false-colour DMS Imagery; (c) NDVI image derived from QuickBird imagery. Weak spots have been identified by white polygons, but not all are due to phylloxera infestation.

Each pixel in a remotely-sensed digital image is a spectrum of reflected solar radiation measured over a number of wavelength intervals called *bands*. Figure 2 contains the reflectance spectra (18 bands) for some pixels in a CASI image of an Upton vineyard (from Renzullo *et al.*, 2004). The displayed curves correspond to groups of pixels that ground surveys had confirmed belonged to grapevines that were

either phylloxera-infested (red curve), uninfested (blue curve), or in a weak spot, the cause for which is uncertain but was *not* phylloxera related (green curve). The figure illustrates the similarity in spectral response for grapevines infested by phylloxera and those in a region of low canopy vigour. The red and green curves differ from the blue curve in the broad spectral region between 600-700 nm (known as the chlorophyll well) and 800-950 nm (the near infrared, or NIR).

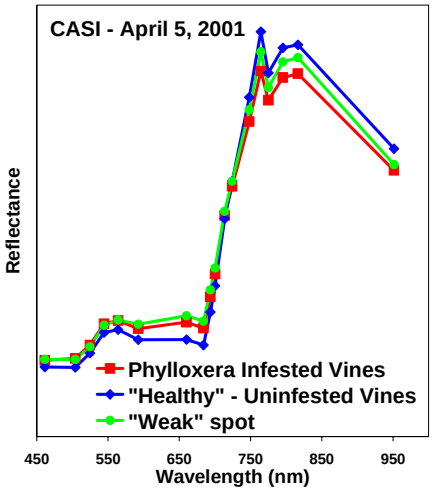


Figure 2: Spectral response from regions of pixels in a CASI image.

Whatever the cause of the weak spot, it is clear that it is spectrally quite similar in shape to that of phylloxera infestation. An index like NDVI, for example, which exploits NIR and red (650-700nm) reflectances to enhance the vegetation signal will give a similar values for both the red and green curves in Figure 2, but a different value for the blue (healthy) curve (e.g. Figure 1c). Similarly for other indices, such as NIR-to-green (550 nm), green-to-red or blue (450 nm)-to-green, as reported by London (personal communication (email) from A. London, Phylloxera and Grape Industry Board of South Australia., 2004).

Furthermore, the signal measured by the remote sensing system is a contribution of canopy foliage, vine trunk, canopy understory vegetation (e.g. grasses, weeds), soil, shadowing from leaves and neighbouring grapevines, and finally atmospheric and sensor calibration effects (Renzullo, 2004). All these factors combine to obfuscate the spectral characteristics of grapevine stress, be it due to phylloxera infestation or any other stressor.

In conjunction with the HPLC measurements, ground-based spectral reflectance measurements were made on leaves collected from the glasshouse level of infestation trial (Trial 1), the field trial (Trial 2) and stressed grapevines grown under controlled (glasshouse) conditions (Trial 3).
Spectral reflectance measurements were made over the full range of the solar reflective region of the electromagnetic spectrum, i.e. between 400-2500 nm using an instrument with 1 nm spectral resolution. These data are referred to as *hyperspectral*

as they are collected over 2101 bands; in contrast to many *multispectral* remote sensing systems that measure reflectances in 4–6 bands (Note that the airborne CASI described earlier measures radiation over 18 bands but is still regarded as a multispectral system).

1.3 Chemical fingerprinting using nuclear magnetic resonance techniques

Previous studies have shown that phylloxera infestation of the roots of *V. vinifera* produces changes in levels of sugars, free amino acids, starch, proteins and phenolics in the nodosities produced by the infestation and also in non-feeding sites on the roots (Schaefer, 1985; Ryan et al., 2000). Furthermore, in *Vitis* species susceptible to the gallicole (leaf-feeding) forms of phylloxera, the phylloxera leaf galls have been shown to have a discernibly different metabolism to unaffected leaf tissue (Schaefer, 1972; Warick and Hildebrandt, 1966). To date there seems to have been very limited investigation of the effects of phylloxera infestation on metabolism in parts of the plant remote to the point of infestation (Kellow, 2001).

The aim of this research was therefore to investigate whether phylloxera infestation of grapevine (*V. vinifera*) roots induces metabolic changes in more accessible parts of the plant, in particular the leaves, and, if such changes do occur, whether any of the changes observed could serve as a chemical fingerprint for the presence of phylloxera. The research utilised ^{1}H Nuclear Magnetic Resonance (NMR) spectroscopy and principal component analysis (PCA) to investigate the metabolic profiles of grape leaf extracts. Such approaches have been widely adopted over the past 6 - 7 years, particularly in the detection of disease by the examination of biofluids (eg Lindon et al., 2000) but also in the characterisation of beer (Duarte *et al*., 2002) and quality control of coffee (Charlton *et al*., 2002) among many other applications and the term "metabonomics" has been coined to describe the technique.

^{1}H NMR spectroscopy is particularly suitable for this type of investigation for the following reasons:

i. All compounds containing hydrogen atoms (ie essentially all organic compounds) produce a signal, ensuring all components of the extracts will be detected.

ii. The intensity of the signals produced is directly proportional to the number of molecules of the compound present in the mixture, allowing good estimates of the concentration of components to be made, at least in cases where sufficient resolution of resonances is present. Almost all other forms of spectroscopy or chromatography-spectroscopy show greater sensitivity to particular classes of compounds (some compounds may not be detected at all) and thus cannot be used to determine concentration.

iii. In favourable cases the information available in the form of chemical shift (frequency), coupling and integration can allow the structure (or at least some

structural information) of components to be deduced, even in complex mixtures of compounds.

The shortcomings of NMR spectroscopy are low sensitivity relative to other spectroscopic techniques and overlap of resonances due to the large number of peaks produced for each molecule present. These limitations are reduced by carrying out the NMR measurements at the highest available field strength and the use of PCA to detect small differences between spectra.

2. Instrumentation and Protocols

2.1 High-performance liquid chromatography (HPLC) for pigment determination

Leaf disks of the target grapevines were collected using a cork borer, 1.4 cm diameter, and immediately frozen at -80^{o}C (Trial 1 and 2) or in liquid nitrogen (Trial 3) for later pigment analysis by HPLC. Pigment extraction followed the methodology of Dunn *et al*. (2004).

Frozen leaf disks were ground using a mortar and pestle with a small amount of acid washed sand and liquid nitrogen. 300µl of cold 100% acetone was added to the ground sample and the slurry was transferred to an Eppendorf tube containing a small amount of $NaHCO_3$. The mortar and pestle were rinsed twice with 300µl of 100% acetone and both washes were added to the Eppendorf tube. Samples were stored on ice, in the dark for 20 minutes prior to centrifugation for 3 mins at 14,000 rpm. The supernatant was removed and the pellet was re-extracted with 300µl of cold 85% acetone using a polypropylene tissue grinder (Crown Scientific, Sydney, Australia). The suspension was stored for a further 10 mins on ice, in the dark, before centrifugation as before. The supernatant was removed and the pellet was re-extracted a second time. The supernatants were combined, made up to 1500 µl with 85% acetone and filtered through a 0.45 µm PTFE syringe filter (Alltech, Sydney, Australia) into amber HPLC vials immediately before HPLC analysis. Samples were kept at –20°C before analysis and were quantified within 24 h of extraction.

Plant pigments were quantified by HPLC using a method adapted from Gilmore and Yamamoto (1991). Samples (30-50 µL) were injected into a Shimadzu HPLC system [Shimadzu Scientific Instruments (Oceania) Pty Ltd Rydalmere, NSW, Australia] by autosampler (Model SIL-10Ai, Shimadzu) at a flow rate of 2 mL min $^{-1}$. Solvent A (acetonitrile:methanol:Tris-HCL buffer 0.1M pH 8.0; 85:10:5) ran isocratically from 0 to 4 min, followed by a 3 min linear gradient to 100% solvent B (methanol:N-hexane; 4:1) which then ran isocratically from 7 to 14 min. Flow rate was decreased from 2 to 1.5 mL min $^{-1}$ from 7 to 12 min and then run at 1.5 mL min^{-1} until 13 min to maintain stable pressure. The column was re-equilibrated with solvent A between samples. Pigments were separated on an Allsphere ODS1 column (Alltech, Sydney, Australia) and quantified by integration of peak areas, detected at 440nm using a photo diode array detector (Model SPD-M10AVP; Shimadzu) using the Class VP software package (v 5.03, Shimadzu).

2.1.1 Statistical Analysis of HPLC data

In Trial 1, Kruskal-Wallis analysis of variance (ANOVA) was used to investigate any relationship in the phylloxera population data and to determine the response of the grapevines to phylloxera infestation by investigating changes in their pigment content as determined by HPLC analysis. In Trial 2 ANOVA were performed on all data. In

Trial 3, REML (restricted maximum likelihood) was used to investigate any relationships in the pigment content data. All analyses were performed using Genstat software (Version 8).

2.2 Spectral reflectance measurements - the portable spectroradiometer

Spectral reflectance profiles of target grapevines and/or vine leaves were acquired using a ASD FieldSpec® Pro FR spectroradiometer (Analytical Spectral Devices, Boulder, CO, USA) (ASD, 2005) fitted with a 5° field of view fore-optic (Figure 3). Spectra were acquired in the 350–2500 nm spectral region with a sampling interval of 1.4 nm between 350 and 1050 nm, and 2 nm between 1050 and 2500 nm. Measured irradiance was converted into reflectance by also collecting irradiance spectra from a 0.4 m x 0.4 m $BaSO_4$ calibration panel. All irradiance measurements were recorded as an average of 20 individual measurements (minus dark current) at an optimised integration time. Initially (Trial 1), spectral reflectance measurements were collected under ambient light conditions, however, for subsequent trials (Trials 2 & 3), a Li-Cor integrating sphere attachment was used to allow collection of stable bi-hemispherical reflectance measurements that were independent of variations in ambient light conditions. Moreover, the integrating sphere provided a consistent, fixed set of geometries with which leaf samples were viewed and illuminated. Although the spectrometer has a broad spectral sensitivity, only those reflectance values within the wavelengths region 400–1600 nm were used in the investigations due to the low intensity of the integral halogen lamp in the UV and SWIR wavelength regions.

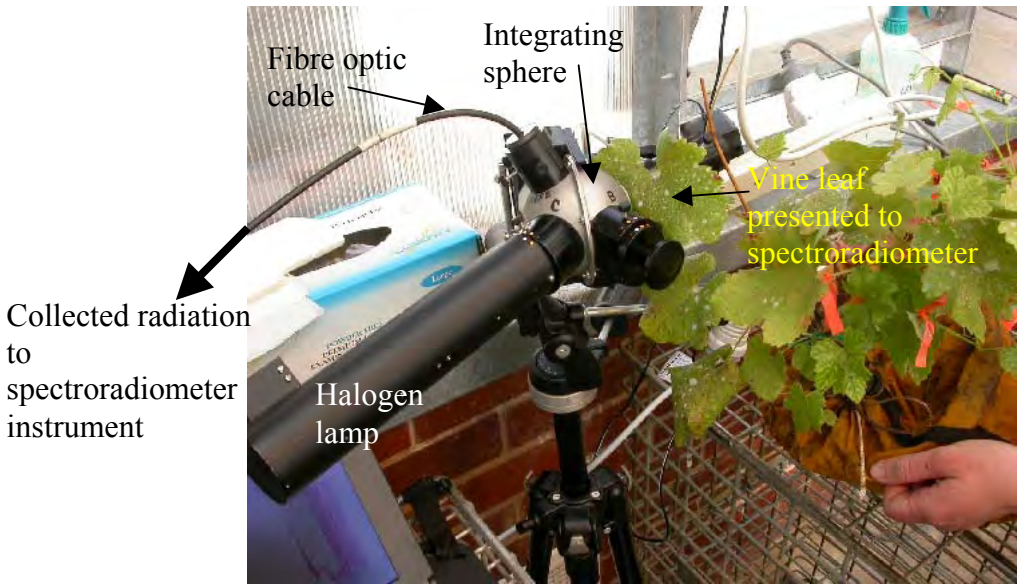


Figure 3: Portable field spectroradiometer used to acquire grapevine leaf spectral reflectance profiles.

2.2.1 Statistical Analysis of Spectral Reflectance Profiles

Penalized discriminant analysis (PDA, Hastie *et al.* 1995) was used on both glasshouse stress response and field trial spectral reflectance data (Trials 2 and 3, respectively) to determine whether the reflectance data could be separated into the various groups and to identify the key spectra regions where the differentiation occurs.

A modified version of the PDA algorithm, referred to in this work as OSLASSO, was also applied to the data of Trial 2 to identify the key wavelengths useful for group separation. Like PDA it uses a regularized method of regression known as *lasso* regression (Tibshirani, 1996), but unlike PDA it provides an automated method of selection by setting the discriminant variable coefficients of many wavelengths to zero. The OSLASSO procedure and the choice of appropriate levels of model complexity are detailed in Renzullo *et al*. (2006a).

2.3 Nuclear magnetic resonance (NMR) spectroscopy

2.3.1 Preparation of extracts

After collection (see Sections 2.1 and Appendix 5), the leaves were oven dried for 48 hours at 45^{o}C. The dried leaves were placed in 250 ml conical flasks, covered with redistilled dichloromethane (25 ml) and extracted at room temperature for 40 - 50 hours. The extracts were filtered and the filtrate evaporated to dryness on a rotary evaporator. Initially, extracts were evaporated individually in round bottom flasks while later extracts were evaporated in 45 ml vials, fitted with sintered glass enclosures, using an ACTEvap device, allowing the simultaneous evaporation of ten extracts. The residues were further dried under high vacuum. Typical weights of extract were about 10% of the dry weight of leaf extracted.

Each extract was then dissolved in dichloromethane (2 ml) and an aliquot of appropriate volume to contain 9 mg of extract (or 6 mg for later experiments (glasshouse trial, Buckland Valley and Upton 2005 samples)) was transferred to a 4 ml vial. The solvent was removed (either using a stream of nitrogen at room temperature or later using the ACTEvap, allowing simultaneous evaporation of 35 samples) and the samples further dried under high vacuum.

2.3.2 NMR Spectroscopy

^{1}H NMR spectra were measured at 750 MHz in deuterochloroform ($CDCl_3$) solution, at a concentration of 9 mg / 700 μL or 6 mg / 700 μL at 30^{o}C, using a Bruker Avance 750 FTNMR Spectrometer with a 5 mm TXI XYZ 1H-13C-15N probe. After Fourier transformation, spectra were manually phase corrected and baseline corrected, ensuring uniformity between spectra.

2.3.3 Principal Component Analysis

The binning and principal component analysis of spectra were carried out using the Bruker Amix 3.1.6 software package. For analyses covering the full spectral width (0 - 10 ppm) a bin width of 0.1 or 0.05 ppm was used (resulting in 100 or 200 bins, respectively). The region from 7.3 to 7.2 (incorporating the residual chloroform signal from the solvent) was omitted from calculations. Analyses of smaller regions of the spectra were conducted with a bin size of 0.05 or 0.02 ppm. To observe the linolenic/linoleic acid ratio, spectra were binned from 2.82 to 2.75 ppm, with a bin width of 0.01 ppm, omitting the bin from 2.80 to 2.79 from calculations.

3. Glasshouse Infestation Level Trial (Trial 1)

A glasshouse pilot study was established to determine (i) the level of phylloxera infestation required to initiate a detectable host plant response in leaf pigments and (ii) grapevine varietal response to infestation. Conclusions drawn from the pilot study were utilised to optimise the protocol for the second, more comprehensive stress response trial (Trial 3) discussed in the section 5.

3.1 Plant Material

Four grapevine varieties were included in the study. One-year old ungrafted *Vitis vinifera* L. cv. Semillon clone DA161612, Cabernet Sauvignon clone CW44 and Sauvignon Blanc clone F4V6 were purchased from Sunraysia Nurseries, Sturt Hwy, Gol Gol, NSW. One-year old *Vitis vinifera* L. cv. Shiraz clone PT23 were purchased from Boulevarde Nurseries, Mildura Pty Ltd. Varietal choice was based on varieties being tested concurrently under field conditions at commercial vineyards (Section 4). All rootlings were potted into 20 cm pots in a mixture of potting mix and perlite at a ratio of 3:1. Plants were maintained in a quarantine glasshouse at DPI Victoria-Rutherglen until the commencement of the trial.

3.2 Trial Design and Infestation Method

Phylloxera eggs of G4 genotype (Corrie *et al*. 2003) were sourced from the DPI-Rutherglen laboratory stock maintained on excised root bioassay plates (modified method of de Benedictis and Granett, 1993). Eggs were originally collected at a vineyard in the King Valley PIZ, which was also the site of a field trial (Section 4). Twenty four grapevines of each variety were used in the trial, representing a total of 96 grapevines. Six grapevines of each variety were used as healthy controls, which were not infested with phylloxera eggs. The remaining six grapevines of each variety were infested with 20 phylloxera eggs and identified as the "low" infestation level, 30 phylloxera eggs were placed on the "medium" level infestation group, and 40 phylloxera eggs on the "high" level infestation group. To infest the grapevines the eggs were placed onto dampened filter paper, approximately 40 mm x 8 mm, the filter paper was gently wrapped around a lignified root piece teased out from the root mass of the potted vine. The vine was repotted and the pot was placed inside a 53µm mesh bag, sealed around the trunk with Tanglefoot™ to prevent phylloxera insects spreading to surrounding grapevines (Figure 4). The grapevines were arranged in a Randomised Block Design (Figure 5) inside the glasshouse and maintained at approximately 24°C throughout the day and 17°C overnight, illuminated with Son-T Agro 400 globes (Philips) for 12 hours daily plus an additional hour boost at 2:00am and watered for 2 minutes daily via drip irrigation, for a nine-week period (24/04/03-27/06/03).



Figure 4: All potted grapevines were placed into a 53 µm gauze mesh bag to prevent cross contamination by phylloxera crawlers

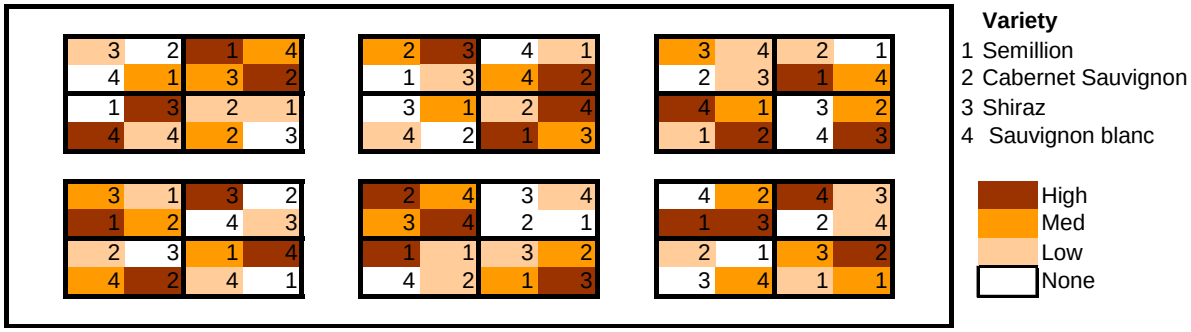


Figure 5: Randomised block design showing potted grapevine position in a single room of a glasshouse. Legend shows the colour scheme layout of the four varieties and four different infestation levels included in the nine-week trial.

3.3 Data collection for HPLC analysis and leaf reflectance

At the end of the nine-week period preliminary, *in situ* leaf spectral reflectance measurements (under ambient light conditions) were acquired from a single, randomly chosen small, medium and large sized leaf from each of the 96 grapevines included in the trial. Following the reflectance measurements the same small, medium and large sized leaves were removed from eight of the grapevines of each variety, two from each treatment group and stored at –80ºC for subsequent HPLC analysis (Section 2.1).

3.4 Phylloxera population counts

At the end of the nine-week period each vine was removed from its pot and the infested root piece was detached, washed in tap water through a 53µm sieve to collect all phylloxera life-stages present. The insects were counted using a bifocal microscope. Root pieces were oven-dried for 48 hours at 60°C and weighed, giving a total number of phylloxera per gram of dry root.

3.5 Results & Discussion (Trial 1)

3.5.1 Phylloxera infestation levels

Variability between infested pots was high and there was no significant relationship identified between the initial number of eggs used to infest a pot and the final population counted at the end of the trial (Figure 6) or between the variety and number of phylloxera present at the end of the trial. The highest single population numbers were observed on the Cabernet Sauvignon and Shiraz varieties, 850 and 763 respectively. This was approximately a 20-fold increase from the initial number of eggs used for infestation at the start of the trial. Treatments were grouped into infested and uninfested to overcome the variability observed. The mean number of phylloxera per variety (values log transformed using $\log_{10}$) were: Cabernet Sauvignon 1.13; Shiraz 1.20; Semillon 0.82; Sauvignon Blanc 0.64 (SEM $\pm$ 0.229; P=0.251).

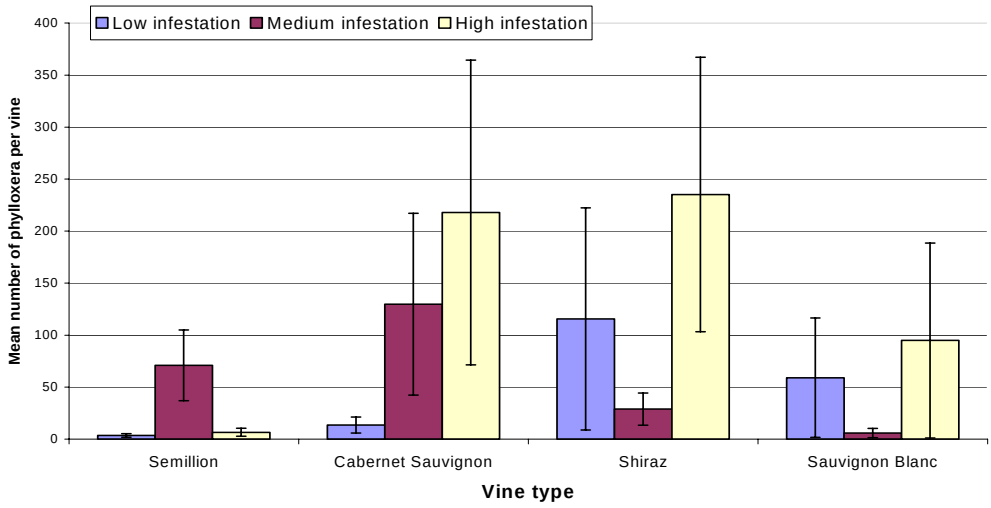


Figure 6: Mean phylloxera population per treatment and grapevine variety included in glasshouse trial. Data collected nine weeks after commencement of the trial.

3.5.2 Spectral measurements

The spectral data collected during the pilot study identified problems in using the variable amount of natural light available for reflectance measurements. Since the reflectance measurements were taken under the ambient lighting conditions of the glasshouse, a large amount of variation was observed in the spectra that were attributable to the change in solar elevation angle and the concomitant different levels of (greenhouse) glass opacity; both of which impacted on the intensity of sunlight that was transmitted to the leaves while the data was recorded. Moreover, initial measurements were taken with a bare fibre into a foreoptic (5 degree field-of-view) pointed at the leaves whilst they were still on the plant. This meant that leaf angle, foreoptic angle and mutual shadowing of the leaves contributed to the variation between spectra.

3.5.3 HPLC analysis

A subset of the samples collected were analysed by HPLC. Due to the high levels of variability in phylloxera population levels the groups were treated as either infested or uninfested (healthy). Figure 7 shows the average total chlorophyll content per gram leaf tissue for each variety. Significant differences were observed in the total chlorophyll content and ratio of chlorophyll a/chlorophyll b between varieties (Figure 8). Significant differences were also observed in the total chlorophyll content of the infested and uninfested Cabernet Sauvignon and Shiraz varieties (mean for Cabernet Sauvignon and Shiraz varieties respectively – infested 1670, uninfested 1111; infested 1441, uninfested 1779) (Table 1).

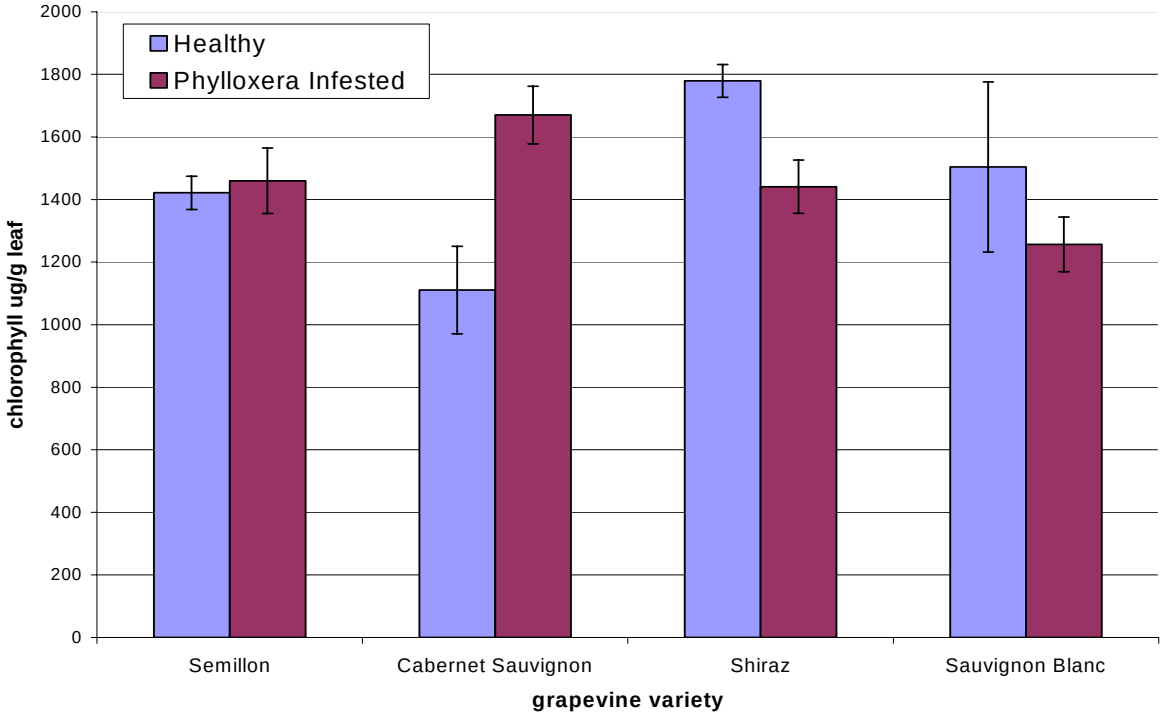


Figure 7: Average total chlorophyll content per gram of leaf tissue from infested and uninfested grapevines of each variety. Data collected nine weeks after commencement of trial.

Table 1: Mean chlorophyll concentration and pigment ratios of healthy and phylloxera infested grapevines.

Variety	Pigment	Mean Healthy (µg/g)	Mean Infested (µg/g)	Treatment P value	LSD
Semillon	Total chlorophyll	1421	1460	0.893	509.6
	Ratio a/b	2.02	2.07	0.869	0.554
Shiraz	Total chlorophyll	1779	1441	0.220	455.7
	Ratio a/b	1.602	1.485	0.575	0.375
Sauvignon Blanc	Total chlorophyll	1502	1256	0.518	665.2
	Ratio a/b	2.01	2.34	0.370	0.615
Cabernet Sauvignon	Total chlorophyll	1111	1670	0.047*	546.5
	Ratio a/b	3.34	2.55	0.116	0.711

*Significant ($p<0.05$)

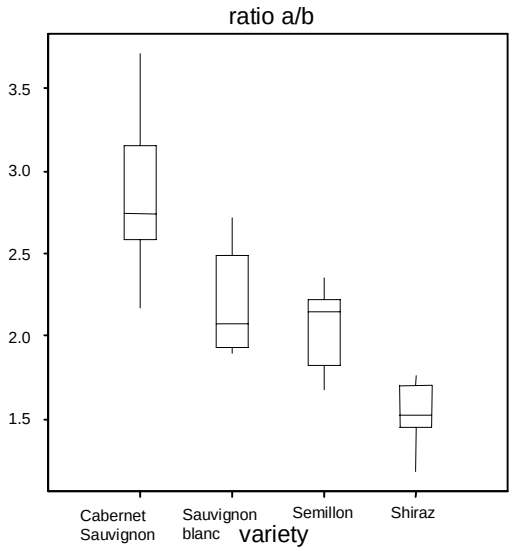


Figure 8: Box and whisker plot indicating varietal effect on the ratio of chlorophyll a / chlorophyll b (ratio a/b).

Significant differences in the total chlorophyll concentration between the infested and uninfested treatments were only observed for the Shiraz and Cabernet Sauvignon varieties. However, the Cabernet Sauvignon phylloxera infested grapevines were actually showing a higher concentration of total chlorophyll, indicating they were less stressed than the uninfested grapevines, this could have been caused by the small sample number used for comparisons. The lack of significant differences in the Semillon and Sauvignon Blanc varieties may have been due to the relatively low phylloxera populations observed on the roots (Figure 6). The differences observed in the phylloxera populations at the end of the trial were difficult to assess because the insects were free to move about the entire root system of the potted grapevines. The difficulty in the establishment of phylloxera on the Semillon and Sauvignon Blanc varieties could have been due to the difference in root morphology of those varieties at the commencement of the trial. However, root morphology was not assessed at the time.

3.6 Key Recommendations

Future glasshouse screening for phylloxera - grapevine interactions should take into account

- the method of assessing phylloxera population density on grapevine roots as the populations need to be tightly confined to the root zone,
- the root physiology and morphological characteristics of grapevine varieties, and
- the difficulty in obtaining spectral reflectance data using ASD Field-Spec Pro; due to changing light conditions an integral light source and integrating sphere should be used.

4. Fieldwork (Trial 2)

Following a pilot study (Held, 2001), fieldwork was conducted at four selected commercial vineyard sites in Phylloxera Infested Zones (control areas for the purpose of preventing the spread of grape phylloxera) in North Eastern Victoria (Figure 9).

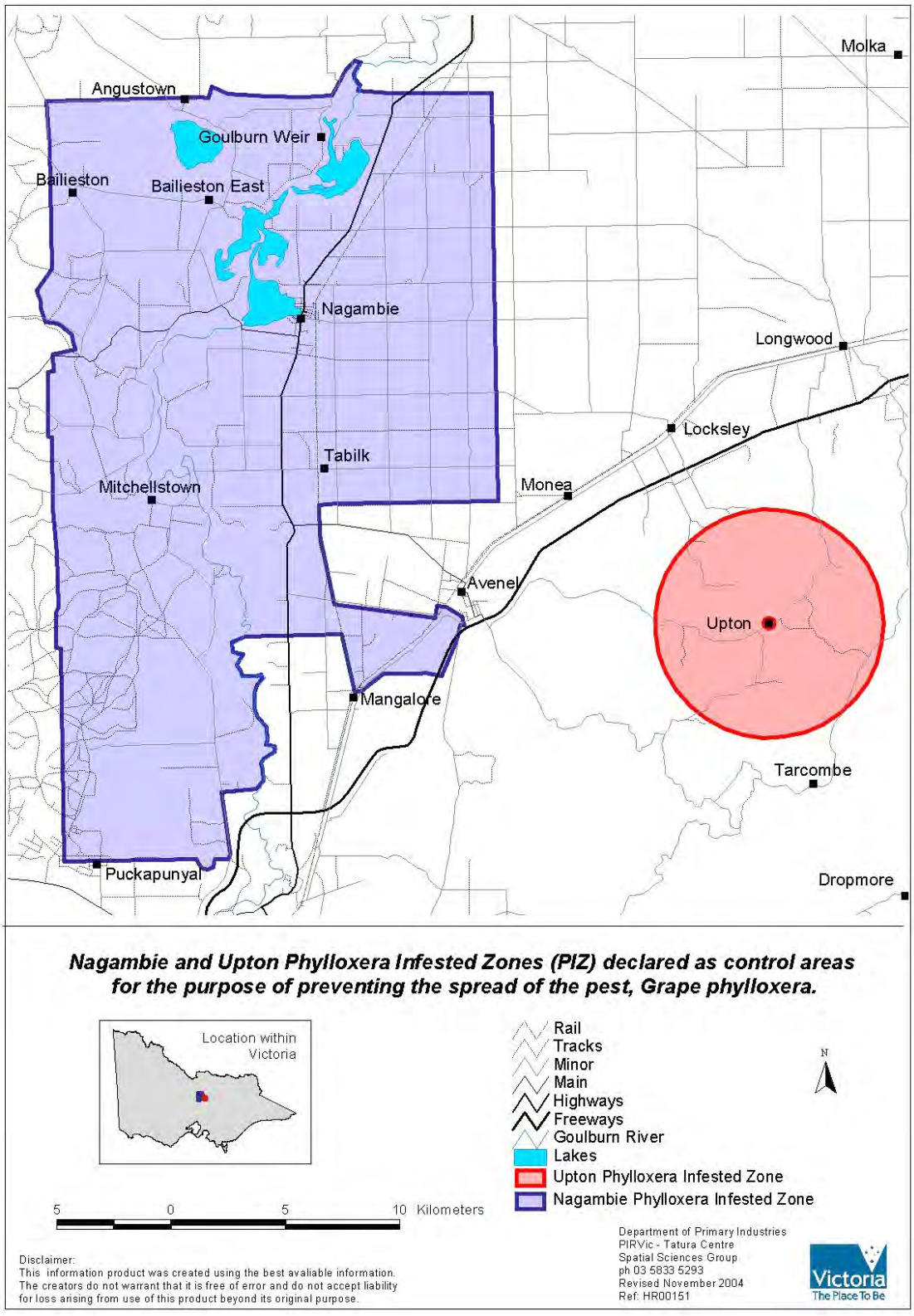


Figure 9a: Nagambie and Upton Phylloxera Infested Zones (PIZ)

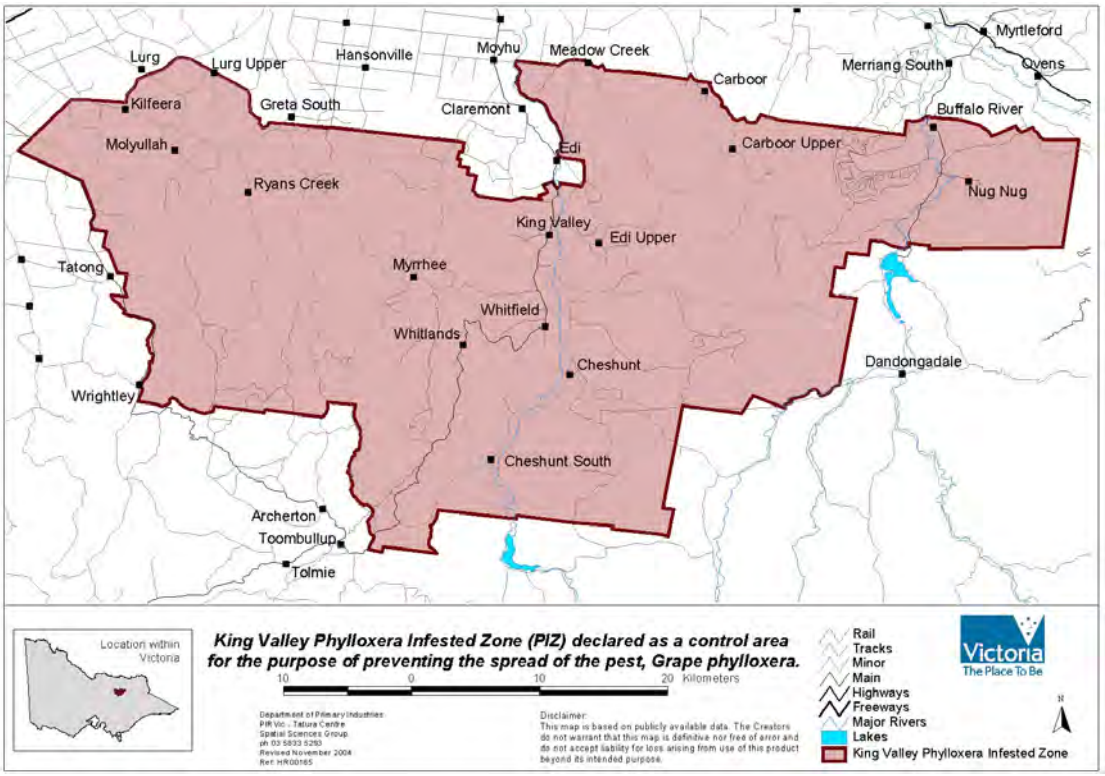


Figure 9b: King Valley PIZ

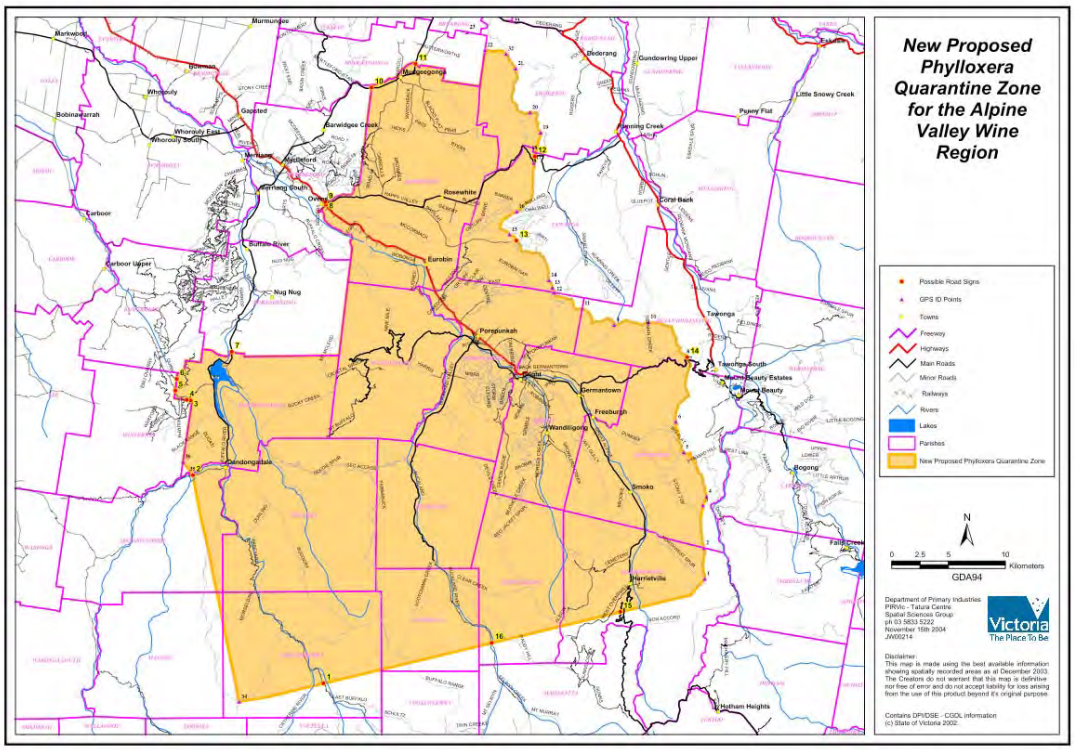


Figure 9c: Alpine Valley PIZ

4.1 Site details

The most suitable sites for detailed investigation were those that contained phylloxera infested and uninfested grapevines in the same varietal block, hence the majority of the field work was completed at two sites - the first in the Upton Phylloxera Infested Zone (Figure 9a), where an outbreak was detected in April 2000. The second was in the Buckland Valley (Figure 9c) where an outbreak was detected in December 2003. All sites and the varieties studied at each site are listed in Table 2. Ground surveys were conducted to verify phylloxera infestation status. Root samples were collected once during each growing season and the relative phylloxera infestation level of targeted grapevines was determined.

Table 2: Sites at which field work was conducted and the grapevine varieties investigated at each site.

Vineyard location	Grapevine variety	Phylloxera free grapevines	Phylloxera infested grapevines	Detection date
Upton	Cabernet Sauvignon Cabernet Franc Merlot	Yes Yes Yes	Yes Yes Yes	2000
Buckland Valley	Pinot Noir	Yes	Yes	2003
King Valley	Riesling Sauvignon Blanc	No No	Yes Yes	1997
Nagambie	Shiraz Semillon	No No	Yes Yes	1969

Fieldwork was conducted at different time points during the growing season; inflorescence fully developed (November), bunch closure (January) and prior to harvest (March) (Table 3). Phylloxera populations generally peak at the trial sites in January (Powell, 2003, 2006) and, to optimise detection potential, sampling times also coincided with this peak (Figure 10).

Table 3: Months in which fieldwork was conducted at the sample sites in Northeast Victoria.

Vineyard location	Grape-growing season					
	2002/2003		2003/2004			2004/2005
King Valley	January	March	November	January	DC	DC
Nagambie	January	March	November	January	DC	DC
Upton	January	March	November	January	March	January
Buckland Valley	NA	NA	NA	January	February	January

NA - not applicable as first detected in December 2003;
DC - discontinued due to difficulty in obtaining control (uninfested) grapevines.

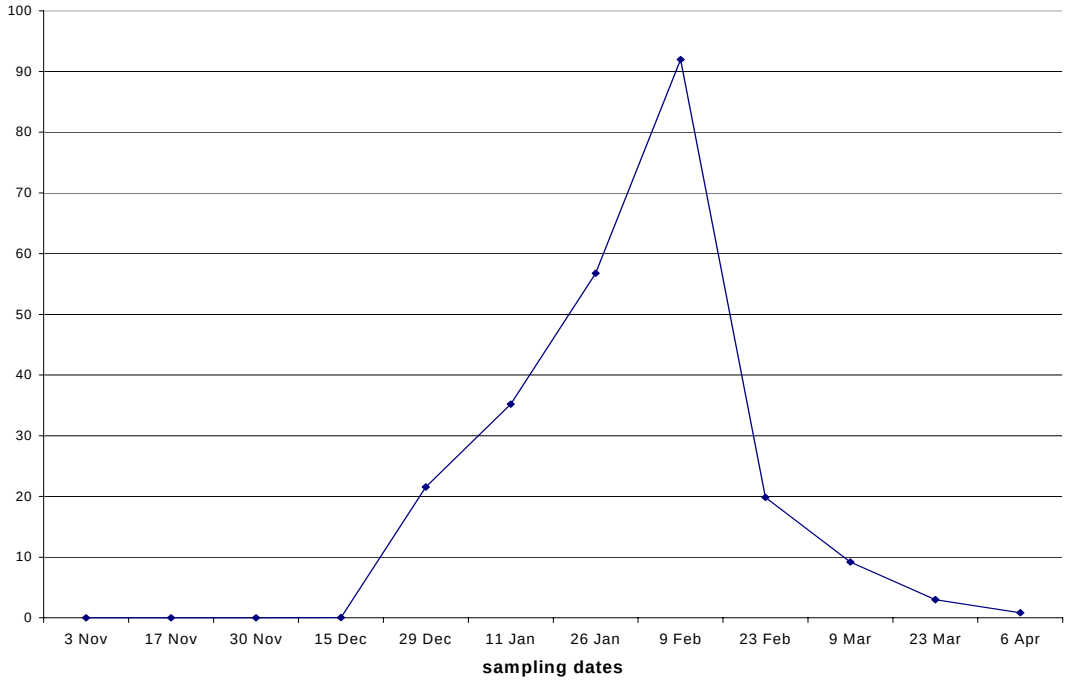


Figure 10: Phylloxera emergence peak taken from trap sampling in Buckland Valley 2004/2005 season.

4.2 Sampling strategy

A varying number of grapevines were selected at each site (Appendix 1) for sampling. Grapevines were selected at each site according to previous or existing experiments conducted at the sites (Powell, 2003, 2006). Grapevines at the Buckland Valley vineyard were chosen based on phylloxera infested and uninfested areas within the Pinot Noir block. Selected grapevines were tagged for identification and the same grapevines were sampled on each field trip. During the 2003 sampling period three leaves were taken from each tagged vine, a small, medium and large leaf representing different age leaves to compare with the sampling strategy used in trial 1. Subsequent sampling strategies included sampling only one leaf per vine. Each leaf sampled was of a uniform green colour and large size, showing no visible sign of chlorosis. During the final field trip, to the Buckland Valley and Upton sites in January 2005, three leaves of uniform large size and green colour were sampled from each tagged grapevine. Sampling strategies are shown in Appendix 1. Leaves were detached from the tagged grapevines, three leaf reflectance measurements were recorded immediately (Section 2.2), a leaf disk was then taken using a 1.4 cm cork borer and the disk was immediately frozen in liquid nitrogen for subsequent HPLC analysis (Section 2.1). Additional leaves were taken from the reference grapevines for NMR analysis (Section 2.3). In conjunction with this study phylloxera populations were monitored as reported in Powell (2006).

4.3 Results & Discussion - Pigments

The following results focus on the Upton and Buckland Valley field sites to enable comparisons between phylloxera infested and uninfested grapevines. Nagambie and King Valley sites did not have sufficient uninfested grapevines. Cabernet Sauvignon from the Upton field site results are shown in Tables 4-7, due to sample storage problems insufficient Cabernet Franc samples were analysed by HPLC to allow statistical analysis of those results. Pinot Noir from the Buckland Valley field site results are shown in Tables 4-8.

4.3.1 Pigment Results - Upton

4.3.1.1 Total chlorophyll content

There was no significant difference in the total chlorophyll content between phylloxera infested and uninfested for the Cabernet Sauvignon leaves on any sampling date (Jan 04, March 04, Jan 05) (Tables 4-6). However, the phylloxera infested samples did show markedly less total chlorophyll content on each date than the uninfested samples (Figure 11). There was no significant difference in the total chlorophyll content between each sampling date, and no significant date by phylloxera interaction (Table 7). A trend was observed, albeit not significant, where the total chlorophyll content of phylloxera infested sample leaves remained relatively static across the three sampling dates whereas it fluctuated across the three sampling dates in the uninfested samples (Figure 11).

4.3.1.2 Total carotenoid content

There was no significant difference in the total carotenoid content between phylloxera infested and uninfested for the Cabernet sauvignon leaves on any sampling date (Jan 04, March 04, Jan 05) (Tables 4-6). However, the phylloxera infested samples did show less total carotenoid content on each date than the uninfested samples except for January 2005, where total carotenoid concentration was almost equal. There was no significant difference in the total carotenoid content between each sampling date, and no significant date by phylloxera interaction was observed (Table 7). A similar trend as was seen in the total chlorophyll content was observed, where the total carotenoid content of phylloxera infested sample leaves remained relatively static across the three sampling dates whereas it fluctuated across the three sampling dates in the uninfested samples.

4.3.1.3 Total carotenoid to total chlorophyll ratio

A trend was observed where phylloxera infested samples showed higher total carotenoid to total chlorophyll ratios than the uninfested samples for the Cabernet Sauvignon variety on each sampling date (Jan 04, March 04, Jan 05). However no significant difference was observed (Tables 4-6) (Figure 12). There was a significant difference in the total carotenoid to total carotenoid ratio between sampling dates

($p<0.001$), the ratio increased in March 2004 compared to both January sampling dates, however January 2005 was also lower than January 2004 (Figure 12). No significant date by phylloxera interaction was observed (Table 7).

4.3.1.4 Total xanthophyll cycle pigments to total chlorophyll ratio (VAZ/Tchlorophyll)

(A, antheraxanthin; Z, zeaxanthin; V, violaxanthin)

A trend was observed where phylloxera infested samples showed higher xanthophyll cycle pigment to total chlorophyll ratios than the uninfested samples for the Cabernet sauvignon variety, however no significant difference was observed (Tables 4-6). There was no significant difference in the VAZ to total chlorophyll ratio between each sampling date, and no significant date by phylloxera interaction was observed (Table 7).

4.3.1.5 Xanthophyll cycle pigment ratio (AZ/VAZ)

A trend was observed where phylloxera infested samples showed consistently higher xanthophyll cycle pigment ratios than the uninfested samples for the Cabernet Sauvignon variety on each sampling date (Jan 04, March 04, Jan 05), however no significant differences were observed (Tables 4-6). There was a significant difference in the xanthophyll cycle pigment ratio between sampling dates ($p<0.001$) (Table 7). The ratio was higher in January 2005 than either sampling dates in 2004. However, no significant date by phylloxera interaction was observed (Table 7).

4.3.1.6 β-carotene to total chlorophyll ratio

There was no significant difference in the β-carotene to total chlorophyll ratio between phylloxera infested and uninfested samples for the Cabernet Sauvignon samples (Tables 4-6). There was a significant difference in the β-carotene to total chlorophyll ratio between dates ($p<0.001$) and a significant date by phylloxera interaction ($p<0.001$) (Table 7). The ratio was lower in samples from January 2005 compared to all other sampling dates.

Table 4: Table of predicted means and P value for Cabernet Sauvignon leaves sampled from a vineyard in the Upton PIZ, January 2004.

Pigment ($nmolsg^{-1}$)	Infested	Uninfested	P value	df	Wald statistic
Total chlorophyll	1282	1747	0.144	1	2.13
Total carotenoid	566.2	715.6	0.119	1	2.43
Tcarot/ Tchlorophyll	0.449	0.413	0.704	1	0.14
VAZ/ Tchlorophyll	0.186	0.148	0.640	1	0.22
AZ/VAZ	0.552	0.520	0.802	1	0.06
β-carot/ Tchlorophyll	0.125	0.130	0.705	1	0.14

* significant ($P<0.05$)

Table 5: Table of predicted means and P value for Cabernet Sauvignon leaves sampled from a vineyard in the Upton PIZ , March 2004.

Pigment ($nmolsg^{-1}$)	Infested	Uninfested	P value	df	Wald statistic
Total chlorophyll	1242	1456	0.636	1	0.22
Total carotenoid	583.9	624.5	0.842	1	0.04
Tcarot/ Tchlorophyll	0.482	0.433	0.683	1	0.17
VAZ/ Tchlorophyll	0.201	0.163	0.705	1	0.14
AZ/VAZ	0.571	0.493	0.706	1	0.14
β-carot/Tchlorophyll	0.124	0.122	0.902	1	0.02

* significant (P<0.05)

Table 6: Table of predicted means and P value for Cabernet Sauvignon leaves sampled from a vineyard in the Upton PIZ, January 2005.

Pigment ($nmolsg^{-1}$)	Infested	Uninfested	P value	df	Wald statistic
Total chlorophyll	1398	1558	0.711	1	0.14
Total carotenoid	552.1	551.7	0.996	1	0
Tcarot/ Tchlorophyll	0.398	0.298	0.287	1	1.14
VAZ/ Tchlorophyll	0.170	0.119	0.261	1	1.26
AZ/VAZ	0.780	0.602	0.425	1	0.64
β-carot/Tchlorophyll	0.110	0.088	0.41	1	0.68

* significant (P<0.05)

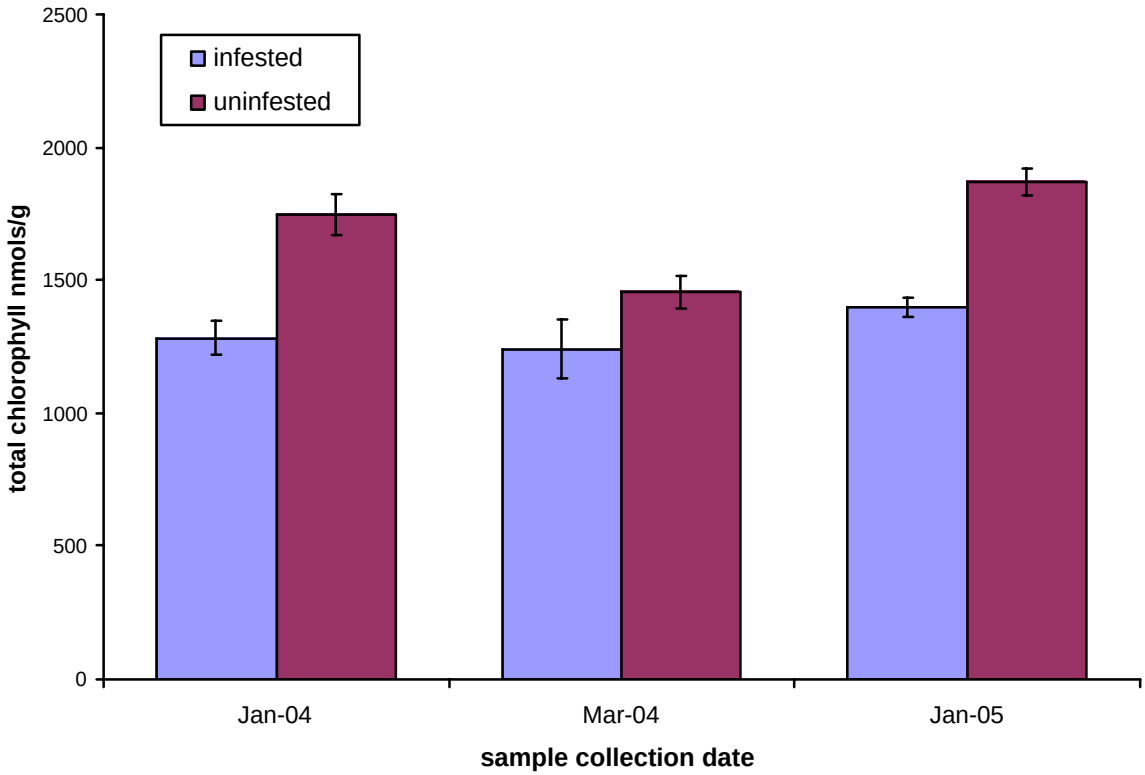


Figure 11: Total chlorophyll content of Cabernet Sauvignon sampled from a field site in the Upton PIZ on three sampling dates.

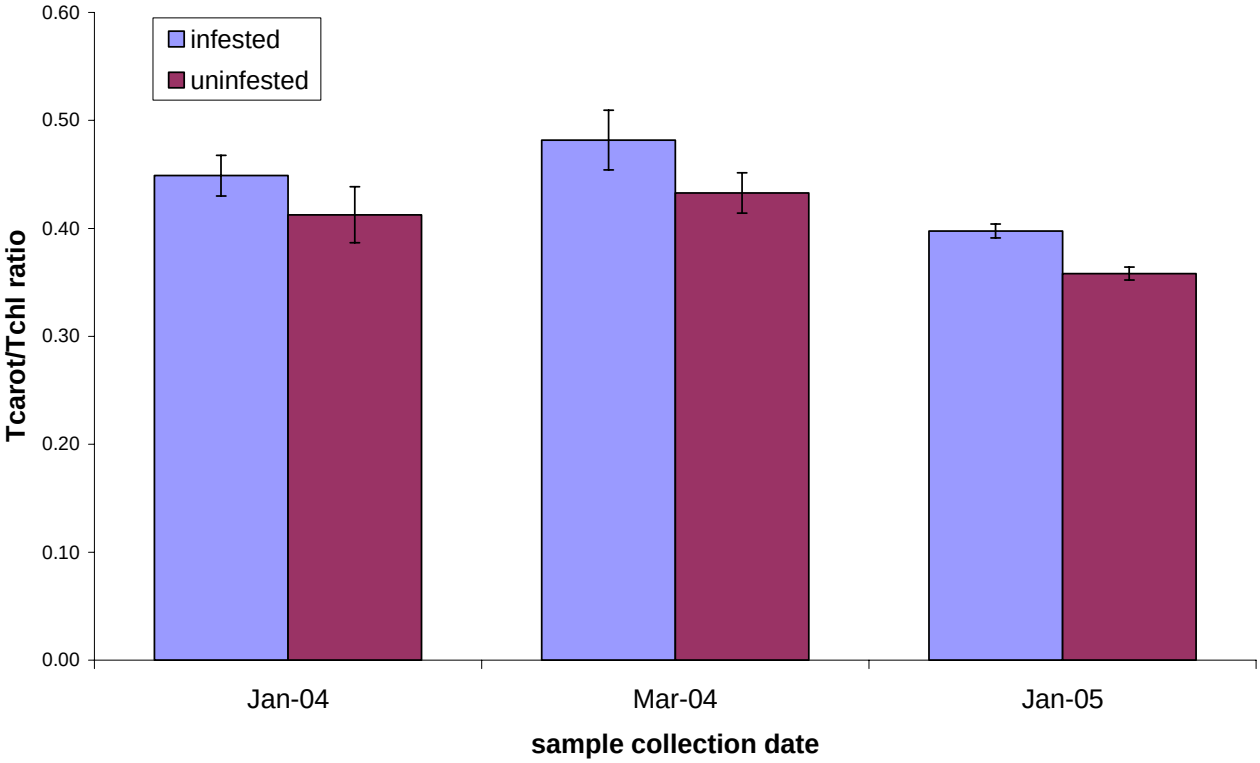


Figure 12: Total carotenoid to total chlorophyll ratio of Cabernet Sauvignon sampled from a field site in the Upton PIZ on three sampling dates.

Table 7: Cabernet Sauvignon Upton field data - all collection dates, infested and uninfested samples. Table of predicted means and p-value.

Pigment/ pigment ratio (nmolsg^{-1})	Phylloxera	20/01/04	23/03/04	18/01/05	Variable	P value	df	Wald statistic
Total chlorophyll	Infested	1282	1242	1398	Date	0.284	2	2.52
					Phylloxera	0.57	1	0.32
	Uninfested	1743	1456	1558	Date.phylloxera	0.341	2	2.15
Total carotenoids	Infested	566.2	583.9	552.5	Date	0.169	2	3.56
					Phylloxera	0.784	1	0.08
	Uninfested	715.6	624.5	551.7	Date.phylloxera	0.185	2	3.37
Tcarot/ Tchlorophyll	Infested	0.449	0.482	0.398	Date	<0.001*	2	33.63
					Phylloxera	0.479	1	0.5
	Uninfested	0.407	0.433	0.298	Date.phylloxera	0.319	2	2.28
VAZ/ Tchlorophyll	Infested	0.186	0.201	0.170	Date	0.051˜	2	5.96
					Phylloxera	0.571	1	0.32
	Uninfested	0.148	0.163	0.119	Date.phylloxera	0.898	2	0.22
AZ/VAZ	Infested	0.552	0.571	0.780	Date	<0.001*	2	36.09
					Phylloxera	0.472	1	0.52
	Uninfested	0.509	0.493	0.602	Date.phylloxera	0.137	2	3.98
β-carot/ Tchlorophyll	Infested	0.125	0.124	0.110	Date	<0.001*	2	68.33
					Phylloxera	0.57	1	0.32
	Uninfested	0.128	0.122	0.088	Date.phylloxera	<0.001*	2	14.08

*significant (P<0.001) ˜ significant (P<0.1) n=12, Where AZ = antheraxanthin + zeaxanthin, VAZ = violaxanthin + antheraxanthin + zeaxanthin

4.3.2 Pigment Results - Buckland Valley

4.3.2.1 Total chlorophyll

In January 2004, one month after phylloxera was first detected at the site, the total chlorophyll content of phylloxera infested and uninfested samples did not differ significantly (Table 8). However, there was a significant difference in the total chlorophyll content between phylloxera infested and uninfested for the Pinot Noir samples in February 2004 and January 2005 (Table 9 & 10) but not in March 2005 (Table 11). The phylloxera infested samples showed less total chlorophyll content than the uninfested samples on each date (Figure 13) (Tables 8-11). Total chlorophyll content of the leaves was markedly lower in February 2004 and a significant difference in the total chlorophyll content between sampling dates was recorded ($p<0.001$), however no significant date by phylloxera interaction was observed (Table 12).

4.3.2.2 Total carotenoid content

Although total carotenoid levels were generally lower in the infested samples than uninfested samples, there was no significant difference in the total carotenoid content between phylloxera infested and uninfested on any sampling date (Jan 04, Feb 04, Jan 05, March 05) (Table 8-11). Phylloxera infested samples showed less total carotenoid content than the uninfested samples on each date except January 2004 (Table 8). Total carotenoid content of the leaves was dramatically lower in February 2004 and a significant difference in the total carotenoid content between sampling dates was recorded ($p<0.001$), however no significant date by phylloxera interaction was observed (Table 12).

4.3.2.3 Total carotenoid to total chlorophyll ratio

A trend was observed where phylloxera infested samples showed higher total carotenoid to total chlorophyll ratios than the uninfested samples for the Pinot Noir variety on each sampling date, except March 2005 (Figure 14) (Table 11). A significant difference was only observed in the samples collected in January 2005 (Table 10). There was a significant difference in the total carotenoid to total chlorophyll ratio between sampling dates ($p<0.001$) and a significant date by phylloxera interaction ($p<0.001$) (Table 12).

4.3.2.4 Total xanthophyll cycle pigments to total chlorophyll ratio (VAZ/Tchlorophyll)

A trend was observed where phylloxera infested samples showed higher xanthophyll cycle pigment to total chlorophyll ratios than the uninfested samples for the Pinot Noir variety on each sampling date, except March 2005 (Tables 8-11). However a significant difference was observed in the samples collected in January 2005 only (Table 10). There was a significant difference in the VAZ to total chlorophyll ratio

between each sampling date ($p<0.001$), and a significant date by phylloxera interaction ($p<0.001$) (Table 12).

4.3.2.5 Xanthophyll cycle pigment ratio (AZ/VAZ)

A trend was observed where phylloxera infested samples showed higher xanthophyll cycle pigment ratios than the uninfested samples for the Pinot noir variety on each sampling date (Jan 04, Feb 04, Jan 05, March 05) (Tables 8-11), however no significant differences were observed. There was a significant difference in the xanthophyll cycle pigment ratio between sampling dates ($p<0.001$) (Table 12), however, no significant date by phylloxera interaction was observed (Table 12).

4.3.2.6 β-carotene to total chlorophyll ratio

There was a trend towards phylloxera infested samples having higher β-carotene to total chlorophyll ratios than uninfested, however the only significant difference between phylloxera infested and uninfested samples for the Pinot Noir variety was observed in February 2004 ($p<0.1$) (Table 9). There was a significant difference in the β-carotene to total chlorophyll ratio between dates ($p<0.001$) and no significant date by phylloxera interaction was observed (Table 12).

Table 8: Table of predicted means and P value for Pinot Noir leaves sampled from a vineyard in the Buckland Valley, January 2004.

Pigment ($nmolg^{-1}$)	Infested	Uninfested	P value	df	Wald statistic
Total chlorophyll	3016	3232	0.848	1	0.04
Total carotenoid	931.3	899.0	0.904	1	0.01
Tcarot/ Tchlorophyll	0.309	0.281	0.414	1	0.67
VAZ/Tchlorophyll	0.96	0.75	0.441	1	0.59
AZ/VAZ	0.387	0.307	0.736	1	0.11
β-carot/ Tchlorophyll	0.101	0.089	0.380	1	0.77

* significant ($P<0.05$)

Table 9: Table of predicted means and P value for Pinot Noir leaves sampled from a vineyard in the Buckland Valley, February 2004.

Pigment ($nmolg^{-1}$)	Infested	Uninfested	P value	df	Wald statistic
Total chlorophyll	1963	2709	0.006*	1	7.67
Total carotenoids	573.4	706.3	0.147	1	2.1
Tcarot/ Tchlorophyll	0.289	0.260	0.199	1	1.65
VAZ/Tchlorophyll	0.076	0.056	0.268	1	1.23
AZ/VAZ	0.566	0.443	0.571	1	0.32
β-carot/ Tchlorophyll	0.098	0.089	0.094	1	2.8

* significant ($P<0.05$)

Table 10: Table of predicted means and P value for Pinot Noir leaves sampled from a vineyard in the Buckland Valley, January 2005.

Pigment ($nmolg^{-1}$)	Infested	Uninfested	P value	df	Wald statistic
Total chlorophyll	2065	2591	<0.001*	1	12.38
Total carotenoids	755.4	843.3	0.286	1	1.14
Tcarot/Tchlorophyll	0.362	0.328	0.028*	1	4.82
VAZ/Tchlorophyll	0.136	0.105	0.043*	1	4.09
AZ/VAZ	0.789	0.728	0.563	1	0.34
β-carot/Tchlorophyll	0.113	0.109	0.23	1	1.44

* significant (P<0.05)

Table 11: Table of predicted means and P value for Pinot Noir leaves sampled from a vineyard in the Buckland Valley, March 2005.

Pigment ($nmolg^{-1}$)	Infested	Uninfested	P value	df	Wald statistic
Total chlorophyll	2666	2733	0.778	1	0.08
Total carotenoids	883.5	981.2	0.308	1	1.04
Tcarot/Tchlorophyll	0.329	0.359	0.138	1	2.2
VAZ/Tchlorophyll	0.115	0.140	0.059	1	3.57
AZ/VAZ	0.796	0.780	0.496	1	0.46
β-carot/Tchlorophyll	0.105	0.107	0.617	1	0.25

* significant (P<0.05)

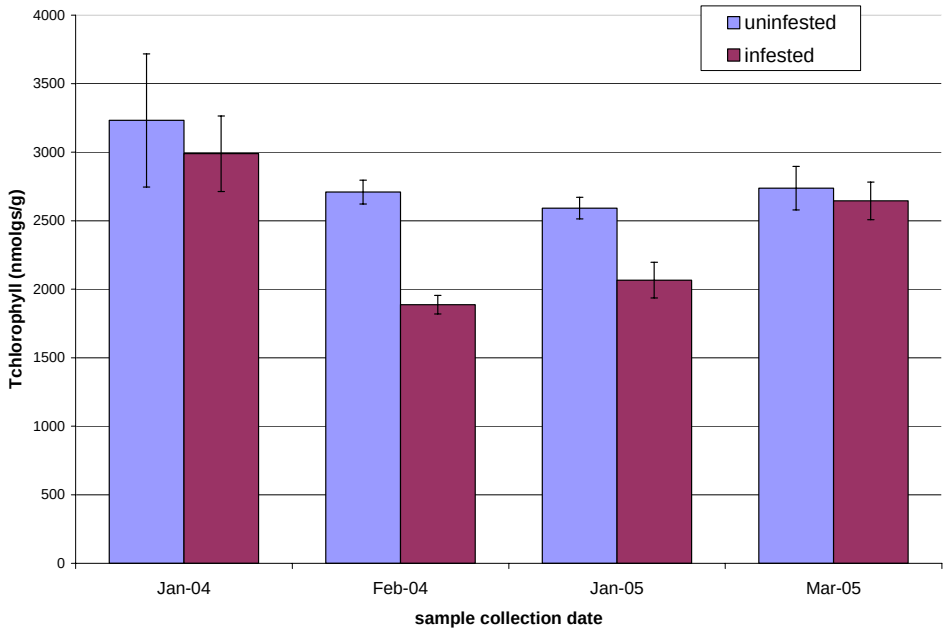


Figure 13: Total chlorophyll content of leaves from phylloxera infested and uninfested Pinot Noir vines taken from a vineyard in the Buckland Valley on four sampling dates.

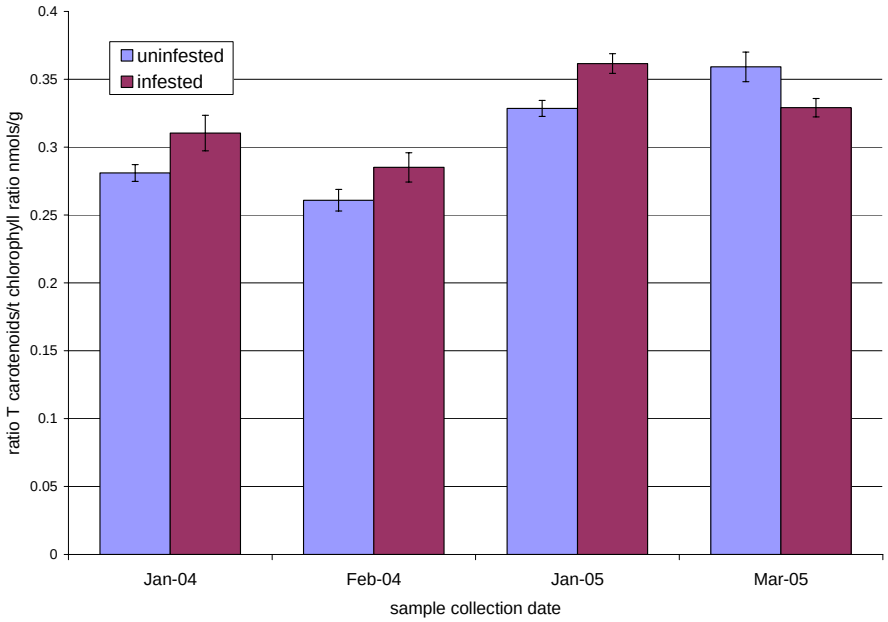


Figure 14: Total carotenoid to total chlorophyll ratio of leaves from phylloxera infested and uninfested Pinot Noir vines taken from a vineyard in the Buckland Valley on four sampling dates.

Table 12: Buckland Valley field data - all sample dates, infested and uninfested samples.
Table of predicted means and P-value.

Pigment/ pigment ratio ($nmolsg^{-1}$)	Phylloxera	20/01/04	24/02/04	19/01/05	09/03/05	Function	P value	df	Wald statistic
Total chlorophyll	Infested	3001	1974	2063	2644	Date	<0.001*	3	18.27
						Phylloxera	0.009*	1	6.89
	Uninfested	3255	2733	2589	2736	Date.phylloxera	0.253	3	4.08
Total carotenoids	Infested	929.5	577.1	742.6	871.2	Date	<0.001*	3	17.49
						Phylloxera	0.11	1	2.55
	Uninfested	918.4	725.9	845.7	983.4	Date.phylloxera	0.806	3	0.98
Tcarot/ Tchlorophyll	Infested	0.311	0.292	0.361	0.329	Date	<0.001*	3	43.49
						Phylloxera	0.122	1	2.39
	Uninfested	0.282	0.262	0.329	0.359	Date.phylloxera	<0.001*	3	20.72
VAZ/ Tchlorophyll	Infested	0.096	0.077	0.135	0.113	Date	<0.001*	3	41.85
						Phylloxera	0.199	1	1.65
	Uninfested	0.076	0.059	0.106	0.141	Date.phylloxera	<0.001*	3	24.81
AZ/VAZ	Infested	0.389	0.586	0.784	0.797	Date	<0.001*	3	147.59
						Phylloxera	0.429	1	0.63
	Uninfested	0.274	0.482	0.725	0.783	Date.phylloxera	0.538	3	2.17
β-carot/ Tchlorophyll	Infested	0.102	0.100	0.112	0.105	Date	<0.001*	3	30.65
						Phylloxera	0.198	1	1.66
	Uninfested	0.0891	0.0889	0.109	0.107	Date.phylloxera	0.108	3	6.07

*significant (P<0.005) n=12, Where AZ = antheraxanthin + zeaxanthin,
VAZ = violaxanthin + antheraxanthin + zeaxanthin

4.3.3 Discussion - Pigments

The relationship between leaf age and chlorophyll content has been studied in grapevines (Poni *et al*. 1994; Lovisolo *et al*. 1996) although some uncertainty still exists about this relationship. Lovisolo *et al*. (1996) showed chlorophyll content per unit leaf area reached maximum values in 20 – 30 day old leaves. Poni *et al*. (1994) found chlorophyll content increased then remained constant for some time after full leaf size attainment, peak concentration was obtained at 70 – 80 days and a consistent decline was observed after four months of age. In our study the strategy of sampling different sized leaves was not continued after the first sampling period because no significant difference was observed in the reflectance spectra of the samples of different sized leaves. The age of the sampled leaves was unknown, and leaf size may not be an accurate estimation of leaf age. It is possible all leaves were older than 50 days hence no further accumulation of chlorophyll would take place. It was assumed all leaves sampled on subsequent dates were full leaf size and older than 50 days, but not four months of age. They would therefore contain their maximum chlorophyll content and not be in decline. Any difference in chlorophyll content observed in the samples was assumed to be not attributable to leaf age.

Phylloxera infested samples from both Upton and Buckland Valley sites showed changes in their pigment content that agree with those symptoms observed due to plant stress. That is a trend for lower total chlorophyll concentrations than uninfested samples; an increase in total carotenoid to total chlorophyll ratio; an increase in the VAZ to total chlorophyll ratio and an increase in the β-carotene to total chlorophyll ratio. Greater differences were observed between the infested and uninfested Pinot Noir samples from Buckland Valley. This may be due to a varietal effect or the shorter period of time the Buckland Valley site has been infested. The concentrations of pigments in the Cabernet Sauvignon leaves appeared to remain more constant over the sampling periods in the infested samples compared to the uninfested samples, suggesting the grapevines are severely stressed and incapable of achieving the fluctuations commonly observed with seasonal patterns. Significant changes were not observed in the xanthophyll cycle pigments, however changes in pigment content of this cycle occur rapidly and continuously throughout a day as a leaf is gradually exposed to full sun and this ratio is an indicator of short term stress events.

Significant differences were observed between sample dates within and across seasons at both Upton and Buckland Valley sites. Samples taken at the end of February 2004 or March 2005 did not show higher total carotenoid to chlorophyll ratios than those taken in January 2004 or January 2005. This suggests those samples were not beginning to show autumnal seasonal change associated with senescence, but were showing general stress symptoms associated with the higher ratio seen in the infested samples. Generally, the degradation of carotenoids is slower than chlorophylls during senescence (Suzuki and Shioi 2004), resulting in an increase in the relative concentration of carotenoids with respect to chlorophyll that is often

observed when plants are subjected to stress and in senescing leaves (Young and Britton 1990).

4.3.4 Conclusion - Pigments

Leaf pigment content provides information about the physiological condition of a plant. HPLC analysis provided a means for the accurate calculation of leaf pigment content which enabled further understanding of the effect phylloxera infestation has on grapevine health. However, limited numbers of phylloxera free grapevines were available for testing in commercial vineyards in PIZs so testing was restricted to only a few locations and hence only a few varieties. The small sample size limited statistical analysis hence many trends were observed but could not be labelled significant.

Results demonstrate the extreme natural variation in leaf pigment content throughout a block of field grown grapevines. Variation is caused by changes in the environment and differences were observed in pigment content of samples between the two sampling seasons, as well as between sampling dates within a season. Phylloxera infested samples showed changes in their pigment content and pigment ratios which are indicators of general stress symptoms. At this stage a phylloxera specific response was not discernible. However, trends were observed which suggest that future investigations are warranted (Blanchfield *et al*., 2006. Differences between sites were also observed which could imply that factors such as (i) phylloxera genotype, (ii) site variability, (iii) vine age and variety, and (iv) vineyard management could all be important factors in determining the severity of the grapevine's response to phylloxera infestation.

4.4 Results & Discussion - Spectral Reflectance

Examples of reflectance spectra for phylloxera-infested and uninfested grapevines are given in the following figures. Some important broad spectral regions that will be referred to throughout this document are as follows:

Green peak, reflectances from 500-600 nm with maxima around 550 nm;
Chlorophyll well, reflectances between 550-700 nm;
Red edge, wavelengths between 700-760 nm;
NIR plateau, wavelengths between 750-1300 nm; and
Water absorption features, minor absorption features occurring around 950 and 1150 nm, and major absorption around 1450 nm.

At the canopy level, the most striking difference between infested and uninfested reflectance spectra occurs for wavelengths on the NIR plateau. NIR radiation lacks the energy to excite electron transition in the molecules within a leaf and is therefore either scattered through the leaf (i.e. transmitted) or reflected back out through the

incident surface. This process is an additive effect so the more leaves in the canopy the more radiation is scattered and reflected out towards the sensor. The fact that phylloxera-infested grapevines have, in general, less foliage means that there will be lower reflectances in the NIR than a healthier counterpart. This is demonstrated in Figure 15.

Considerable vine-to-vine variation in canopy-level reflectance spectra (Figure 16a) was also observed. As with the remotely-sensed observation, this variation may be due to background reflectance contribution, mutual shadowing of leaves and other grapevines, relative solar and sensor geometries, and changes in the ambient light conditions between measurements. These factors come into play to hamper efforts in understanding the difference in spectral response between infested and uninfested grapevines. Therefore, in this study the emphasis was on analysing leaf-level reflectances measured with an integrating sphere. The integrating sphere provided a stable, consistent light environment and fixed illumination and viewing geometry between leaf measurements. Resulting spectra had reduced variably (Figure 16b), compared to canopy level spectra, in which variations (we could confidently assume) were due to chemical composition and physical structure and not the lighting environment.

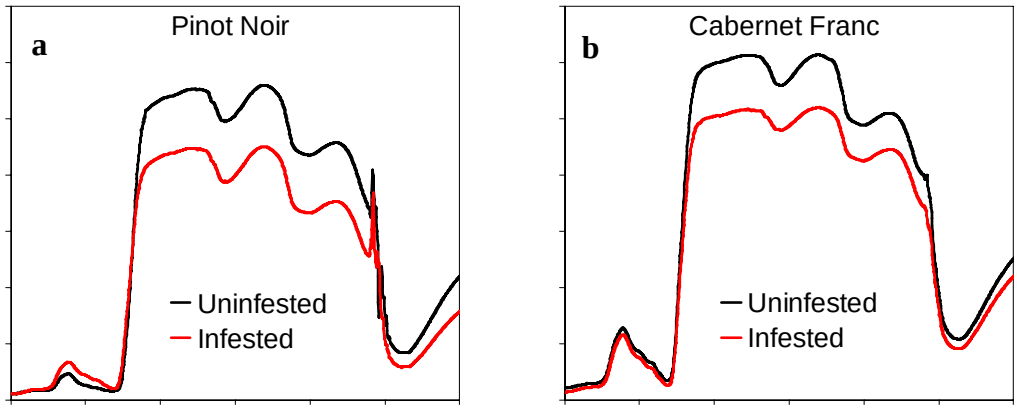


Figure 15: Differences in canopy-level reflectance spectra for two varieties of phylloxera-infested and uninfested grapevines taken at the (a) Buckland Valley and (b) Upton field sites.

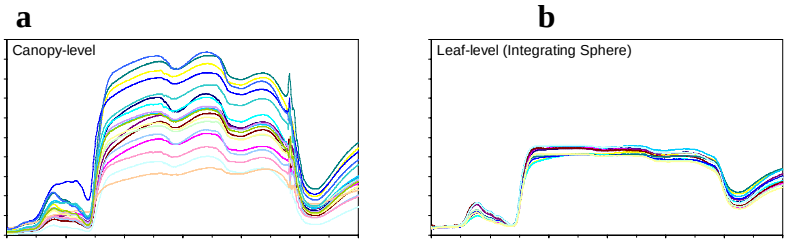


Figure 16: The range of variability between (a) canopy-level and (b) leaf-level reflectance spectra for the same Riesling grapevines taken at the King Valley field site.

Another advantage of using the integrating sphere is that it provides consistency for the assessment of inter-annual (Figure 17) and seasonal (Figure 18) variability in leaf-level spectral response. Figure 17 shows that there is very little inter-annual change in reflectances for Cabernet Sauvignon leaves. Most of the differences are on the NIR plateau that may be linked to plant development (through early development, maturation and senescence). In this case, however, we suspect that the differences are not statistically significant, based on the observations in Figure 18.

Figure 18 shows changes in leaf reflectances of Cabernet Franc over a grape-growing season. Statistical test of significance via the *F*-statistic show that over the growing season, the spectra reflectance curves for an uninfested sample differ most around the green peak (500-600 nm) and along the red edge (680-750 nm). These regions are known to be affected by leaf development. Early in the growing season (November), young leaves are bright green and have higher reflectances in the green peak. As the leaves grow, the increase in chlorophyll content and leaf thickness contribute to a decrease in green peak reflectances by around January. By March the leaves are beginning to senesce, meaning lower chlorophyll concentrations, and the green peak reflectances start to rise again. Changes in red-edge reflectances (as we shall see below) are also related to leaf chlorophyll concentrations. Figure 18b shows that there are no regions of statistically significant differences between the reflectance spectra over the growing season for the phylloxera-infested Cabernet Franc, whereas there are significant changes for uninfested vines (Figure 18a).

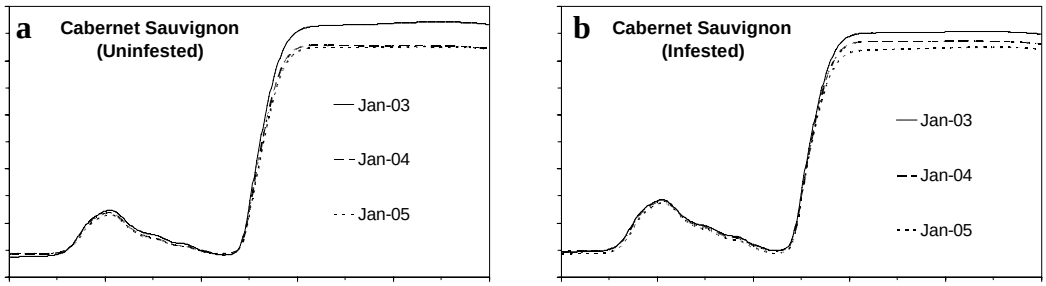


Figure 17: Inter-annual variability in mean leaf-level spectral response for (a) uninfested and (b) infested Cabernet Sauvignon vines taken at the Upton field site.

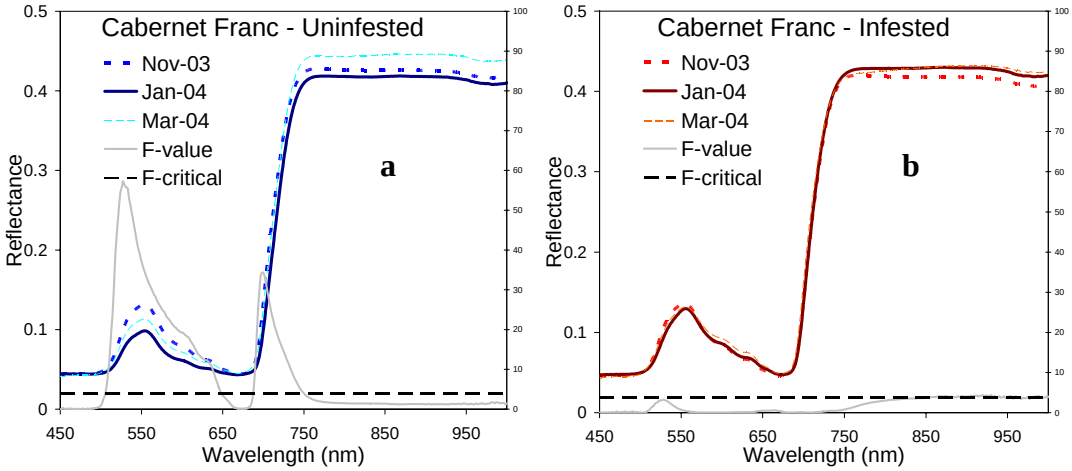


Figure 18: Leaf reflectance spectra showing phenological changes over the grape-growing season for (a) uninfested and (b) infested Cabernet Franc vines at the Upton field site. Grey line shows calculated F-values; dashed horizontal lines mark critical F-value for a 95% level of statistical significance.

The most commonly observed differences in the reflectance spectra of uninfested and infested samples occur around the green peak and into the chlorophyll well (Figure 19). These regions are known to be affected by chlorophyll content in response to plant stress (Carter, 1993). The higher reflectances in the highlighted regions are due to lower chlorophyll contents as the vine relocates resources to the roots to help repair the damage cause by phylloxera (Peterson and Johnson, 2000).

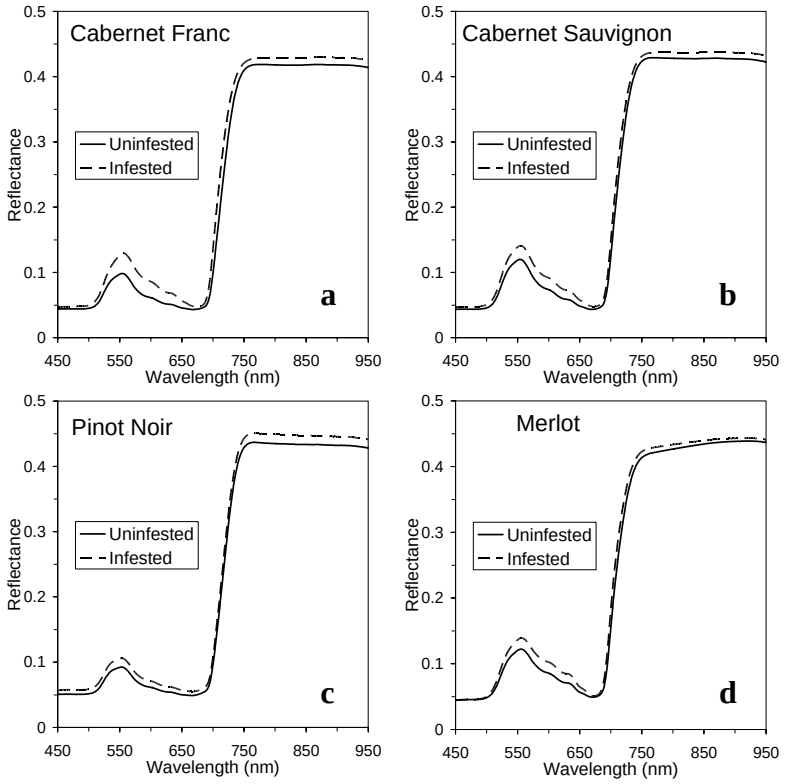


Figure 19: Mean leaf reflectance spectra for uninfested and infested (a) Cabernet Franc, (b) Cabernet Sauvignon (c) Pinot Noir and (d) Merlot vines. These data were acquired in January 2004 at the Upton (a)(b) and (d) Buckland Valley (c) field sites.

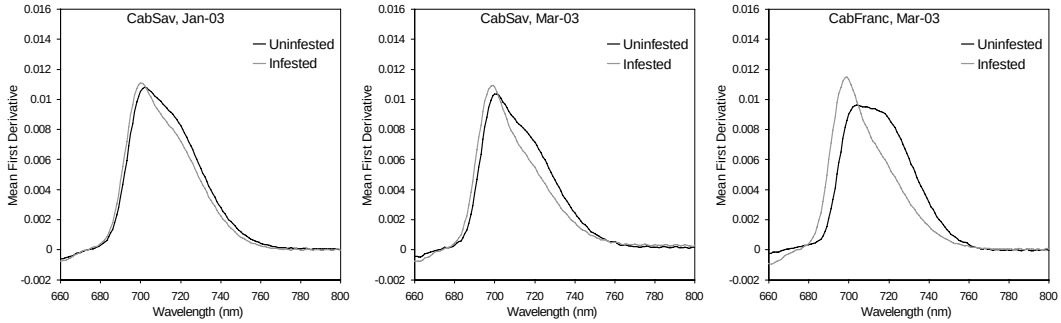


Figure 20: Derivative spectra of some of the grapevine leaves measured at the Upton field site.

Derivative operators were also of interest in this work because of their well-known ability to detect subtle changes in curvature in reflectance spectra that are related to pigment and chemical absorption (Tsai and Philpot, 1998; Clark *et al.*, 2003). Of particular interest is the shape of resulting derivative spectra around the red edge (660-760 nm) and its relationship with leaf chlorophyll content and pre-visual stress detection (Zarco-Tejada *et al.*, 2003).

Figure 20 gives some examples of derivative spectra. Displayed are first derivative spectra (estimated by finite differences) for phylloxera-infested and uninfested samples of grapevines acquired in January 2003 and March 2003. We observe that for infested samples, the spectra have sharper looking peaks that are more skewed to the lower wavelengths than the uninfested samples. The wavelength corresponding to the maximum in the first derivative spectrum is known as the *red edge inflection point* (REIP). A shift in REIP towards shorter wavelengths (as is observed for infested samples above) is commonly attributed to plant stress and, as Figure 21 illustrates, a decrease in leaf chlorophyll content.

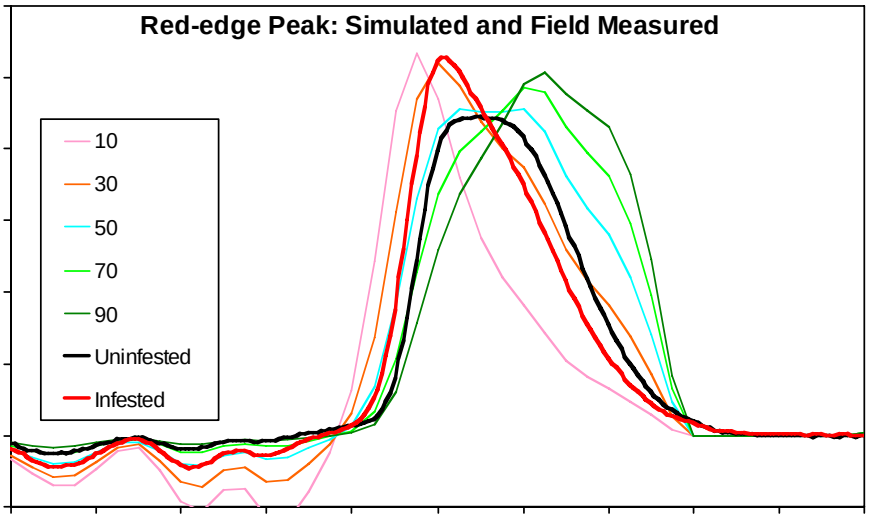


Figure 21: Illustration of how the shift in the peak and shape of the derivative spectra are related to leaf chlorophyll content. The thick black and red curves are the estimated first derivate curves of actual field-measured reflectance spectra for uninfested and infested grapevines. The thinner coloured curves are simulated spectra estimated by the PROSPECT radiative transfer model for different levels of leaf chlorophyll content.

Figure 22a shows the grouping of phylloxera infested and uninfested Cabernet Sauvignon spectra for both January and March 2003. This illustrates that PDA found it much easier to separate the data from different months (which is identified by the first discriminant variable) than the phylloxera-infestation levels (which is identified by the second discriminant variable). In other words the effect of leaf age was more discernable than the stress caused by phylloxera. In March, however, the separation of the infestation levels is more pronounced than in the January data.

Figure 22b shows the group separation of the grapevine varieties. The results displayed suggest that Shiraz vines were spectrally more distinct from the other varieties than the other grapevines. Overall, however, there seems to be considerable confusion (i.e. overlap of the groups) between varieties. The PDA shown was conducted with a low level of model complexity (see Renzullo *et al*. (2006) for further explanation of model complexity in regards to PDA). The expectation is that the group separation for the different grapevine variates will increase with a slight increase in model complexity.

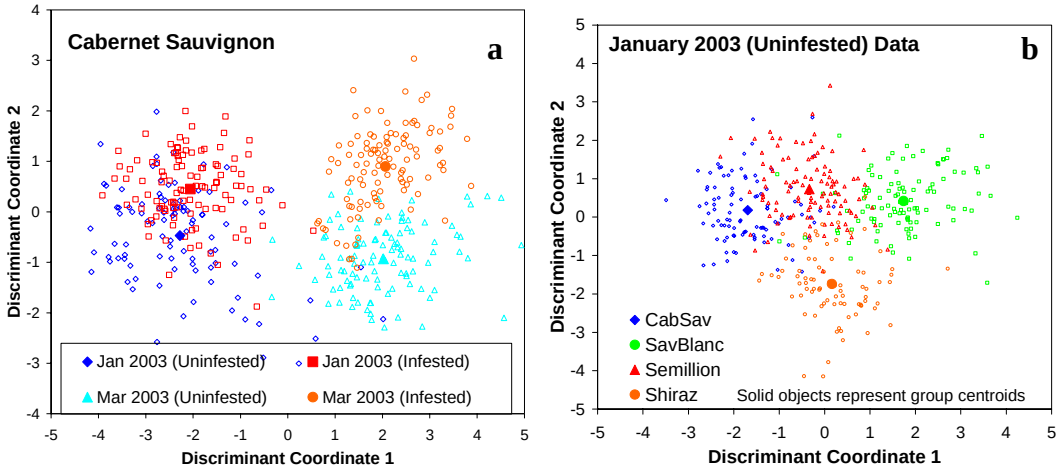


Figure 22: Discriminant plots of the first and second discriminant variables (coordinates) for some of the field-measured reflectance spectra. Small shapes represent individual spectra, group means are represented by the corresponding large solid shapes.

Figure 23 shows spectral separation of groups of reflectance spectra acquired in January 2005. The two varieties considered, Pinot Noir and Cabernet Sauvignon, are separated by the second discriminant variable, whereas the infestation levels are separated by the first discriminant variables.

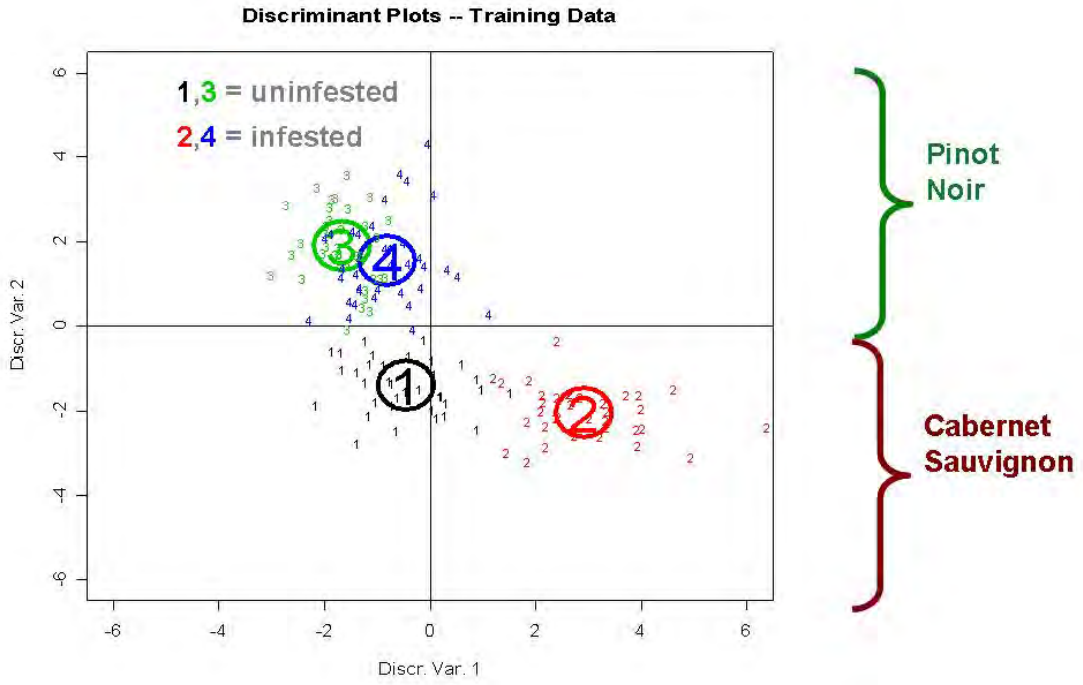


Figure 23: Discriminant plots of the reflectance spectra from phylloxera-infested and uninfested Pinot Noir and Cabernet Sauvignon vines acquired at the Buckland Valley and Upton field sites respectively in January 2005.

The phylloxera-infested Cabernet Sauvignon is quite clearly separated from the uninfested grapevines, however, there is some confusion between the infested and uninfested Pinot Noir. We speculate that this may be due to the respective lengths of time the grapevines have been infested with phylloxera, the relative virulence of the phylloxera genetic strains or that when sampled the grapevines were at different phenological stages due to differences in climatology and/or soil type between vineyards.

4.5 Results & Discussion - NMR and Chemical Fingerprinting

4.5.1 NMR Results - Introduction

Figure 24 shows a typical ^{1}H NMR spectrum of the dichloromethane extract of a grape leaf (Cabernet Sauvignon collected in March 2004). The spectrum is dominated by the resonances produced by protons from the lipid component of the extract, in particular the resonance centred at δ1.25 caused by the nearly equivalent protons of the methylene chain of fatty acids (either free or esterified), containing approximately 8 - 30 protons per fatty acid chain (depending on the chain length and degree of unsaturation).

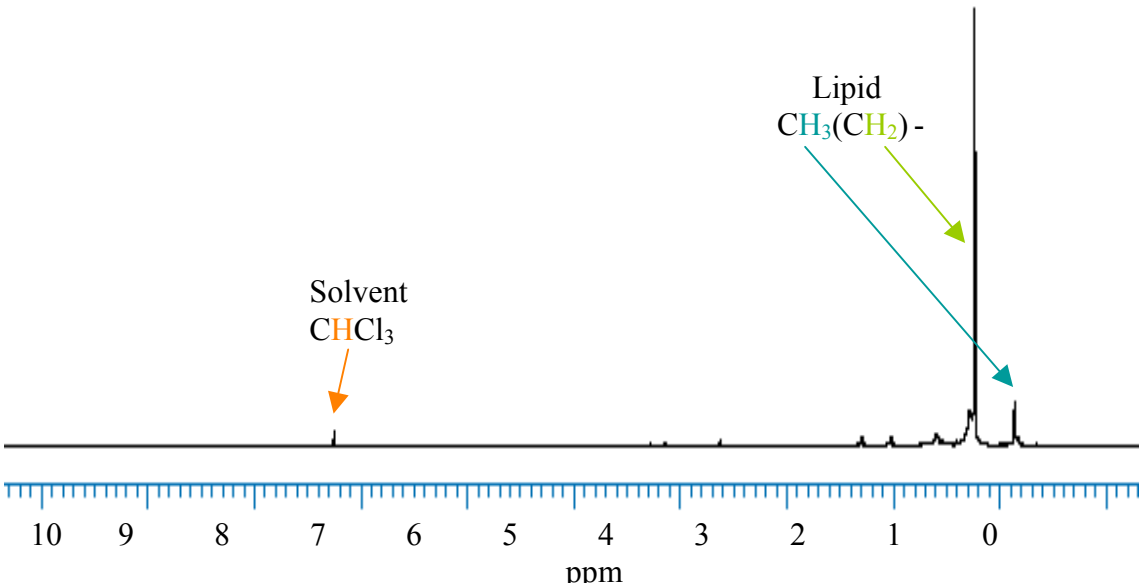


Figure 24: ^{1}H NMR spectrum of the dichloromethane extract of a Cabernet Sauvignon leaf

On expansion (vertically and horizontally) of the spectrum, a large number of additional resonances can be seen (Figure 25), including further lipid resonances but also resonances from other minor constituents of the extract. The intensity (and sometimes presence) of these minor resonances changes depending upon a large number of variables including grapevine variety, time of collection and phylloxera infestation status and it is these changes (followed by PCA) which were used to search for a fingerprint for phylloxera infestation.

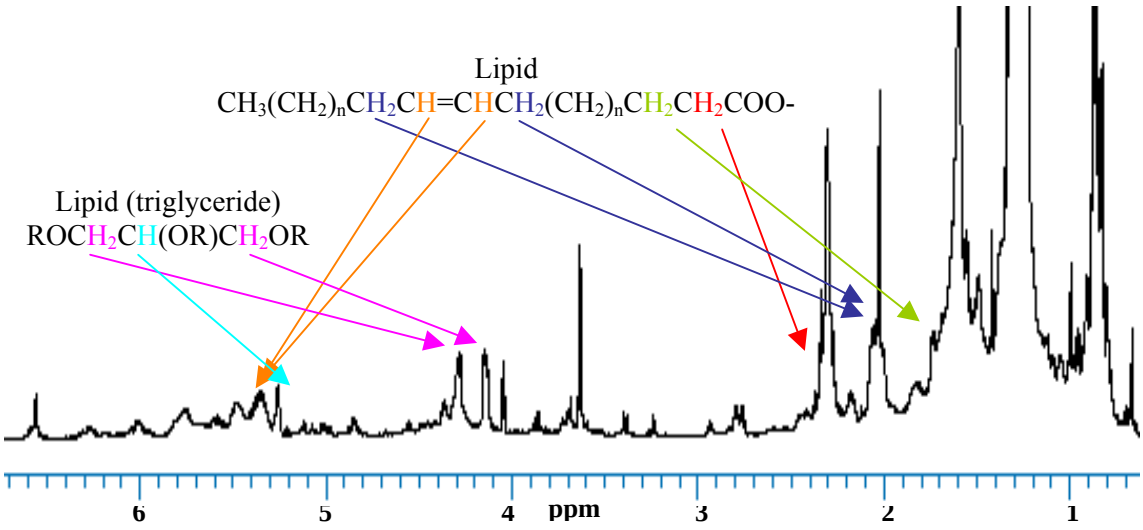


Figure 25: Expansion of the ^{1}H NMR spectrum of the DCM extract of a Cabernet Sauvignon leaf.

4.5.2 NMR Results - Upton

(Cabernet Sauvignon, Blocks 20 (uninfested) and 21 (infested))

4.5.2.1 November 2003

In this collection both large and small leaves were collected, as during collection of leaf samples it was observed that there was a marked difference in the colour of small leaves between infested grapevines (green leaves) and uninfested grapevines (pink leaves). There were no obvious visual differences between large leaves.

Figure 26 shows the PCA results for extracts from large leaves, which showed discernible differences between infested and uninfested grapevines. The scores plot illustrates that PC4 gives the greatest discrimination between the two classes, although three grapevines from the infested block (212126, 212110 and 212310) show borderline scores.

The loadings plot reveals that the sections of the spectrum which contribute to PC4 (in the direction of the uninfested grapevines) are 0.9 - 0.8, 1.7 - 1.6 and 1.6 - 1.5 ppm, containing the resonances for the terminal methyl and β-methylene of fatty acids. The bins corresponding to phylloxera infestation in PC4 are 5.4 – 5.3, 1.8 – 1.7 and 1.40 - 1.30 ppm. The bin at 5.4 - 5.3 ppm contains the resonance for the vinyl protons of unsaturated fatty acids, a broad multiplet centred at δ5.35, suggesting that infestation leads to an increase in the amount of unsaturated fatty acids or an increase in the degree of unsaturation. A comparison of the actual ^{1}H NMR spectra of all of the leaf extracts, in the region from δ2.9 - 0.1, reveals that the spectra from infested grapevines (with the exception of 212118 and 212110) have additional sharp singlets at δ1.35 and 1.76 (see Figure 27). The shape of the resonances suggest they are due to tertiary methyl groups, with the one at δ1.76 being attached to a double bond, while the relative sizes of the peaks implies that they may not belong to the same molecule.

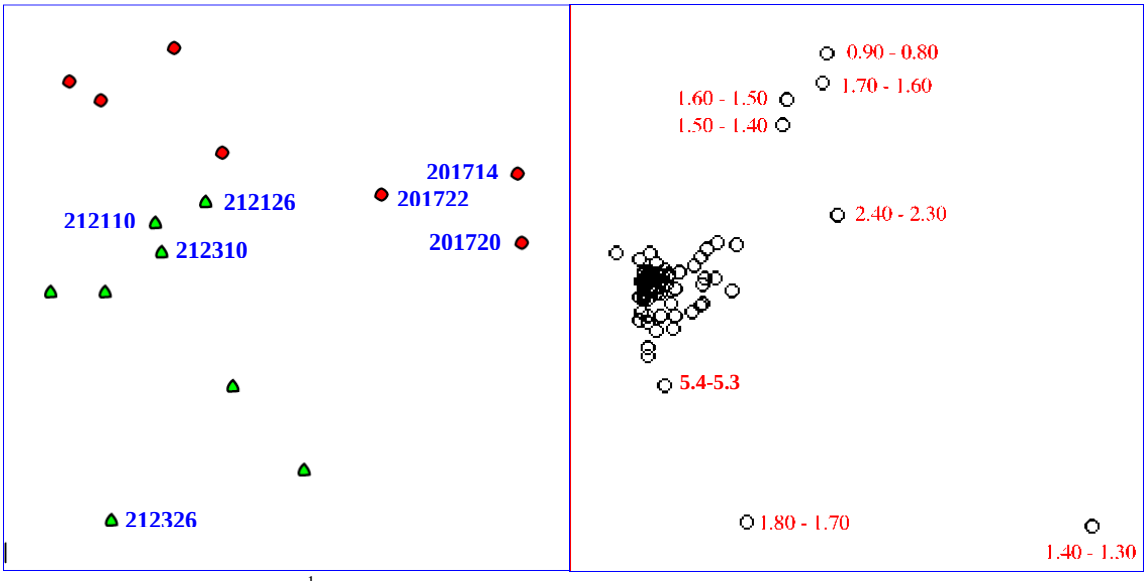


Figure 26: PCA results for ^{1}H NMR spectra (10-0 ppm range) of DCM extracts of leaves collected in November 2003, large mature leaves only.
Left: Scores plot (PC4 v PC1), red circles - uninfested vines; green triangles - infested vines.
Right: Loadings plot, influential regions of the ^{1}H NMR spectrum are labelled (in ppm) in red.

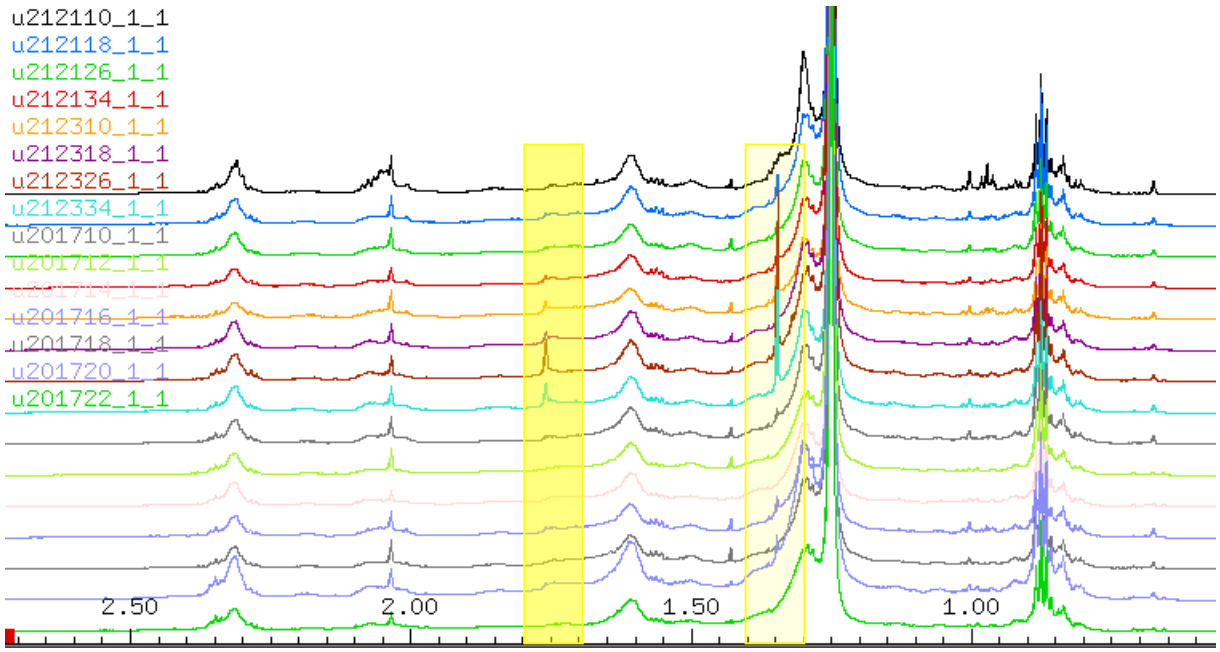
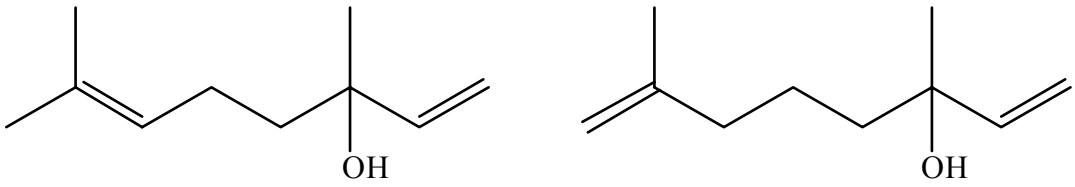


Figure 27: ^{1}H NMR spectra (2.9-0.1 ppm range) of DCM extracts of leaves collected in November 2003, mature leaves only. Yellow shaded areas indicate regions corresponding to the highest loadings for infestation in Figure 26.

As the shift of the resonance at δ1.76 suggested the presence of a double bond in the molecule, the region of the spectrum from δ7 to δ4 was investigated by PCA. This allowed the typical range for protons attached to double bonds (δ5 - 6) to be observed without the dominating effects of the lipid methylene resonances present in the full scale spectrum. In this case, PC3 best distinguishes between the infested and uninfested samples (see Figure 28). As in Figure 26, vine 212126 groups with the uninfested samples. The largest loadings for spectra of uninfested grapevines were from 5.4 - 5.3, corresponding to the vinyl protons of unsaturated fatty acids, while infested grapevines showed a number of additional vinyl protons resonances, indicated by the loadings plot and visible in the spectra (Figure 29). Close inspection of the spectrum of 212326 revealed the following resonances δ5.95 (dd J17.6, 10.8 Hz), 5.27 (br d J17.6 Hz), 5.21 (br d J10.8 Hz), 5.02 (br s), 4.98 (br s), all integrating for approximately one proton. The first three resonances suggested a similar coupling pattern to that shown by the terminal double bond of linalool (**1**), a common metabolite of a wide range of plant species, although the resonances were slightly shifted relative to those of linalool (δ5.90, 5.18 and 5.05) and lacked the vinyl multiplet belonging to the internal double bond.

Based on their chemical shift and their broad singlet shape, the additional two vinyl resonances could constitute a vinyl methylene group and the compound is tentatively assigned as α-linalool (3,7-dimethyl-1,7-octadien-3-ol) (**2**). α-linalool occurs less commonly than linalool but has been reported as a component of plant essential oils and as an aroma component of wine (Mallouchos *et al.* 2003, Kourkoutas *et al.* 2001). No NMR data for this compound was easily available for comparison and the assignment as α-linalool should be considered tentative.



1 (linalool) **2 (α-linalool)**

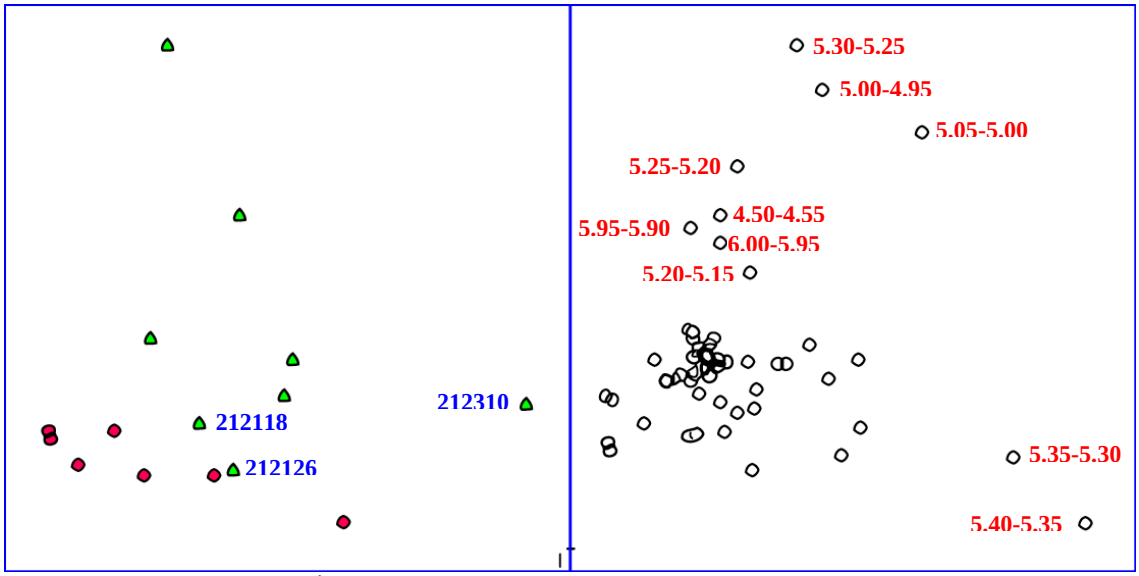


Figure 28: PCA results for ^{1}H NMR spectra (7-4 ppm range) of DCM extracts of leaves collected in November 2003, large mature leaves only.
Left: Scores plot (PC3 v PC2), red circles - uninfested vines; green triangles - infested vines.
Right: Loadings plot, influential regions of the ^{1}H NMR spectrum are labelled (in ppm) in red.

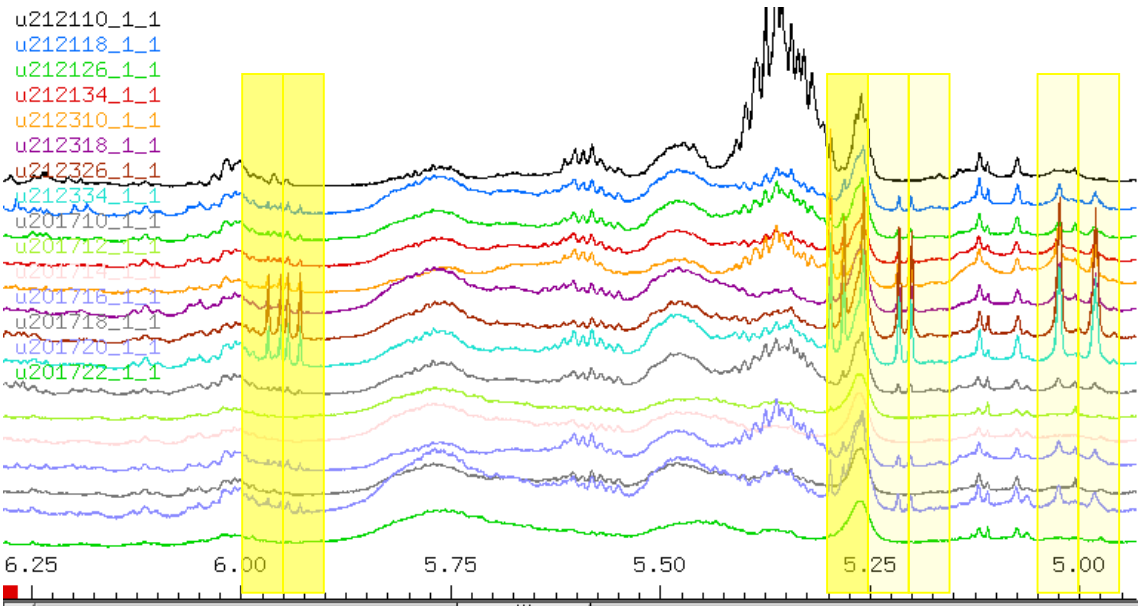


Figure 29: ^{1}H NMR spectra (6.25-5.00 ppm range) of DCM extracts of leaves collected in November 2003, mature leaves only. Yellow shaded areas indicate regions corresponding to the highest loadings for infestation in Figure 28**.**

Three grapevines (212126, 212110 and 212310) showed borderline scores in Figures 26 and 28 and although growing in Block 21, which is known to be phylloxera-infested, it seemed possible that these grapevines may not actually be infested or may have a lower degree of infestation. No counts of phylloxera populations on the roots of these grapevines during November 2003 were available to confirm this proposal. The phylloxera population on the roots of 212126 was counted in January 2004 and this grapevine was found to be heavily infested, although 212110 showed a much lower degree of infestation. In PCA analysis of NMR data from leaves collected in January 2004, 212126 clustered with infested grapevines (see next section).

Inspection of the spectra of the anomalous grapevines, 212126, 212110 and 212310, revealed that the extract of 212126 contained a small amount of α-linalool and 212310 contained a slightly larger amount. Thus their grouping close to the uninfested grapevines in the scores plots may be a result of a higher level of the compounds associated with the loadings for the uninfested grapevines rather than a lack of the compounds associated with infestation. However, 212110 showed no trace of α-linalool and 201710, 201716 and 201720 (uninfested grapevines) also contain trace amounts of this compound. The content of 201716 and 201720 was about roughly equal to that of 212126, the content of 212710 was less. Vine 201710 was found to be phylloxera free when checked in January 2004. By altering the binning to narrow the part of the spectrum observed to the range from δ5.23 to 4.95 (all other α-linalool resonances suffered overlap with those of other compounds) a PCA analysis reflecting essentially only the α-linalool concentration of each extract is achieved (see Figure 30). In this case PC1 gives the greatest differentiation between infested and uninfested grapevines. This method may prove a useful method of detecting infested grapevines or at least grapevines requiring close monitoring but this experiment must be repeated with a much larger sample of grapevines before the results can be regarded as reliable.

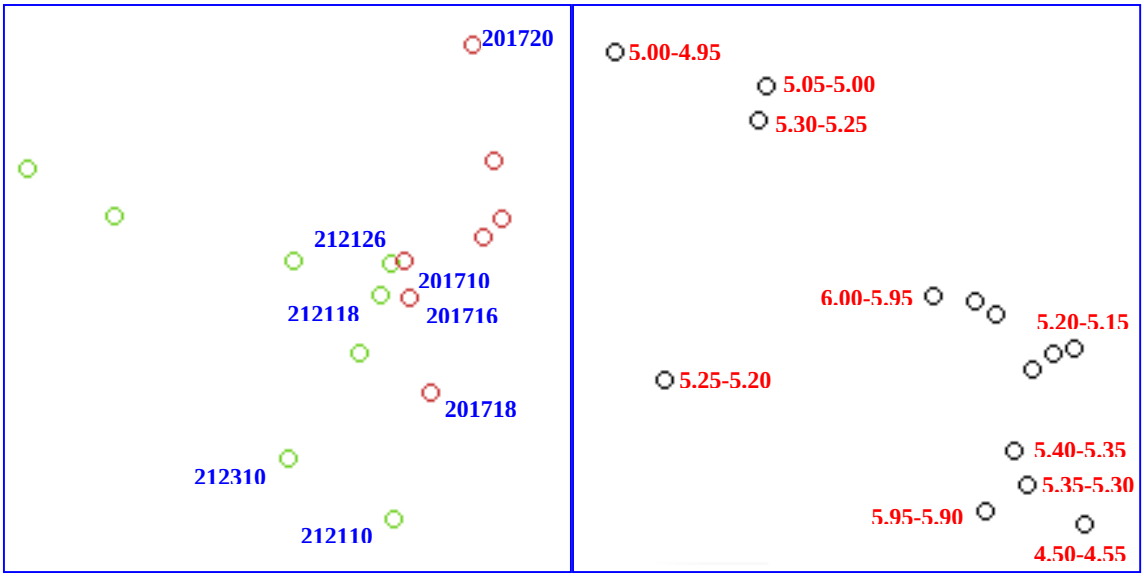


Figure 30: PCA results for ^{1}H NMR spectra (5.23 - 4.95 ppm range) of DCM extracts of leaves collected in November 2003, mature leaves only.
Left: Scores plot (PC2 v PC1), red circles - uninfested vines; green circles - infested vines.
Right: Loadings plot, influential regions of the ^{1}H NMR spectrum are labelled (in ppm) in red.

In the case of small leaves, PC3 produces some division between infested and uninfested grapevines (see Figure 31) with 212126 again grouping with uninfested grapevines and 212110 and 212310 being near the borderline. The major loadings for infestation were δ5.3 - 5.2, δ5.4 - 5.3 and δ0.9 - 0.8, while δ2.4 - 2.3 was the major loading for uninfested grapevines. Resonances in the region from δ5.3 - 5.2 are produced by the vinyl protons of a large range of terpenoids (and other compounds) and a definite assignment was not possible. The resonance from δ5.4 - 5.3 can be attributed to the vinyl protons of unsaturated fatty acids, while 2.4 - 2.3 is due to the α- methylene protons of all fatty acids. This suggests that infestation was associated with an increase in the proportion of unsaturated acids (or the degree of unsaturation) in the lipids of the small leaves. No spectra of small leaves showed any appreciable amount of α-linalool, although 212326, which had the largest proportion of α-linalool in the large leaves, did show trace amounts.

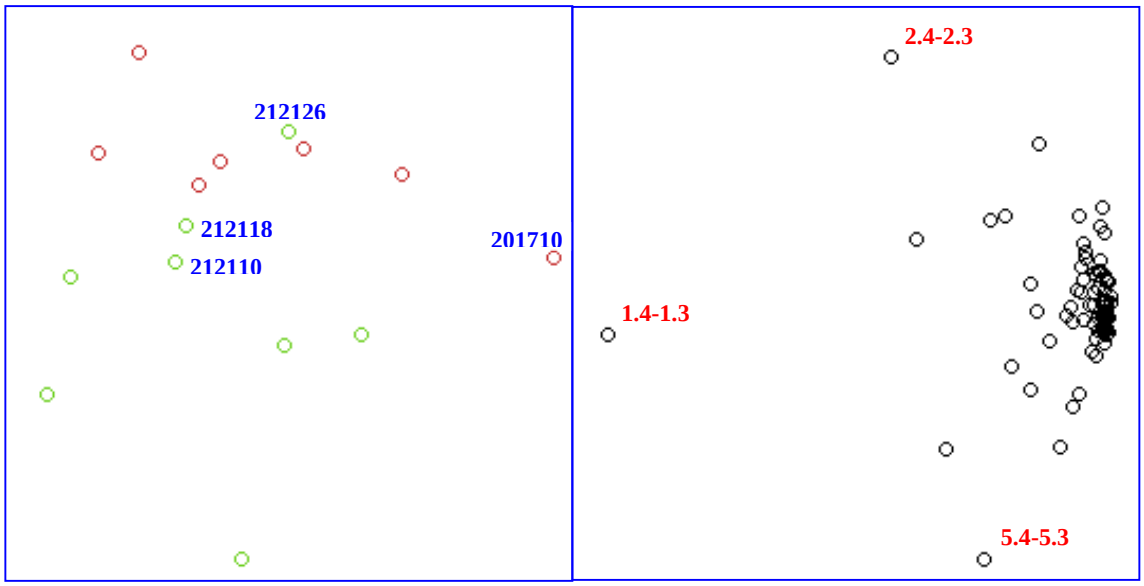


Figure 31: PCA results for ^{1}H NMR spectra (10-0 ppm range) of DCM extracts of leaves collected in November 2003, small leaves only.
Left: Scores plot (PC3 v PC1), red circles - uninfested vines; green triangles - infested vines.
Right: Loadings plot, influential regions of the ^{1}H NMR spectrum are labelled (in ppm) in red.

As the small uninfested leaves change from pink to green as they mature, it seemed possible that the small infested leaves, which were green, were older than uninfested leaves of a corresponding size and that the phylloxera infestation was slowing the rate of growth of the leaves. To investigate this, PCA of the spectra of both large and small leaves was carried out (see Figure 32). It can be seen that the small leaves cluster separately from the large leaves but the infested small leaves do show a tendency to be closer to the large leaves, suggesting that they may in fact be older than uninfested leaves of the same size and hence the difference seen in Figure 31 may be a reflection of the age of the leaves, rather than directly indicating infestation. This is supported by the loadings plot where two of the major loadings for the large leaves, 5.4 - 5.3 and

2.1 - 2.0, indicate a greater amount of unsaturation in the fatty acids, the same differentiator as proposed for infestation in small leaves. The bins that contributed to this differentiation by leaf size, 1.8 - 1.7, 1.7 - 1.6 and 1.6 - 1.5 were removed from the PCA calculation, resulting in PC4 discriminating between infested and uninfested grapevines for small leaves (see Figure 33). The major loading for infestation in PC4 was 0.9 - 0.8. Inspection of the spectra revealed that the only major peak in this region is the approximate triplet due to the terminal methyl of fatty acids. As the integrals for each bin are scaled relative to that of the largest bin, the lipid methylene peak, this implies an increase in the ratio of the terminal methyl to the chain methylenes, i.e. a decrease in chain length. As this distinction relies on changes in the intensity of a peak that is present in all spectra (infested and uninfested) rather than the presence or absence of a characteristic peak, it is unlikely to provide a useful marker for infestation. Small leaves were not investigated in subsequent collections.

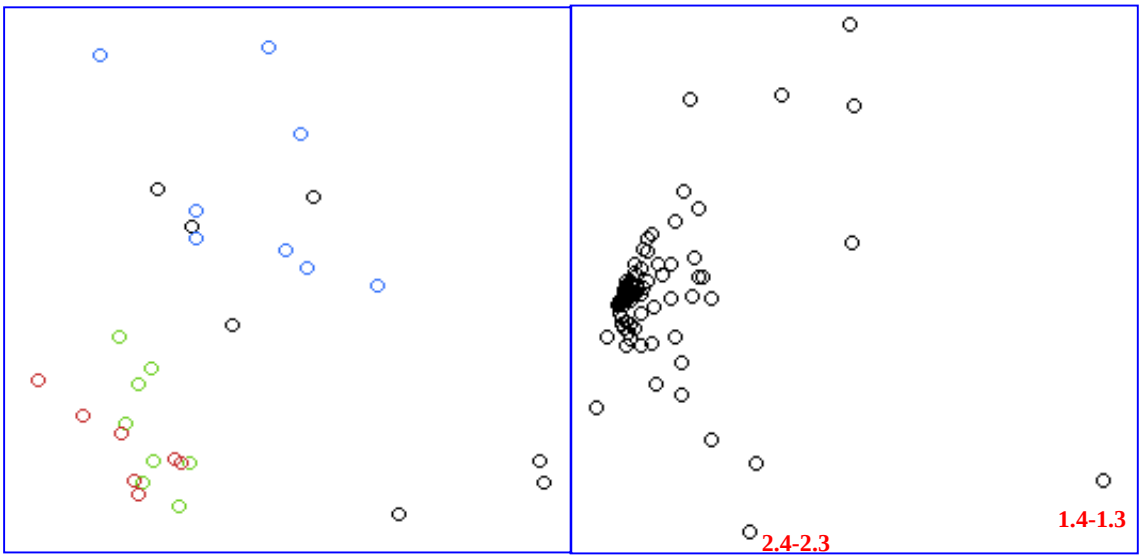


Figure 32: PCA results for ^{1}H NMR spectra (10-0 ppm range) of DCM extracts of leaves collected in November 2003, both large and small leaves.
Left: Scores plot (PC2 v PC1), small leaves: red circles - uninfested, green circles - infested vines; large leaves: black circles - uninfested, blue circles - infested vines.
Right: Loadings plot, influential regions of the ^{1}H NMR spectrum are labelled (in ppm) in red.

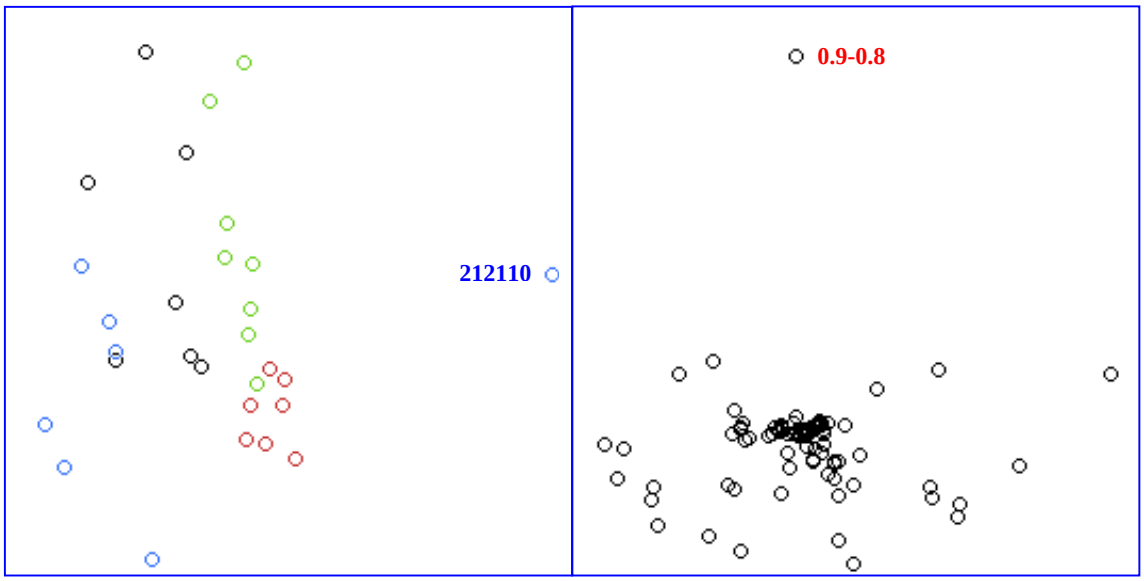


Figure 33: PCA results for NMR spectra (10-0 ppm range, excluding 1.8 – 1.3 ppm) of DCM extracts of leaves collected in November 2003, both large and small leaves.
Left: Scores plot (PC4 v PC3), small leaves: red circles - uninfested, green circles - infested vines; large leaves: black circles - uninfested, blue circles - infested vines.
Right: Loadings plot, influential regions of the ^{1}H NMR spectrum are labelled (in ppm) in red.

4.5.2.2 January 2004

The PCA scores plot for the ^{1}H NMR spectra of extracts of leaves collected in January 2004 shows close clustering of the uninfested grapevines and reasonable distinction from infested grapevines (see Figure 34). Some grapevines are separated using PC1 but the majority is distinguished via PC3. The major loadings are 1.7 - 1.6, 2.1 - 2.0 and 1.6 - 1.5 for PC1 and 1.8 - 1.7 and 2.2 - 2.1 for PC3. ^{1}H NMR spectra of 212326 and 211724 (large influence on PC1) were compared with the spectrum of 201708 (known to be uninfested by field survey of roots in January 2004) to investigate the resonances corresponding to these loadings (see Figure 35), as were spectra of 211708 (large effect of PC1 and PC3) and 212118 (large PC3, small PC1) (see Figure 36).

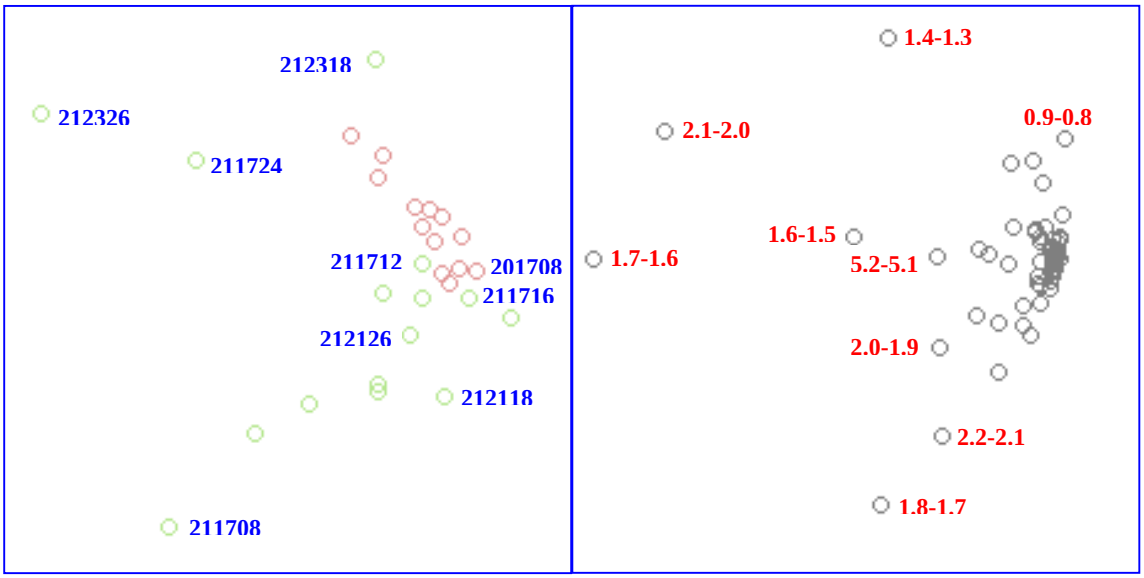


Figure 34: PCA results for NMR spectra (10-0 ppm range) of DCM extracts of leaves collected in January 2004.
Left: Scores plot (PC3 v PC1), red circles - uninfested vines, green circles - infested vines.
Right: Loadings plot, influential regions of the ^{1}H NMR spectrum are labelled (in ppm) in red.

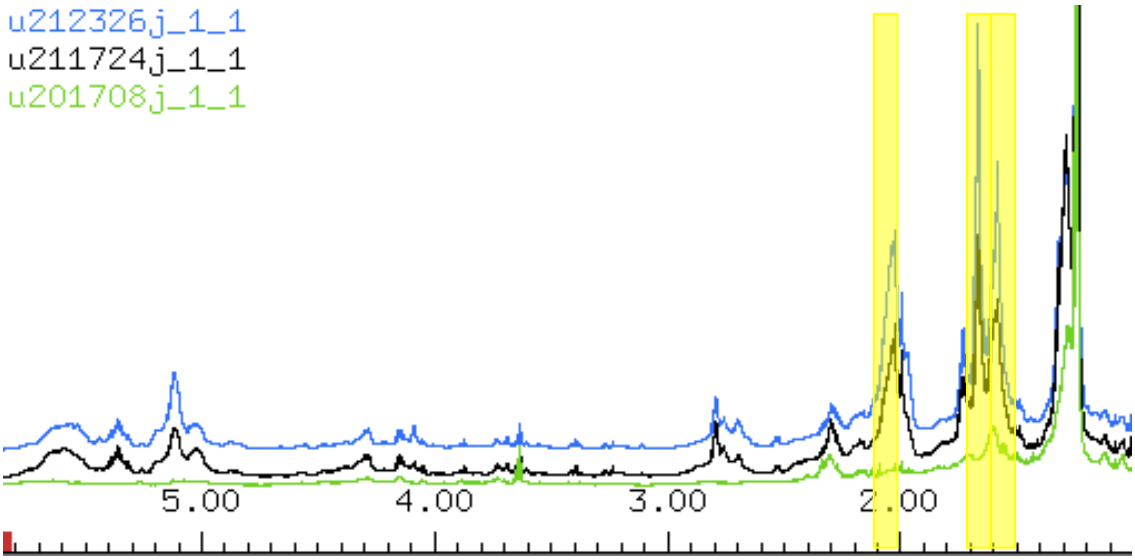


Figure 35: Some ^{1}H NMR spectra of DCM extracts of leaves collected in January 2004. Yellow shaded areas indicate regions corresponding to the highest loadings for PC1 in Figure 34.

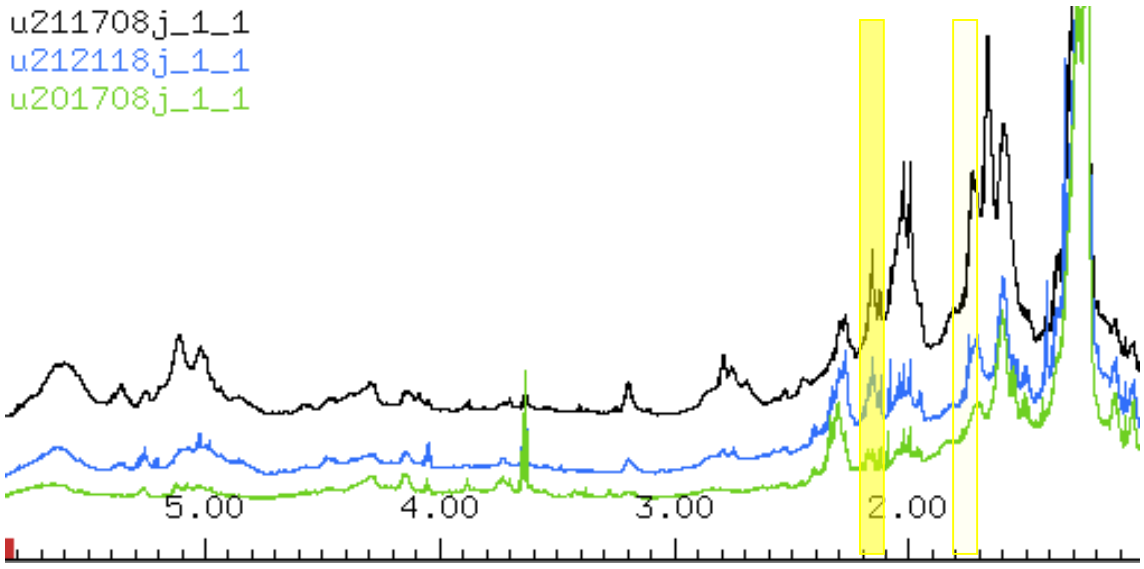
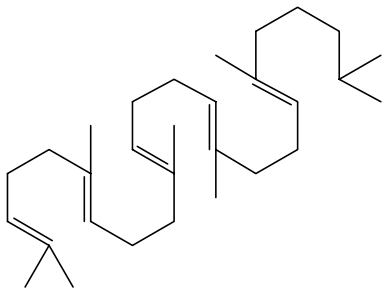


Figure 36: Some ^{1}H NMR spectra of DCM extracts of leaves collected in January 2004. Yellow shaded areas indicate regions corresponding to the highest loadings for PC3 in Figure 34.

From Figure 35, it can be seen that the major differences in the spectrum of 212326 (relative to that of 201708) are the presence of two sharp singlet resonances at δ1.68 and 1.60 (assignable as methyl groups attached to double bonds) and broad peaks at δ2.03 (methylene next to double bond) and δ5.12 (proton attached to a double bond). This information suggested that the additional compound might be squalene (**3**). This was confirmed by comparison with literature values of the ^{1}H NMR spectrum of this compound (δ1.67, 1.59, 5.11, 2.07, 1.98) (Sobolev *et al.* 2005).



3 (squalene)

Additional peaks in 211708 (Figure 36) are at δ1.73, 2.16, 2.80, 3.21, 5.02 and 5.38.

The resonance at δ2.80 is due to the bis - allylic methylene protons of linolenic acid (there is also a peak at δ2.77 due to the corresponding protons of linoleic acid), while the peak at δ5.38 is due to the vinyl protons of the unsaturated fatty acids. As found for the November 2003 data, this indicates that phylloxera infestation causes an increase in the amount of unsaturated acids in the extract.

The small resonance at δ5.29 (visible in 201708 as well) is due to the sn2 proton of glycerol, in the form of triglycerides. For the triglyceride with three linolenic acid residues, this should have an intensity one eighteenth of that of the double bond protons,

while for triolein the ratio would be one sixth. As this ratio appears to be roughly one half in 211708 (this figure is very approximate due to the difficulty of achieving accurate integrals because of the overlap of peaks in this region of the spectrum), this would suggest that all the fatty acids in this extract (and probably all the other extracts as well) are in the form of triglycerides and that saturated acids constitute a considerable proportion of the total fatty acids.

Koussa *et al.* (2002) conducted an investigation (utilising gas chromatography to quantify the individual fatty acids) into the effects on the fatty acid profile caused by eutypiose, a disease caused by infection with the fungus, *Eutypa lata*. They measured levels of fatty acids for infected and uninfected grapevines (Cabernet Sauvignon) at three stages of the growing season and found that the level of unsaturation decreased upon infection (see Table 13), the opposite result to that suggested in this work for infestation by phylloxera. They proposed that water stress caused by eutypiose led to increased levels of abscisic acid, which in turn altered the lipid metabolism. As water stress seems a likely effect of phylloxera infestation due to the impact of reduced water uptake from the damaged root system, it seems unusual that this study should show opposite results but may indicate that there are other metabolic changes being caused by phylloxera in addition to a response to water stress. Koussa *et al.* did find an increase in the linoleic acid content upon infection and hence an increase in the linoleic/linolenic acid ratios. This also appears to be the case with phylloxera infestation. However, the ^{1}H NMR spectra exhibited a great deal of variability in the amount of unsaturation, with respect to both the vinyl proton resonance (δ5.32) and the linolenic acid methylene resonance (δ2.80), for both infested and uninfested grapevines. Furthermore, Koussa *et al.* found that the lipid profile changes during the growing season, an observation also made during this work (see Section 4.5.2.4). Because of the large variation in lipid profiles between individuals and the additional complication of variation induced by other factors, including the stage of the growing season and water status of the grapevine, it would be difficult to define a normal value for the lipid profile of a grapevine. Hence change in the lipid profile, although an interesting response to phylloxera infestation, seems unlikely to prove a useful indicator for determining phylloxera status although use of the linolenic/linoleic acid ratio warrants further investigation.

Table 13: Effect of Eutypa on water content, ABA and fatty acids in leaves of cv. Cabernet Sauvignon at three stages; buds (BF), flowering (F) and closed clusters (FG) (S: healthy; A.S.: apparently healthy; M: diseased; MS: dry weight; C18 = C18:0 + C18:1 + C18:2 + C18:3) from Koussa et al. (2002).

Stades (stages)		BF			Fl			FG	
Etat (State)	S	Ap. S	M	S	Ap. S	M	S	Ap. S	M
Eau (Water) %	77.0	76.0	75.3	77.8	77.0	75.3	69.0	68.0	65.0
ABA (mg 100 g^{-1} MS)	22.4	28.2	28.0	12.4	18.3	24.5	15.6	28.9	45.3
Teneurs (Contents):									
AGS (mg g^{-1})	6.4	7.3	7.7	5.6	4.8	6.4	4.2	4.2	4.6
AGI (mg g^{-1})	19.1	21.4	22.5	23.1	18.4	17.9	15.0	13.2	11.6
AGT (mg g^{-1})	25.4	28.7	30.2	28.7	23.3	24.3	19.2	17.5	16.1
Proportions (%):									
C16 :0	20.5	22.1	22.4	17.0	17.6	22.0	19.0	20.4	21.8
C18 :0	2.6	2.4	2.3	1.9	2.4	3.7	2.2	3.0	5.2
C20 :0	2.0	0.9	0.8	0.6	0.8	0.7	0.5	0.9	1.3
C18 :1	4.1	3.6	2.7	3.5	2.9	3.3	4.0	3.0	3.5
C18 :2	21.3	23.4	24.8	15.7	19.8	22.1	8.4	12.0	14.7
C18 :3	49.5	47.6	47.0	61.4	56.5	48.2	65.8	60.7	53.4
Rapports (Ratios):									
AGS/AGI	0.3	0.3	0.3	0.2	0.3	0.4	0.3	0.3	0.4
C16 :0/C18	0.3	0.3	0.3	0.2	0.2	0.3	0.2	0.3	0.3
C18 :0/C18 :1	0.6	0.7	0.9	0.6	0.8	1.1	0.6	1.0	1.5
C18 :1/C18 :2	0.2	0.2	0.1	0.2	0.2	0.2	0.5	0.3	0.2
C18 :2/C18 :3	0.4	0.5	0.5	0.3	0.4	0.5	0.2	0.2	0.3

In order to search for indications of infestation other than changes in the lipid profile, the region of the spectra from δ4 - 3, which is largely free of lipid resonances, was investigated. One resonance, a triplet centred at δ3.64, due to the α-methylene protons of a long chain alcohol, which was present in all the spectra, was removed by excluding the bins from 3.66 to 3.62 from the PCA calculation. In this case the scores plot (see Figure 37) shows reasonable separation of the infested and uninfested grapevines based on a combination of PC1 and PC2.

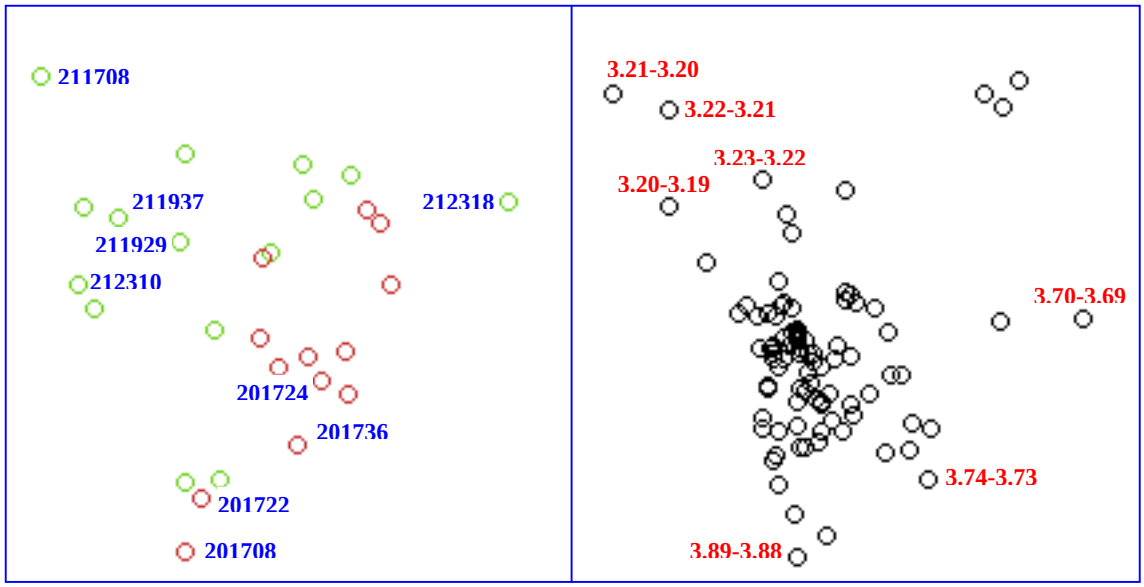


Figure 37: PCA results for ^{1}H NMR spectra (4 - 3 ppm range) of DCM extracts of leaves collected in January 2004.
Left: Scores plot (PC2 v PC1), red circles - uninfested vines, green circles - infested vines.
Right: Loadings plot, influential regions of the ^{1}H NMR spectrum are labelled (in ppm) in red.

The loadings plot in Figure 37 reveals that the loadings reflecting infestation range from 3.19 - 3.22, while for uninfested grapevines the major loadings centre around 3.74 and 3.88. This is illustrated in Figure 38, which shows the ^{1}H NMR spectra of some of the extracts. It is not possible to ascertain which compounds are associated with these changes in the NMR spectrum or if the new peak at δ3.21 is due to part of the same molecule as the other additional resonances (at δ1.73, 2.16, 2.80, 5.02 and 5.38) found in the spectrum of 211708 (Figure 35).

Isolation of the compound(s) by preparative chromatography followed by structural elucidation by NMR spectroscopy of the purified compound(s) should be attempted, as it may provide another potential marker for infestation.

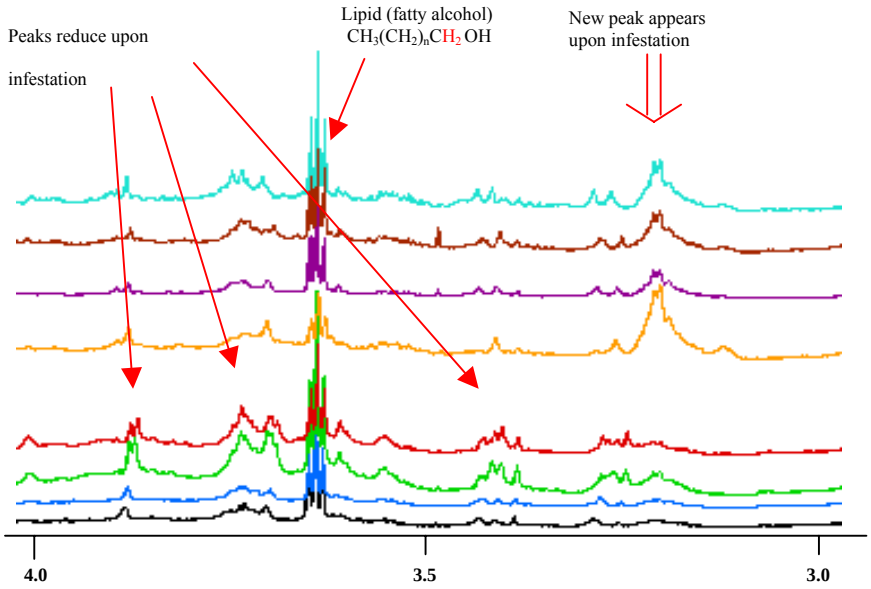


Figure 38: Some ^{1}H NMR spectra (δ4 - 3) of DCM extracts of leaves collected in January 2004. The samples are (from the top) 212310, 211929, 211937, 211708, 201724, 201736, 201722 and 201708.

Some of the infested grapevines showed the presence of α-linalool but a binning plan to produce PCA results reflecting the α-linalool concentration, as was used for the November 2003 data (Figure 30), was not feasible in this case because of the overlap with other much larger peaks in the range δ5.23 - 4.95. Although in the case of infested grapevines the α-linalool resonance centred at δ5.95 was free from overlap, for uninfested grapevines an additional resonance was present in many cases, preventing the use of this region as well. Instead the presence or absence of α-linalool was determined by direct observation of the spectra (see Figures 39 and 40).

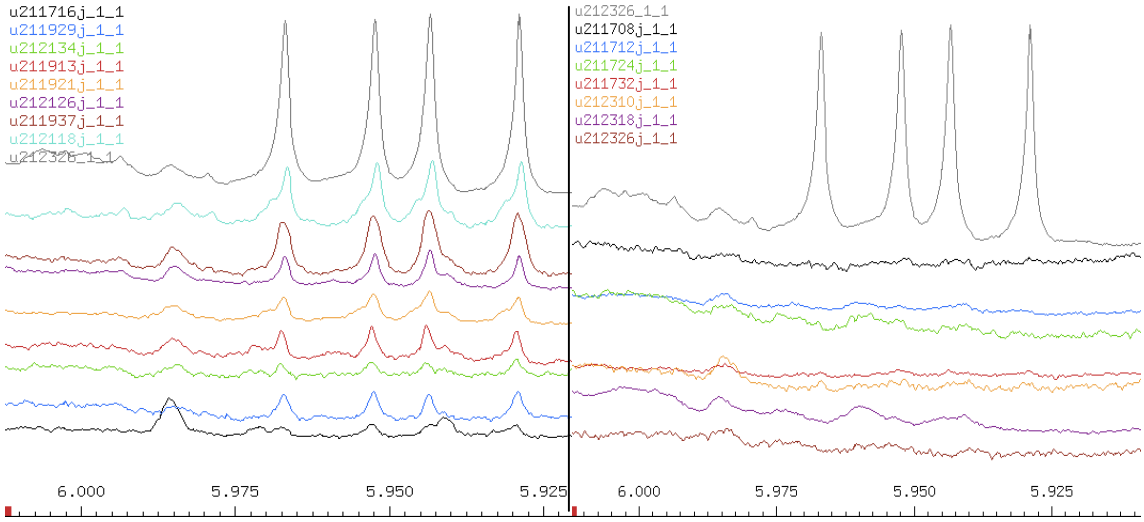


Figure 39: ^{1}H NMR spectra (δ6.0 - 5.92) of DCM extracts of infested leaves collected in Jan. 2004.
Left: Spectra showing the presence of α-linalool.
Right: Spectra with no α-linalool.
The top spectrum in each case is 212326 collected in Nov. 2003, to illustrate α-linalool resonances.

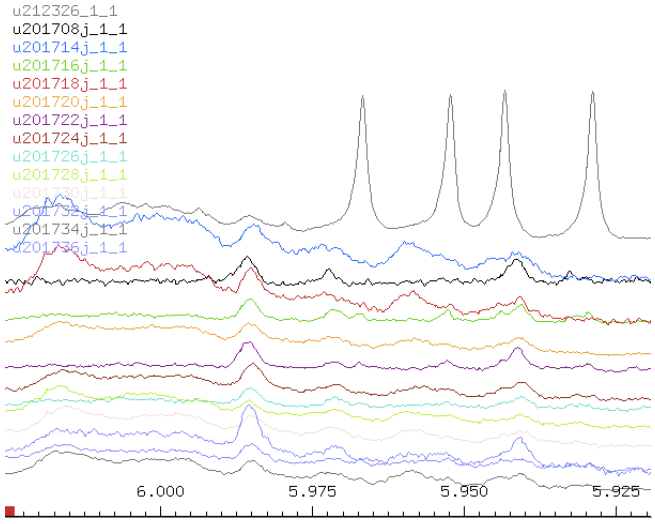


Figure 40: ^{1}H NMR spectra (δ6.0 - 5.92) of DCM extracts of uninfested leaves collected in January 2004. The top spectrum is an infested sample, 212326, collected in November 2003, to illustrate α-linalool resonances.

Among the infested grapevines that showed no presence of α-linalool were 212326 and 211724, the grapevines that showed the greatest score for PC1 in Figure 34. Thus, if the presence of α-linalool is truly an indicator of phylloxera infestation, this suggests that PC1 does not reflect phylloxera status and hence the squalene content of these grapevines is not related to phylloxera infestation. This was proven to be the case, as in the March 2004 collection all grapevines showed the presence of squalene (see next section). Interestingly, 212326 was the grapevine which showed the highest α-linalool concentration of those measured in November, 2003 (211724 was not measured at that time) and it seems possible that if α-linalool production is indeed a response to

phylloxera infestation, it may be only a transient one. Similarly, 211708, which showed the highest score for PC3 in Figure 34, also showed no α-linalool although 211929, which had the second highest score, did. In general there appeared to be no correlation between the scores for PC3 and the presence of α-linalool in the extract. However, of the grapevines that showed no α-linalool, three had shown α-linalool in November 2003 and none of the others had been investigated then. It seems possible that production of α-linalool may take place early in the growing season and the compound responsible for PC3 is produced later in the season (there was no peak at δ3.21 present in any of the spectra of extracts from November 2003).

4.5.2.3 March 2004

PCA analysis of the NMR data from the March 2004 collection of grapevine leaves produced only limited distinction between infested and uninfested grapevines when the full ^{1}H NMR spectrum (10 - 0 ppm) was examined. However by reducing the spectral range that was binned to 10 - 5 ppm, reasonable separation between the two classes was achieved (see Figure 41). The major loadings for the uninfested grapevines were from 5.4 - 5.3 ppm due to vinyl protons of unsaturated acids, the opposite trend to that which had been found for collections in November 2003 and January 2004, where the amount of unsaturation increased with infestation. The major loadings for the infested grapevines were due to an increase in intensity of very broad peaks at δ5.6 - 5.5, 5.22 - 5.18 and 5.07 - 4.98. All of these resonances were present in the uninfested grapevines as well and so would make a less useful marker. All spectra of grapevines collected in March 2004 showed intense peaks corresponding to squalene.

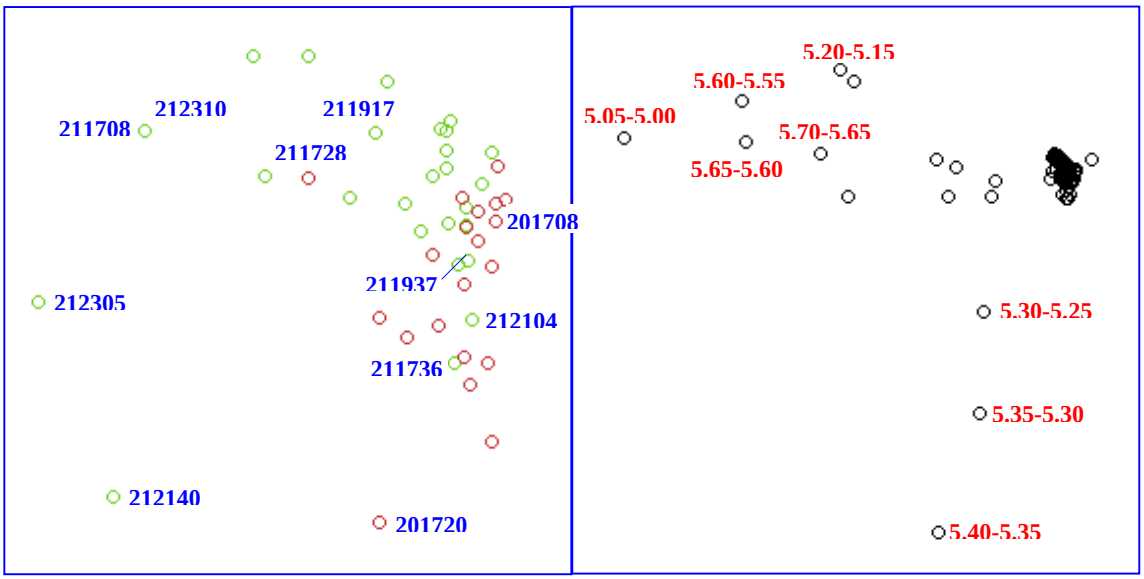


Figure 41: PCA results for ^{1}H NMR spectra (10 - 5 ppm range) of DCM extracts of leaves collected in March 2004.
Left: Scores plot (PC2 v PC1), red circles - uninfested vines, green circles - infested vines.
Right: Loadings plot, influential regions of the ^{1}H NMR spectrum are labelled (in ppm) in red.

By restricting the binning to the part of the spectrum from 7 - 6 ppm, a slightly better separation was achieved (see Figure 42). Observation of the loadings plot and the spectra (see Figure 43) reveal that the major effect of infestation is an increase in a peak

at δ6.49. This peak was present to a lesser degree in uninfested grapevines as well. For uninfested grapevines one of the major loadings was due to a peak at δ6.37, which was substantially decreased in intensity and often missing in infested grapevines. A reinvestigation of spectra from January 2004 showed that this peak was present in uninfested grapevines and also much reduced in infested grapevines during this period as well. Investigation of the structure of the compound responsible for this resonance should be carried out, as low or zero levels of this compound may be an indicator of infestation.

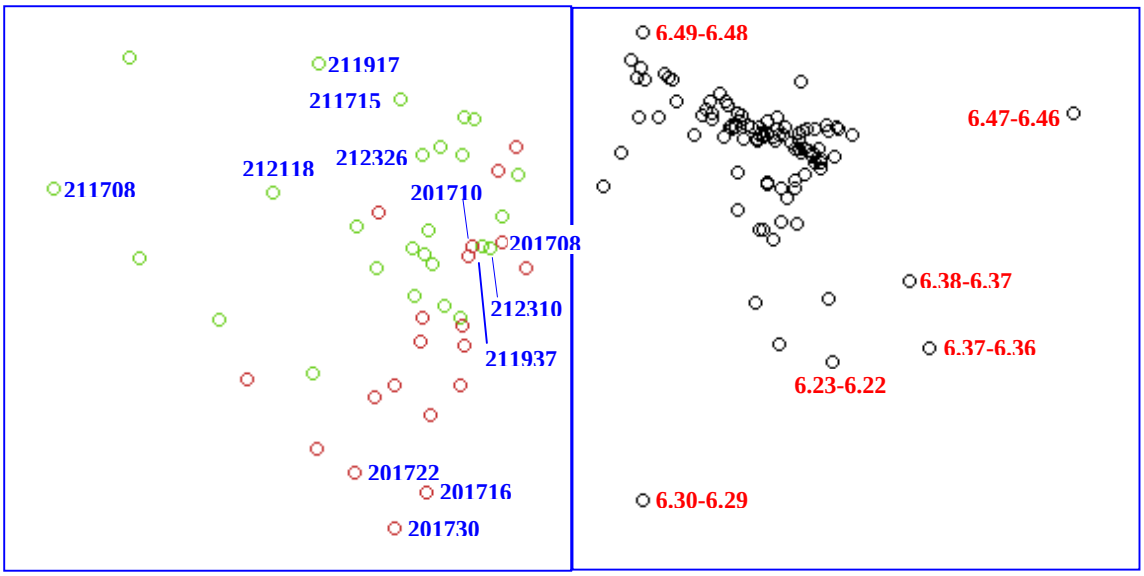


Figure 42: PCA results for ^{1}H NMR spectra (7 - 6 ppm range) of DCM extracts of leaves collected in March 2004.
Left: Scores plot (PC2 v PC1), red circles - uninfested vines, green circles - infested vines.
Right: Loadings plot, influential regions of the ^{1}H NMR spectrum are labelled (in ppm) in red.

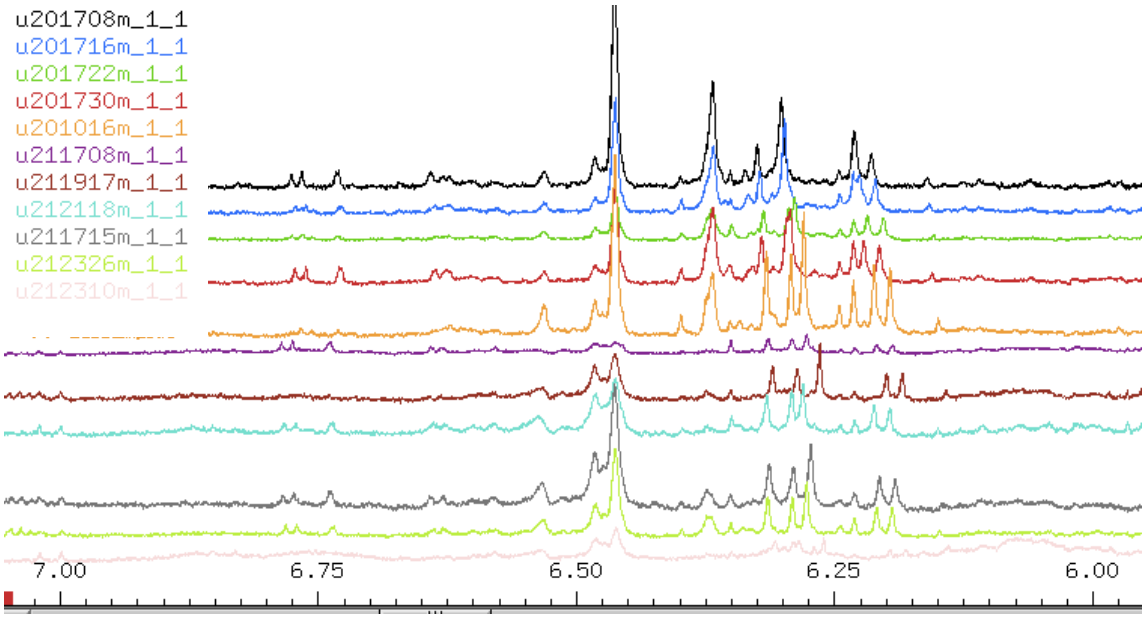


Figure 43: Some ^{1}H NMR spectra (δ7.0 - 6.0) of DCM extracts of leaves collected in March 2004. The top five spectra represent uninfested grapevines and the bottom five infested grapevines.

The ratio of linoleic/linolenic acids was also investigated for this collection and again found to be larger for infested grapevines (see Figure 44). The loadings plot (not shown) associated with the scores plot shown in Figure 44 indicated that the major loadings for PC1 were 2.81 - 2.80 (linolenic acid) for uninfested and 2.78 - 2.77 and 2.77 - 2.76 (linoleic acid) for infested grapevines.

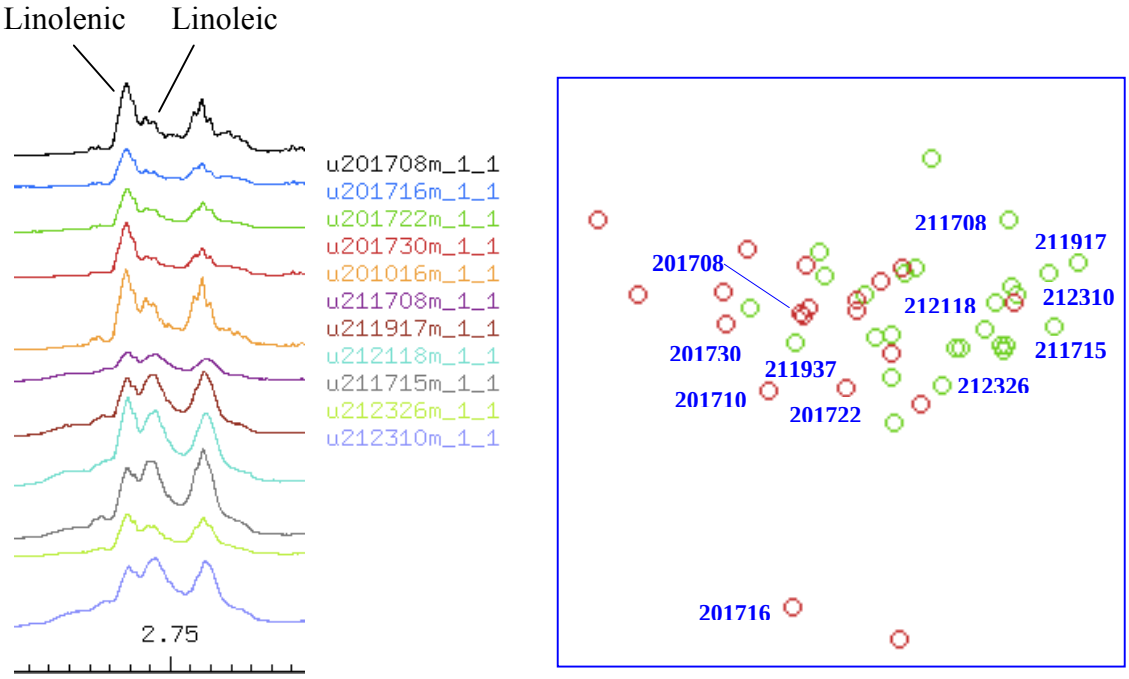


Figure 44: Left: Some ^{1}H NMR spectra (δ2.95 - 2.55) of extracts of leaves collected in March 2004. Right: PCA results for ^{1}H NMR spectra (δ2.82 - 2.76) of extracts of leaves collected in March 2004 - Scores plot (PC2 v PC1), red circles - uninfested vines, green circles - infested vines.

4.5.2.4 Variation in extracts during growing season

As noted earlier there was a substantial change in the metabolite profile of the extracts throughout the growing season. This is illustrated in Figure 45, which shows distinct clustering for each collection. The loadings indicate that the major difference between the November 2003 and January 2004 collections is the chain length and degree of unsaturation of the fatty acids (the ratio of δ1.32 to δ1.25 is a measure of the amount of unsaturated acids present, the ratio of δ1.25 to δ0.88 reflects chain length), whereas for January and March 2004 the squalene content is the important distinguishing factor. The March data is more diverse, perhaps because of the larger sample size but probably also because the longer time of growth has allowed differences in individual vigour, microclimate and soil to have a greater effect. Even in this PCA plot, which is dominated by the effects of the time of the growing season, there appears to be some discernible effects of infestation. The infested grapevines from January show a trend to be closer to the March data, possibly indicating an acceleration of the ageing process. There is also some separation of the March data, possibly reflecting a change in the unsaturation of the fatty acids.

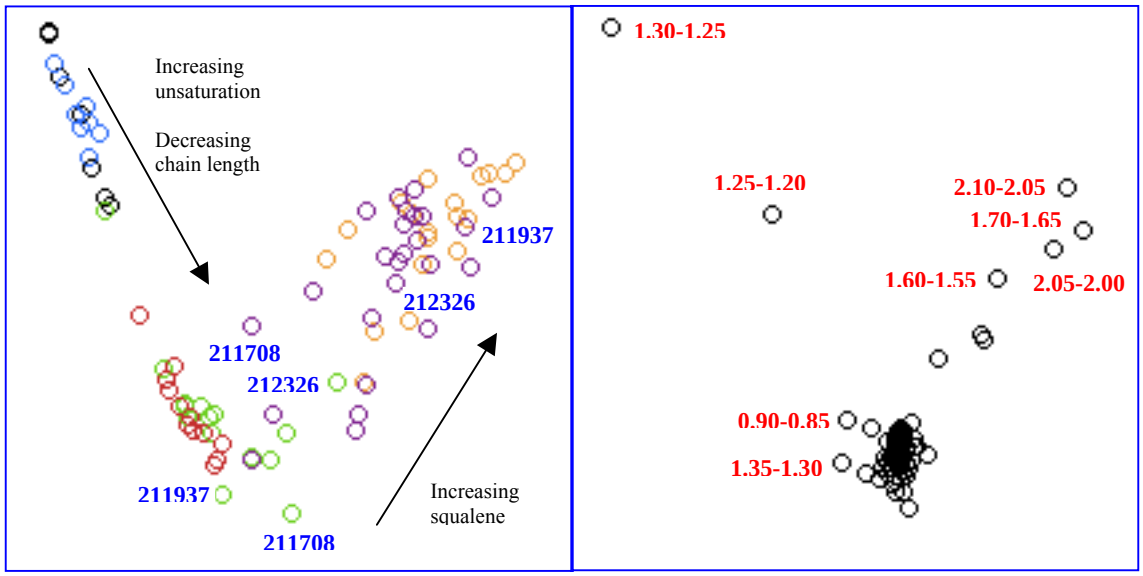


Figure 45: PCA results for ^{1}H NMR spectra (10 - 0 ppm range) of DCM extracts of all leaves collected in 2003 / 2004.
Left: Scores plot (PC2 v PC1), black circles - uninfested vines, blue circles - infested vines, Nov. 2003, red circles - uninfested vines, green circles - infested vines, January 2004,
orange circles - uninfested vines, purple circles - infested vines, March 2004.
Right: Loadings plot, influential regions of the ^{1}H NMR spectrum are labelled (in ppm) in red.

Since the results from the November 2003 collection had shown promise but were based on only a small sample size, further leaves from that collection were processed approximately 5 months after the first batch. When the NMR spectra from the second batch were included in the PCA, they were found to vary considerably from the initial data (see Figure 46). The second batch clustered more closely with the January 2004 data with respect to PC2 but with the original November 2003 data with respect to PC1. The loadings from PC1 suggest that it is reflecting an increase in squalene content and unsaturation, those of PC2 reflect a change in chain length. As all of the leaves collected were dried at 45^{o}, the changes taking place after collection would be limited to decomposition reactions rather than metabolic processes. It seems likely that the apparent decrease in chain length is a result of some decomposition of unsaturated acids due to aerial oxidation, resulting in an increase in the ratio of C16 to C18 acids, as the C16 acid content of Cabernet Sauvignon leaves is virtually all saturated (palmitic) acid (Koussa *et al.*, 2002) and hence not as susceptible to oxidative degradation.

Thus it is important that all samples should be processed as quickly as possible after collection and only data collected from extracts prepared at the same time should be compared.

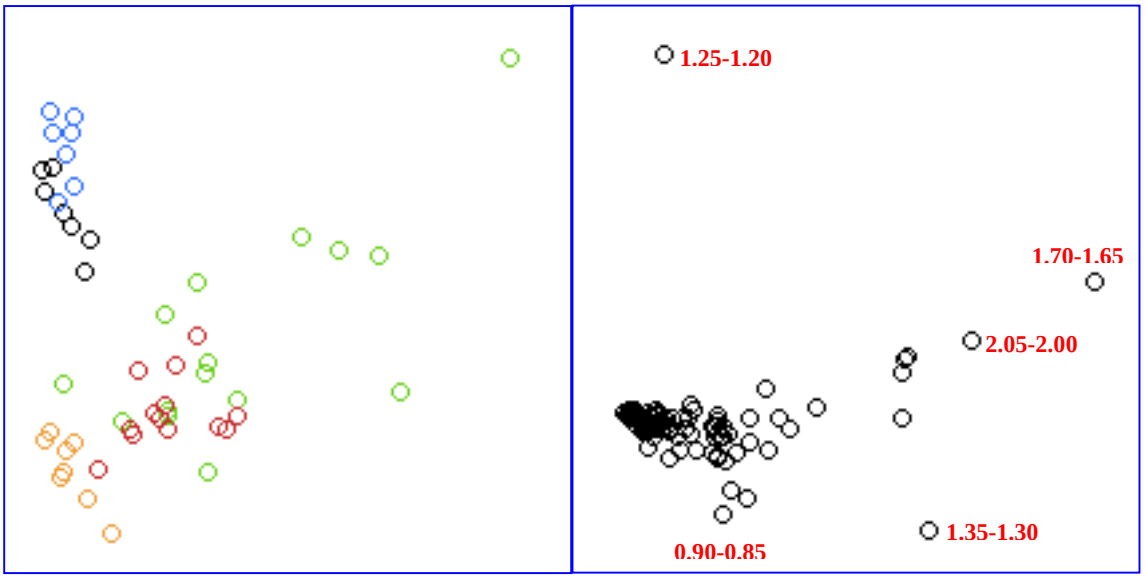


Figure 46: PCA results for ^{1}H NMR spectra (10 - 0 ppm range) of DCM extracts of leaves collected in November 2003 and January 2004.
Left: Scores plot (PC2 v PC1), black circles - uninfested vines, blue circles - infested vines, Nov. 2003, red circles - uninfested vines, green circles - infested vines, January 2004,
orange circles - uninfested vines, November 2003, second batch.
Right: Loadings plot, influential regions of the ^{1}H NMR spectrum are labelled (in ppm) in red.

4.5.2.5 January 2005

A scores plot of PC2 v PC3 (see Figure 47) gives quite good separation of the infested and uninfested grapevines. The major loading for infestation is 1.70 - 1.65, a region which includes one of the squalene methyl peaks. However, other squalene peaks (δ1.60, 2.07, 1.98) are within the bins associated with uninfested grapevines, suggesting that a second compound, having a resonance overlapping the squalene methyl peak, is responsible for the loading for infested grapevines. Fractionation of the extract may be required to verify this.

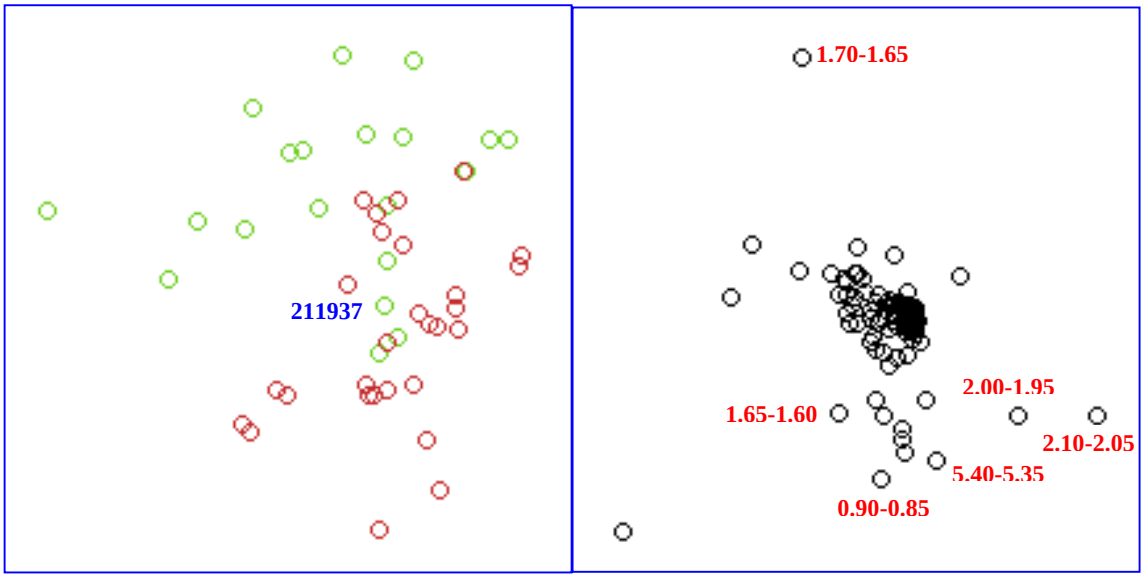


Figure 47: PCA results for ^{1}H NMR spectra (10 - 0 ppm range) of DCM extracts of leaves collected in January 2005.
Left: Scores plot (PC3 v PC2), red circles - uninfested vines; green circles - infested vines.
Right: Loadings plot, influential regions of the ^{1}H NMR spectrum are labelled (in ppm) in red.

PCA with binning to observe the linolenic/linoleic acid ratio gives good separation (see Figure 48). The two infested grapevines that cluster with the uninfested data present interesting cases. Firstly, 211937, which also groups with uninfested grapevines in the other January 2005 and all of the March 2004 PCA, had clustered with infested grapevines in January 2004 and had α-linalool in its extract at that time. Without phylloxera population counts for this grapevine at the time of each collection, it is difficult to reconcile this variation. Secondly, three leaves were taken from 212110 in this collection. One labelled 212110b groups with the uninfested grapevines, while the other two grapevines behave as expected. This is perhaps due to the difficulty in obtaining accurate integration of the linolenic and linoleic methylene resonances, which are not well resolved in the ^{1}H NMR spectra, and suggests that an alternative method for determining this ratio such as gas chromatography, following hydrolysis of the triglycerides and methylation of the resulting fatty acids, may produce more accurate results.

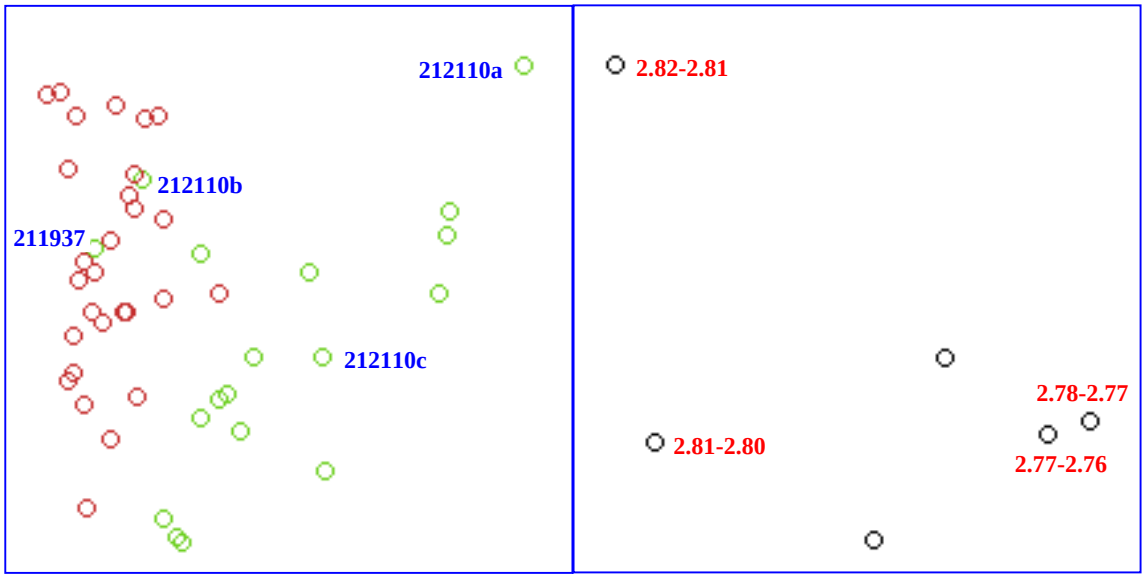


Figure 48: PCA results for ^{1}H NMR spectra (2.82 - 2.76 ppm range) of DCM extracts of leaves collected in January 2005.
Left: Scores plot (PC2 v PC1), red circles - uninfested vines; green circles - infested vines.
Right: Loadings plot, influential regions of the ^{1}H NMR spectrum are labelled (in ppm) in red.

4.5.2.6 Variation in extracts between growing seasons

The ^{1}H NMR spectra of leaves collected in January 2005 were quite different to those of leaves from the January 2004 collection, the major difference being a large increase in the squalene content. This can be clearly seen in PCA of the spectra (see Figure 49). Whether this is an effect of differing climatic conditions or management methods from season to season or an effect of increasing age of the grapevines is uncertain and would require observation over a number of years to provide a definitive answer. However it does have implications for attempts to identify chemical fingerprints of infestation, as it prevents the establishment of invariant baseline data for healthy grapevines, with which the data of infested grapevines can be compared. Despite this, some separation based

on phylloxera status is visible (largely PC2) but is small when compared to the differences due to the year of collection (mainly PC1).

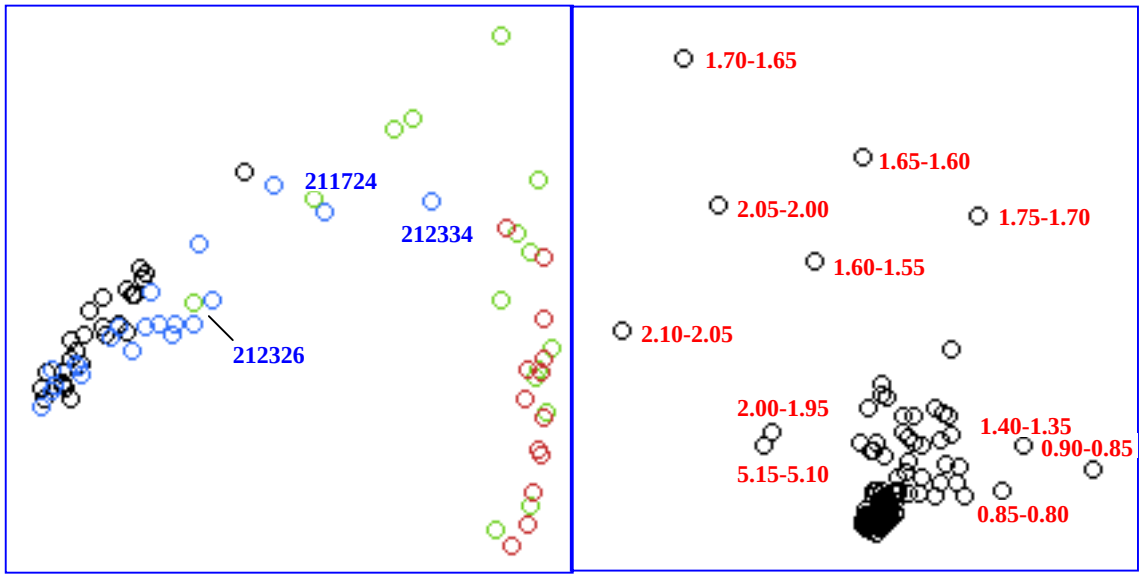


Figure 49: PCA results for ^{1}H NMR spectra (10 - 0 ppm range) of DCM extracts of leaves collected in January 2004 and January 2005.
Left: Scores plot (PC2 v PC1), black circles - Jan. 2005 – uninfested, blue circles - Jan. 2005 - infested, red circles - January 2004 – uninfested, green circles - January 2004 – infested.
Right: Loadings plot, influential regions of the ^{1}H NMR spectrum are labelled (in ppm) in red.

4.5.3 NMR Results - Buckland Valley (Pinot Noir, Blocks 117 - 119 (uninfested) and 128 - 132 (infested))

4.5.3.1 January and February 2004

The spectra of DCM extracts from Pinot grapevine leaves were visibly different to those from Cabernet Sauvignon leaves with the major differences being a large increase in the amount of squalene, which was the major component of the Pinot Noir extracts, and in the amount of unsaturation of the fatty acids, observable in the ratio of the δ1.32 to δ1.25 peaks and the increase in the δ5.35 peak (see Figure 50).

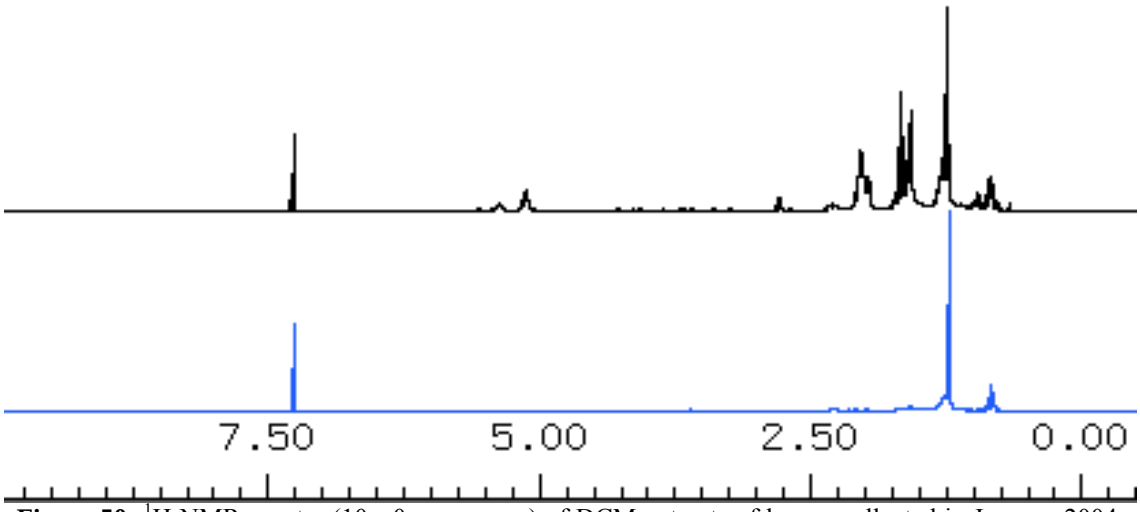


Figure 50: ^{1}H NMR spectra (10 - 0 ppm range) of DCM extracts of leaves collected in January 2004. Top Pinot Noir - Buckland Valley. Bottom Cabernet Sauvignon - Upton.

PCA of the ^{1}H NMR spectra showed some separation (with PC2) of the two classes (see Figure 51) with the major loadings for infestation being an increase in a triplet peak centred at δ1.75. This peak is present in the spectra of uninfested grapevines as well and was also in the spectra of Cabernet Sauvignon grapevines. A large number of infested grapevines group with the uninfested grapevines. A survey made during the 2004/5 growing season revealed that 11 of the 25 grapevines surveyed in the infested block were not infested (Powell 2006) or only lightly infested (less than 5 crawlers captured during the entire season). This figure might be expected to be even lower in this (previous) season and could count for the apparent incorrect clustering of some grapevines.

Using binning restricted to the region of the linolenic/linoleic methylene region also gave some separation of the infested and uninfested grapevines but with some seemingly incorrect grouping as above (see Figure 51). The grapevines which grouped incorrectly were the same grapevines that were incorrectly grouped in the PCA of the full spectral width, being mainly grapevines in the range 130-45 to 130-53 and it seems possible that infestation hadn't spread to this region of the vineyard at the time of collection.

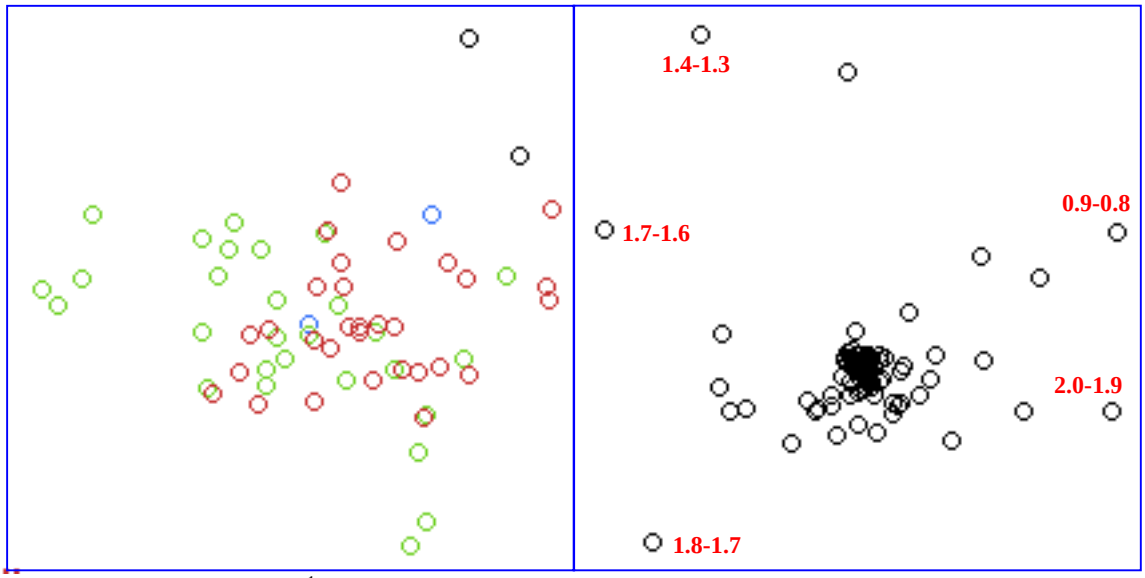


Figure 51: PCA results for ^{1}H NMR spectra (δ10.0 - 0.0 range) of DCM extracts of leaves collected in January and February 2004.
Left: Scores plot (PC4 v PC2), black circles - uninfested vines, blue circles - infested vines, Jan. 2004, red circles - uninfested vines, green circles - infested vines, February 2004.
Right: Loadings plot, influential regions of the ^{1}H NMR spectrum are labelled (in ppm) in red.

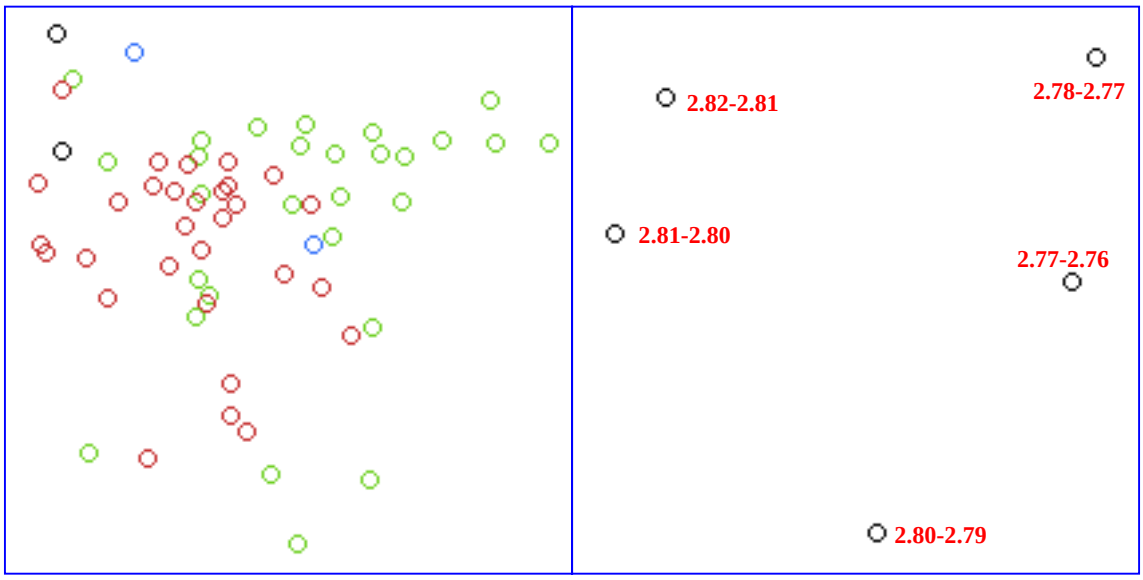


Figure 52: PCA results for ^{1}H NMR spectra (δ2.82 - 2.76 range) of DCM extracts of leaves collected in January and February 2004.
Left: Scores plot (PC2 v PC1), black circles - uninfested vines, blue circles - infested vines, Jan. 2004, red circles - uninfested vines, green circles - infested vines, February 2004.
Right: Loadings plot, influential regions of the ^{1}H NMR spectrum are labelled (in ppm) in red.

4.5.3.2 November 2004

PCA of the ^{1}H NMR spectra of extracts of leaves collected in November 2004 gave some separation of infested and uninfested grapevines (see Figure 53). The loadings indicate that, as was found for Cabernet Sauvignon, infestation led to an increase in unsaturation of the fatty acids. Again a number of grapevines in the infested block group with uninfested grapevines. In most cases this can be explained by the fact that these grapevines had low counts for phylloxera early in the season (two or less crawlers emerged by December 29 2004) but two grapevines, 132-53 (61 crawlers) and 128-65 (9 crawlers) gave anomalous results, while other grapevines which had low rates of infestation at this stage of the season still grouped with the infested grapevines. Inspection of the individual spectra for these grapevines did not reveal any features which could explain this behaviour and again this illustrates that lipid resonances, which are often broad and poorly resolved and hence may be influenced by the presence of other underlying peaks, provide less reliable indicators of infestation. Investigation of the region of the spectrum from δ2.83 to δ2.75 did not give a good distinction between the two classes based on the linolenic/linoleic acid ratio.

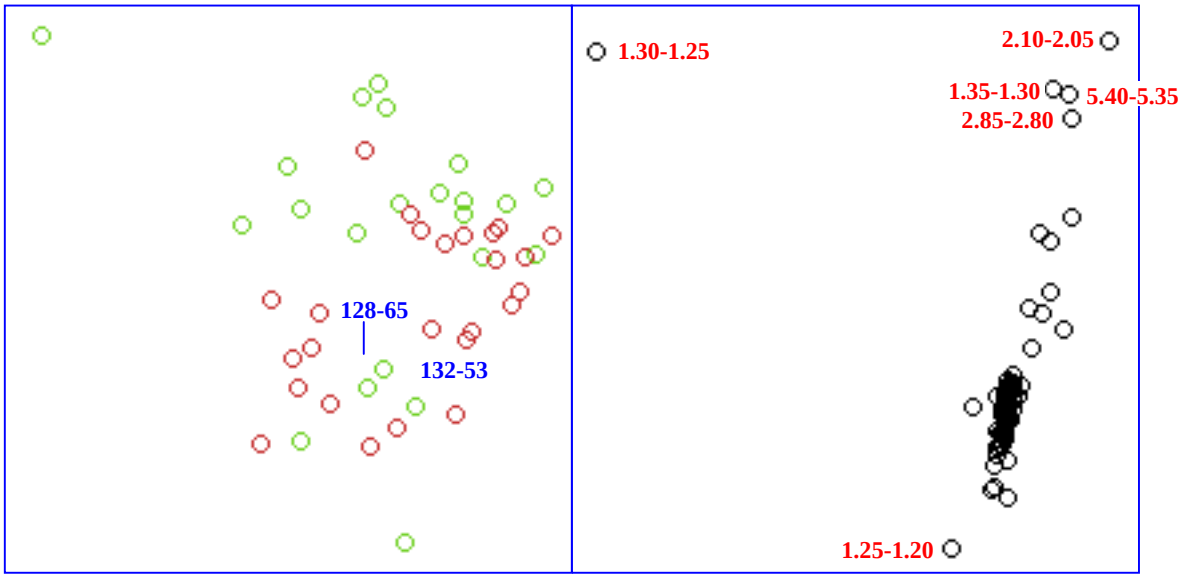


Figure 53: PCA results for ^{1}H NMR spectra (δ10 - 0 range) of DCM extracts of leaves collected in November 2004.
Left: Scores plot (PC2 v PC1), red circles - uninfested vines, green circles - infested vines.
Right: Loadings plot, influential regions of the ^{1}H NMR spectrum are labelled (in ppm) in red.

4.5.3.3 January 2005

Figure 54a shows a scores plot of PC4 v PC1 for leaves collected in January 2005. The loadings plot (not shown) indicates that PC1 is a measure of squalene content while PC4 reflects the degree of unsaturation of the fatty acids. PC4 achieves some separation based on phylloxera status but, as in November 2004, there is no good explanation for the grouping of some infested peaks with uninfested grapevines.

The linolenic/linoleic acid ratio does give a reasonable separation based on phylloxera status (see Figure 54b). In this case the infested grapevines which group with the uninfested grapevines are those that have low or zero phylloxera counts despite being in the infested block.

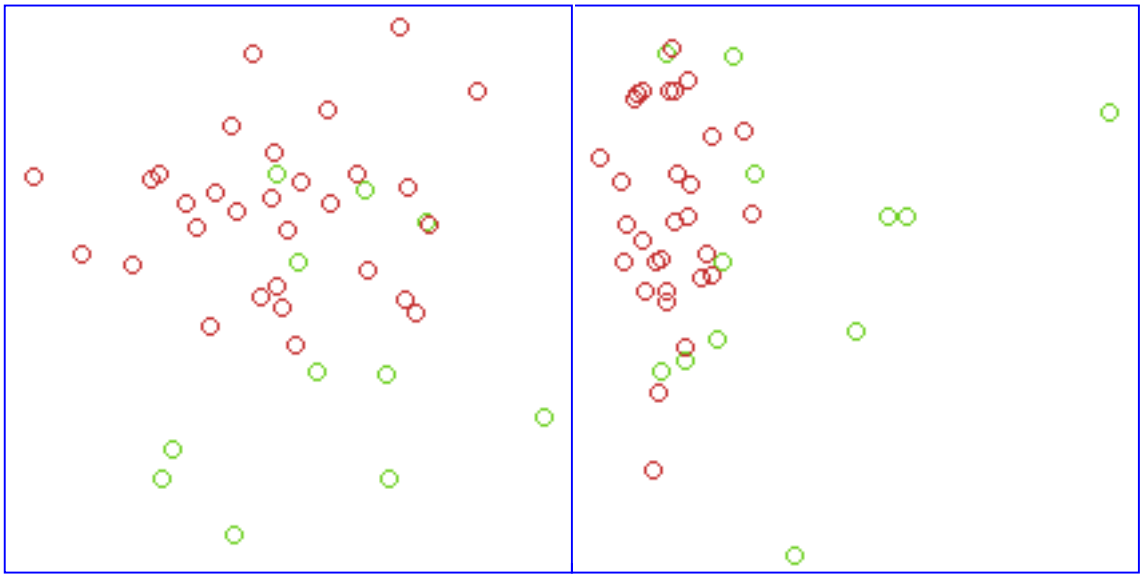


Figure 54: PCA results for ^{1}H NMR spectra of DCM extracts of leaves collected in January 2005.
(a) Left: Scores plot (PC4 v PC1) (δ10 - 0 range), red circles - uninfested, green circles - infested vines.
(b) Right: Scores plot (PC2 v PC1) (δ2.82-2.75 range), red circles - uninfested, green circles – infested.

4.5.3.4 March 2005

PC2 gives good separation of the two classes (see Figure 55) with several of the wrongly grouped grapevines proving to be the grapevines from the infested block that were found to have low levels of infestation (one or no crawlers trapped during the entire season). These are indicated with boxes in Figure 55. However one grapevine (131-59) grouped strongly with the infested grapevines despite having a phylloxera count of one crawler throughout the season.

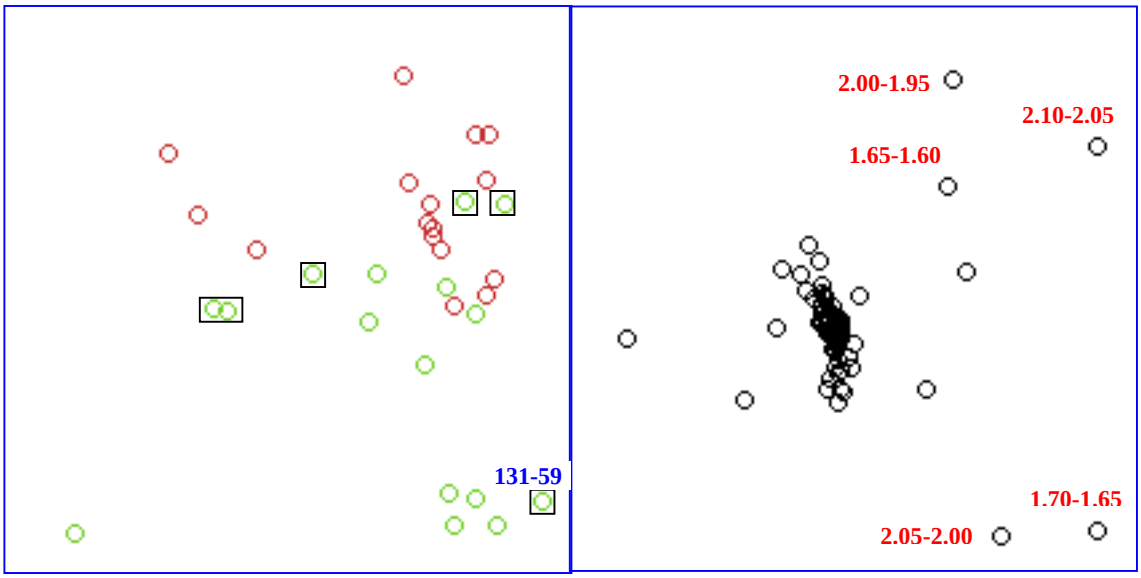


Figure 55: PCA results for ^{1}H NMR spectra (10 - 0 ppm range) of DCM extracts of leaves collected in March 2005.
Left: Scores plot (PC2 v PC1), red circles - uninfested vines, green circles - nominally infested vines, Green circles enclosed in a box are grapevines that had a phylloxera (crawler) count of 0 or 1.
Right: Loadings plot, influential regions of the ^{1}H NMR spectrum are labelled (in ppm) in red.

The meaning of the loadings plot is uncertain, as regions of the ^{1}H NMR spectrum corresponding to squalene resonances appear in the loadings for PC2 for both infested and uninfested vines. This suggests that there are other resonances underlying the squalene resonances and inspection of the spectra revealed that there are shoulders on both methyl resonances belonging to squalene, possibly due to a compound related to squalene. The loadings plot may be reflecting a change in the ratio of these two compounds. To further investigate this, the PCA was repeated on a narrower region of the spectra (δ2.03 - 1.55), with the binning narrowed to give greater resolution (see Figure 56). This gives a very similar separation to the full spectral width PCA, with grapevine 131-59 again grouping with the infested grapevines, as does the nominally uninfested grapevine 118-83. Again, this illustrates the difficulty in getting reliable results from PCA of overlapping or poorly resolved peaks. The loadings plot in this case reveals that the loadings correspond to the centre of the two squalene methyl peaks and do not involve the shoulders of these peaks. As the ratio of peaks from the same molecule cannot vary, this indicates that one of the peaks has an overlapping resonance that is changing in intensity upon infestation. Separation of the extracts by chromatography would be required to verify this assumption and to determine the nature of this compound.

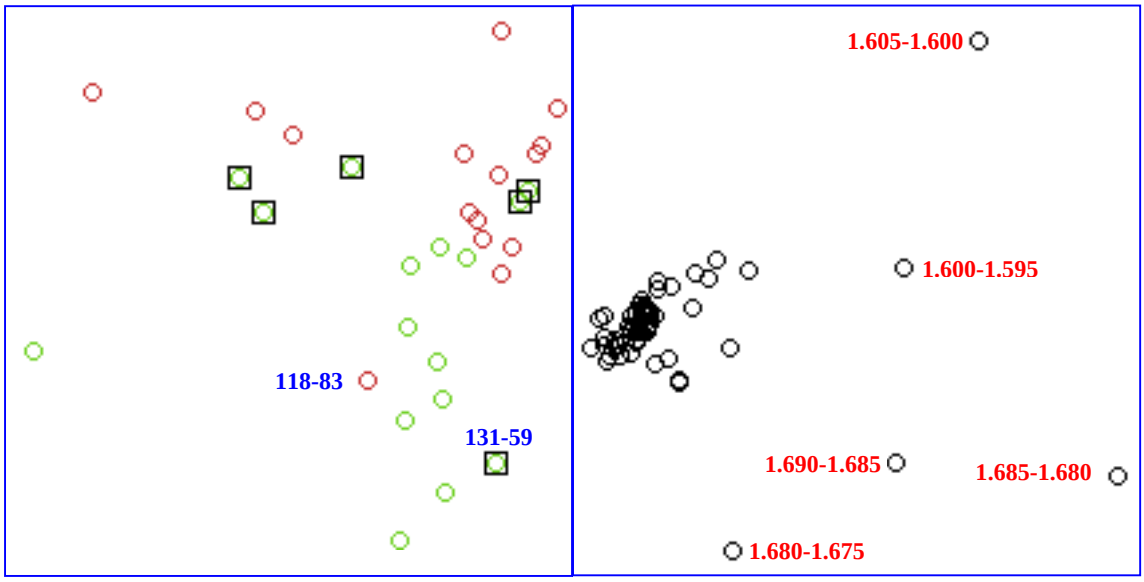


Figure 56: PCA results for ^{1}H NMR spectra (2.03 - 1.55 ppm range) of DCM extracts of leaves collected in March 2005.
Left: Scores plot (PC2 v PC1), red circles - uninfested vines, green circles - nominally infested vines, Green circles enclosed in a box are vines that had a phylloxera (crawler) count of 0 or 1.
Right: Loadings plot, influential regions of the ^{1}H NMR spectrum are labelled (in ppm) in red.

Using the binning scheme optimised to determine the linolenic/linoleic acid ratio, PC1 gives separation between the classes (see Figure 57) but some grapevines do not group in the expected way. In particular, 131-59 again groups with the infested grapevines.

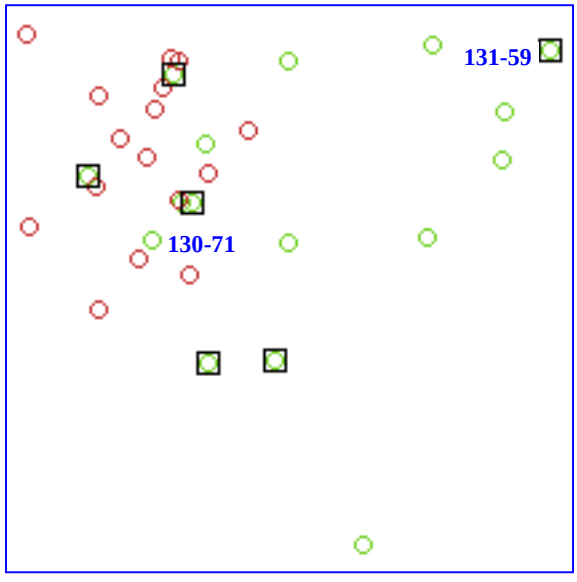


Figure 57: PCA results for ^{1}H NMR spectra (2.82-2.75 ppm range) of DCM extracts of leaves collected in March 2005.
Left: Scores plot (PC2 v PC1), red circles - uninfested vines, green circles - nominally infested vines, Green circles enclosed in a box are grapevines that had a phylloxera (crawler) count of 0 or 1.
Right: Loadings plot, influential regions of the ^{1}H NMR spectrum are labelled (in ppm) in red.

4.5.3.5 Variation in extracts during growing season

PCA analysis of the ^{1}H NMR spectra of extracts from the collections of Pinot Noir leaves made in November 2004, January 2005 and March 2005 leads to a separation (PC1) based on the stage of the growing season (see Figure 58). The loadings plot (PC1) indicates that squalene concentration increases through the season while PC2 is influenced by the degree of unsaturation of the fatty acids, although it does not give good separation based on phylloxera status. Interestingly, grapevine 131-59 from the January 2005 collection groups with the grapevines from the November 2004 collection, indicating that its development appears to be retarded, and may explain why this grapevine grouped with the infested grapevines despite having a low phylloxera count. This may suggest that the separation between infested and uninfested grapevines being seen in the previous PCA analyses was an indicator of any stress rather than specifically due to phylloxera status. This grapevine did group with others from the same collection at the other two stages of the season.

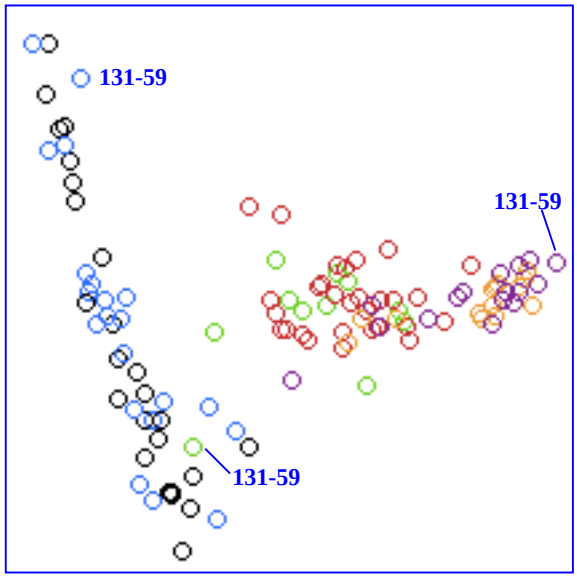


Figure 58: PCA results for ^{1}H NMR spectra (10 - 0 ppm range) of DCM extracts of all leaves collected in 2004 / 2005.
Scores plot (PC2 v PC1), black circles - uninfested vines, blue circles - infested vines, Nov. 2004,
red circles - uninfested vines, green circles - infested vines, January 2005,
orange circles - uninfested vines, purple circles - infested vines, March 2005.

5. Glasshouse Grapevine Stress Detection Trial (Trial 3)

Ungrafted *Vitis vinifera* L. Cabernet Sauvignon and Shiraz were chosen for use in this second glasshouse trial because higher populations of phylloxera were observed on those two varieties at the completion of Trial 1. The optimum number of phylloxera eggs used to infest a pot was selected to be 20 based on data from Trial 1.

This second glasshouse trial was conducted to observe the evolution of stress symptoms in the reflectance spectra and leaf pigment content over time, with the aim of identifying the appropriate wavelengths and pigment profiles allowing the different stress treatments to be discriminated. Furthermore, NMR measurements were also performed to characterize chemical species present in the leaves of phylloxera infested and phylloxera-free grapevines.

5.1 Plant material

Three-year old rootlings of ungrafted *Vitis vinifera* L. cv Shiraz, clone PT23 and ungrafted *Vitis vinifera* L. cv Cabernet Sauvignon, clone LC10 were sourced from Boulevarde Nurseries, Mildura, Victoria. The Shiraz vines were sourced one season prior to the Cabernet Sauvignon, hence were four and a half years old at the commencement of the study, whereas the Cabernet Sauvignon were three and a half years old. All plants were potted into 20 cm pots in a 3:1 ratio mix of potting mix and perlite and maintained in a shadehouse at DPI-Rutherglen. "Yates" Thrive-all purpose soluble fertiliser was applied monthly, 8g was dissolved in 4.5L water, as per manufacturers recommendations. A final application was conducted one month before the commencement of the trial. All plants were moved to a glasshouse one week before the commencement of the trial.

5.2 Trial design

A total of 96 grapevines were included in the glasshouse trial, 48 of each variety. Eight grapevines of each variety were used for each treatment group. The six treatments included: unstressed control grapevines; nitrogen deficient; water deficient; phylloxera infested; phylloxera infested and nitrogen deficient; phylloxera infested and water deficient. The control grapevines (termed "healthy") and grapevines without phylloxera treatment were replanted with fresh potting mix and placed back into their original pots. Plants were then supplemented with either 2.00 g ammonium nitrate or deprived of this fertiliser (termed "nitrogen deficient"). All treatments received 2.50 g "Yates" Trace Elements Essential Nutrients. All pots were sealed in a 53 μm mesh bag, secured at the base of the grapevine trunk with Tanglefoot™ applied around the neck of the bag where it contacted with the grapevine trunk (Figure 59a).

5.3 Infestation method

Vines to be infested with phylloxera were removed from their pots and one medium sized lignified root was teased out. Twenty phylloxera eggs of G4 genotype were sourced from excised root piece bioassays (de Benedictis and Granett 1993) maintained at DPI-Rutherglen laboratory and were placed on dampened filter paper strips, approximately 40 mm x 10 mm. The filter paper was placed on polyamide gauze fabric of 53 μm mesh. The mesh was then rolled around the root so the eggs were in contact with the root piece, and secured with cable ties and Tanglefoot™ was applied to prevent phylloxera crawlers escaping into the main root mass (Burns & Powell, submitted) (Figure 59b). Plants were repotted and received trace elements and nitrogen fertiliser, except for the nitrogen deficient treatment group, before being bagged, as before.

5.4 Trial conditions

All plants were placed in a single room of a glasshouse and arranged in 8 randomised blocks according to a 2x3x2 random factorial design created using GenStat Release 6.1 (Figure 60). All plants except those of the water deficient treatment groups were watered for 2 mins daily via a drip irrigation system. Plants subjected to the water deficiency treatment were originally given half the water of the controls, however after the first week of the trial the watering regime for the water deficiency treatments was reduced to approximately 70 % less water than the control group received. Plants were visually assessed for symptoms of severe water stress and were given additional water when required. The glasshouse was maintained at approximately 24°C throughout the day and 17°C overnight and was illuminated using Son-T Agro 400 globes (Philips) for 12 hours daily plus an additional hour boost at 2:00 am.

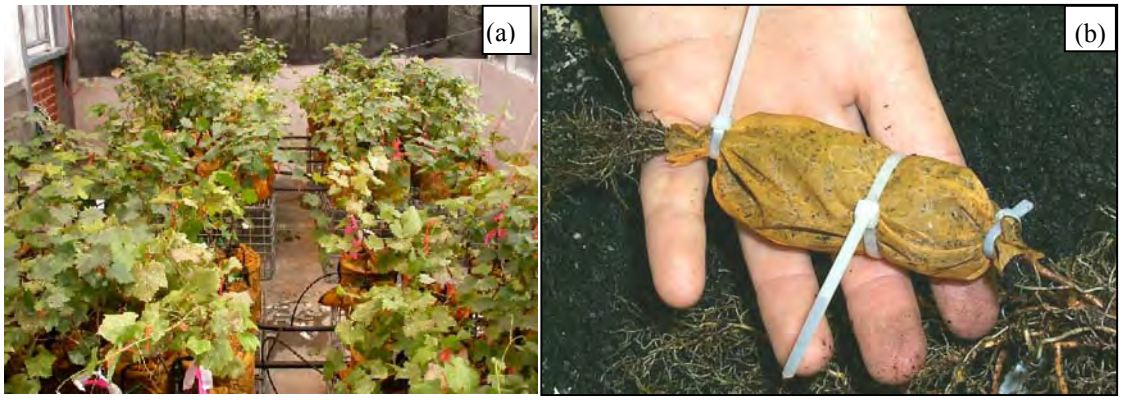


Figure 59: (a) Potted grapevines were placed in 53 μm mesh bags before positioning inside a single room of a glasshouse.
(b) Pots were infested by securing phylloxera eggs to a medium sized lignified root inside a 53 μm mesh "snag" to prevent crawlers spreading throughout the root system.

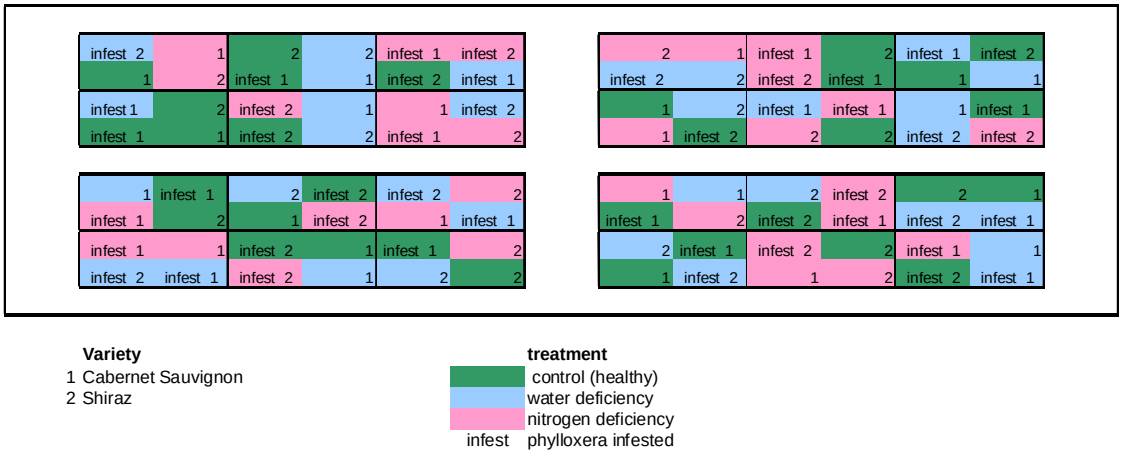


Figure 60: Randomised potted grapevine placement. Varieties and treatment are colour-coded according to the legend.

The potted grapevines were monitored at approximately 10-day intervals over a period of nine weeks (30/3/04 – 2/6/2004). The 6 time intervals were designated Time 0 - Time 5.

5.5 Pigment Analysis

Pigment extraction and quantification followed the procedure described in section 2.1, with the exception that the extracted pigments were separated on a SphereClone 5u ODS1 column (Phenomenex, Sydney, Australia) and quantified as before. The HPLC methodology was as described in Section 2.1 with the modification that solvent A was adjusted to acetonitrile:methanol:Tris-HCL buffer 0.1M pH 8.0; 85:9:6.

5.6 Spectral reflectance measurements

Spectral reflectance measurements were taken throughout the trial from the same leaves taken for HPLC analysis. However, this time individual leaf-level reflectance spectra were acquired using an ASD FieldSpec-Pro® spectroradiometer coupled with a Li-Cor Integrating Sphere in order to overcome the lighting problems encountered during the first trial (Section 3.2.2). The fibre optic cable was held at a fixed position in the integrating sphere's chamber, leaves were held at the same position in the clip, and the same integrated light source was used to illuminate the samples (Figure 3).

5.7 NMR measurements

NMR measurements of collected samples followed the protocol described earlier (Section 2.3).

5.8 Nitrogen content and phylloxera populations

At the end of the trial the plants were removed and all foliage and root matter was weighed as an indicator of plant vigour. Three fresh leaves from each plant were weighed, dried, then weighed again to determine leaf water content. The leaves were then sent, following quarantine regulations, to CSIRO Christian Laboratories, Canberra for nitrogen content analysis.

Each grapevine was then removed from their pot and the root enclosures where the phylloxera were initially attached were removed. The excised root piece was washed, phylloxera collected and the populations counted as described in Section 3.4.

5.9 Results & Discussion (Trial 3)

5.9.1 Phylloxera populations

The number of phylloxera counted on each infested grapevine at the completion of the trial showed considerable variation. There was a significant difference between the variety of grapevine and the number of phylloxera observed at the end of the trial ($P<0.001$). Greater numbers of phylloxera were observed on the Cabernet Sauvignon grapevines than on the Shiraz, the mean number of phylloxera (log transformed) on Shiraz and Cabernet Sauvignon varieties was 0.97 and 1.99 respectively. The maximum number of phylloxera observed on a single grapevine was 816 per 0.1g dried root. This represented a 40-fold increase from the initial 20 eggs placed on the root piece. There was no significant difference between treatments and the number of phylloxera observed at the end of the trial ($P=0.946$) and there was no significant grapevine variety and treatment interactions ($P=0.816$) (Figure 61).

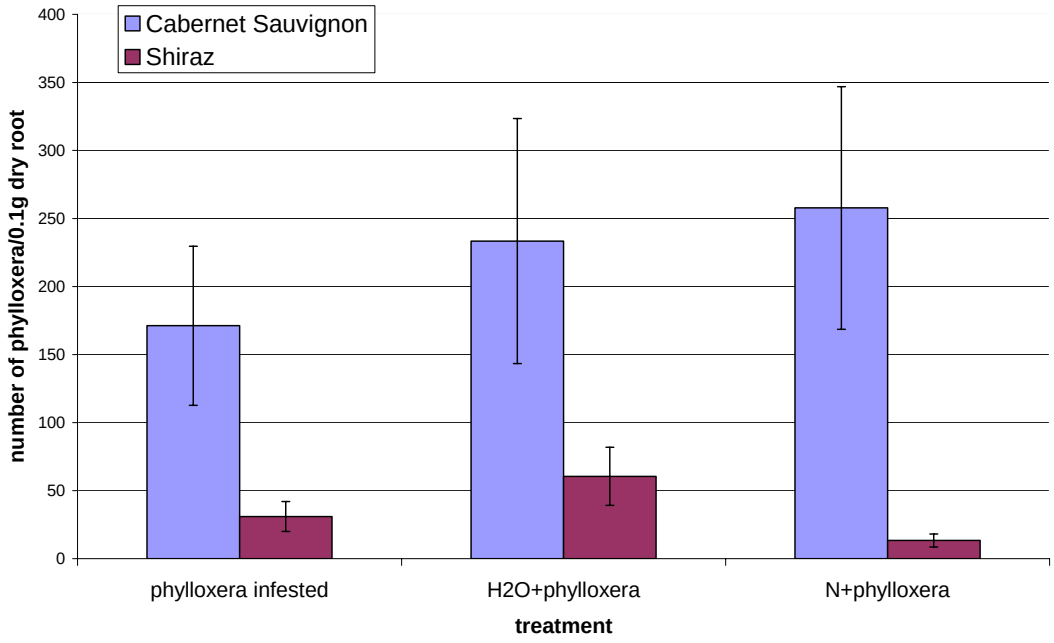


Figure 61: Mean number of phylloxera per potted grapevine for both varieties and each treatment included in Glasshouse Trial 3.

5.9.2 Vigour Assessment

Considerable variation was observed in the fresh root weight due to excess wetness in some pots. Significant differences were observed between the grapevine varieties for the shoot weight but not in root weight (Table 13).

Table 13: Mean shoot and root weight (g) from both varieties.

	Shiraz	Cabernet Sauvignon	P value	LSD
Mean shoot weight (g)	60.1	44.2	<0.001 *	9.20
Mean Root weight (g)	177.3	175.0	0.873	26.01

* = Significant ($p<0.05$)

Significant differences were observed in the fresh root weight between the phylloxera infested and uninfested Cabernet Sauvignon. However there was no difference between treatments or interaction between phylloxera and treatments for root weight (Table 14a). Phylloxera infested grapevines had reduced root mass, compared to the healthy controls. Similar observations have been reported by Powell and Herbert (2005). The greatest differences were observed between the combination treatment of water deficiency and phylloxera and the healthy control (Table 14a). The root mass of the combination treatment grapevines were severely reduced.

Significant differences were not observed in the fresh root weight between the phylloxera infested and uninfested Shiraz vines (Table 14b). There was also no difference between treatments or interaction between phylloxera and treatments for root weight (Table 14b). All treatments showed a reduction in their root mass compared to the healthy control, again the combination treatment of water deficiency and phylloxera were severely reduced, being the lowest weight on average.

Table 14a: Cabernet Sauvignon mean root weight (g) for each treatment group.

	phylloxera			
Treatment	no	yes	P value	LSD
Water stress	177	133	Phylloxera 0.030 *	Phylloxera 43.3
Nitrogen deficiency	242	165	Treatment 0.179	Treatment 53.0
Healthy (control)	182	158	Treatment.phylloxera 0.607	Treatment.phylloxera 74.9

* = Significant ($p<0.05$)

Table 14b: Shiraz variety mean root weight (g) for each treatment group.

	phylloxera			
Treatment	no	yes	P value	LSD
Water stress	162.7	154.9	Phylloxera 0.138	Phylloxera 30.79
Nitrogen deficiency	200.7	171.8	Treatment 0.246	Treatment 37.71
Healthy (control)	202.4	170.1	Treatment.phylloxera 0.777	Treatment.phylloxera 53.33

* = Significant ($p<0.05$)

Significant differences were not observed in the shoot weight between the phylloxera infested and uninfested Cabernet Sauvignon. However phylloxera infested grapevines generally showed less vigour than the healthy control grapevines. There was a significant difference between the healthy control and the treatments. The healthy controls showed significantly more vigour than either the water stressed grapevines or the nitrogen deficient grapevines, however there was no significant difference between the water stressed grapevines, the nitrogen deficient grapevines or between those treatments and the phylloxera infested grapevines. There was no significant interaction between phylloxera and treatments (Table 15a).

Significant differences were not observed in the shoot weight between the phylloxera infested and uninfested Shiraz vines. There was a significant difference between the healthy controls and the treatments. The water stressed grapevines showed significantly less vigour than the healthy controls, however there was no significant difference between the nitrogen deficient grapevines and the healthy controls or the water stressed grapevines and the nitrogen deficient grapevines. There was no significant difference between the three stress treatments of water deficiency, nitrogen deficiency or phylloxera infestation. There was no significant interaction between phylloxera and treatments, however those grapevines infested by phylloxera and water stressed showed considerably less vigour than other treatments (Table 15b).

Table 15a: Mean shoot weight (g) of the Cabernet Sauvignon variety for each treatment group.

	phylloxera			
Treatment	no	yes	P value	LSD
Water stress	43.7	41.2	Phylloxera 0.063	Phylloxera 9.47
Nitrogen deficiency	37.4	34.1	Treatment 0.009 *	Treatment 11.60
Healthy (control)	64.8	43.8	Treatment.phylloxera 0.202	Treatment.phylloxera 16.41

* = Significant ($p<0.05$)

Table 15b: Mean shoot weight (g) of Shiraz variety for each treatment group.

	phylloxera			
Treatment	no	yes	P value	LSD
Water stress	44.6	40.5	Phylloxera 0.678	Phylloxera 15.80
Nitrogen deficiency	58.7	67.3	Treatment 0.006 *	Treatment 19.36
Healthy (control)	77.9	72.7	Treatment.phylloxera 0.789	Treatment.phylloxera 27.37

* = Significant ($p<0.05$)

5.9.3 Leaf nitrogen content

The treatment group where the application of ammonium nitrate was withheld showed significantly less nitrogen content in their leaves than other groups - mean % nitrogen of total dry leaf weight; healthy 2.257, water stress 2.272, nitrogen stress 1.928 (Table 16). A significant difference was also seen in the water content of the leaves between the two varieties, but not between treatments (Table 16). Statistical comparisons were made between varieties (V), treatments of water or nitrogen deficiency (T) and phylloxera infestation (I) and interactions (Table 16).

Table 16: P-value of the interactions for nitrogen and water content of leaves.

	Variety	Treatment	Infestation	VxT	VxI	IXT	VxIxT
Nitrogen content (%)	0.355	<0.001 *	1.000	0.863	0.567	0.627	0.918
Water content (%)	<0.001 *	0.777	0.848	0.961	0.434	0.920	0.653

V - variety, I - infestation treatment, T - treatment of water deficiency or nitrogen deficiency.
* = Significant ($p<0.05$)

5.9.4 Pigment analysis

A significant difference was observed in the concentration of total chlorophyll and total carotenoids between varieties (Figures 62 and 63). Varieties were then analysed independently to eliminate the varietal effect on the pigment concentrations.

5.9.4.1 Total chlorophyll

There was a significant difference in the total chlorophyll content between treatments for the Cabernet Sauvignon variety, but not between the phylloxera infested treatment and healthy control (Table 17). There was a significant difference between the total chlorophyll content of the healthy control, the water stressed and the nitrogen deficient treatments, the healthy control showing the highest concentration of chlorophyll (Figure 62). However, there was no significant difference between the water stress and nitrogen deficient treatments. There was a significant difference between the phylloxera infested treatment and the nitrogen deficient treatment, however not between the water stress and phylloxera infested treatments. Both the water stress and nitrogen deficient treatment had less chlorophyll than the phylloxera infested treatment, the nitrogen deficient treatment being the lowest chlorophyll concentration of all treatments. Those treatments receiving both phylloxera infestation and water or nitrogen deficiency treatments, although lower, did not show significantly lower chlorophyll concentrations than those treatments receiving only single stress treatments.

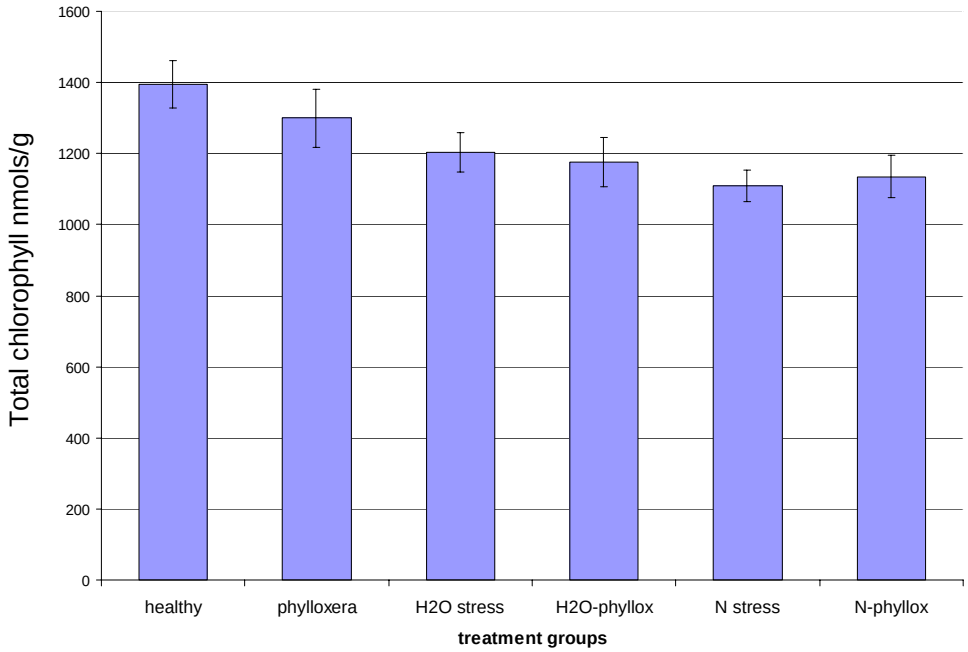


Figure 62: Total chlorophyll content (nmols/g) of leaves from Cabernet Sauvignon variety for each treatment group included in the glasshouse stress detection trial.

There was a significant difference in the total chlorophyll content between phylloxera infested and healthy control grapevines for the Shiraz variety (Table 18). The healthy control treatment had a higher concentration of chlorophyll per gram of fresh leaf material than the phylloxera infested treatment (Figure 63). A significant difference was observed between the nitrogen stress treatment and the healthy control, however not between the water stress and healthy or water stress and nitrogen stress. The water stress and phylloxera infestation combination treatment showed a significantly lower chlorophyll concentration than the water stress alone treatment, however there was no significant reduction in the chlorophyll content of the nitrogen deficient with phylloxera infestation combination treatment compared to nitrogen deficiency alone.

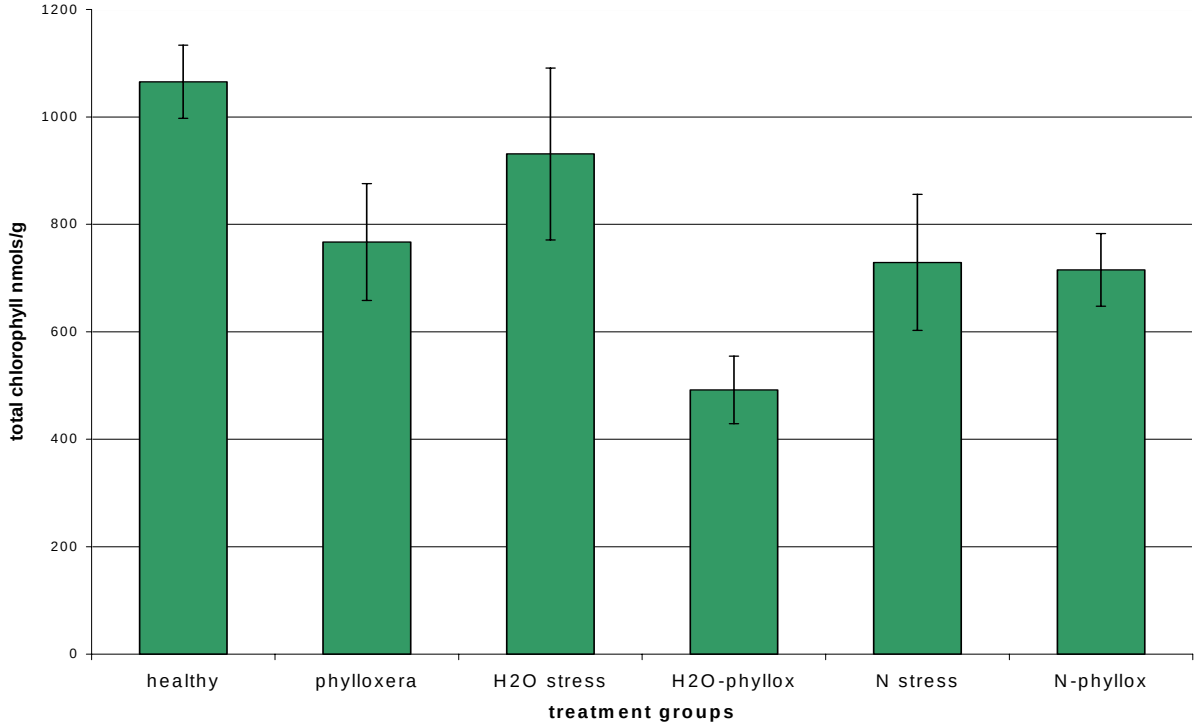


Figure 63: Total chlorophyll content (nmols/g) of leaves from Shiraz variety for each treatment group included in glasshouse stress detection trial.

5.9.4.2 Total carotenoid content

There was a significant difference in the total carotenoid content between treatments for the Cabernet Sauvignon variety (Table 17). There was a significant difference between the total carotenoid content of the healthy control, the water stressed and the nitrogen deficient treatments, the healthy control showing the highest concentration of carotenoids. However, there was no significant difference between the water stress and nitrogen deficient treatments. There was a significant difference between the phylloxera infested treatment and the nitrogen deficient treatment, however not the water stress and phylloxera infested treatments. Those treatments receiving both phylloxera infestation and water or nitrogen deficiency did not show significantly less total carotenoid concentrations than single stress treatments.

There was a significant difference in the total carotenoid content between phylloxera infested and healthy control grapevines for the Shiraz variety (Table 18). The healthy control treatment showing the greatest concentration of chlorophyll per gram and the water stress with phylloxera infestation treatment showed the lowest chlorophyll concentration per gram (Figure 64). A significant difference was observed between the nitrogen stress treatment and the healthy control, however not the water stress to healthy or water stress to nitrogen stress treatment. The combined water stress with phylloxera infestation treatment showed a significantly lower chlorophyll concentration than single stress treatments, but there was no significant reduction in the combined nitrogen deficient and phylloxera infestation treatment compared to nitrogen deficiency alone.

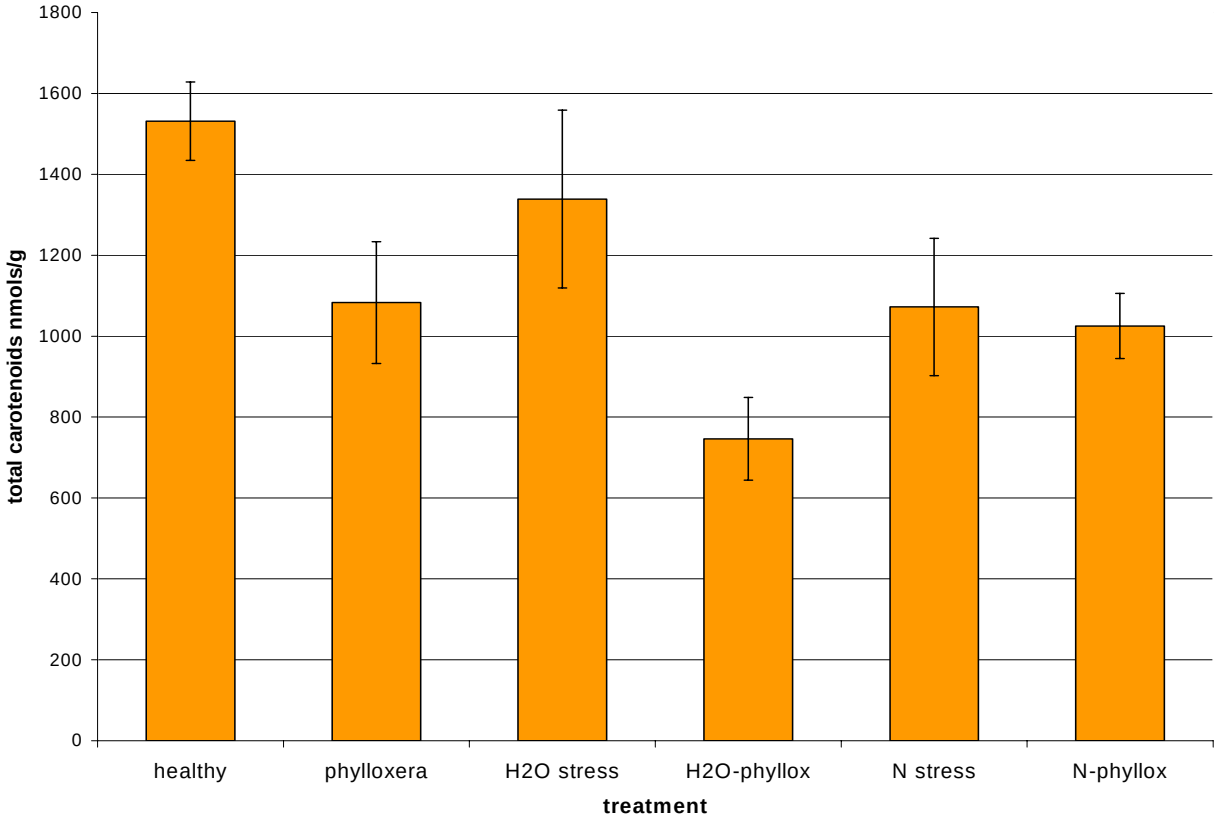


Figure 64: Total carotenoids concentration (nmols/g) of leaves sampled from Shiraz variety of each treatment included in the stress detection glasshouse trial.

5.9.4.3 Total carotenoids to total chlorophyll ratio

A trend was observed where stress treatments showed higher Tcar/Tchl ratios than the healthy control treatment for both Cabernet Sauvignon and Shiraz varieties (except phylloxera infested Shiraz treatment), however no significant difference was observed for any of the treatments (Table 17 & 18).

5.9.4.4 Xanthophyll cycle pigment ratio (AZ/VAZ)

No significant differences were observed between treatments or phylloxera infestation for either Cabernet Sauvignon or Shiraz varieties. Ratios were not showing the predicted trend where stress treatments would induce a higher ratio of AZ/VAZ (Table 17 & 18).

5.9.4.5 Total xanthophyll cycle pigments to total chlorophyll ratio (VAZ/Tchlorophyll)

A trend was observed where stress treatments showed higher ratios than the healthy control treatment for both Cabernet Sauvignon and Shiraz varieties (except water stressed and phylloxera infested Shiraz treatment). However, no significant difference was observed for any of the treatments (Table 17 & 18).

5.9.4.6 β-carotene to total chlorophyll ratio

There was a significant difference in the β-carotene to total chlorophyll ratio between treatments for the Cabernet Sauvignon variety (Table 17) (Figure 65). As anticipated, stress treatments showed higher ratios in β-car/Tchl than the healthy control treatment. There was a significant difference between the water stress, nitrogen deficiency and healthy treatments, however not between water stress and nitrogen deficiency treatments. The phylloxera infested treatment was significantly lower than the water stressed or nitrogen deficient treatments. Those treatments receiving a combination of stresses were not significantly different to single stress treatments.

There were no significant differences observed for the β-carotene to total chlorophyll ratio between the stress treatments for the Shiraz variety, however stress treatments showed a trend of increased ratios compared to the healthy control treatment as predicted (Table 18).

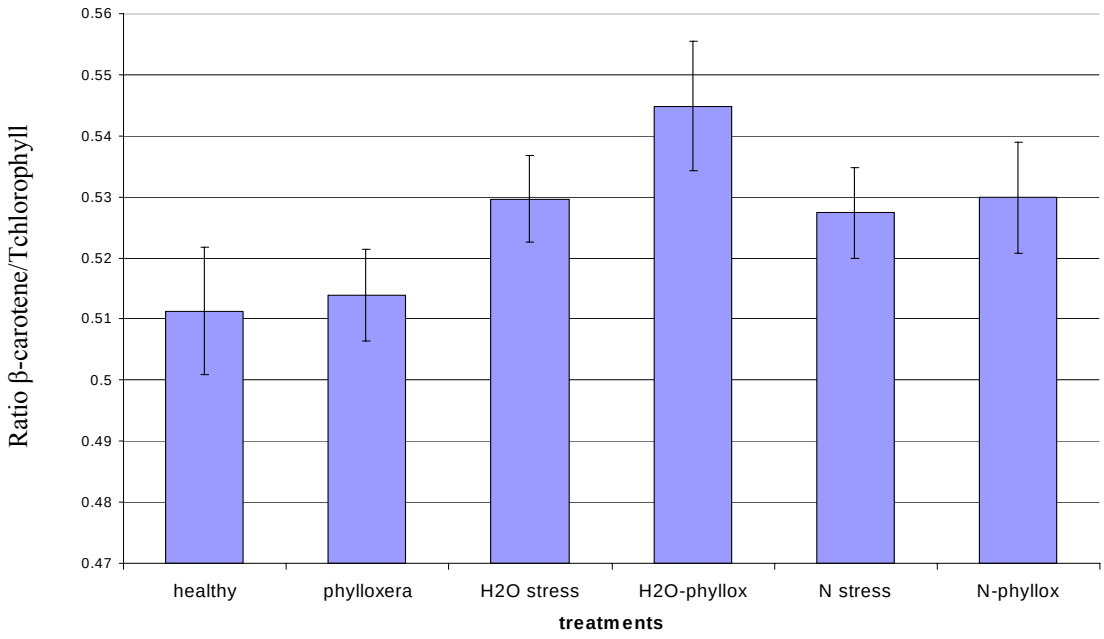


Figure 65: β-carotene to total chlorophyll ratio for leaves samples from Cabernet Sauvignon variety for each treatment.

Table 17: Cabernet Sauvignon - Mean pigment content and P-value of the interactions for treatment and phylloxera infestation.

Pigment/Ratio	Phylloxera	H_2O stress	Healthy	N stress	Interaction	P value	LSD
Total chlorophyll	no	1211	1407	1109	Treatment	0.004*	134.3
	yes	1176	1300	1135	Phylloxera	0.476	109.6
					Treatment.phylloxera	0.607	189.9
Total carotenoids	no	1684	1888	1557	Treatment	0.014*	174.0
	yes	1650	1797	1602	Phylloxera	0.700	142.1
					Treatment.phylloxera	0.729	246.1
Tcarot/Tchl	no	1.394	1.340	1.407	Treatment	0.066	0.044
	yes	1.408	1.383	1.416	Phylloxera	0.225	0.036
					Treatment.phylloxera	0.709	0.062
AZ/VAZ	no	0.099	0.177	0.191	Treatment	0.202	0.058
	yes	0.183	0.153	0.175	Phylloxera	0.141	0.047
					Treatment.phylloxera	0.236	0.082
VAZ/Tchlorophyll	no	0.152	0.144	0.153	Treatment	0.247	0.016
	yes	0.168	0.154	0.142	Phylloxera	0.433	0.013
					Treatment.phylloxera	0.244	0.023
β-carot/Tchl	no	0.532	0.511	0.528	Treatment	0.014*	0.017
	yes	0.545	0.514	0.531	Phylloxera	0.386	0.014
					Treatment.phylloxera	0.774	0.024

*=significant ($p<0.05$)

Table 18: Shiraz - Mean pigment content and P-value of the interactions for treatment and phylloxera infestation.

Pigment/Ratio	Phylloxera	H_2O stress	Healthy	N Stress	Interaction	P value	LSD
Total chlorophyll	No	931	1065	729	Treatment	0.110	213.8
	Yes	499	767	715	Phylloxera	0.007*	174.6
					Treatment.phylloxera	0.143	302.4
Total carotenoids	No	1339	1531	1072	Treatment	0.127	289.8
	Yes	757	1083	1025	Phylloxera	0.004*	236.6
					Treatment.phylloxera	0.164	409.8
Tcarot/Tchl	No	1.47	1.438	1.578	Treatment	0.521	0.147
	Yes	1.516	1.431	1.453	Phylloxera	0.633	0.120
					Treatment.phylloxera	0.493	0.208
AZ/VAZ	No	0.151	0.139	0.145	Treatment	0.775	0.061
	Yes	0.138	0.108	0.129	Phylloxera	0.421	0.050
					Treatment.phylloxera	0.951	0.087
VAZ/Tchlorophyll	No	0.1296	0.1366	0.1484	Treatment	0.421	0.025
	Yes	0.1307	0.123	0.1405	Phylloxera	0.510	0.021
					Treatment.phylloxera	0.841	0.036
β-carot/Tchl	No	0.5236	0.5165	0.5405	Treatment	0.659	0.038
	Yes	0.5396	0.5173	0.524	Phylloxera	0.996	0.031
					Treatment.phylloxera	0.694	0.544

*=significant ($p<0.05$)

5.9.5 Spectral reflectance measurements

Reflectance measurements were made at all 6 sampling intervals over the nine week period (Time 0, Time 1, …, Time 5). The mean green peak reflectance spectra for each group of Cabernet Sauvignon and Shiraz grapevines measured at Times 0, 3 and 5 are displayed in Figure 66. The decrease in reflectance values between Time 0 and Time 3 were interpreted as all the grapevines recovering from the stress caused through handling and positioning in the initial set up of the experiment.

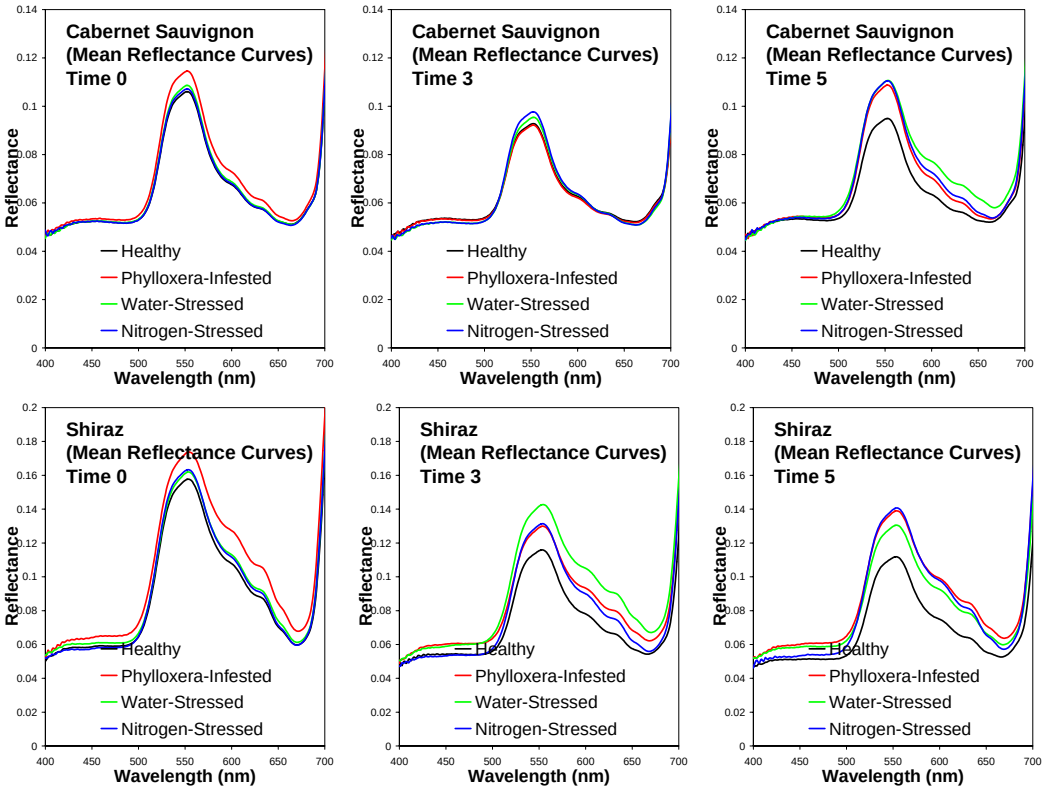


Figure 66: The evolution of the green peak reflectance spectra for four of the six treatment groups of grapevines investigated.

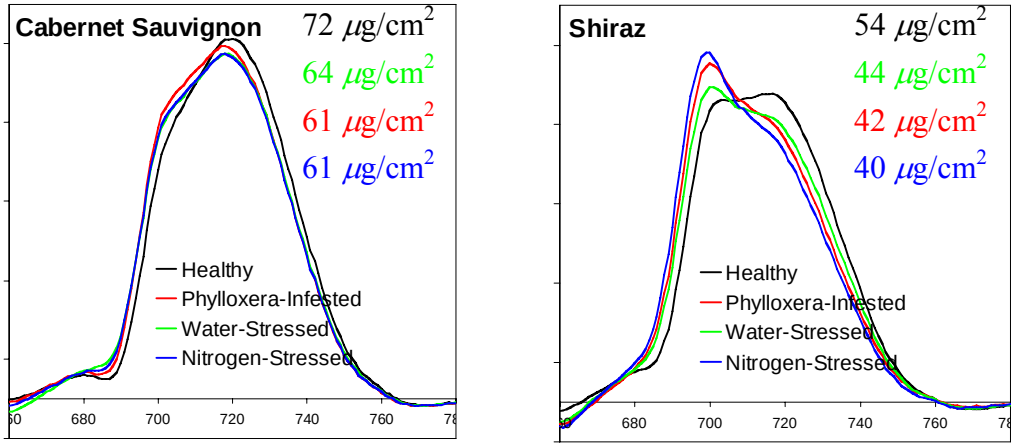


Figure 67: Mean first derivative spectra around the red edge for the two grapevine varieties measured at Time 5. Also displayed are the PROSPECT estimates (discussed later) of chlorophyll content for each curve.

By Time 3 we observed that the groups of Cabernet Sauvignon grapevines had very similar spectral responses. For the Shiraz vines it appeared that the stressed groups did not completely recover from the initial stress. By the end of the experiment (Time 5) we observe the stressed groups for both grapevine varieties possessed the characteristic higher reflectances in the green peak and chlorophyll well compared to the control grapevines.

We also observed changes in the shape of the first derivative spectra for these data consistent with previous findings (Figure 67). Moreover, Figure 67 shows that subtle changes in the shape of the derivate spectra are related to large changes in leaf chlorophyll content. This supports the claim (Tsai and Philpot, 1998; Zarco-Tejada *et al.* 2000; 2002; 2003) that derivative analysis of hyperspectral reflectance data may be a useful tool for the pre-visual detection of plant stress. This type of derivative analysis is not possible with multispectral data.

The values of chlorophyll content displayed in Figure 67 were estimated from the reflectance spectra and the PROSPECT leaf radiative transfer software (Jacquemoud and Baret, 1990). Specifically the PROSPECT software was used in a function minimisation procedure (full details in Renzullo *et al.* 2005) to infer estimates of leaf chlorophyll content for a subset of the reflectance data. The agreement between PROSPECT-derived and HPLC estimates of total leaf chlorophyll content observed in these leaves is illustrated in Figure 68.

Figure 68 shows that the Cabernet Sauvignon had generally higher leaf chlorophyll contents than the Shiraz leaf samples. It also suggests that on average the PROSPECT model estimates were within 11 μg/cm^2 of those estimated using HPLC.

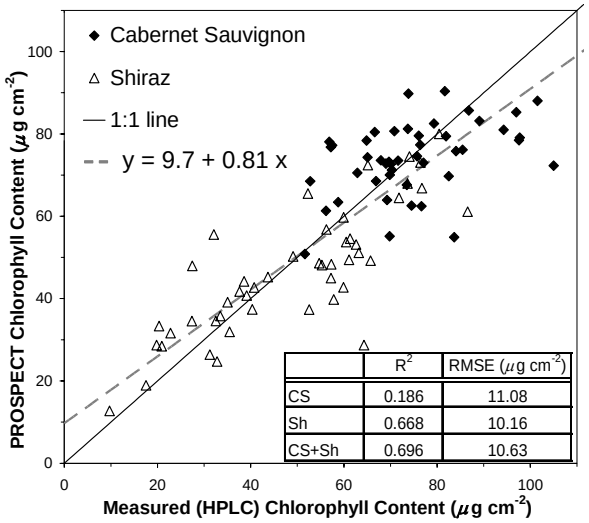


Figure 68: PROSPECT and HPLC estimates of leaf chlorophyll content for a subset of the leaves measured in glasshouse experiment. Coefficients of determination (R^2) and root mean squared error (RMSE) are displayed for the two grapevine varieties individually and combined.

PDA was applied to the glasshouse reflectance spectra to explore group separation. Figure 69 shows the groups of treatment Cabernet Sauvignon spectra. It illustrates the improved separability of the data as the stresses progress through time. PDA was proposed by Hastie *et al.* (1995) as a way of classifying data that were high-dimensional and ill-posed (namely many more highly correlated variables, i.e. wavelengths, than there are observations). It uses a regularized regression method known as ridge regression (Hoerl and Kennard, 1970) to assign spectra to one of the various groups. A result of PDA is a set of coefficients that, when applied to the spectral data, form the *discriminant variables*. We use the magnitude of the coefficients of these discriminant variables to give an indication of the importance of a particular wavelength in contribution to the separation of the groups.

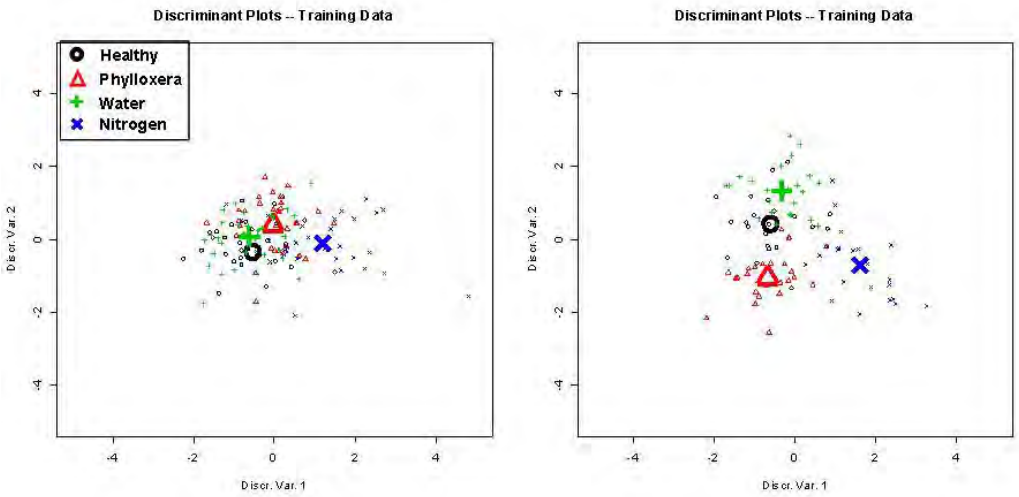


Figure 69: Discriminant plots from PDA of Cabernet Sauvignon reflectance data. The figure shows increased group separation through time.

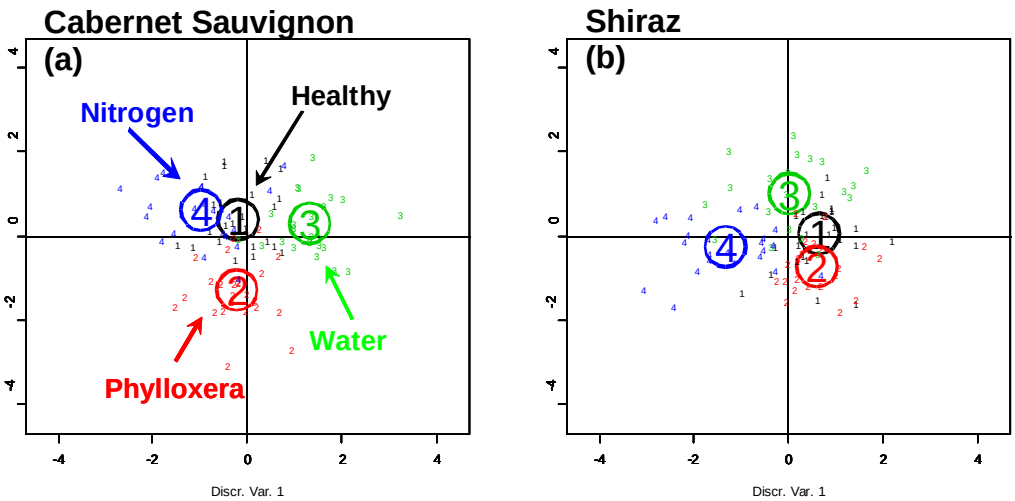


Figure 70: OSLASSO discriminant plots of the above Time 5 data for both grapevine varieties.

Figure 70 gives examples of the spectral separation achieved using OSLASSO on the (a) Cabernet Sauvignon and (b) Shiraz samples measured at Time 5. Here we give a brief description of the interpretation of these figures by considering the role of the first and second discriminant variables separately.

For the Cabernet Sauvignon data, Figure 70a shows that the first discriminant variable differentiates the water- and nitrogen-stressed groups from the healthy group, while the second discriminant variable separates the phylloxera-infested group from the healthy group. The normalized coefficients of the second discriminant variable in Figure 71a shows the phylloxera-infested group of grapevines differs most from the control grapevines at wavelengths around 530, 660 and 740 nm, but the separation is dominated by wavelengths in the region above 900 nm (note that PDA coefficients of the same variable are displayed for comparison purposes).

For the Shiraz vines, we observe in Figure 71b that the nitrogen-deficient grapevines differ from the healthy grapevines at the wavelength identified by the coefficients of the first discriminant variable, plotted for both PDA and OSLASSO in Figure 70b. Some of the wavelengths exploited in separating the nitrogen stressed groups from the healthy group of grapevines (Figure 71) are located around 530 nm; 660, 680 and 700 nm; 730 and 760 nm; and 950 and 1150 nm.

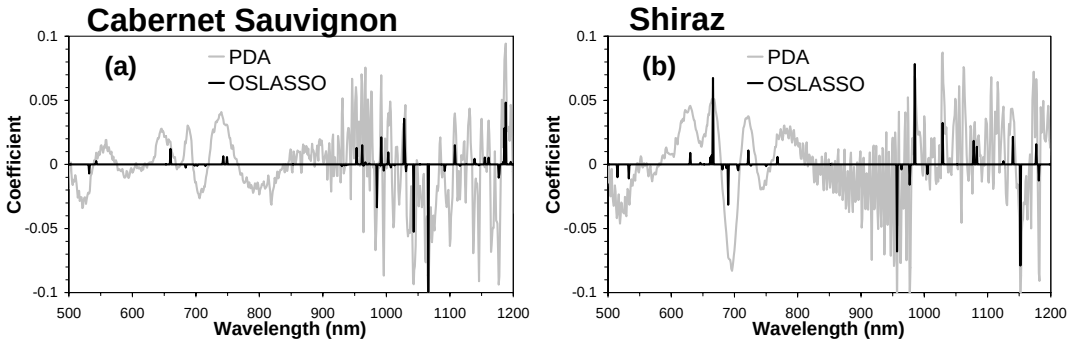


Figure 71: PDA and OSLASSO (a) second and (b) first discriminant variables for the Cabernet Sauvignon and Shiraz vines, respectively.

In Figure 71, we observed for the Shiraz vines that some of the wavelengths selected that separate the N from the H group of grapevines occurred in the chlorophyll well. This suggests that chlorophyll absorption may be one of the distinguishing features between the nitrogen-deficient grapevines and control grapevines. This is supported by the finding reported Renzullo *et al.* (2005) showing the nitrogen-deficient grapevines overall had lower total leaf chlorophyll content compared with other grapevines in the glasshouse experiment. Wavelengths in the water absorption regions were also selected but they play more of a dominant role in the separation of

phylloxera-infested Cabernet Sauvignon from the control grapevines. Investigations have yet to confirm if leaf water content was significantly different between groups.
It was also observed that the selected wavelengths were in the location of the zero-crossings of the first- and higher-order derivative spectra (Figure 72). Derivative zero-crossings are known to correspond to absorption features in reflectance spectra (Tsai and Philpot, 1998; Clark *et al.*, 2003; Hsu, 2003). Derivative operators, however, are also notorious for highlighting noise, particularly the higher-order derivatives. Both the PDA and OSLASSO procedures often selected wavelengths in noisy parts of the reflectance on the near-infrared plateau at wavelengths above 800 nm, which is also the location of numerous water absorption features. When the groups of data are very similar and it is difficult to identify "physically meaningful" changes in curvature to exploit, the procedures tend to use the noisy parts of the spectrum to separate the groups. The procedures' sensitivity to noise needs to be further investigated.

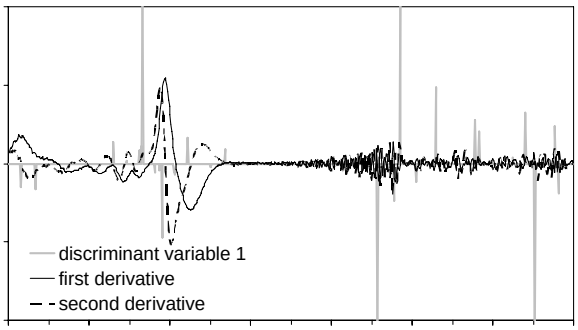


Figure 72: First and second order derivative spectra and coefficients of the first discriminant variable to separate N and H groups of Shiraz vines.

Finally, bootstrap resampling (Efron and Tibshirani, 1993) was employed as a means of assessing the repeatability of the wavelength selection of the OSLASSO. The procedure was applied to 100 bootstrap samples of the original reflectance data from the glasshouse experiment. This resulted in 100 replicates of the discriminant variables. The number of times a wavelength was given a non-zero discriminant variable coefficient is displayed in the frequency histograms of Figure 73. Note that the coefficients from the OSLASSO were grouped into 10-nm bins between 450–1600 nm. The units on the y-axes of the histograms are normalized counts (i.e. the sum of squared counts over all wavelengths equals unity) to facilitate comparisons between the two datasets. Figure 73 demonstrates that the wavelengths selected by both procedures fall in comparable spectral regions.

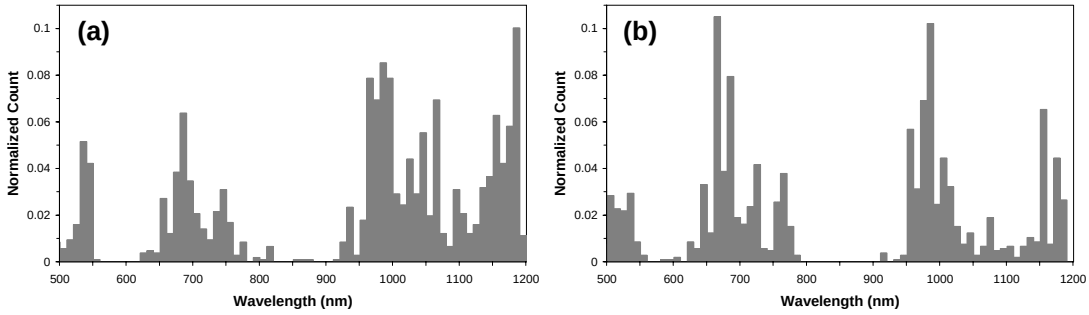


Figure 73: Frequency histograms for the wavelength selection of 100 bootstrap samples of the (a) Cabernet Sauvignon (b) Shiraz reflectance data. The data displayed are related to the number of time wavelengths in a 10-nm bin were given non-zero weighting.

Wavelength selection was based on the magnitude of the normalized coefficients of the discriminant variables of interest. For the OSLASSO this is straightforward; wavelengths whose corresponding coefficient is non-zero are selected. Throughout these investigations, wavelengths of a few spectral regions were continually being selected. Moreover, these regions are known to correspond to spectral features related to plant physiology. For example there are: xanthophylls cycle pigments known to be spectrally active between 500-530 nm which are important for photo-protection; chlorophyll *a* and *b,* whose influence ranges from the maximum in the green peak around 550 nm, the chlorophyll well between 660-690 nm, the red-edge inflection point between 700-730 nm, and also the reported fluorescence feature around 760 nm (Zarco-Tejada *et al.*, 2003); and leaf water, with minor absorption features centred on 950, 1050, 1150 nm, and a major feature at 1450 nm.

The discriminant analysis has shown that the stresses can be separated but the separation is achieved by obtaining linear combinations of reflectances at wavelength in similar spectral region. The linear combinations are governed by the magnitude of the discriminant variable coefficients, which vary depending on which group is to be separated from which other group. The same spectral regions are selected throughout. No regions unique to phylloxera infestation have been identified in this trial. However this does not discount the possibility that regions may be present and further analysis is required.

5.9.6 NMR measurements

The studies on grapevine leaves from field infested Cabernet Sauvignon (Section 4.5.2) and Pinot Noir (Section 4.5.3) have shown that grapevines did cluster according to their phylloxera status but it was not possible to tell whether the indicators found were specific to phylloxera infestation or a sign of any stress in the plant. Therefore glasshouse trials using Cabernet Sauvignon and Shiraz vines were carried out to investigate this. PCA analysis was carried out on NMR spectra from grapevines collected at Time Stage 0 (immediately after establishment of the experiment) and Stage 5 (completion of experiment).

PCA of the spectra from Cabernet Sauvignon vines showed no significant separation of the different treatments at either Stage 0 or at Stage 5 while the Shiraz vines showed no separation at Stage 0 but grouping based upon the treatments was discernible at Stage 5. Only the results for Shiraz vines at Stage 5 will be discussed further.

For grapevines with no imposed water or nutrient stresses, a plot of PC2 against PC1 achieves reasonable separation between phylloxera infested and uninfested grapevines (see Figure 74). Three nominally infested grapevines, 11, 30 and 64, were found to have very low phylloxera populations at the completion of the trial (less than 7 individuals, including eggs, for 11 and 64 and no phylloxera were found for grapevine 30). However, two uninfested grapevines, 5 and 14, grouped with the infested grapevines (all uninfested grapevines were verified as uninfested at the end of the trial). These two grapevines did have a lower dry leaf weight than all other uninfested grapevines, suggesting that they may have been less healthy, which would imply that the PCA is indicating grapevine health rather than phylloxera infestation.

The loadings are difficult to interpret but possibly indicate an increase in unsaturation and / or chain length upon infestation, although the loading of the bin at 1.35 - 1.30 is difficult to reconcile as this bin is also usually associated with unsaturation due to the peak at δ1.30 (this falls in both the 1.35 - 1.30 and the 1.30 - 1.25 bins) for methylenes beta to a double bond. Presumably another resonance is underlying this broad resonance.

The spectrum of grapevine 19 reveals the presence of α-linalool but this compound is not present in any of the other grapevines.

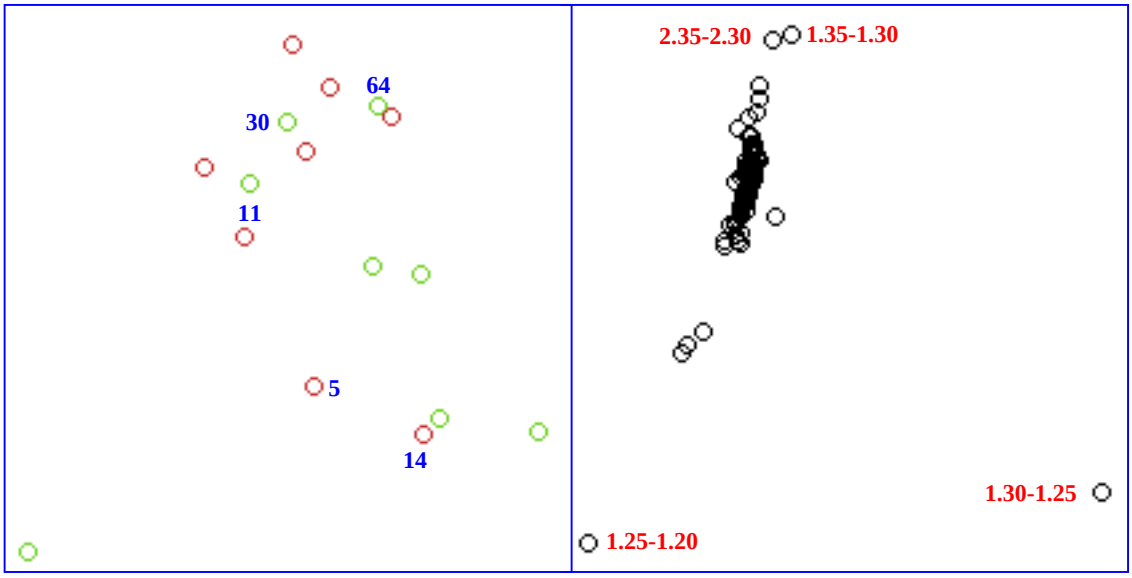


Figure 74: PCA results for ^{1}H NMR spectra (10 - 0 ppm range) of DCM extracts of leaves from Shiraz vines, grown during the glasshouse trial, no stresses.
Left: Scores plot (PC2 v PC1), red circles - uninfested vines, green circles - nominally infested vines.
Right: Loadings plot, influential regions of the ^{1}H NMR spectrum are labelled (in ppm) in red.

Observation of the linolenic/linoleic acid ratio gives separation with PC1 but some grapevines group incorrectly, namely grapevines 14 and 48 (uninfested) and in this case grapevines 11 and 30 group with infested but grapevine 64 still groups with the uninfested grapevines (see Figure 75).

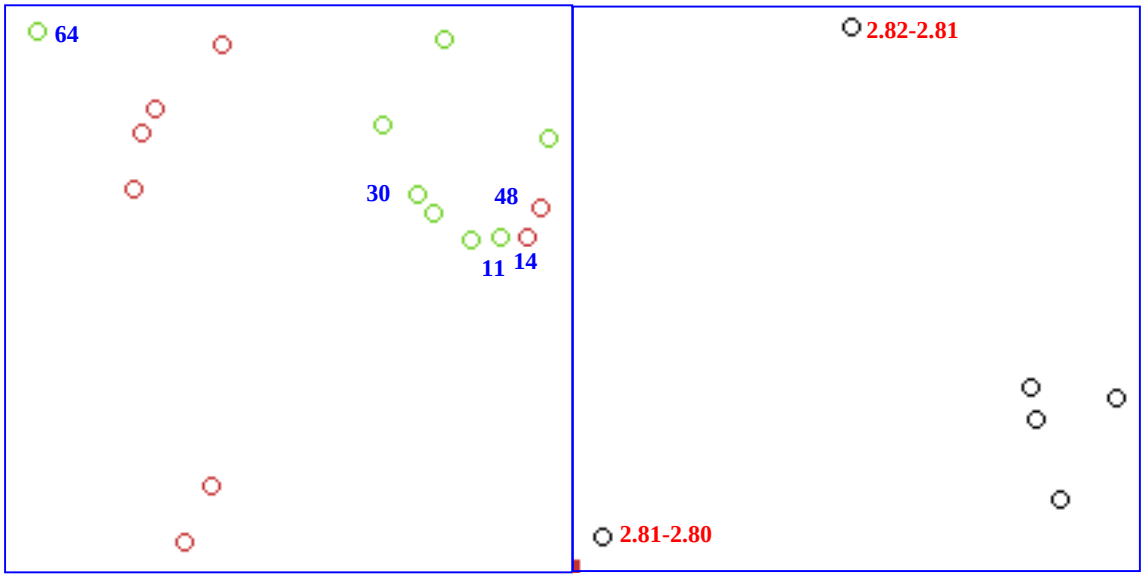


Figure 75: PCA results for ^{1}H NMR spectra (2.82 - 2.75 ppm range) of DCM extracts of leaves from Shiraz grapevines, grown during the glasshouse trial, no stresses v phylloxera infestation.
Left: Scores plot (PC2 v PC1), red circles - uninfested vines, green circles - nominally infested vines.
Right: Loadings plot, influential regions of the ^{1}H NMR spectrum are labelled (in ppm) in red.

In the case of grapevines subjected to water stress, a plot of PC4 against PC3 gives separation between grapevines suffering water stress and unstressed grapevines (see Figure 76). Two water-stressed grapevines, 20 and 77, group with the unstressed grapevines. These grapevines have dry leaf weights similar to those of most of the

healthy grapevines and suggest that the low water regime that they were subjected to may not have adversely affected their health. Grapevine 5 again groups with the stressed grapevines, supporting the proposal that it was not healthy, but grapevine 14 this time groups with the unstressed grapevines. The important loadings are quite different to those shown in Figure 74 for phylloxera infestation.

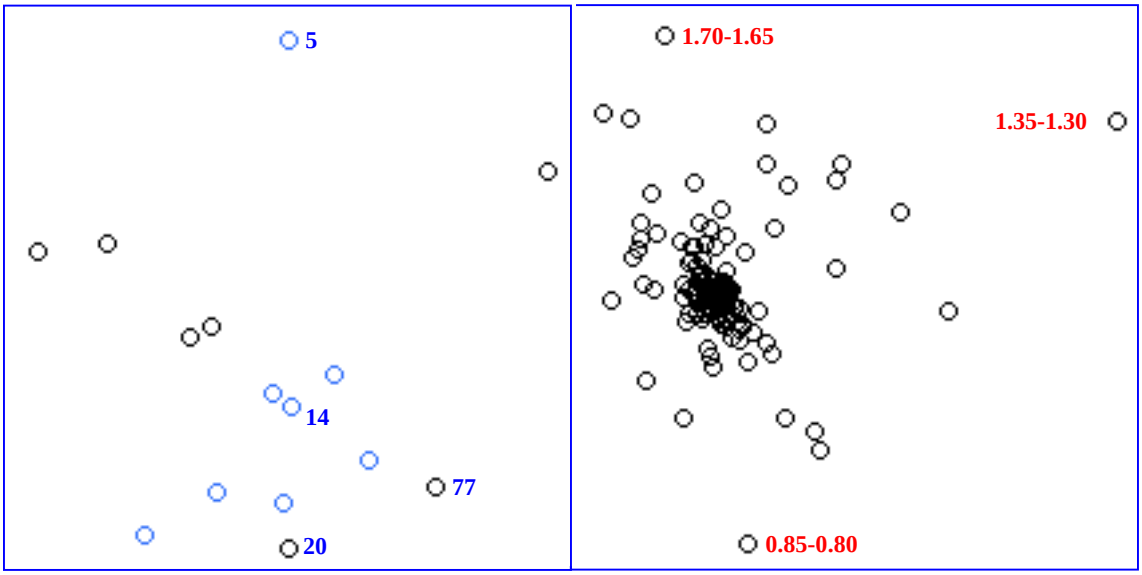


Figure 76: PCA results for ^{1}H NMR spectra (10 - 0 ppm range) of DCM extracts of leaves from Shiraz vines, grown during the glasshouse trial, no stresses v water stress.
Left: Scores plot (PC4 v PC3), blue circles - unstressed vines, black circles - water-stressed vines. Right: Loadings plot, influential regions of the ^{1}H NMR spectrum are labelled (in ppm) in red.

Using the binning pattern designed to observe the linolenic/linoleic acid ratio, PC1 gives separation based on this ratio but the separations found do not have any obvious relationship to the water stress applied or the grapevine vigour deduced from the leaf dry weight.

When the effects of phylloxera infestation and water stress are analysed together, including grapevines suffering both water stress and phylloxera infestation, a plot of PC 6 v PC1 (see Figure 77) allows distinction between infested and uninfested grapevines, regardless of their water stress status. Only some of the nominally phylloxera infested grapevines (19, 22, 41, 58, 79 and 95) had appreciable phylloxera counts when the grapevines were investigated at the completion of the experiment.

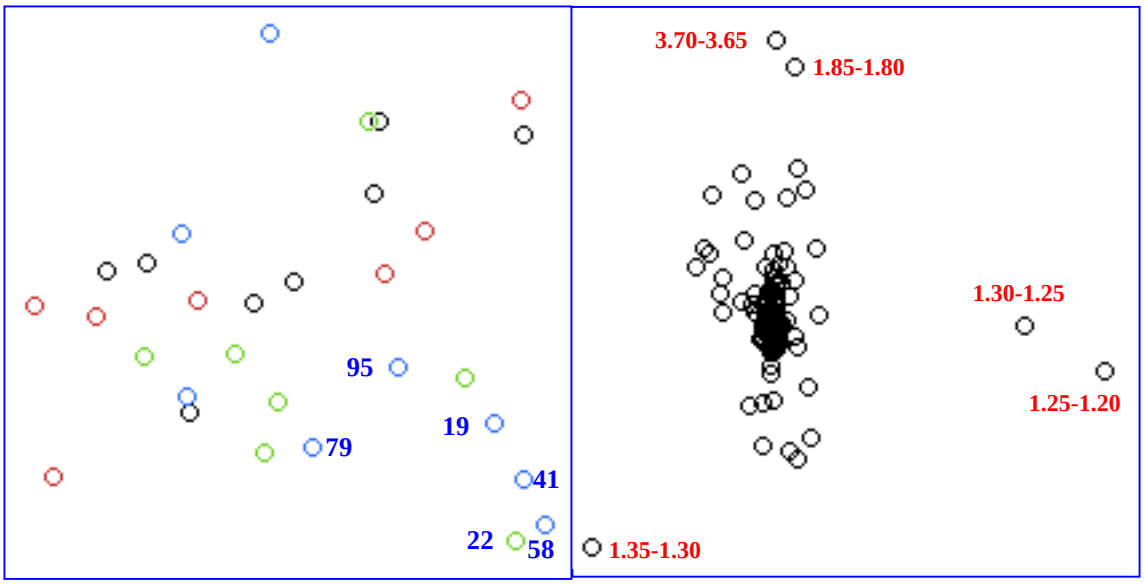


Figure 77: PCA results for ^{1}H NMR spectra (10 - 0 ppm range) of DCM extracts of leaves from Shiraz vines, grown during the glasshouse trial, no stresses v water stress v infested v infested+water stress. Left: Scores plot (PC6 v PC2), black circles - unstressed vines, blue circles - infested vines, red circles - water-stressed vines, green circles - infested+ water-stressed vines.
Right: Loadings plot, influential regions of the ^{1}H NMR spectrum are labelled (in ppm) in red.

Vines grown under conditions of nitrogen stress can be distinguished from healthy grapevines by a plot of PC2 v PC1 (see Figure 78). Again grapevines 14 and 48 group incorrectly as they did when the linolenic/linoleic acid ratios for infested and uninfested grapevines were analysed. The loadings suggest that nitrogen stress results in a decrease in unsaturation of the fatty acids.

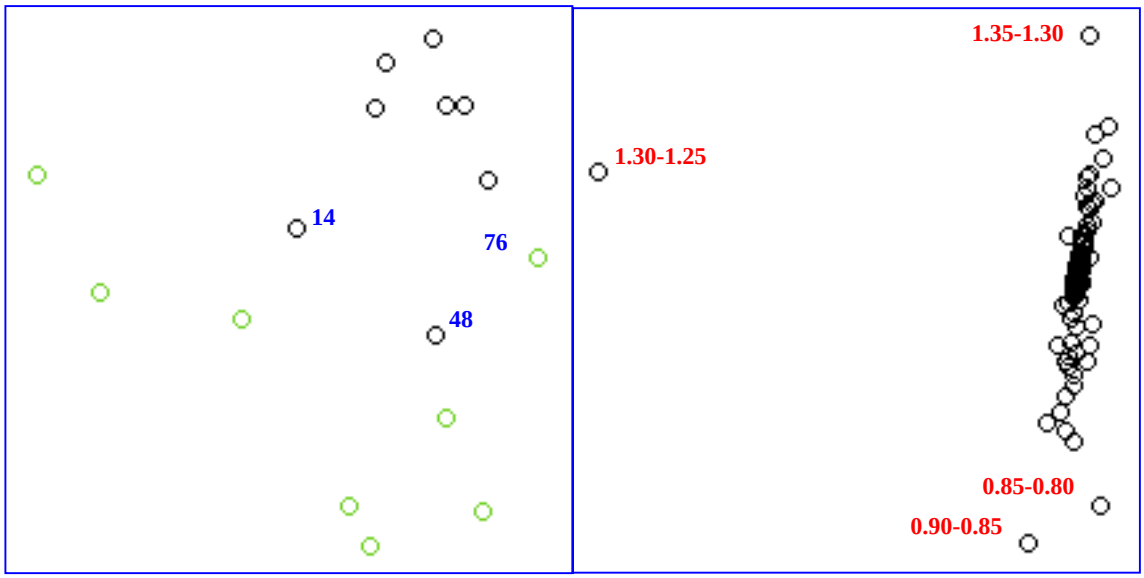


Figure 78: PCA results for ^{1}H NMR spectra (10 - 0 ppm range) of DCM extracts of leaves from Shiraz vines, grown during the glasshouse trial, no stresses v nitrogen stress.
Left: Scores plot (PC2 v PC1), black circles - unstressed vines, green circles - nitrogen-stressed vines.
Right: Loadings plot, influential regions of the ^{1}H NMR spectrum are labelled (in ppm) in red.

Nitrogen stress also results in a decrease in the linolenic/linoleic acid ratio (see Figure 79). The same grapevines group incorrectly as in the full spectral width PCA.

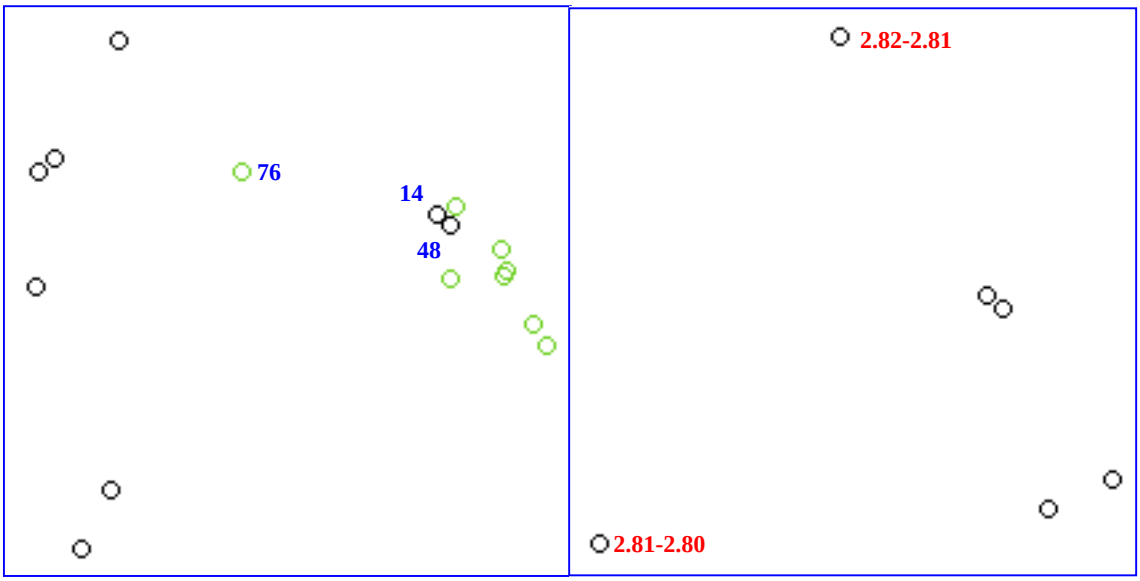


Figure 79: PCA results for ^{1}H NMR spectra (2.82 - 2.75 ppm range) of DCM extracts of leaves from Shiraz vines, grown during the glasshouse trial, no stresses v nitrogen stress.
Left: Scores plot (PC3 v PC2), black circles - unstressed vines, green circles - nitrogen-stressed vines.
Right: Loadings plot, influential regions of the 1H NMR spectrum are labelled (in ppm) in red.

When the effects of phylloxera infestation and nitrogen stress are considered together, PC2 v PC1 separates the grapevines according to their nitrogen status (see Figure 80). Grapevines 14 and 48 group with the nitrogen stressed vines, while 76 groups with the unstressed grapevines as before. The loadings suggest that this effect is an increase in unsaturation as seen previously for nitrogen stress and a reduction in chain length of the fatty acids. The phylloxera-infested grapevines tend to group in a position intermediate between the two classes of uninfested grapevines. This is perhaps to be expected in those grapevines suffering both infestation and nitrogen stress (only 43, 55 and 89 showed appreciable presence of phylloxera) where the effects of infestation and nitrogen stress appear to produce opposite effects on the degree of unsaturation and so may cancel each other. However, the grapevines with only phylloxera infestation would be expected to have more unsaturated fatty acids and so be at the opposite extreme to the nitrogen-stressed grapevines. It may be that the loading at 1.35-1.30 ppm is reflecting an underlying peak (as was proposed for Figure 74 as well) and not the methylenes of unsaturated fatty acids. This requires further investigation with a larger sample size and longer time frame for the experiment to allow the effects of infestation to become more pronounced.

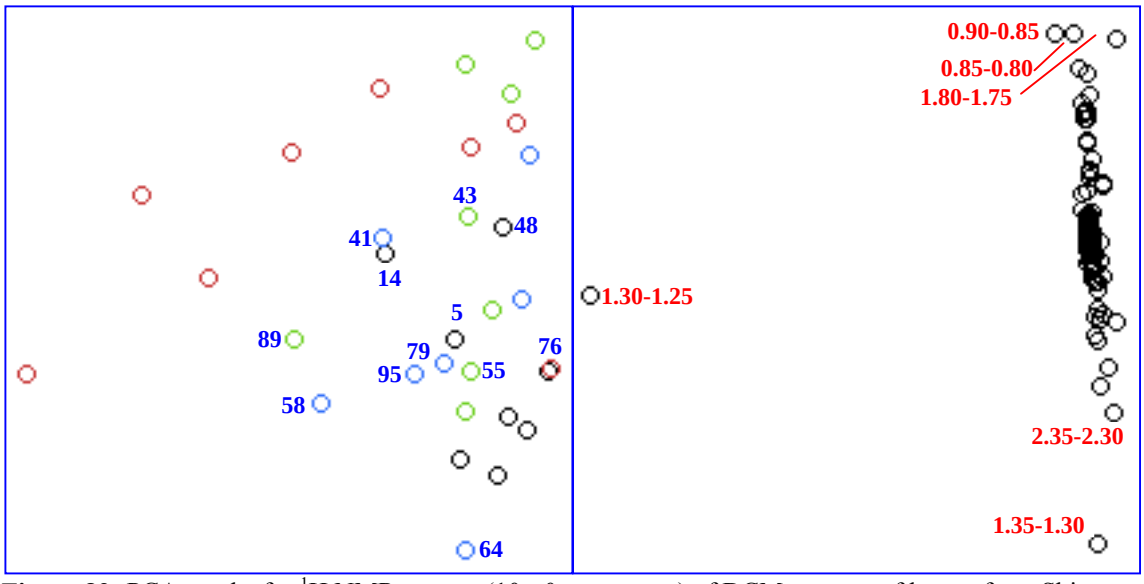


Figure 80: PCA results for ^{1}H NMR spectra (10 - 0 ppm range) of DCM extracts of leaves from Shiraz vines, grown during the glasshouse trial, no stresses v nitrogen stress v infested v infested+nitrogen stress.
Left: Scores plot (PC2 v PC1), black circles - unstressed vines, blue circles - infested vines, red circles - nitrogen-stressed vines, green circles - infested + nitrogen-stressed vines.
Right: Loadings plot, influential regions of the ^{1}H NMR spectrum are labelled (in ppm) in red.

Removal of the grapevines that had both stresses from the calculations produces a similar scores plot of PC1 v PC2 with the nitrogen stressed grapevines separating from the unstressed grapevines, with the exception of grapevines 11, 14, 41, 48 and 76 which group incorrectly (See Figure 81). The loadings plot (not shown) is virtually identical to that shown in Figure 80. This provides further evidence that nitrogen stress produces different metabolic changes to those induced by phylloxera infestation.

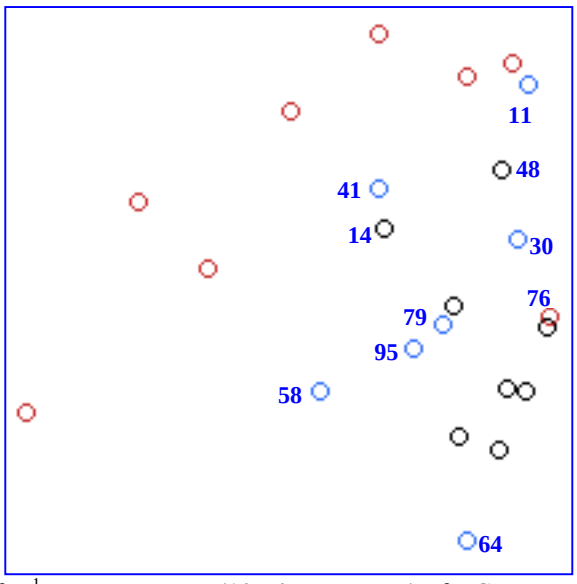


Figure 81: PCA results for ^{1}H NMR spectra (10 - 0 ppm range) of DCM extracts of leaves from Shiraz vines, grown during the glasshouse trial, no stresses v nitrogen stress v infested.
Left: Scores plot (PC2 v PC1), black circles - unstressed vines, blue circles - infested vines, red circles - nitrogen-stressed vines.
Right: Loadings plot, influential regions of the ^{1}H NMR spectrum are labelled (in ppm) in red.

Using the binning scheme designed to measure the linolenic/linoleic acid ratio results in separation of unstressed vines from the stressed grapevines (see Figure 82), which implies that this binning method cannot be used to distinguish phylloxera infestation from nitrogen stress but that it does provide a good indicator of grapevines that are under stress.

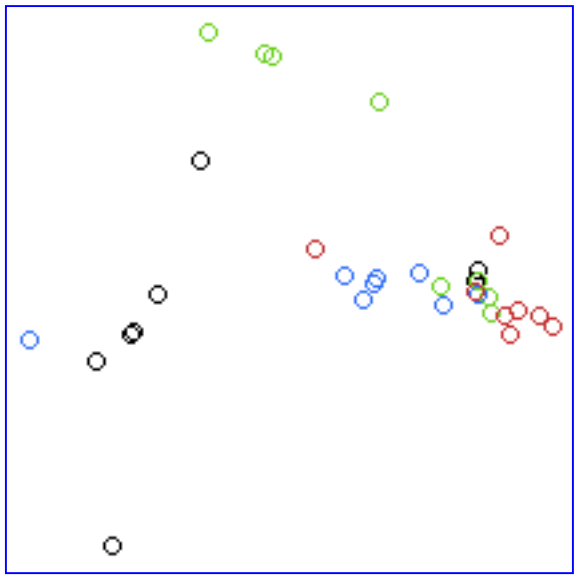


Figure 82: PCA results for ^{1}H NMR spectra (2.82-2.75 ppm range) of DCM extracts from Shiraz leaves, grown during the glasshouse trial, no stresses v nitrogen stress v infested v infested+nitrogen stress.
Left: Scores plot (PC2 v PC1), black circles - unstressed vines, blue circles - infested vines, red circles - nitrogen-stressed vines, green circles - infested+nitrogen -stressed vines.
Right: Loadings plot, influential regions of the ^{1}H NMR spectrum are labelled (in ppm) in red.

6. Global Conclusions and Recommendations

6.1 Phylloxera infestation

The method for infesting the pots with phylloxera eggs was greatly improved for this second trial. Placement of the eggs near the root piece, and keeping the developing insects enclosed around the root piece in a mesh bag allowed the population at the end of the trial to be quantified more easily.

The number of phylloxera counted on each infested grapevine at the completion of this trial still showed considerable variation. In light of the more stringent confinement of the populations to the grapevine roots, this suggests the survival rate of the phylloxera eggs through to adulthood and oviposition and fecundity was variable. Variation in phylloxera population numbers could be attributed to a number of factors. Some variation could be attributed to:

(i) handling the fragile eggs during experiment set-up or egg viability
(ii) the position of the dripper on each pot may have caused wet or dry patches in the pot which could effect phylloxera survival
(iii) a small amount of fungus was observed on the roots of some wetter pots at the end of the trial which could also effect phylloxera survival and root viability.

Moreover, a significant difference was observed between varieties and this could be attributable to either the above-mentioned factors, or the difference in the age of the grapevines when they were infested, or differences in root morphology (making it more difficult for the phylloxera to establish on the Shiraz variety). This particular issue requires further investigation

Future glasshouse screening for phylloxera-grapevine interactions should take into account:

- the method of infesting roots with phylloxera and the accuracy of assessing the phylloxera population density on the grapevine roots;
- root physiology of grapevine varieties and variation of root morphology with age of grapevines; and, given the effect of these extenuating factors on the rate of *in situ* population development,
- the length of the trial.

6.2 Treatment assessment

Nitrogen content analysis and vigour assessment, in terms of root mass and shoot growth, allowed for quantification of the effectiveness of each treatment. Water stress was more difficult to assess however vigour decline was observed for those treatments suggesting the grapevines were affected by the limited amount of water made available to them. Significant differences were not observed in the shoot weight of the infested and uninfested Cabernet Sauvignon or Shiraz varieties, however this may have been due to the variable phylloxera numbers observed at the end of the trial and

the short length of the trial. Differences were not observed between the vigour of the stress treatments and the phylloxera treatment. This needs further investigating as current remote sensing imaging used for the detection of phylloxera highlights areas of reduced vigour amongst vineyard blocks.

Future glasshouse screening for the above-ground effect of phylloxera infestation on grapevines compared to other stresses should take into account

- the population density on the grapevine roots needed to observe a visual symptom,
- the method of implementing water stress and assessing the degree of severity (iii) assessment of root mass should be of oven-dried roots, and
- the length of the trial to allow adequate development of symptoms.

6.3 Leaf Pigment content

Significant differences were observed in the total chlorophyll concentration and chlorophyll a / chlorophyll b ratio between varieties as expected. The chlorophyll a / chlorophyll b ratio is not an indicator of plant stress, but highlights the natural variation in pigment content between grapevine cultivars. The ratio changes with different plant species and demonstrates whether a plant is adapted to growing in high light conditions or prefers shaded positions. Changes in canopy management, for example, could influence this ratio. This needs to be taken into consideration when investigating commercial vineyards growing different varieties or with varying canopy management strategies in place.

The pigments and pigment ratios chosen to include in this investigation as indicators of plant stress include: total chlorophyll (chlorophyll a + chlorophyll b); total carotenoids (neoxanthin + violaxanthin + antheraxanthin + lutein + zeaxanthin + α-carotene + β-carotene); total carotenoids to total chlorophyll ratio; the xanthophyll cycle pigments ratio (antheraxanthin + zeaxanthin to violaxanthin + antheraxanthin + zeaxanthin) xanthophyll pigments to total chlorophyll ratio (violaxanthin + antheraxanthin + zeaxanthin to total chlorophyll) and β-carotene to total chlorophyll ratio. Total chlorophyll is an accepted indicator of plant stress (Gitelson *et al*., 2003). The carotenoid pigments and xanthophyll cycle pigment ratios were chosen because of their role in protecting the photosynthetic apparatus from photooxidation which can occur under stress conditions. These pigments are commonly used by other authors as indicators of stress (Chaumont *et al*., 1997,Young and Britton, 1990). The xanthophyll cycle pigments can be used to assess short term stress events and total carotenoid content or β-carotene can be used to measure longer term stress events (S. Robinson, personal communication). The same pigments and ratios are used during analysis of both the stress detection glasshouse and field studies (Section 2).

The two varieties appeared to respond differently to both stress treatments and phylloxera infestation, as reflected by the different, significant changes in pigment concentration and pigment ratios for each variety. Significant differences were

recorded between treatments in total chlorophyll, total carotenoid and β-carotene to total chlorophyll ratio for the Cabernet Sauvignon variety but not the Shiraz variety. Significant differences were recorded for the phylloxera infested and healthy control treatment for the Shiraz variety but not the Cabernet Sauvignon. This is surprising because lower phylloxera numbers were observed on the Shiraz vines compared to the Cabernet Sauvignon at the end of the trial. Differences in the phylloxera population could be attributable to the difference in the age of the grapevines when the trial commenced. This could have affected the root morphology and phylloxera establishment and development rate.

Increases in the relative concentration of carotenoids with respect to chlorophyll are often observed when plants are subjected to stress (Penuelas and Filella, 1998). A trend was observed towards the stress treatments and phylloxera infested treatments having higher ratios. This may have become more significant over time as the total carotenoid to total chlorophyll ratio is an indicator of long term stress events.

The pigments of the xanthophyll cycle did not show an increase in the antheraxanthin and zeaxanthin concentrations as predicted, however this ratio changes quickly over the course of one day and is particularly affected by high light conditions. The time of day the samples were collected could have affected this ratio as sample collection for HPLC analysis was taken after leaf reflectance measurements were taken from the same leaf and it took most of the day to collect samples from all 96 grapevines included in the trial. Samples collected during the morning and late afternoon would have lower ratios then those collected between 11:00am and 1:00pm, the ideal sampling time. Samples analysed are not an accurate representation of the changes expected under high light conditions for stressed grapevines. The artificial lighting used in the glasshouse could also affect the pigment ratio because they may not subject plants to light levels as high as would occur naturally when the sun reaches its zenith, so would not give an accurate level of xanthophyll cycle pigment concentration.

Grapevines included in the stress detection evaluation glasshouse trial exhibited general symptoms of plant stress by the end of the trial as shown by reduced vigour and the deviation in pigment concentration and pigment ratios from the healthy control treatments. Where pigment ratios were not showing predicted changes it was attributable to experimental error which could not be overcome because the restricted size of the glasshouse allowed only low numbers of replicates to be included in the trial. A distinct phylloxera infested symptom was not identified however this was possibly due to the large variation in phylloxera numbers observed at the end of the trial on the phylloxera treated grapevines and the length of the experiment.

Future glasshouse screening for the effect of phylloxera infestation on grapevine pigments compared to other stresses should take into account:

- the population density on the grapevine roots needed to produce a symptom;
- the method of implementing water stress and assessing the degree of severity;
- the length of the trial to allow adequate development of symptoms and
- the effect of artificial lighting on leaf pigments.

6.4 Spectral Reflectance Profiles

The following are conclusions and recommendations based on the spectral analysis component of the project.

There is still much to be done before remote sensing can be used operationally to detect phylloxera infestation in Australian vineyards without the need for ground-based verification. These investigations have shown that, in terms of key spectral regions, phylloxera affects grapevine spectral response in similar manner to dehydration and nitrogen deficiency. To date, no regions unique to phylloxera infestation have been identified. Discriminant analysis has been demonstrated to exploit reflectances in the identified spectral regions by different amounts to successfully separate (classify) the stresses.

Discriminant analysis needs to be "trained" on reflectance data belonging to specific stress groups – operationally difficult to do. It is recommended that the same analysis be done over much greater range of grapevine samples under different sets of environmental conditions. The same spectral regions need to be identified for a much larger range of samples. The boot strapping exercise described above assumes the samples investigated are a representative of the larger population, which is certainly not the case.

The emphasis of analysis of certain wavelength regions for the separation of certain stress groups over others suggests a close relationship with leaf chemical composition. These results need to be analysed in conjunction with a leaf chemical analysis (e.g. HPLC) to establish a causal link.

We have demonstrated the potential for hyperspectral data to detect subtle changes at the leaf-level that can be used in pre-visual detection of grapevine stress. However, a remotely-sensed signal is a contribution of leaf- and canopy-level reflectances, as well as other environmental factors (shadow, soil, atmosphere etc.). It may be of interest to explore the use of hyperspectral remote sensing data for the early detection of vineyard stress. One may also consider modelling the canopy-leaving reflectance spectra with radiative transfer models to see if subtle changes at the leaf level propagate to the remotely-sensed signal.

Finally, reflectance spectra are only one source of remotely-sensed information. Future research may consider integrating reflectance data with other sources of information to improve classification/detection of grapevine stress. Other sources of remotely-sensed information may include maps of: soil type and profile, soil moisture, surface temperature, and terrain elevation. Another potentially useful source of information may be historical data, e.g. previous surveys, which can be incorporated into the classification scheme.

6.5 NMR Fingerprinting

Principal component analysis of ^{1}H NMR spectra of dichloromethane extracts from grape leaves has shown that phylloxera infestation causes identifiable changes to the metabolic profile of Cabernet Sauvignon and Pinot Noir vines grown in the field. These differences are detectable at each stage of the growing season. The most obvious changes are in the degree of unsaturation and in the chain length of the fatty acids that constitute the triglyceride fractions of the extracts. Investigation of Shiraz vines grown in the glasshouse reveals that these characteristics also change when grapevines are subjected to water or nitrogen stress but these changes can be distinguished from those induced by phylloxera infestation.

Additional possible indicators of infestation were found, two compounds, α-linalool and an unknown compound, from Cabernet Sauvignon and one unknown compound from Pinot Noir. The occurrence of these compounds is transient, being limited to particular (different) stages of the growing season. Additionally, phylloxera infestation was associated with a decrease to near zero levels of an unknown compound that was found in the extracts of leaves from healthy Cabernet Sauvignon vines, collected in January and March 2004. Further investigation by fractionation of the extract by preparative chromatography is required to identify these unknown compounds. The identification of α-linalool as a possible marker was done using a limited number of extracts and this finding should be verified with a larger sample size. Signals belonging to the two unknown compounds were not visible in any spectra from the glasshouse trial and so these trials did not give any information on whether the unknown compounds are specific indicators of phylloxera infestation or are merely symptomatic of grapevine stress. The occurrence of α-linalool may be a general reaction to stress as it was found in one water-stressed grapevine (and one phylloxera infested grapevine without other stresses) but this needs to be investigated further, with a more extensive glasshouse experiment.

The original aim of this research was to identify potential markers that could be detected by more widely available analytical methods such as GC or HPLC. The complications introduced by changes in the metabolite profile of all grapevines throughout the growing season and from season to season and upon storage of the leaves, in addition to the transient nature of some of the markers found, prevent the

establishment of a meaningful universal metabolite profile for a healthy or an infested grapevine. This necessitates that extracts must be compared only with others prepared simultaneously from grapevines collected at the same time and so for large-scale comparisons of many extracts, ^{1}H NMR spectroscopy followed by PCA remains as the most convenient method of doing such analysis. However, an HPLC method for the detection of α-linalool in grape leaf extracts should be developed, as any occurrence of α-linalool should be treated as, at least, a sign of a stressed grapevine and, as it appears early in the growing season, may detect stress well before the grapevines exhibit any visible symptoms. Similarly, the measurement of the linolenic/linoleic acid ratio, which appears to be a general indicator of grapevines stress) could be achieved by GC (after hydrolysis of the triglyceride and derivatisation of the resulting acids) or HPLC (which would probably require a specialised column and detector) but NMR may still prove to be the most efficient method for comparing this ratio between extracts as no threshold value for the ratio needs to be chosen.

The analysis of leaf extracts was chosen for this research to complement the investigation of leaf pigments by HPLC and visible spectrometry in other parts of the project. To date only dichloromethane, which would be expected to best extract the majority of pigments, has been used as an extraction solvent. The use of a more polar solvent would allow the observation of other potentially interesting compounds, such as phenolics, and may prove fruitful. However, as drying and extraction of the leaves are extremely time consuming and constitute a considerable fraction of the experimental time, the investigation of fruit, in particular the juice from the fruit, would avoid the need for those stages of the experimental method. The metabolic changes observed in grape leaves upon infestation with phylloxera suggest that such changes may take place throughout the plant and that the presence of a chemical fingerprint of infestation in grape juice is quite possible. The juice obtained from crushing a single grape could be quickly filtered (if necessary) and directly placed in an NMR tube (or a flow NMR system could be employed) greatly reducing preparation time. The NMR procedure would be slightly more complex as solvent suppression of water would be required but this is a straight forward process.
Should a chemical marker of infestation be found in grape juice and a satisfactory method of its analysis developed, juice could be collected for testing when it is produced during the crush in the winemaking process, simplifying the sampling procedure and avoiding the quarantine issues involved with leaves. Of course, any markers would be likely to be present in very low concentrations as the juice from infested grapevines would be diluted by juice from healthy grapevines and so would require a more sensitive analytical technique such as LCMS for the trace detection of the compounds originally identified by the NMR procedure.

6.6 An integrated approach to phylloxera detection

The outcomes of this research have shown that, whilst there is no simple solution to phylloxera detection, the use of an integrated approach, using spectral, chemical and pigment fingerprinting is clearly warranted and is much more sensitive than the conventional approaches. The methods used here do demonstrate that with further refinement the opportunity exists to develop more targeted approaches to area-wide surveillance and detection of phylloxera. Hyperspectral sensors, which are currently limited in their commercial availability, are being developed for both airborne and satellite systems for the foreseeable future and are being used for monitoring of the physiological status of crops. Our study has shown that with ground-based sensors at the leaf level certain spectral wavebands are clearly associated with vine stress. This can be related to changes in specific pigment ratios and aid in the detection of phylloxera. However, even though the system is more sensitive than currently used multispectral systems, further refinement in the use of hyperspectral sensors is required to utilise this system at a canopy level for phylloxera detection. Chemical fingerprinting using nuclear magnetic resonance has identified some potential chemical markers that may be unique to phylloxera infestation. However this particular area of research requires further validation under controlled conditions and would also benefit from the application of the more sophisticated statistical treatment that was applied to the data from spectral reflectance measurements.

Appendix 1: Communication

(*bold text denotes project staff)

Scientific Publications (refereed)

Blanchfield, A.L., Robinson, S.A., **Renzullo, L.J.** & **Powell, K.S.** (2006) 'Phylloxera-infested grapevines have reduced chlorophyll and increased photoprotective pigment content – can leaf pigment composition aid pest detection?' *Functional Plant Biology,* **33,** 507 - 514.

Blanchfield, A.L., Robinson, S.A., **Renzullo, L.J. & Powell, K.S.** (2006) Preliminary investigations of pigment responses to phylloxera infestation. *Acta Horticulturae* (submitted).

Renzullo, L. J., Blanchfield, A. L., Guillermin, R., **Powell, K. S.** & **Held, A. A**. (2006) 'Comparison of Prospect and HPLC estimates of leaf chlorophyll contents in a grapevine stress study', *International Journal of Remote Sensing*, **27**, 817-823

Renzullo, L. J., Blanchfield, A. L. & Powell, K. S. (2006) 'A method of wavelength selection and spectral discrimination of hyperspectral reflectance spectrometry', *IEEE Transactions on Geoscience and Remote Sensing,* accepted Dec 2005.

Renzullo, L.J., Blanchfield, A.L., Powell, K.S (2006) Insights into the early detection of grapevine phylloxera (*Daktulosphaira vitifoliae* Fitch) from *in situ* hyperspectral data. *Acta Horticulturae* (submitted).

Tucker, D.J., Powell, K.S., Lamb, D.W., Murison, R.D., Blanchfield, A.L. & Brereton, I.M. (2006) Detection of phylloxera infestation in grapevines by NMR. *Acta Horticulturae* (in prep.)

Research Conference, Seminars, Workshop Presentations and Technical Reports (non-refereed)

Renzullo, L., Held, A., Powell, K. & **Blanchfield, A.** (2004) Investigations into the Early Detection of Phylloxera Infestation using Remotely-sensed and Field Spectrometry In *Proc 22nd International Congress on Entomology*, Brisbane, Qld.

Blanchfield, AL; Renzullo, LJ; Robinson, SA; Powell KS (2005) Linking leaf pigment composition and reflectance spectra as a means of fingerprinting grapevine phylloxera In *Proc 7th International Symposium on Aphids,* Fremantle, WA.

Renzullo, L.J., Blanchfield, A.L., Powell, K.S. (2005) Insights into the early detection of grapevine phylloxera infestation using *in situ* hyperspectral data. In *Proc 3rd International Phylloxera Symposium*, Fremantle, WA.

Seminars

Blanchfield, A.L. (2004) How stressed is it? Detecting the subtle, early signs of plant stress. DPI Rutherglen Centre Seminar Series 2004.

Renzullo, L., Blanchfield, A., Powell, K., Held, A. & **Barrett, D.** (2005), '*Variable Selection and Discrimination in Vineyard Spectrometry'*, CSIRO Earth Observation Centre, Annual Science Meeting, 8-10 March, Hobart, Tasmania.

Renzullo, L.J. (2005) 'The Spectral Fingerprint of Phylloxera Infestation and Other Grapevine Stresses', invited presentation, CRC for Greenhouse Accounting, Weekly Seminar Series, 11 April, Australian National University, Canberra, ACT.

Tucker, D.J. (2004) Detection of Phylloxera Infestation in Grapevines using NMR Methods, invited presentation, 29 October, School of Biological, Biomedical and Molecular Sciences, University of New England, Armidale, NSW.

Posters & Conference Proceedings

Blanchfield AL, Renzullo LJ, Robinson SA & Powell KS (2005) Investigating pigment changes as indicators of phylloxera infestation in Proc *The 15th Biennial Australasian Plant Pathology Society Conference Handbook "Innovations for sustainable plant health*", Geelong, Vic.

Blanchfield AL, Renzullo LJ, Robinson SA & Powell KS (2005) Identification of unique pigment responses to phylloxera infestation in *Proc 3rd International Phylloxera Symposium,* Fremantle, WA.

Blanchfield A.L., Renzullo L.J., Powell K.S. & Robinson S.A. (2006) Early detection of grapevine phylloxera by linking leaf pigment composition with reflectance spectra at Cool Climate Symposium, Christchurch, NZ.

Frazier, P., Whiting, J., **Lamb, D.W.**, & **Powell, K.** (2004) Characterising the development of grape phylloxera infestation with multi-temporal near-infrared aerial photography. in *Proc 12th Australian Wine Industry Technical Conference* (Australian Wine Industry Technical Conference Inc.), Melbourne, Vic.

Powell, KS, Tucker, DJ, Lamb DW, Murison RD, Blanchfield AL, & Brereton IM (2005) Detection of phylloxera infestation in grapevines by NMR methods in Proc *The 15th Biennial Australasian Plant Pathology Society Conference Handbook "Innovations for sustainable plant health*", Geelong, Vic.

Renzullo, L., Held, A., Powell, K. & Blanchfield, A. (2004) Characterising grapevine spectral response to phylloxera infestation. in *Proc 12th Australian Wine Industry Technical Conference* (Australian Wine Industry Technical Conference Inc.), Melbourne, Vic.

Renzullo LJ, Blanchfield AL, Powell KS (2005) Discriminant analysis: A tool for the spectral fingerprinting of grapevine stress including phylloxera at *CRC for Viticulture Symposium*, Mildura, Vic. * note Third Prize poster award.

Tucker, D.J., **Brereton, I.M.**, **Murison, R.D.**, **Powell, K.**, **Lamb, D.W. & Held A.A.** (2004) Detection of phylloxera infestation in grapevines using NMR methods at ANZMAG 2004 (5th Biennial Conference of the Australian and New Zealand Society for Magnetic Resonance), Barossa Valley, SA.

Tucker, D.J., Lamb, D.W., Murison, R.D., Powell, K., Blanchfield, A. & Brereton, I.M. (2004) Detection of phylloxera infestation in grapevines using NMR methods. in *Proc 12th Australian Wine Industry Technical Conference* (Australian Wine Industry Technical Conference Inc.), Melbourne, Vic.

Tucker, D.J., Lamb, D.W., Murison, R.D., Powell, K., Blanchfield, A. & Brereton, I.M. (2005) Detection of phylloxera infestation in grapevines using NMR methods at *CRC for Viticulture Symposium,* Mildura, Vic.

Tucker, D.J., Powell, K.S., Lamb, D.W., Murison, R.D., Blanchfield, A.L. & Brereton, I.M. (2005) Detection of phylloxera infestation in grapevines by NMR in *Proc 3rd International Phylloxera Symposium,* Fremantle, WA.

Tucker, D.J., Powell, K.S., Lamb, D.W., Murison, R.D., Blanchfield, A.L. & Brereton, I.M. (2006) Detection of phylloxera infestation in grapevines by NMR Cool Climate Symposium, Christchurch, NZ.

Tucker, D.J., Powell, K.S., Lamb, D.W., Murison, R.D., Blanchfield, A.L. & Brereton, I.M. (2006) Detection of phylloxera infestation in grapevines by NMR methods at ANZMAG 2006 (6th Biennial Conference of the Australian and New Zealand Society for Magnetic Resonance), Murramarang, NSW.

Workshops

Blanchfield, A.L. Early detection of grapevine stress symptoms and pests using reflectance spectrometry. Presentation at four National Phylloxera Management and Idenfication Workshops, three in Jan 2005, one in Jan 2006.

Powell, K.S. Early detection of grapevine phylloxera in ungrafted vineyards. Presentation at two National Phylloxera Management and Identification Workshops, Dec 2005, Jan 2006

Renzullo, L.J. Early detection of grapevine phylloxera using reflectance spectrometry. Presentation at two National Phylloxera Management and Identification Workshops, Jan 2004.

Technical Reports and Industry Journal articles (non-refereed)

Edwards, J., Lewis, M., **Powell, K.**, Hackworth, P. & **Lamb, D.W**. (2004), Identification of Phylloxera from high-resolution aerial imagery: a comparative study between airborne imagery types. *Australian Grapegrower & Winemaker, **488**, 51-54*.

Frazier, P., Whiting, J., **Powell, K. & Lamb, D.W.** (2004) Characterising the development of grape phylloxera infestation with multi-temporal near-infrared aerial photography, *Australian Grapegrower & Winemaker, Annual Technical Edition*, 133-136

Renzullo, L., Held, A., **Powell, K. & Blanchfield, A.** (2004). Remote sensing phylloxera infestation: current capabilities and future possibilities for early detection. *The Australian and New Zealand Grapegrower and Winemaker* (32nd Annual Technical Issue), 126-130. (**Corrections** to Fig. 7. published in August Issue of *Grapegrower and Winemaker* 2004)

Reprints of Publications

International Journal of Remote Sensing
Vol. 27, No. 4, February 2006, 817–823

Taylor & Francis
Taylor & Francis Group

Comparison of PROSPECT and HPLC estimates of leaf chlorophyll contents in a grapevine stress study

L. J. RENZULLO*†‡, A. L. BLANCHFIELD†§, R. GUILLERMIN¶,
K. S. POWELL†§ and A. A. HELD‖

†Cooperative Research Centre for Viticulture, PO Box 154, Glen Osmond, SA 5064, Australia

‡CSIRO Land and Water, GPO Box 1666, Canberra, ACT 2601, Australia

§Primary Industries Research Victoria (PIR Vic), Department of Primary Industries, Rutherglen Centre, RMB 1145 Chiltern Valley Road, Rutherglen, Victoria 3685, Australia

¶Institut National des Sciences Appliquées de Strasbourg, 24 Boulevard de la Victoire, 67084 Strasbourg Cedex, France

‖CSIRO Office of Space Science and Applications, GPO Box 3023, Canberra, ACT 2601, Australia

(*Received 10 May 2005; in final form 23 June 2005*)

This letter describes how PROSPECT, updated with a 1 nm chlorophyll absorbance database, was used to infer total chlorophyll content from the measured reflectance spectra of grapevine leaves. Modelled and measured reflectance spectra agreed on average to within 13% over the range 400–1600 nm. However, discrepancies between modelled and measured reflectances of up to 40% were observed in the spectral region dominated by chlorophyll content. In terms of estimating total chlorophyll content, PROSPECT gave estimates that were on average within 10 $\mu g\,cm^{-2}$ of those obtained using high performance liquid chromatography.

1. Introduction

Leaf radiative transfer (RT) models (e.g. PROSPECT of Jacquemoud and Baret 1990, Leaf Incorporating Biochemistry Exhibiting Reflectance and Transmittance Yields (LIBERTY) of Dawson *et al.* 1998, Stochastic model for Leaf Optical Properties Extended for fluorescence (SLOPE) of Maier 2000, and Fluorescence–Reflectance–Transmittance (FRT) model of Zarco-Tejada *et al.* 2002) are useful tools to investigate the effects that variation in leaf pigment and chemical composition, as well as structural properties, will have on leaf reflectance and transmittance spectra. Perhaps the best demonstration of the utility of leaf RT models is when coupled with canopy RT models to simulate the top-of-canopy reflectance as observed by a wide range of remote sensing systems (Jacquemoud *et al.* 1995). For the study to be described in the following, the modelling of leaf-level effects on reflectance spectra is of interest.

*Corresponding author. Email: Luigi.Renzullo@csiro.au

International Journal of Remote Sensing
ISSN 0143-1161 print/ISSN 1366-5901 online © 2006 Taylor & Francis
http://www.tandf.co.uk/journals
DOI: 10.1080/01431160500239164

One of the most desirable features of leaf RT models is that they may be used as a non-destructive method of inferring estimates of pigment concentration from measured reflectance spectra. The most important pigments in the analysis of plant stress with remote sensing technologies are chlorophyll *a* and *b* (Zarco-Tejada *et al.* 2002). It is the purpose of this letter to describe how the PROSPECT model was modified and adapted to the estimation of total leaf chlorophyll content (i.e. chlorophyll $a+b$) from measured reflectance spectra of a grapevine stress study. The estimates obtained are compared to those measured using high performance liquid chromatography (HPLC).

2. Data acquisition

The data in this letter were collected as part of a project investigating the remote sensing of grapevine phylloxera infestations in Australian vineyards (Renzullo *et al.* 2004). From March to June 2004, an experiment was conducted which aimed to monitor changes in leaf spectral response for two varieties of *Vitis vinifera* (referred to here as Cabernet Sauvignon and Shiraz) that were subjected to various stresses in a controlled glasshouse environment. Eight vines of each variety were set aside as the healthy (H) control group, while a further eight were subjected to one of the following stresses: water stress (W), caused by reducing the amount of water supplied to the vine; nitrogen deficiency (N), achieved by withholding application of ammonium nitrate; and phylloxera infestation (P), where 20 phylloxera eggs were attached by a nylon gauze fabric to one medium-sized feeder vine root (Burns and Powell 2005). Double-stressed groups were formed by subjecting vines to phylloxera infestation and either water stress (PW) or nitrogen deficiency (PN). Finally the vines were arranged in a randomized block design generated using GenStat 6.1 (GenStat 2005).

Reflectance measurements were recorded on six dates over a nine-week period with an Analytical Spectral Devices FieldSpec® Pro FR spectroradiometer (ASD 2005). A LiCor integrating sphere attachment was also used to allow collection of stable bi-hemispherical reflectance measurements that were independent of variations in ambient light conditions. The integrating sphere further provided a consistent, fixed set of geometries with which leaf samples were viewed and illuminated. Although the spectrometer has a broad spectral sensitivity, only those reflectance values within the wavelengths region 400–1600 nm were used in this investigation, due to the low intensity of the halogen lamp in the ultraviolet (UV) and short-wave infrared (SWIR) wavelength regions (figure 1(*a*)). Over 2300 reflectance spectra were measured over the course of the experiment. For brevity, only the measurements acquired at the end of the experiment are considered.

For leaves whose reflectance spectra were measured, leaf disks were collected using a cork borer (1.4 mm diameter) and immediately frozen in liquid nitrogen for subsequent pigment analysis by HPLC. Ground leaf tissue samples were added to 100% acetone solution and the method of pigment extraction and quantification followed that described by Dunn *et al.* (2004) with minor modifications. The final concentrations of total chlorophyll content derived from the HPLC analysis were transformed into a mass per area ($\mu g\,cm^{-2}$) for consistency with units used in PROSPECT. The distribution of total chlorophyll content values for the two grape varieties is presented in figure 1(*b*).

In total there were 96 reflectance measurements, each with an associated value of total chlorophyll content.

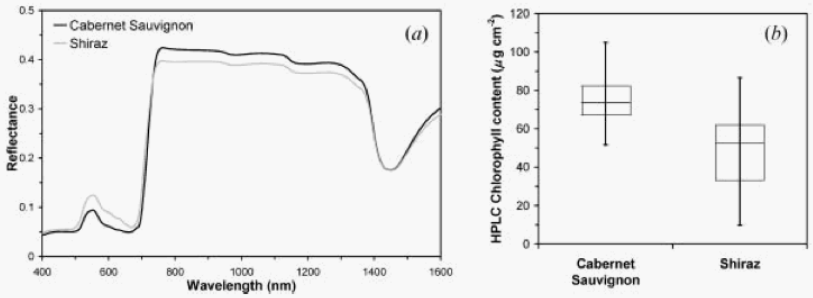


Figure 1. Summary of the data acquired during a glasshouse experiment from Cabernet Sauvignon and Shiraz grapevine varieties: (*a*) mean reflectance curves; and (*b*) the distribution of HPLC estimates of total chlorophyll content ($\mu g\,cm^{-2}$) (centre line marks the median value, 25% and 75% quartiles are the bottom and top of the box, respectively, while minimum and maximum values are the ends of the whiskers).

3. Comparative analysis

The PROSPECT model of Jacquemoud and Baret (1990) simulates leaf reflectance and transmittance over the range 400–2500 nm at 5-nm intervals. The first task was to modify the code to incorporate the 1 nm absorbance data of Jacquemoud (2004) to facilitate direct comparisons between spectra measured by the spectroradiometer and those simulated by PROSPECT.

The attraction to PROSPECT for this work includes its relative ease of use and demonstrated ability to provide accurate estimations of spectra with comparatively few input parameters. In this case, the reflectances and transmittances were modelled using estimates of total chlorophyll content (*Cab*, in $\mu g\,cm^{-2}$), leaf water content (*Cw*, in cm of water), dry matter content (*Cm*, in g cm^{-2}) and mesophyll structure parameter, *N*, which is effectively the number of layers in the plate model.

It was recognized that PROSPECT could be used to infer estimates of the four input parameters by minimizing the difference between measured and modelled spectra. In the absence of transmittance measurements, a procedure may be employed to obtain a fit between PROSPECT-modelled ($R_{\mathrm{modelled}i}$) and measured ($R_{\mathrm{measured}i}$) reflectance spectra that minimizes the merit function

$$\chi^2 = \sum_{i=1}^{p} \left(\frac{R_{\mathrm{modelled}i} - R_{\mathrm{measured}i}}{R_{\mathrm{measured}i}} \right)^2 \quad (1)$$

where *p* denotes the number of wavelength intervals between 400–1600 nm and the summand is the squared relative difference. The set of *Cab*, *Cw*, *Cm* and *N* values that resulted in the lowest χ^2 for each spectrum was deemed the 'best' set of input parameters. From these χ^2 values a root mean squared relative difference (RMSRD), calculated as $(\chi^2/p)^{1/2}$, may serve as a measure of the overall goodness of fit between 400–1600 nm. Investigations showed that the Levenberg–Marquardt method (Press and Vettering 1992) was a suitable procedure for minimizing equation (1) and, irrespective of the values used for the initial set of input parameters, the procedure converged rapidly to the same 'best' set (Guillermin 2004).

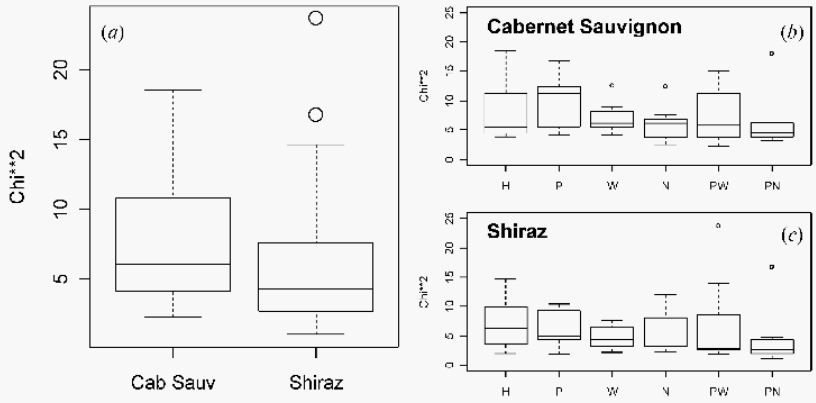


Figure 2. Distribution of χ^2 values for (*a*) all the Cabernet Sauvignon and Shiraz vines, and the individual groups of (*b*) Cabernet Sauvignon and (*c*) Shiraz vines, respectively. The χ^2 value represents a relative measure of fits between PROSPECT-modelled and measured reflectance spectra. Extreme values outside 1.5 times the interquartile range are represented as circles.

4. Results and discussion

The Levenberg–Marquardt minimization routine was applied to the 96 measured reflectance spectra. The distribution of χ^2 values for the two grape varieties and different groups (i.e. H, P, etc., §2) are displayed in figure 2. With the exception of one outlier (a chlorotic Shiraz vine) χ^2 values were less than 20, which corresponds to an RMSRD of 13%. Generally lower χ^2 values were observed for the Shiraz vines. It appears that PROSPECT was able to reproduce the sharper looking green-peak (500–700 nm) that was typically observed for the Shiraz rather than the Cabernet Sauvignon variety (figure 1(*a*)). In the same way, good fits were observed for the stressed groups of vines, particularly the PN (displayed in figure 3(*a*)), as green peak reflectances are generally higher in leaves of low chlorophyll content. For chlorotic leaves, however, poorer fits were observed (figure 3(*b*)).

The overall differences between PROSPECT-modelled reflectances relative to the measured reflectances are illustrated in figure 3(*c*). On average the relative difference over the range 400–1600 nm is around 12%, which is consistent with the calculated RMSRD above. The figure, however, also shows that discrepancies between modelled and measured reflectances of around 35–40% may be observed between 400–720 nm. Leaf chlorophyll content plays a dominant role in the reflected signal in this region. Whilst not directly relevant to the topic of this letter, wavelengths above 720 nm were of interest in other investigations on vine stress because of the reported chlorophyll fluorescence signatures around 760 nm (Zarco-Tejada *et al.* 2000, 2002) and leaf water content (970 and 1450 nm).

From the 'best' set of input parameters, the value of *Cab* formed a data pair with the corresponding estimate from HPLC analysis for each leaf. The modelled and measured values for both the Cabernet Sauvignon (CS) and Shiraz (Sh) leaves are displayed in figure 4. The figure shows a distribution of points for both grape varieties that is consistent with figure 1(*b*); the displayed coefficient of determination (R^2) reflecting the range of values for the individual datasets (CS and Sh), and the

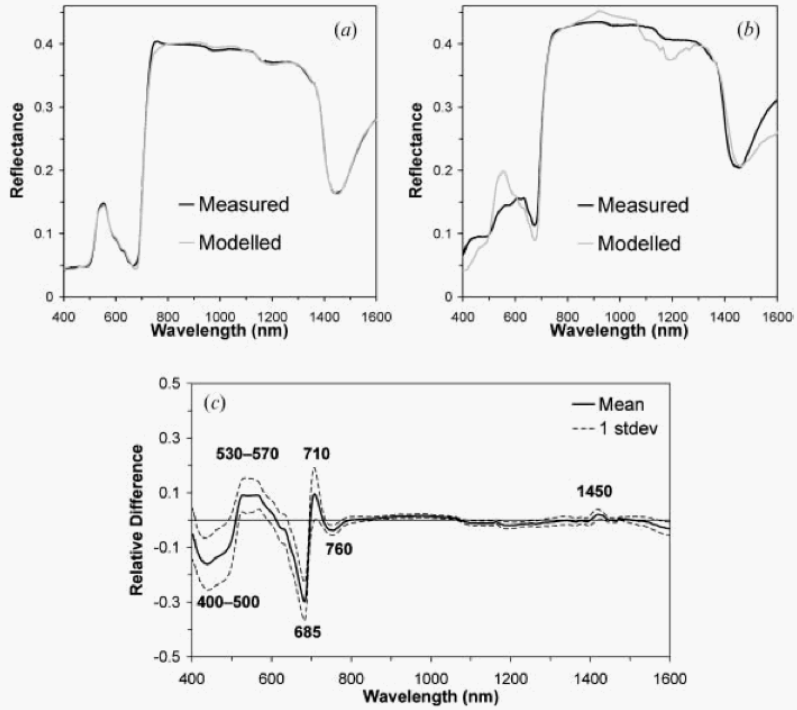


Figure 3. Examples of (*a*) the best and (*b*) the worst fit of the PROSPECT-modelled reflectance to that measured. (*c*) The relative difference between measured and modelled spectra averaged over all 96 estimates (solid line, dashed lines indicating one standard deviation limits). Some spectral regions of note are annotated on the figure.

combined dataset (CS + Sh). The root mean squared errors (RMSE) show that PROSPECT agreed with the HPLC estimates to an accuracy of similar magnitude previously reported (Jacquemoud and Baret 1990, Jacquemoud 2004). Furthermore, an uncertainty of around $\pm 10\,\mu g\,cm^{-2}$ is inside the order of the within-leaf variability often observed in this experiment (unpublished result). The least squares line of best fit of the combined dataset is displayed to show an overall trend that has also been previously observed (Zarco-Tejeda *et al*. 2002).

5. Conclusions

In spite of the complex nature of the biophysical interactions and processes occurring within a leaf that is exposed to light, the PROSPECT model was able to estimate grapevine leaf reflectance spectra that were on average within 13% of measured spectra. Furthermore, the model estimates of total chlorophyll content are within an uncertainty level acceptable for the described study of grapevine stress, and can thus be used to provide estimates of total chlorophyll content for the 2000 or so reflectance spectra for which we do not have HPLC measured values.

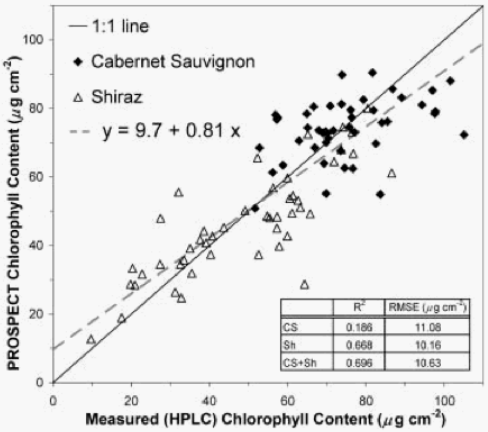


Figure 4. Total chlorophyll content estimates from PROSPECT model inversion and HPLC analysis for both Cabernet Sauvignon (CS, black diamonds) and Shiraz (Sh, triangles) vines. For the individual datasets and the combined dataset (i.e. CS + Sh) the coefficient of determination (R^2) and the root mean squared error (RMSE) are displayed. The 1 : 1 line (thin black solid curve) and least squares line of best fit to the combined dataset (dashed grey curve) are also displayed.

Much research has been devoted recently to incorporating chlorophyll fluorescence into leaf radiative transfer models, particularly in relation to pre-visual detection of plant stress (Maier 2000, Zarco-Tejada *et al.* 2000, 2002). The spectral regions most affected by fluorescence are consistent with the regions identified in this work as showing the greatest discrepancy between PROSPECT and the measured spectra (i.e. 685 and 760 nm). It is therefore expected that a significant improvement in the model will result with the addition of fluorescence signature to the model.

Acknowledgments

This research was supported by the Commonwealth Cooperative Research Centre Program and conducted through the CRC for Viticulture with support from Australia's grapegrowers and winemakers through their investment body the Grape and Wine Research and Development Corporation, with matching funds from the Federal Government.

References

ASD, 2005, FieldSpec® Pro product specifications. Available on line at: http://www.asdi.com/products_specifications-FSP.asp (accessed 14 June 2005).

Burns, A.E. and Powell, K.S., 2005, A novel approach for rapid screening of grapevine rootstocks for resistance to grape phylloxera. *Australian Journal of Grape and Wine Research* (submitted).

Dawson, T.P., Curran, P.J. and Plummer, S.E., 1998, LIBERTY—modeling the effects of leaf biochemical concentration on reflectance spectra. *Remote Sensing of Environment*, **65**, pp. 50–60.

Dunn, J.L., Turnbull, J.D. and Robinson, S.A., 2004, Comparison of solvent regimes for the extraction of photosynthetic pigments from leaves of higher plants. *Functional Plant Biology*, **31**, pp. 195–202.

GENSTAT, 2005, GenStat product details. Available online at: http://www.vsn-intl.com/genstat/gsprod_details.htm (accessed 14 June 2005).

GUILLERMIN, R., 2004, Etude des effets de l'infestation du Phylloxéra sur l'espèce Vitis Vinifera par analyse statistique de paramètres optiques et chimiques dérivés du modèle PROSPECT de la feuille. Department of Civil Engineering and Topography, Strasbourg, Institut National des Sciences Appliquées de Strasbourg: 76.

JACQUEMOUD, S., 2004, New calibration of PROSPECT, unpublished report.

JACQUEMOUD, S. and BARET, F., 1990, PROSPECT: a model of leaf optical properties spectra. *Remote Sensing of Environment*, **34**, pp. 75–91.

JACQUEMOUD, S., BARET, F., ANDRIEU, B., DANSON, F.M. and JAGGARD, K., 1995, Extraction of vegetation biophysical parameters by inversion of the PROSPECT + SAIL models on sugar beet canopy reflectance data. Application to TM and AVIRIS Sensors. *Remote Sensing of Environment*, **52**, pp. 163–172.

MAIER, S.W., 2000, Modeling the radiative transfer in leaves in the 200 nm to 2.5 μm wavelength region taking into consideration chlorophyll fluorescence—the leaf model SLOPE. PhD thesis, Technische Universität München, Germany.

PRESS, W.H. and VETTERING, W.T., 1992, *Numerical Recipes in FORTRAN: The Art of Scientific Computing*, pp. 1–963 (Cambridge: Cambridge University Press).

RENZULLO, L., HELD, A., POWELL, K. and BLANCHFIELD, A., 2004, Remote sensing phylloxera infestation: current capabilities and future possibilities for early detection. *Australian and New Zealand Grapegrower and Winemaker, 32nd Annual Technical Issue*, No. 485a, pp. 126–130.

ZARCO-TEJADA, P.J., MILLER, J.R., MOHAMMED, G.H., NOLAND, T.L. and SAMPOSON, P.H., 2000, Chlorophyll fluorescence effects on vegetation apparent reflectance: II. Laboratory and airborne canopy-level measurements with hyperspectral data. *Remote Sensing of Environment*, **74**, pp. 596–608.

ZARCO-TEJADA, P.J., MILLER, J.R., MOHAMMED, G.H., NOLAND, T.L. and SAMPSON, P.H., 2002, Vegetation stress detection through chlorophyll a + b estimation and fluorescence effects on hyperspectral imagery. *Journal of Environmental Quality*, **31**, pp. 1437–1441.

CSIRO PUBLISHING
www.publish.csiro.au/journals/fpb *Functional Plant Biology*, 2006, **33**, 507–514

Phylloxera-infested grapevines have reduced chlorophyll and increased photoprotective pigment content — can leaf pigment composition aid pest detection?

Annette L. Blanchfield[A,B], *Sharon A. Robinson*[C,E], *Luigi J. Renzullo*[B,D] *and Kevin S. Powell*[A,B]

[A]Primary Industries Research Victoria, Department of Primary Industries, Rutherglen Centre, RMB 1145, Chiltern Valley Road, Rutherglen, Vic. 3685, Australia.
[B]Cooperative Research Centre for Viticulture, PO Box 154, Glen Osmond, SA 5064, Australia.
[C]Institute for Conservation Biology, Department of Biological Sciences, University of Wollongong, Wollongong, NSW 2522, Australia.
[D]CSIRO Land and Water, GPO Box 1666, Canberra, ACT 2601, Australia.
[E]Corresponding author. Email: sharonr@uow.edu.au

This paper originates from a presentation at ECOFIZZ 2005, North Stradbroke Island, Queensland, Australia, November 2005.

Abstract. Grape phylloxera (*Daktulosphaira vitifoliae* Fitch) is a root-feeding pest of grapevines. In Australia, phylloxera-infested vineyards are subjected to quarantine restrictions and early detection remains vital for the timely implementation of post-outbreak quarantine protocols. Current detection methods rely on time-consuming ground surveying, which involves detailed examination of grapevine (*Vitis vinifera* L.) root systems. Leaf pigment composition is often a sensitive indicator of plant stress. The increasing popularity of remote sensing systems, which exploit those changes in pigments observed with plant stress, offers a real possibility for the development of a phylloxera-specific remote detection system. Our objective was to investigate changes in grapevine leaf pigments associated with phylloxera infestation and to relate any changes to appropriate reflectance indices. This was achieved with a glasshouse experiment in which the responses of two vine cultivars (Cabernet Sauvignon and Shiraz) to phylloxera infestation were compared with their responses to water and nitrogen deficiencies. The responses of leaf pigments to phylloxera infestation were also investigated in Pinot Noir and Cabernet Sauvignon grapevines grown under field conditions. A reduction in the leaf chlorophyll content and an increase in photoprotective pigment concentrations were observed in leaves of phylloxera-infested grapevines compared with uninfested vines. The photochemical reflectance index (PRI) was found to be most closely associated with the ratio of total carotenoid to chlorophyll in these vines.

Keywords: β-carotene, carotenoids, chlorophylls, phylloxera, phylloxera detection, xanthophyll cycle pigments.

Introduction

Grape phylloxera is a root-feeding member of the Aphidoidea super family. Feeding on the roots of grapevines, it causes the formation of galls and feeding sites can also act as access points for secondary fungal infections (Omer *et al*. 1995). The resulting damage to and decay of the root system causes a reduction in yield and quality of grapes, making phylloxera an insect pest of economic significance to viticultural industries worldwide. In Australia, phylloxera-infested vineyards are subjected to quarantine regulations.

Phylloxera outbreaks and infestations in the states of Victoria and New South Wales (NSW), both historically (late 19th century) and more recently (December 2003), have highlighted the Australian viticulture industry's vulnerability and the need for vigilance, awareness and on-going research into early detection. Owing to the cost of phylloxera-

Abbreviations used: A, antheraxanthin; β-car, β-carotene; Chl, chlorophyll$_{a+b}$; HPLC, high-performance liquid chromatography; L, lutein; N, neoxanthin; PIZ, phylloxera infested zone; PRI, photochemical reflectance index; Tcar, total carotenoid; V, violaxanthin; VAZ, xanthophyll cycle pigments; Z, zeaxanthin.

© CSIRO 2006 10.1071/FP05315 1445-4408/06/050507

resistant rootstock material, the shortage of supply and the extra cultural management required for grafted vines, the proportion of total vineyard area in Australia planted as own-rooted vines is unlikely to decrease appreciably over the next 20 years.

To date, detection methods have relied predominantly on ground surveying techniques, which involve detailed examination of the grapevine root system for the presence of insects and galls. However, ground surveying alone, which is still used in NSW, is by its very nature costly, time-consuming and not very effective (Herbert *et al*. 2003). Above-ground, symptoms of phylloxera-infested vines are expressed as premature yellowing of the leaves or canopy reduction. However, this may go unnoticed for 2–3 years, by which time there is irreversible and economically significant damage to the vines and a high risk of a breakdown in quarantine. In cases where a low-virulence phylloxera genotype is present it could take much longer than 3 years before visible symptoms are expressed (KS Powell personal observation).

In Australia, remote sensing techniques were first applied to phylloxera detection in Victoria in the mid-1990s with near-infrared aerial imagery (Frazier *et al*. 2004). Further improvements in remote sensing have led to the use of high-resolution multispectral imaging sensors for surveying large areas of South Australia (Edwards *et al*. 2004), reducing the costs associated with ground truthing by targeting 'weak spots' for ground inspection. According to the National Phylloxera Management Protocols (NVHSC 2003), viticulture regions must undertake expensive, labour-intensive ground surveys over three consecutive years in order to be eligible for 'phylloxera-free' status.

Current remote sensing methods for phylloxera detection use multispectral airborne sensors to detect visual changes in the grapevine canopy induced by stresses imposed on the root system by phylloxera feeding. While these systems highlight weak spots in vineyard blocks (Hall *et al*. 2002), such canopy variability is also caused by other abiotic or biotic variables such as water stress, nutrient deficiencies or drainage issues. Therefore, any positive identification of phylloxera infestation still requires follow-up ground surveying by the same protocol employed in the absence of a phylloxera-specific remote sensing system.

Leaf pigment composition is sensitive to plant stress, with a range of abiotic and biotic factors responsible for either loss of photosynthetic pigments (e.g. chlorophylls) or the production of photoprotective pigments [such as zeaxanthin or β-carotene (Demmig-Adams and Adams 1992)]. Changes in leaf pigment content of grapevines has previously been examined in response to growth light, water stress, cold-temperature stress and virus infection (Chaumont *et al*. 1997; Flexas *et al*. 2000, 2001; Maroco *et al*. 2002; Medrano *et al*. 2002; Sampol *et al*. 2003; Bertamini and Nedunchezhian 2004; Bertamini *et al*. 2004, 2005; Hendrickson *et al*. 2004). Chlorophyll and carotenoid content clearly acclimate to changes in growth light (Chaumont *et al*. 1995, 1997; Flexas *et al*. 2001; Medrano *et al*. 2002; Bertamini and Nedunchezhian 2004). However while significant reduction of chlorophyll content in response to drought has been shown in some studies (Flexas *et al*. 2000; Maroco *et al*. 2002) this is not a consistent response (Chaumont *et al*. 1997; Medrano *et al*. 2002). In addition, drought stress did not affect carotenoid composition in field-grown vines in contrast to other Mediterranean species (Demmig *et al*. 1988; Medrano *et al*. 2002). Virus-infected vines showed decreased chlorophyll, increased carotenoid / chlorophyll content and increased non-photochemical quenching (Sampol *et al*. 2003), which was attributed to xanthophylls-mediated heat dissipation (Balachandran *et al*. 1997). In general, grapevines maintain large pools of the photoprotective xanthophyll pigments and have been shown to utilise photoprotective heat dissipation via xanthophyll pigments to avoid photoinhibition (Chaumont *et al*. 1997; Medrano *et al*. 2002; Hendrickson *et al*. 2004).

Several studies have shown that changes in pigment composition are quantifiable as subtle changes in crop-level reflectance (Held and Jupp 1994; Nichol *et al*. 2000; Carter and Knapp 2001). In addition, specific spectral indices have been developed that correlate with plant stress indicators such as a decline in photosynthetic efficiency (Gamon *et al*. 1997; Lovelock and Robinson 2002). In grapevines attempts have been made to establish remote methodologies for determining water stress (Flexas *et al*. 2000; Evain *et al*. 2004).

The aim of this study was to investigate whether changes in grapevine leaf pigments occur before visible symptoms of phylloxera infestation. High-performance liquid chromatography (HPLC) was used to analyse the pigment content of field-grown, ungrafted *Vitis vinifera* leaf samples collected from commercial vineyards in Phylloxera Infested Zones (PIZ) in north-eastern Victoria, Australia. In a separate glasshouse experiment the response of grapevine pigments to infestation with phylloxera was compared with that produced by other stressors such as nitrogen or water deficiency. Pigment concentration and pigment ratios were compared for phylloxera-infested and uninfested grapevines with the aim of determining grapevine response to phylloxera infestation and to identify pigment changes that might provide additional tools for early detection of grapevine infestation, either as stand-alone markers or preferably to enhance the capability of remote sensing methodologies.

Materials and methods

Glasshouse experiment

Plant material

Three-year old rootlings of ungrafted *Vitis vinifera* L. cv. Shiraz, clone PT23 and ungrafted *V. vinifera* cv. Cabernet Sauvignon, clone LC10 were sourced from Boulevarde Nurseries, Mildura, Victoria,

Australia. The Shiraz vines were sourced one season before the Cabernet Sauvignon, hence were 4.5 years old at the commencement of the study, whereas the Cabernet Sauvignon were 3.5 years old. All plants were potted into 20-cm pots in a 3 : 1 ratio mix of potting mix and perlite and maintained in a shade-house on the premises of DPI Victoria, Rutherglen. 'Yates' Thrive (all purpose soluble fertiliser, Arthur Yates and Co. Limited, Homebush, NSW) was applied monthly; 8 g was dissolved in 4.5 L water, according to the manufacturer's recommendations. The final application was 1 month before the commencement of the trial. All plants were moved to a glasshouse 1 week before the commencement of the trial.

Trial design and infestation method

Eight vines of each variety were used for each treatment group (total 96 vines). The six treatments included unstressed control vines, nitrogen deficient, water deficient, phylloxera-infested, phylloxera-infested and nitrogen deficient, phylloxera-infested and water deficient. The control vines and vines without phylloxera treatment were replanted with fresh potting mix and placed back into their original pots. Plants were then supplemented with either 2 g ammonium nitrate or deprived of this fertiliser (termed 'nitrogen deficient'). All treatments received 2.5 g 'Yates' Trace Elements Essential Nutrients (Arthur Yates and Co. Limited). Each pot was sealed in a 53-µm mesh bag, secured at the base of the vine trunk and Tanglefoot™ was applied around the neck of the bag where it contacted with the vine trunk, to prevent phylloxera cross-contamination.

Vines to be infested were removed from their pots and one medium-sized lignified root was teased out. Phylloxera eggs of G4 genotype (Corrie *et al*. 2002) were sourced from excised root bioassays (de Benedictis and Granett 1993) maintained at DPI Victoria, Rutherglen laboratory and 20 eggs were placed on dampened filter paper strips ~40 × 15 mm. The filter paper was placed on polyamide gauze fabric of 53-µm mesh. The mesh was then rolled around the root, so the eggs were in contact with the root piece, and secured with cable ties and Tanglefoot™ was applied. Plants were repotted and received trace elements and nitrogen fertiliser, except for plants in the nitrogen-deficient treatment group, before being bagged, as before.

The plants were placed in a single glasshouse room and arranged in eight randomised blocks according to a 2 × 3 × 2 random factorial design created with GenStat (GenStat release 8.1, Lawes Agricultural Trust, UK). All plants except those of the water-deficient treatment groups were watered for 2 min daily with a drip irrigation system. Plants subjected to the water deficiency treatment were initially given half the water of the controls, however after the first week of the trial the watering regime for the water deficiency treatments was reduced to approximately one-third of that supplied to the control group. Plants were visually assessed for symptoms of severe water stress and were given additional water when required. The glasshouse was maintained at ~24°C throughout the day and 17°C overnight and was illuminated with Son-T Agro 400 globes (Philips, North Ryde, NSW) for 12 h daily, with an additional 1-h boost at 0200 h to maintain appropriate photoperiod. Leaf samples were collected 9 weeks after initial infestation. Leaf disks were collected with a cork borer of 1.4 cm diameter, and immediately frozen in liquid nitrogen for later HPLC analysis. Whole-leaf samples were collected for nitrogen content analysis. Leaves were oven-dried at 45°C for 48 h. Nitrogen content analysis was completed by CSIRO commercial testing laboratories, Canberra, Australia.

Field experiment

Field sites and varieties

Samples were also collected for pigment analysis from grapevines growing in two commercial vineyards in PIZs in north-eastern Victoria, Australia. Ungrafted *V. vinifera* cv. Cabernet Sauvignon vines were situated at a site in the Upton PIZ, where phylloxera was first detected in April 2000. Ungrafted *V. vinifera* cv. Pinot Noir vines were located at a second site in the Buckland Valley, where phylloxera was first detected in December 2003. Above-ground symptoms of phylloxera infestation, including reduced vigour and yield, were first noticed by vineyard staff. Sampling was conducted over the season from bunch closure (January) to just before harvest (March) in 2004. Four vines were identified in each of three rows in phylloxera-infested and uninfested areas at each field site. Phylloxera-affected vines chosen for sampling showed reduced vigour but not leaf chlorosis. Leaves of uniform size and green colour were collected between 1100 and 1500 h on clear, sunny days, from the side of the grapevine receiving maximal exposure to the sun. Leaf disks were collected with a cork borer of 1.4 cm diameter, and immediately frozen in liquid nitrogen for later pigment analysis by HPLC. Root samples were collected from each of the grapevines once during the growing season and examined with a binocular microscope to verify the phylloxera-infested or uninfested status of each vine included in the study.

Pigment extraction and quantification by HPLC

Pigments were extracted from vine leaves with three sequential acetone extractions (100% : 80% : 80%) following the methodology described by Dunn *et al*. (2004), and were quantified by HPLC according to the method of Gilmore and Yamamoto (1991) as described by Dunn *et al*. (2004) with a SphereClone 5-µm ODS1 column (Phenomenex, Sydney, NSW). Solvent A was adjusted to acetonitrile : methanol : Tris–HCL buffer 0.1 M, pH 8.0; 85 : 9 : 6, while Solvent B remained methanol : hexane 80 : 20.

Reflectance measurements

Individual leaf reflectance spectra of leaf samples collected from both glasshouse and the field were acquired with an ASD FieldSpec-Pro® spectroradiometer (Analytical Spectral Devices Inc., Boulder, CO) coupled with a Li-Cor Integrating Sphere (Li-Cor, Lincoln, NE) as described by Renzullo *et al*. (2004). The photochemical reflectance index [$PRI = (R531 - 570) / (531 + 570)$; Gamon *et al.* 1997] was calculated for each sample.

Statistical analysis

Differences in pigment content and pigment ratios as a function of variety, phylloxera infestation and treatment (glasshouse trial only) were analysed by analysis of variance (ANOVA) with Genstat. ANOVA was used to compare nitrogen content of leaves from each treatment group (glasshouse trial only). Linear regression was used to examine the association between the PRI and relative leaf carotenoid composition (including Tcar / Chl, β-car / Chl, VAZ / Chl, AZ / Chl, Z / Chl, AZ / VAZ and Z / VAZ).

Results

Glasshouse experiment

In the glasshouse experiment pot-grown Cabernet Sauvignon and Shiraz varieties were subjected to water and nitrogen deficiency in the presence or absence of phylloxera infestation for 9 weeks before sampling. Although some vines showed visible decline due to treatment effect, such as reduced vigour and leaf chlorosis, leaves targeted for collection did not show any chlorosis. Plants in the treatment groups in which nitrogen was withheld showed significantly lower nitrogen content in their leaves than the other treatment

groups ($P<0.001$). Mean nitrogen contents as percentage of total dry leaf weight were control 2.2, water deficiency 2.3, nitrogen deficiency 1.9, phylloxera-infested control 2.3, water deficiency and phylloxera 2.2, nitrogen deficiency and phylloxera 1.9.

Cabernet Sauvignon leaves had higher chlorophyll$_{a+b}$ and total carotenoid (Tcar) content and higher chlorophyll a / b ratios than Shiraz leaves (Fig. 1; $P<0.001$). However, the Tcar / Chl of Shiraz leaves was higher than that of Cabernet Sauvignon (1.39 : 1.48, $P=0.0043$).

Both grapevine varieties responded similarly to water or nitrogen deficiency by reducing leaf chlorophyll and total carotenoids (Fig. 1; Chl, $P=0.0022$; Tcar, $P=0.0065$) but Tcar / Chl was unaffected by treatment. Chl a / b was higher in water-deficient vines than in nitrogen-deficient vines ($P=0.014$), but neither of these treatments was significantly different from the control vines.

Chlorophyll concentration was reduced by phylloxera infestation in Shiraz but not in Cabernet Sauvignon leaves. Shiraz leaves from phylloxera-infested vines had 28% less chlorophyll than control vines, and 46% less chlorophyll than water-stressed vine leaves (Fig. 1; variety × phylloxera interaction, $P=0.036$). The total chlorophyll concentration in Shiraz leaves was similar in phylloxera-infested and nitrogen treatments both with and without phylloxera, but significantly lower in the phylloxera-infested / water-deficient treatment. Carotenoid concentration was similarly reduced but the Tcar / Chl was not affected by infestation. None of the other pigments in Shiraz were significantly affected by phylloxera infestation. Pigment composition in Cabernet Sauvignon was unaffected by infestation over the course of the experiment.

Field experiment

The field trial consisted of two grapevine varieties, Cabernet Sauvignon and Pinot Noir, growing in different vineyards, and compared infested and uninfested vines, of the same variety, in adjacent blocks, within the same vineyard. Pinot Noir contained approximately twice as much chlorophyll, on a leaf-mass basis, as Cabernet Sauvignon and the Chl a / b was also significantly higher in the former variety (Fig. 2; $P<0.001$). Phylloxera-infested vines of both varieties had reduced chlorophyll content (12–17%, Fig. 2; $P=0.016$) but Chl a / b was unaffected by infestation.

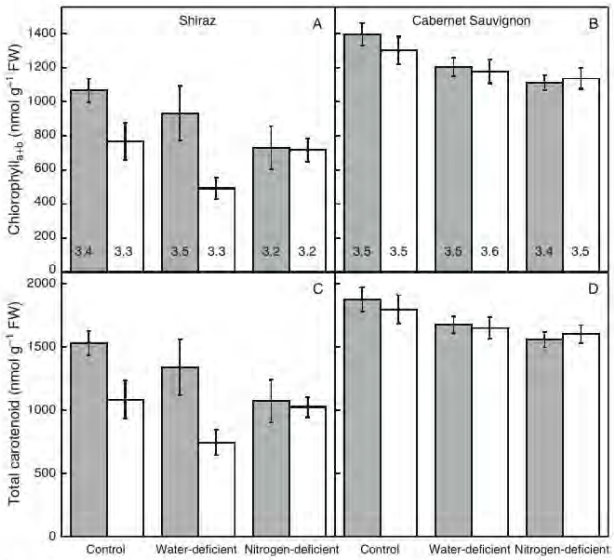


Fig. 1. Effect of phylloxera infestation on chlorophyll (*A*, *B*) and carotenoid (*C*, *D*) concentration of leaves of Shiraz (*A*, *C*) and Cabernet Sauvignon (*B*, *D*) grapevine varieties grown for 9 weeks in a glasshouse trial. Vines were grown with optimum water and nutrients (Control) or subjected to water or nitrogen deficiency. Solid bars denote uninfested vines and open bars show phylloxera-infested vines. Chlorophyll a / b ratios are presented as text in appropriate chlorophyll bars (*A*, *B*). Data represent mean ± s.e. ($n = 8$).

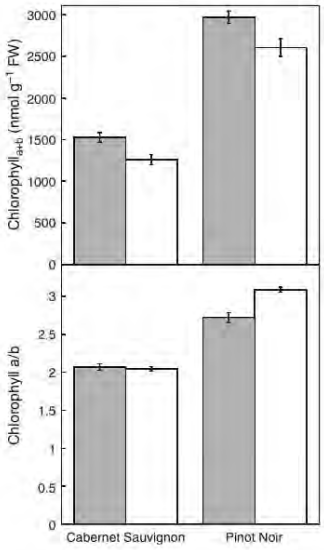


Fig. 2. Effect of phylloxera infestation on chlorophyll concentration and Chl *a* / *b* of leaves of Cabernet Sauvignon and Pinot Noir grapevine varieties grown in the field. Solid bars denote uninfested vines and open bars show phylloxera-infested vines. Data represent mean ± s.e. (Cabernet Sauvignon, $n = 20$; Pinot Noir, $n = 8$).

Relative to chlorophyll, Cabernet Sauvignon leaves had higher concentrations of carotenoids than Pinot Noir leaves, particularly those carotenoids involved in photoprotection such as β-carotene and the xanthophyll cycle pigments (Fig. 3; $P<0.001$). In both varieties, more than 40% of the xanthophyll pool was in the photoprotective form (Fig. 3*D*). However, Cabernet Sauvignon leaves maintained a higher de-epoxidation status than Pinot Noir leaves ($P=0.023$).

Although the total carotenoid content declined in infested leaves, the decline was less pronounced than the reduction in chlorophyll and as a result the Tcar / Chl pool was significantly higher in leaves from infested plants ($P=0.044$). The xanthophyll cycle pigments were responsible for much of this increase, with the relative size of the VAZ / Chl pool increasing 22% and 13% in leaves of infested Cabernet Sauvignon and Pinot Noir respectively. The proportion of this pool in the photoprotective forms (AZ / VAZ) was also higher in leaves from infested vines, albeit not significantly ($P=0.1$). Infested Pinot Noir leaves contained slightly more β-car / Chl than leaves from uninfested vines but there was no difference between phylloxera-infested and uninfested Cabernet Sauvignon for this pigment (Fig. 3*B* variety × phylloxera interaction, $P=0.051$).

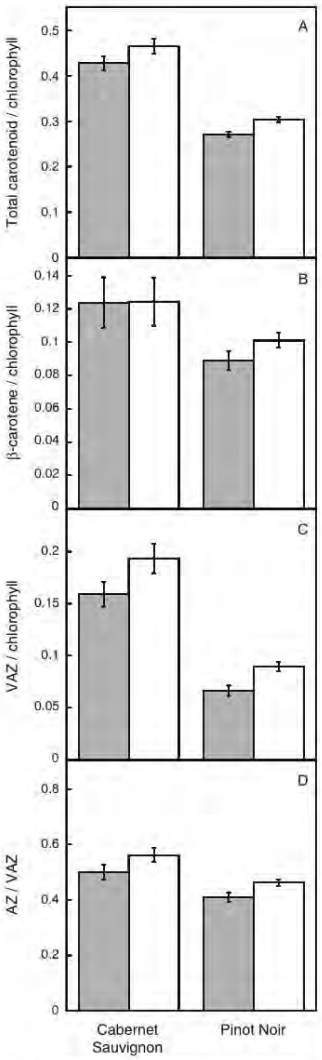


Fig. 3. Effect of phylloxera infestation on carotenoid composition of leaves of Cabernet Sauvignon and Pinot Noir grapevine varieties grown in the field. Total carotenoid / chlorophyll (*A*), β-carotene / total chlorophyll (*B*), xanthophyll cycle (V + A + Z) / total chlorophyll (*C*) and portion of the xanthophyll cycle in the photoprotective forms (A + Z) / (V + A + Z). Solid bars denote uninfested vines and open bars show phylloxera-infested vines. Data represent mean ± s.e. (Cabernet Sauvignon, $n = 20$; Pinot Noir, $n = 8$).

PRI measurements

The PRI was originally developed to estimate changes in concentrations of the photoprotective xanthophyll cycle pigments that are formed when plants are stressed (Gamon *et al*. 1997), but has also been shown to respond to Tcar / Chl (Sims and Gamon 2002). The best associations between PRI and carotenoids for both field- and glasshouse-grown vines are shown in Table 1. For both experiments the strongest associations (r^2=42% for glasshouse-grown vines, 31% for field-grown vines) were between PRI and Tcar / Chl (Fig. 4; Table 1). In the field-grown vines the associations between PRI and β-car / Chl, VAZ / Chl, AZ / Chl and Z / Chl were also significant and their r^2 values were greater than 10% (Table 1). However, for glasshouse samples the r^2 value was only 7% for Z / Chl and the regression for AZ / Chl was not significant.

Discussion

Phylloxera infestation reduces chlorophyll and increases investment in photoprotective pigments

The most notable trend from both the field and glasshouse experiments was an overall reduction in chlorophyll content when vines were infested with phylloxera. This decline was observed in the field for both Cabernet Sauvignon and Pinot Noir varieties and in the glasshouse for Shiraz (after only 9 weeks of infestation). For glasshouse-grown Cabernet Sauvignon the decline in chlorophyll was not significant after 9 weeks and unfortunately the trial was stopped after 10 weeks. However, given the decline observed in the field-grown vines of this variety it seems likely that a significant decline would have been observed within months of infestation. The declines in chlorophyll in the field-grown grapevines also illustrate that this reduction is not an artefact of glasshouse conditions. Phylloxera infestation reduced chlorophyll content in field-grown vines by 12% in Pinot Noir and 17% in Cabernet Sauvignon. The more marked reduction in the Cabernet Sauvignon may reflect that these vines had been infested for longer but we cannot rule out varietal or phylloxera genotype differences at this stage. The added effect of the above-mentioned factors plus varying environmental conditions at the different vineyard locations should also be considered.

In the glasshouse experiment, phylloxera infestation reduced leaf chlorophyll by 28% in control phylloxera-infested Shiraz vines and 46% in water-deficient vines but only 2% in nitrogen-deficient vines. Shiraz vines responded less strongly to water deficiency than to nitrogen deficiency when these stresses were imposed as single treatments; however, when added to phylloxera infestation the water-deficient treatment produced the largest decline in chlorophyll. This may indicate that phylloxera infestation interferes more strongly with water uptake and therefore exacerbates water stress, but has a less significant effect on nitrogen uptake. Further work is required to confirm these results because it was difficult to impose an adequate drought treatment under glasshouse conditions; an open field experiment would provide a more realistic test of this hypothesis.

In other studies pigment composition of grapevines has been shown to be relatively resilient to drought and cold stress (Medrano *et al*. 2002; Hendrickson *et al*. 2004), although changes have been observed as a result of varying growth irradiance and virus infection (Sampol *et al*. 2003; Bertamini and Nedunchezhian 2004; Bertamini *et al*. 2004). Our results are consistent with these findings and suggest that infestation of the roots imposes a considerable stress on the plants, which is reflected in leaf pigments switching away from light harvesting towards a role in energy dissipation. This is particularly clear in the increase in xanthophyll cycle pigments and in the de-epoxidation status of these pigments. Grapevines are known to be highly resistant to photoinactivation of photosynthesis and are able to dissipate a high proportion of absorbed light energy as heat. In previous studies cold- and water-stressed vines have been estimated to dissipate 64–92% of captured light energy via ΔpH-dependent, xanthophyll-mediated non-photochemical quenching (Medrano *et al*. 2002; Hendrickson *et al*. 2004). Phylloxera damage to the roots affecting water uptake would also explain higher levels of photoprotective pigments in

Table 1. Summary of regression analysis of the photochemical reflectance index (PRI) against leaf carotenoids for glasshouse and field grown vines

Only significant regressions with r^2 values greater than 10% are shown; leaf carotenoids tested include total carotenoids / chlorophyll, β-carotene / chlorophyll, VAZ / chlorophyll, AZ / chlorophyll, Z / chlorophyll, AZ / VAZ, Z / VAZ

Experiment	Carotenoid	Regression	r^2 (%)	*P*
Glasshouse	Total carotenoid / Chl	= 1.47 – 2.18PRI	42.6	< 0.0001
Field	Total carotenoid / Chl	= 0.36 – 1.51PRI	31.0	< 0.0001
	β-carotene / Chl	= 0.11 – 0.23PRI	25.4	< 0.0001
	VAZ / Chl	= 0.13 – 0.95PRI	23.1	0.0002
	AZ / Chl	= 0.06 – 0.48PRI	16.9	0.002
	Z / Chl	= 0.03 – 0.22PRI	11.2	0.013

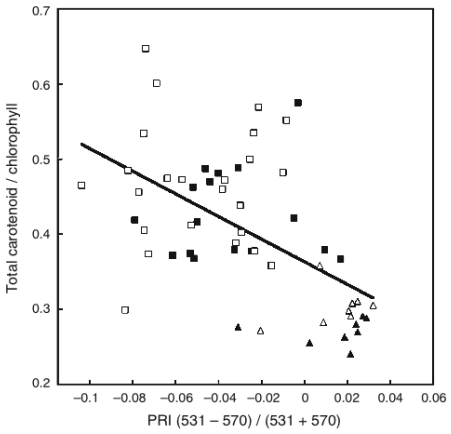


Fig. 4. Total carotenoid / chlorophyll as a function of PRI for Cabernet Sauvignon (□, ■) and Pinot Noir (△, ▲) grapevine varieties grown in the field. Infested vines are denoted by open symbols and uninfested vines are shown by filled symbols. Equation of regression line is given in Table 1.

infested vines in the field. Infestation increases the stress experienced at leaf level and leads to shifts in pigment composition to facilitate greater energy dissipation as heat. This response is similar to that shown in virus-infected plants including vines (Balachandran *et al*. 1997; Sampol *et al*. 2003; Bertamini *et al*. 2004).

High spectral resolution, reflectance spectrometry has been used to characterise the spectral response of vegetation to several stressors (Carter 1993; Gamon *et al*. 1997; Mohammed *et al*. 2000; Zarco-Tejada *et al*. 2003), including mite attack on apple trees (Penuelas and Filella 1998), and remote sensing is increasing in popularity as a tool for assessing plant physiological status. Individual leaf reflectance spectra measured at field sites and in the glasshouse trial, simultaneously with the leaf sampling for HPLC analysis, showed significant differences in key wavelength regions (Renzullo *et al*. 2004, 2006). The most commonly observed differences in the reflectance spectra of phylloxera infested and uninfested samples taken from the field occurred around the green peak (500–600 nm), the chlorophyll well (reflectances between 550 nm–700 nm) and the red edge (660–760 nm). These regions are affected by chlorophyll content in response to plant stress (Carter 1993; Zarco-Tejada *et al*. 2003). The phylloxera-infested leaves of both grapevine varieties taken from the glasshouse trial also possessed characteristic higher reflectances in the green peak and chlorophyll well than the unstressed controls. These results are consistent with the findings of lower chlorophyll levels detected in the leaves of phylloxera-infested vines analysed by HPLC.

Given that changes in pigment composition can be detected before leaves show visible changes, it is possible that they can be used to improve current methods for the early detection of phylloxera infestations. The PRI was originally developed to detect de-epoxidation status of the xanthophyll cycle (Gamon *et al*. 1997) and although it performed adequately with these pigments in our field study, the correlation was much weaker in the glasshouse-grown vines. However, as has recently been observed for a wide range of plant species and leaf structures (Sims and Gamon 2002) we found the best overall relationship was between PRI and Tcar / Chl (Table 1; Fig. 4). The PRI is sensitive to both the Tcar / Chl and changes in the relative xanthophyll cycle pigments, and generally correlates well with the latter in diurnal studies of the same leaves (Sims and Gamon 2002). However, the between-treatment differences in Tcar / Chl in the present study probably swamped the more subtle xanthophyll cycle pigment changes. Given that the relative increase in Tcar / Chl reflects increased vine stress, this is still a promising index for future study. If such indices can be detected at a canopy level there is a real possibility that an appropriately tuned airborne sensor could identify phylloxera infestation earlier then current methods.

Acknowledgments

This research was supported by the Commonwealth Cooperative Research Centre Program through the CRC for Viticulture and a University of Wollongong New Partnership Grant. We gratefully acknowledge the grape growers in north-eastern Victoria, Australia, for allowing us to conduct fieldwork on their vineyards.

References

Balachandran S, Hurry VM, Kelley SE, Osmond CB, Robinson SA, Rohozinski J, Seaton GGR, Sims DA (1997) Concepts of plant biotic stress. Some insights into the stress physiology of virus-infected plants, from the perspective of photosynthesis. *Physiologia Plantarum* **100**, 203–213. doi: 10.1034/j.1399-3054.1997.1000201.x

de Benedictis JA, Granett J (1993) Laboratory evaluation of grape roots as hosts of Californian grape phylloxera biotypes. *American Journal of Enology and Viticulture* **44**, 285–291.

Bertamini M, Nedunchezhian N (2004) Photosynthetic responses for *Vitis vinifera* plants grown at different photon flux densities under field conditions. *Biologia Plantarum* **48**, 149–152. doi: 10.1023/B:BIOP.0000024294.75496.a6

Bertamini M, Muthuchelian K, Nedunchezhian N (2004) Effect of grapevine leafroll on the photosynthesis of field grown grapevine plants (*Vitis vinifera* L. cv. Lagrein). *Journal of Phytopathology* **152**, 145–152. doi: 10.1111/j.1439-0434.2004.00815.x

Bertamini M, Muthuchelian K, Rubinigg M, Zorer R, Nedunchezhian N (2005) Low-night temperature (LNT) induced changes of photosynthesis in grapevine (*Vitis vinifera* L.) plants. *Plant Physiology and Biochemistry* **43**, 693–699. doi: 10.1016/j.plaphy.2005.06.001

Carter G (1993) Responses of leaf spectral reflectance to plant stress. *American Journal of Botany* **80**, 239–243.

Carter G, Knapp A (2001) Leaf optical properties in higher plants: linking spectral characteristics to stress and chlorophyll concentration. *American Journal of Botany* **88**, 677–684.

Chaumont M, Morot-Gaudry JF, Foyer CH (1995) Effects of photoinhibitory treatment on CO_2 assimilation, the quantum yield of CO_2 assimilation, D1 protein, ascorbate, glutathione and xanthophyll contents and the electron transport rate in vine leaves. *Plant, Cell & Environment* **18**, 1358–1366.

Chaumont M, Osorio ML, Chaves MM, Vanacker H, Morot-Gaudry JF, Foyer CH (1997) The absence of photoinhibition during the mid-morning depression of photosynthesis in *Vitis vinifera* grown in semi-arid and temperate climates. *Journal of Plant Physiology* **150**, 743–751.

Corrie AM, Crozier RH, van Heeswijck R, Hoffman AA (2002) Clonal reproduction and population genetic structure of grape phylloxera, *Daktulosphaira vitifoliae*, in Australia. *Heredity* **88**, 203–211.

Demmig B, Winter K, Kruger A, Czygan F-C (1988) Zeaxanthin and the heat dissipation of excess light energy in *Nerium oleander* exposed to a combination of high light and water stress. *Plant Physiology* **87**, 17–24.

Demmig-Adams B, Adams WW (1992) Carotenoid composition in sun and shade leaves of plants with different life forms. *Plant, Cell & Environment* **15**, 411–419.

Dunn JL, Turnbull JD, Robinson SA (2004) Comparison of solvent regimes for the extraction of photosynthetic pigments from leaves of higher plants. *Functional Plant Biology* **31**, 195–202. doi: 10.1071/FP03162

Edwards J, Lewis M, Powell K, Hackworth P, Lamb D (2004) Identification of phylloxera from high resolution infrared aerial imagery: a comparative study between airborne imagery type. *Australian Grapegrower & Winemaker* **488**, 51–54.

Evain S, Flexas J, Moya I (2004) A new instrument for passive remote sensing: 2. Measurement of leaf and canopy reflectance changes at 531 nm and their relationship with photosynthesis and chlorophyll fluorescence. *Remote Sensing of Environment* **91**, 175–185. doi: 10.1016/j.rse.2004.03.012

Flexas J, Briantais JM, Cerovic Z, Medrano H, Moya I (2000) Steady-state and maximum chlorophyll fluorescence responses to water stress in grapevine leaves: a new remote sensing system. *Remote Sensing of Environment* **73**, 283–297. doi: 10.1016/S0034-4257(00)00104-8

Flexas J, Hendrickson L, Wah Soon C (2001) Photoinactivation of photosystem II in high light-acclimated grapevines. *Australian Journal of Plant Physiology* **28**, 755–764.

Frazier P, Whiting J, Powell K, Lamb D (2004) Characterising the development of grape phylloxera infestation with multi-temporal near-infrared aerial photography. *Australian Grapegrower & Winemaker 32nd Annual Technical Edition* 133–136.

Gamon JA, Serrano L, Surfus JS (1997) The photochemical reflectance index: an optical indicator of photosynthetic radiation use efficiency across species, functional types, and nutrient levels. *Oecologia* **112**, 492–501. doi: 10.1007/s004420050337

Gilmore AM, Yamamoto HY (1991) Resolution of lutein and zeaxanthin using a non-endcapped, lightly carbon-loaded C_{18} high-performance liquid chromatographic column. *Journal of Chromatography* **543**, 137–145. doi: 10.1016/S0021-9673(01)95762-0

Hall A, Lamb D, Holzapfel B, Louis J (2002) Optical remote sensing applications in viticulture: a review. *Australian Journal of Grape and Wine Research* **8**, 36–47.

Held AA, Jupp DLB (1994) Use of the compact airborne spectral imager (CASI) for remote sensing of vegetation function and dynamics. In 'Proceedings of the 7th Australasian remote sensing conference. Vol. 2.' Melbourne, Australia. pp. 573–580.

Hendrickson L, Chow WS, Forster B, Furbank RT (2004) Processes contributing to photoprotection of grapevine leaves illuminated at low temperature. *Physiologia Plantarum* **121**, 272–281. doi: 10.1111/j.0031-9317.2004.0324.x

Herbert K, Powell KS, Hoffman A, Parsons Y, Ophel-Keller K, van Heeswijck R (2003) Early detection of phylloxera — present and future directions. *The Australian & New Zealand Grapegrower & Winemaker* **473a**, 93–96.

Lovelock CE, Robinson SA (2002) Surface reflectance properties of Antarctic moss and their relationship to plant species, pigment composition and photosynthetic function. *Plant, Cell & Environment* **25**, 1239–1250. doi: 10.1046/j.1365-3040.2002.00916.x

Maroco JP, Rodrigues ML, Lopes C, Chaves MM (2002) Limitations to leaf photosynthesis in field-grown grapevine under drought — metabolic and modelling approaches. *Functional Plant Biology* **29**, 451–459. doi: 10.1071/PP01040

Medrano H, Bota J, Abadía A, Sampol B, Escalona JM, Flexas J (2002) Effects of drought on light-energy dissipation mechanisms in high-light-acclimated, field-grown grapevines. *Functional Plant Biology* **29**, 1197–1207. doi: 10.1071/FP02016

Mohammed GH, Noland TL, Irving D, Sampson PH, Zarco-Tejada PJ, Miller JR (2000) 'Natural and stress-induced effects on leaf spectral reflectance in Ontario species.' (Ministry of Natural Resources: Ontario, Canada)

National Vine Health Steering Committee (NVHSC) (2003) National phylloxera management protocol http://www.gwrdc.com.au/nvhscphylloxera.htm [verified 7 March 2006].

Nichol CJ, Huemmrich KF, Black TA, Jarvis PG, Walthall CL, Grace J, Hall FG (2000) Remote sensing of photosynthetic-light-use efficiency of boreal forest. *Agricultural and Forest Meteorology* **101**, 131–142. doi: 10.1016/S0168-1923(99)00167-7

Omer AD, Granett JD, De Benedictis JA, Walker MA (1995) Effects of fungal root infections on the vigour of grapevines infested by root-feeding grape phylloxera. *Vitis* **34**, 165–170.

Penuelas J, Filella I (1998) Visible and near-infrared reflectance techniques for diagnosing plant physiological status. *Trends in Plant Science* **3**, 151–156. doi: 10.1016/S1360-1385(98)01213-8

Renzullo L, Held A, Powell KS, Blanchfield AL (2004) Remote sensing phylloxera infestation: current capabilities and future possibilities for early detection. *The Australian and New Zealand Grapegrower & Winemaker 32nd Annual Technical Issue* 126–130.

Renzullo LJ, Blanchfield AL, Powell KS (2006) A method of wavelength selection and spectral discrimination of hyperspectral reflectance spectrometry. *IEEE Transactions on Geoscience and Remote Sensing*, (In press).

Sampol B, Bota J, Riera D, Medrano H, Flexas J (2003) Analysis of the virus-induced inhibition of photosynthesis in malmsey grapevines. *New Phytologist* **160**, 403–412. doi: 10.1046/j.1469-8137.2003.00882.x

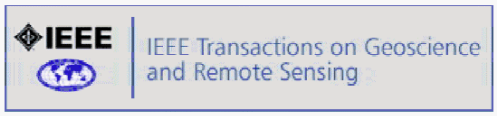
Sims DA, Gamon JA (2002) Relationships between leaf pigment content and spectral reflectance across a wide range of species, leaf structures and developmental stages. *Remote Sensing of Environment* **81**, 337–354. doi: 10.1016/S0034-4257(02)00010-X

Zarco-Tejada PJ, Pushnik JC, Dobrowski S, Ustin SL (2003) Steady-state chlorophyll *a* fluorescence detection from canopy derivative reflectance and *double-peak* red-edge effects. *Remote Sensing of Environment* **84**, 283–294. doi: 10.1016/S0034-4257(02)00113-X

Manuscript received 20 December 2005, accepted 6 March 2006

http://www.publish.csiro.au/journals/fpb

Transactions on Geoscience and Remote Sensing



A Method of Wavelength Selection and Spectral Discrimination of Hyperspectral Reflectance Spectrometry

For Review Only

Journal:	*Transactions on Geoscience and Remote Sensing*
Manuscript ID:	TGRS-2005-00390
Manuscript Type:	Regular paper
Date Submitted by the Author:	08-Aug-2005
Complete List of Authors:	Renzullo, Luigi; CSIRO Land and Water, Environmental Remote Sensing Blanchfield, Annette; Primary Industries Research Victoria, Department of Primary Industries Powell, Kevin; Primary Industries Research Victoria, Department of Primary Industries
Keywords:	Remote sensing

powered by ScholarOne
Manuscript Central™

A Method of Wavelength Selection and Spectral Discrimination of Hyperspectral Reflectance Spectrometry

Luigi J. Renzullo, *Member, IEEE*, Annette L. Blanchfield, and Kevin S. Powell

***Abstract*—Regularized regression was used in a discriminant analysis framework to identify the key spectral regions for the separation of hyperspectral reflectance spectra of grapevine leaves. Out of the 1151 wavelength bands available in the data, the analysis selected 12 or so wavelengths that can be used to differentiate the groups of vines studied. Moreover these wavelengths were repeatedly observed to occur in spectra regions known to be linked to plant physiology and condition.**

***Index Terms*—Reflectance spectrometry, discriminant analysis, cross-validation, regularized regression.**

I. Introduction

THE threat that grape phylloxera (*Daktulosphaira vitifoliae* Fitch) poses to Australian's grape and wine industry has motivated much research over the past decade into the use of remote sensing technologies for the mapping of sites of potential infestation. However, the challenges for the remote sensing community are well known [1], particularly as the above-ground symptoms of phylloxera infestation, which include reduced canopy density (vigour) and premature yellowing of the foliage (chlorosis) in autumn, are similar to poor irrigation or soil nutrient deficiencies, for example. The work presented in this paper resulted from an attempt to understand how the symptoms are manifested in reflectance spectra at the leaf level and, moreover, if the symptoms differ from other abiotic grapevine stresses.

The advent of hyperspectral remote sensing technologies has seen an increased number of spectral bands and, consequently, an improved capability for gaining a greater understanding of the fundamental processes that govern changes in vegetation biophysical/biochemical properties. Reflectance spectrometry are often analysed in an attempt to establish a causal link between observed spectral response and the foliar biochemical composition and/or plant physiology [1]–[6]. Alternatively the data may be analysed for their ability to separate various land-cover types [7] or vegetation species [8]. Fundamental to both analyses is the identification of key spectral regions that, in the first case, explain the variation observed in the chemical of interest or, in the second case, may be exploited for species (group) differentiation.

Methods for processing and analysing hyperspectral reflectance spectrometry are faced with data that are high-dimensional, with band numbers typically in excess of 10–100 times the number of samples, and exhibit a high degree of inter-band correlation, leading to much data redundancy. Ideally, methods should be able to handle the ill-posed nature of the reflectance spectrometry and obtain lower-dimensional representations of the data by selecting only those spectral regions useful for specific problem one seeks to address. This paper argues that discriminant analysis is one such method.

The aim of this paper is to demonstrate the use of discriminant analysis as an exploratory tool for hyperspectral reflectance spectrometry of vegetation. The data used in the demonstration are leaf-level reflectance spectra of grapevine leaves acquired in both vineyard and glasshouse environments. The emphasis is on the method's ability to identify spectral features used to separate the groups of interest; classification accuracy will be used to guide the choice of model complexity. Identified regions may be targeted for further analysis which may be linked with plant biochemistry.

II. Data Description

The data in this paper were collected as part of a project investigating the remote sensing of phylloxera infestation in Australian vineyards [1]. They are described below in two parts: the fieldwork dataset, acquired in January 2005 at a mid-point in the grape-growing season in Australia; and a glasshouse dataset, acquired in May 2004. For all data acquisitions, common varieties of *Vitis vinifera* L. were sampled and the same apparatus were used throughout.

Leaf-level reflectance measurements were recorded using an Analytical Spectral Devices FieldSpec® Pro FR spectroradiometer. A LiCor integrating sphere attachment was also used to allow collection of stable bi-hemispherical reflectance measurements that were independent of variations in ambient light conditions. White reference measurements of a Spectralon plate were made between consecutive leaf

Manuscript received August 8, 2005. The authors are part of the Cooperative Research Centre for Viticulture, Glen Osmond, SA 5064, Australia.

L. J. Renzullo is with CSIRO Land and Water, Canberra, ACT, 2601, Australia (phone: 61-2-6246 5758; fax: 61-2-6246 5800; e-mail: Luigi.Renzullo@csiro.au).

A. L. Blanchfield and K. S. Powell are with Primary Industries Research Victoria (PIR Vic), Department of Primary Industries, Rutherglen Centre, Rutherglen, Victoria 3685, Australia (e-mail: Annette.Blanchfield@dpi.vic.gov.au and Kevin.Powell@dpi.vic.gov.au)

For Peer Review

samples. Although the spectrometer has a broad spectral sensitivity, only those reflectance values within the wavelengths region 450–1600 nm were used in this investigation, due to the low intensity of the halogen lamp in the UV and SWIR wavelength regions

A. Field data

Fieldwork was conducted at two vineyards in north-eastern Victoria, Australia in January 2005. For the first vineyard, phylloxera was identified in a block of Cabernet Sauvignon in the Upton Phylloxera Infested Zone (PIZ) in 2000. The second vineyard, in Buckland Valley located in the NorthEast PIZ, is the site of a relatively recent outbreak (December 2003) of phylloxera in a block of Pinot Noir. Within each vineyard, 9 vines were identified via ground (root) surveying to be either phylloxera-free (uninfested) or phylloxera-infested (infested), and it is from these vines that 3 leaf samples were taken for spectral and chemical analysis. The mean reflectance curves (average of 36 individual spectra) are displayed for the Cabernet Sauvignon and Pinot Noir in Fig. 1(a) and (b), respectively.

B. Glasshouse data

Over a 9-week period between March–June 2004, an experiment was conducted to monitor changes in leaf spectral responses for two varieties of grapevine. Cabernet Sauvignon and Shiraz vines were subjected to various stresses in a controlled glasshouse environment. Eight vines of each variety were set aside as the healthy (H) control group, while a further eight were subjected to one of the following stresses: water stress (W), caused by reducing the amount of water supplied to the vine; nitrogen deficiency (N), achieved by withholding application of ammonium nitrate; and phylloxera infestation (P), where twenty phylloxera eggs, of a single sourced G4 genetic strain, were attached by enclosure within a nylon gauze fabric to one medium-sized lignified vine root [9]. Double-stressed groups were formed by subjecting vines to phylloxera infestation and either water stress or nitrogen deficiency (data not presented). Finally the 96 vines were arranged in a randomized block design generated using GenStat 6.1.

Reflectance measurements were taken for at least 3 leaves per vine, at several time intervals, which over the duration of the experiment amounted to over 2300 spectra. For brevity, only those measured on the final time period are considered here. The mean reflectance curves (average of around 24 individual spectra) for the H, P, W and N groups of the two grapevine varieties are displayed in Fig. 1 (c) and (d).

[Insert Fig. 1 about here]

C. A note on leaf sampling

Every attempt was made to maintain consistency in the leaf sampling strategy in both the field and glasshouse environments. Regardless of the groups to which the leaves belonged, mature leaves of a uniform green color were targeted for spectral data collection. There were however, instances, particularly in the glasshouse, where chlorotic leaves were sampled, but these were in the minority of occurrences.

III. Method

The explicit link between discriminant analysis, canonical correlation analysis and regression is detailed in Hastie *et al.* [10] and [11]. For further details, the reader is referred to these. Here only a brief description is provided for the practical implementation of the regression formulation of discriminant analysis.

To begin, we treat a reflectance spectrum as a p-dimensional vector, $\mathbf{x}_i$, belonging to one of J groups (classes, categories), for $i = 1,\ldots,N$. Each spectrum is assigned a group label $g_i \in \{1, 2,\ldots,J\}$ and the dataset $\{(\mathbf{x}_i, g_i)\}_{i=1}^{N}$ is formed. We then construct an $N \times p$ spectral data matrix, $\mathbf{X} = (\mathbf{x}_1,\ldots,\mathbf{x}_N)^T$, and an $N \times J$ indicator matrix $\mathbf{Y}$ defined as,

$$Y_{ij} = \begin{cases} 1, & g_i = j \\ 0, & \text{otherwise} \end{cases},$$

for $i = 1,\ldots,N$ and $j = 1,\ldots,J$. We choose to center the columns of $\mathbf{X}$ such that $\sum_{i=1}^{N} X_{ij} = 0$ to remove the influence of the magnitude of the reflectance value at different wavelengths, and ensure that there is no y-intercept term in the regression as described below. Note that $\mathbf{Y}^T\mathbf{Y}$ is a diagonal matrix whose elements are the number of spectra in each group.

A. Optimal scoring algorithm

Hastie *et al.* [10] showed that discriminant analysis may be recast as a regression problem by introducing a set of *scorings* that transform the group labels into real numbers so that they can be regressed against the spectra. In this paper, the scorings were performed with a $J \times K$ contrast matrix $\mathbf{\Theta}_0$, where $K = J - 1$. This may be viewed as a matrix of Helmert contrasts, which compares the second group to the first, the third group to the average of the first two, the fourth to the average of the first three, and so on. Alternatively a "treatment-type" matrix may be used, where each group is contrast with a "baseline" group, which may be the first group for example. To illustrate, let $J = 4$ groups. Then

$$\mathbf{\Theta}_0 = \begin{pmatrix} -1 & -1 & -1 \\ 1 & -1 & -1 \\ 0 & 2 & -1 \\ 0 & 0 & 3 \end{pmatrix} \text{ or } \begin{pmatrix} 0 & 0 & 0 \\ 1 & 0 & 0 \\ 0 & 1 & 0 \\ 0 & 0 & 1 \end{pmatrix}$$

for a Helmert or treatment contrast matrix, respectively. The scoring is then applied to the indicator matrix to create a transformed indicator matrix, $\mathbf{Z} = \mathbf{Y}\mathbf{\Theta}_0$, which is appropriately normalised such that $\mathbf{Z}^T\mathbf{Z} = \mathbf{\Theta}_0^T\mathbf{Y}^T\mathbf{Y}\mathbf{\Theta}_0 = \mathbf{I}$, where $\mathbf{I}$ is the $K \times K$ identity matrix.

For Peer Review

The next step is to perform the regression where we seek coefficients that minimize the average sum of squared residuals,

$$ASR = \mathrm{tr}\left(\| \mathbf{Z} - \mathbf{X}\mathbf{B} \|^2\right)/N, \quad (1)$$

where $\mathbf{B} = (\boldsymbol{\beta}_1, \ldots, \boldsymbol{\beta}_K)$ is a matrix of regression coefficients, the estimate of which is denoted $\hat{\mathbf{B}}$ (more details on the estimation of the regression coefficients will be given later in this section). Let the eigenvalues and eigenvectors of $\mathbf{Z}^T\mathbf{X}\hat{\mathbf{B}}$ be denoted as $\Phi = (\phi_1, \ldots, \phi_K)^T$ and $\mathbf{U} = (\mathbf{u}_1, \ldots, \mathbf{u}_K)$ respectively, with $\phi_k < 1$ for $k = 1, \ldots, K$ and $\mathbf{U}^T\mathbf{U} = \mathbf{I}$. It can then be shown that (1) becomes,

$$ASR = \sum_{k=1}^{K} (1 - \phi_k)/N.$$

Finally a set of "optimal" scores [10] is obtained as $\boldsymbol{\theta}_0\mathbf{U}$ as well as a $p \times K$ matrix of coefficients,

$$\mathbf{V} = \hat{\mathbf{B}}\,\mathbf{U}\,\mathbf{D}^{1/2}, \quad (2)$$

where $\mathbf{D} = \mathrm{diag}[\phi_1(1-\phi_1), \ldots, \phi_K(1-\phi_K)]$. It is the columns of $\mathbf{V}$ that, when applied to the spectral data, calculate the *discriminant variables*,

$$\mathbf{v}_k^T\mathbf{x}_i, \quad (3)$$

$i = 1, \ldots, N$.

It is the magnitude of the components of $\mathbf{v}_k$ that determines whether or not a wavelength is selected. Wavelengths that contribute most to the spectral separation between groups are given high coefficient values by the analysis. For visualization purposes in the figures that follow, the coefficients were normalized, that is the values are scaled such that $\|\mathbf{v}_k\|^2 = 1$. The plot of the components of $\mathbf{v}_k$ as a function of wavelength is what we refer to as the coefficient *contour* plots.

B. A note on regression

For the minimization of (1) the usual multiple least squares estimates of the regression coefficients are given as,

$$\hat{\boldsymbol{\beta}}_k = \left(\mathbf{X}^T\mathbf{X}\right)^{-1}\mathbf{X}^T\mathbf{z}_k,$$

where $\mathbf{z}_k$ are the columns of $\mathbf{Z}$ for $k = 1, \ldots, K$. For the hyperspectral reflectance data used in this study, where the number of wavelength bands is much greater than the number of observations (i.e. $p >> N$), the matrix $\mathbf{X}^T\mathbf{X}$ is not of full rank as there can be at most *N* linearly independent rows. Therefore, inversion would result in highly unstable estimates of **B**. A contour plot of the coefficients would reveal their highly variable (oscillatory) nature as the model attempts to overfit the spectral data. To address this problem, one may resort to regularized methods of regression. Regularized regression brings stability to the estimates of the coefficients and ultimately, via (2), stability and improved interpretability of the discriminant variable coefficients, $\mathbf{v}_k$ [12, 13].

Ridge regression [14] is a method of regularized regression that controls the stability of $\hat{\boldsymbol{\beta}}_k$ by imposing a constraint on the size of the coefficients. For ridge regression the objective function is written as,

$$\min \| \mathbf{z}_k - \mathbf{X}\boldsymbol{\beta}_k \|^2 + \lambda \| \boldsymbol{\beta}_k \|^2,$$

which amounts to adding a constant, $\lambda > 0$, to the diagonal elements of $\mathbf{X}^T\mathbf{X}$. Hastie *et al.* [11] used this formulation in the development of penalized discriminant analysis (PDA), for use in situations where there are a large number of highly correlated variables (wavelength bands in our case). The discriminant variable coefficients from PDA tend to have a smoother contour as a result of the regularization, which aids model interpretation [13, 8].

Tibshirani [15] introduced the least absolute shrinkage and selection operator (lasso) as another method of regularized regression. Like ridge regression the lasso can handle ill-posed problems (i.e. large number of correlated variables compared to sample size) and give stable estimates of $\hat{\boldsymbol{\beta}}_k$. However, through the objective function

$$\min \| \mathbf{z}_k - \mathbf{X}\boldsymbol{\beta}_k \|^2 + s \| \boldsymbol{\beta}_k \|^1,$$

where $\| \boldsymbol{\beta}_k \|^1 = \sum_{j=1}^{p} | \beta_{jk} |$ and $0 < s < 1$, lasso sets some of the components of $\hat{\boldsymbol{\beta}}_k$ to zero. Only those wavelengths that exhibit the strongest effect and, through (2), contribute to the separation between groups, are given nonzero weight.

It is this feature that makes lasso regression so attractive in this work on wavelength selection. Lasso regression will be used in the context of the discriminant analysis in what will be referred to in this paper as the OSLASSO procedure, i.e. optimal scoring via lasso regression.

C. Tuning parameter selection

By employing PDA and OSLASSO the goal was to derive a model which would differentiate the grapevines of the various groups from each other and, more importantly, would allow the key spectral regions to be easily identifiable. In other words, we required a model of sufficient complexity to accurately classify the data into the groups investigated and select the wavelengths utilized from the spectral separation was required. Model complexity in both methods is determined by the choice of "tuning parameters": in the case of PDA this is the parameter λ in the ridge regression; and for OSLASSO it is the parameter *s* in the lasso regression.

The effect of choosing two extreme values for the tuning parameter on the PDA of the four groups of Shiraz vines is demonstrated in Fig. 2. The upper plot of the first and second discriminant variables shows the separation of the groups of training data, whereas the lower plots contain the contour of the normalized coefficients of the first discriminant variable. Fig. 2(a) and (c) demonstrates that a PDA model with high complexity can result in a high degree of separation with no misclassification error of the training data, but results in a contour of the discriminant variable coefficients which is highly variable and, thus, makes it difficult to choose the key wavelengths (this is also known as overfitting). Fig. 2(b) and

For Peer Review

(d) demonstrates a model of low complexity in which there is considerable overlap of the groups (i.e. confusion) but leads to a contour from which the spectral regions are easily identified. Further details on the interpretation of these plots will be given in Section IV.

To aid in the choice of appropriate values for tuning parameters, L-fold cross-validation was employed. The principle involves dividing the training data are divided into L subsets of roughly equal size. Sequentially each subset is set aside to serve as a "validation" dataset while the model is trained on the remaining L-1 subsets. This is repeated for different levels of model complexity (i.e. values of the tuning parameter) and estimates of training and validation misclassification error may be obtained (discussed further in Section IV).

[Insert Fig. 2 about here]

IV. Results

The discriminant analysis algorithm employed in this work is written using R programming language and is a modified version of the *fda* routine of the *mda* package, available from the website http://cran.r-project.org/. Modifications included the option to choose the kind of contrast matrix $\mathbf{\Theta}_0$ to be used, and the ability to perform lasso regression, as required by the OSLASSO procedure. The bulk of the original *fda* code, for example the estimation of classification error or percentage variation explained, remains unaltered. Note that the *mda* package has a built-in ridge regression routine, as required for PDA. The lasso regression was performed with the *lars* (i.e. least angle regression) package also available from the above website.

In the following, the PDA and OSLASSO procedures are applied to the reflectance spectra acquired a) in the field and b) in the glasshouse experiment. Datasets consist of J = 4 groups with N = 144 or 96 for the field data or glasshouse respectively. Each spectrum is composed of p = 1151 wavelength bands spaced at 1-nm intervals between 450–1600 nm.

A. Field-measured reflectance spectra

The four groups of field-measured spectra consisted of phylloxera-infested and uninfested Cabernet Sauvignon and Pinot Noir vines. In this example a matrix of Helmert contrasts was used for both methods of discriminant analysis. L-fold cross-validation was used to choose appropriate values for λ and s. In this case, each group consisted of 36 spectra, so the data were split into L = 6 subsets. The estimated training and validation errors are displayed in Fig. 3. Note that model complexity increases along the x-axis from left to right and the vertical bars represent the standard error of the calculated mean.

In Fig. 3(a) it can be observed that a value of λ = 0.003 results in a perfect fit to the training data and a minimum validation misclassification error of around 14%. It is, however, likely that the contour of the discriminant variable coefficients would be highly variable and difficult to interpret. In Fig. 3(b) a minimum in the validation misclassification error is obtained for values of s between 0.025–0.05. Increasing s in this case would result in the model complexity increasing, leading to a perfect fit to the training data for s = 0.2 but decreasing the fit to the validation data for higher values of s.

In the interest of parsimony, the choices of tuning parameters values for PDA and OSLASSO were λ = 0.15 and s = 0.03, respectively. The associated training and validation errors for what we call the *optimal* tuning parameters were on average less than 12% and 20% respectively.

[Insert Fig. 3 here]

The spectral separation of the groups for PDA and OSLASSO using the optimal choice of tuning parameters is illustrated in the discriminant plots of Figs. 4(a) and (b) respectively. The data in both cases are the original field-measured spectra. The first and second discriminant variables (x and y axes respectively) for both methods account for over 90% of the between-group variation, with a training misclassification error of less than 13%. Both methods show good separation between the Cabernet Sauvignon and Pinot Noir groups, and the phylloxera-infested Cabernet Sauvignon are clearly separable from the other groups. Most of the confusion, and thus misclassification, observed is between infested and uninfested Pinot Noir vines—this is more pronounced in the OSLASSO results than in those of the PDA.

[Insert Fig. 4 about here]

The normalized coefficients of the first discriminant variables from PDA and OSLASSO for the chosen values of the tuning parameters are displayed in Fig. 5. Recall that it is the magnitude of the coefficients that gives an indication of the importance of a given wavelength in explaining the spectral separation between groups. Fig. 5 demonstrates the two methods' abilities to identify wavelengths in similar broad spectral regions. These wavelengths are interpreted, in conjunction with Fig. 4, as contrasting the two grapevine varieties (Cabernet Sauvignon and Pinot Noir) and the phylloxera-induced stress in the Cabernet Sauvignon.

[Insert Fig. 5 about here]

In this example, however, it is difficult to identify those wavelengths that differentiate the vine varieties from the stress. One may choose to rotate the axes in Fig. 4 clockwise by 45°, in which case the interpretation of the second discriminant variable is that it contrasts the Cabernet Sauvignon from the Pinot Noir, and the first discriminant as contrasting the phylloxera-infested vines from the uninfested ones. However, this paper addresses the spectral separation of various vine stresses in the following section using glasshouse reflectance data.

B. Glasshouse-measured reflectance spectra

PDA and OSLASSO were applied to the Cabernet Sauvignon and Shiraz vines in the glasshouse experiment (see

For Peer Review

Section II) separately to avoid the influence of grapevine variety on the discriminant analysis. In this example, comparisons between the P, W and N groups of vines and the baseline control group, H, were achieved by a treatment-type contrast matrix (see Section III).

Cross-validation was once again used to aid in the selection of an appropriate choice of tuning parameter values for spectral separation of the four groups of vines. The results of cross-validation for both methods on the Cabernet Sauvignon vines are displayed in Fig. 6. Estimated misclassification errors for the range of λ and s were observed to be on average around 67% for both PDA and OSLASSO. Similarly high estimates of validation misclassification errors were observed for the Shiraz vines (data not presented).

[Insert Fig. 6 about here]

In this case, the choice of optimal tuning parameter values was governed on the methods' ability to achieve a training misclassification error < 20% without becoming overly complex. For both the Shiraz and Cabernet Sauvignon varieties, the optimal choices were $\lambda = 0.002$ and $s = 0.075$.

The spectral separation of the groups of vines resulting from the application of the OSLASSO to the Shiraz and Cabernet Sauvignon reflectance data is illustrated in Fig. 7(a) and (b), respectively. In this example, over 75% of the between-group variance was explained by the first and second discriminant variables with training misclassification errors of 25% and 17% for the Shiraz and Cabernet Sauvignon vines, respectively. The first and second discriminant variables from PDA explained a similar percentage of variation, but had misclassification errors of 21% and 16% for the Shiraz and Cabernet Sauvignon data respectively.

[Insert Fig. 7 about here]

In this example, a treatment contrast matrix was used. Therefore the coefficients of the discriminant variables are interpreted as identifying the spectral regions where one of the stress groups (i.e. P, W or N) differs from the control group (H). For the Shiraz vines, we observe in Fig. 7(a) that the nitrogen-deficient vines (N) differ from H at the wavelength identified by the coefficients of the first discriminant variable, plotted for both PDA and OSLASSO in Fig. 7(c). Using the magnitude of the coefficients as a guide, some of the wavelengths exploited in separating the N groups from the H group of vines are located around 530 nm; 660, 680 and 700 nm; 730 and 760 nm; and 950 and 1150 nm.

For the Cabernet Sauvignon data, Fig. 7(b) shows that the first discriminant variable differentiates the W and N groups from the H group, while the second discriminant variable separates the P group from the H group. The coefficients of the second discriminant variable in Fig. 7(d) shows the phylloxera-infested group of vines differ most from the control vines at wavelengths around 530, 660 and 740 nm, but the separation is dominated by wavelengths in the region above 900 nm.

Note that similar spectral regions are identified by both PDA and OSLASSO.

C. Wavelength selection and derivative analysis

An understanding of the significance of the wavelengths identified by OSLASSO is gained through derivative analysis. Changes in the curvature of reflectance spectra may be identified using derivative operators. For example, local curvature extrema and inflection points are highlighted by first and second order derivative operators, with high-order derivatives identifying more subtle changes in curvature. Most of these changes in curvature may be linked to absorption features and even instrument noise [16]-[18].

For these data the interest is not in individual reflectance curves, but the difference between two spectra. For example, let us consider Shiraz vines and the contrast between N and H groups. Let $\mathbf{m}_N$ and $\mathbf{m}_H$ be the p-dimensional mean reflectance curves of the N and H group of Shiraz vines, respectively. The difference in the mean spectral response of both groups is defined as $\mathbf{R} = \mathbf{m}_N - \mathbf{m}_H$. The finite difference approximation is employed to calculate the first-order derivative of the reflectance spectra,

$$D_i^{(1)} = \frac{\mathrm{d}\mathbf{R}}{\mathrm{d}\lambda} \approx \frac{R_{i+1} - R_{i-1}}{2},$$

for $i = 2, \ldots, p-1$, and the second-order derivative as,

$$D_i^{(2)} = \frac{\mathrm{d}^2\mathbf{R}}{\mathrm{d}\lambda^2} \approx \frac{D_{i+1}^{(1)} - D_{i-1}^{(1)}}{2},$$

for $i = 3, \ldots, p-2$. The estimates of the first and second derivative spectra are displayed, along with the OSLASSO coefficients of the first discriminant variable in Fig. 8(a) (note that the second derivative spectrum was smoothed by a 9-point moving-average filter for presentation purposes). The same calculations were performed for the Cabernet Sauvignon data, however the difference in the mean spectral response was between the phylloxera-infested and control groups. These are displayed with the OSLASSO coefficients of the second discriminant variable in Fig. 8(b). The data in Fig. 8 were scaled for clarity.

[Insert Fig. 8 about here]

Fig. 8 shows that most of the wavelengths selected by the OSLASSO correspond to the location of zero-crossings in the first- and second-order derivative spectra. It is important to remember that the zero-crossings of the nth-order derivative are associated with the crests or troughs in the (n-1)th order derivative spectrum. Therefore, wavelengths selected that coincide with a crest or trough in the second derivative will coincide with a zero-crossing of the third derivative spectrum. Third and higher-order derivate spectra have not been displayed to maintain clarity.

D. Repeatability of wavelength selection

To assess the repeatability of the wavelength selection, PDA and OSLASSO (using the optimal choices of λ and s) were

For Peer Review

applied to 100 bootstrap samples of the training data from the glasshouse experiment. This resulted in 100 replicates of the discriminant variables, $\mathbf{v}_k^{(n)}$ for $n = 1,\ldots,100$ and $k = 1,\ldots,3$.

For illustration, we consider the discriminant variables displayed in Fig. 7 (c) and (d). The wavelength selection for the normalized coefficients was based on the following criteria:

$$\left|v_{jk}^{(n)}\right| > 0.025 \text{ for PDA; and}$$

$$v_{jk}^{(n)} \neq 0 \quad \text{for OSLASSO,}$$

where $n = 1,\ldots,100$, $j = 1,\ldots,p$ and $k = 1$ or 2 depending on grapevine variety (see Fig. 7). The number of times a given wavelength satisfied the above criteria is displayed in the frequency histograms for Fig. 9 for both the Cabernet Sauvignon and Shiraz vines. Note that the coefficients from the OSLASSO were grouped into 10-nm bins between 450–1600 nm. The units on the y-axes of the histograms are normalized counts (i.e. the sum of squared counts over all wavelengths equals unity) to facilitate comparisons between the two methods. Fig. 9 demonstrates that the wavelengths selected by both procedures fall in comparable spectral regions.

[Insert Fig. 9 about here]

V. Discussion

An optimal scoring algorithm was used to discriminate between groups of leaf-level hyperspectral reflectance spectra and, in so doing, identify the wavelengths exploited for separating the groups. Two versions of the algorithm were investigated: the first used ridge regression [14] in what is known as penalized discriminant analysis (PDA) [11]; the second used lasso regression [15] in what is referred to in this paper as the OSLASSO procedure. Both approaches employ methods of regularized regression, and can handle the ill-posed nature of the problem (i.e. many more wavelengths than observations) and control the stability of the estimated coefficients. However the lasso selects only a comparatively small subset of the wavelengths, compared to ridge regression which uses the full spectrum.

A. Model complexity and classification accuracy

The amount of regularization and therefore complexity of the derived PDA and OSLASSO models was governed by their respective tuning parameters. In the absence of an independent validation set of spectra, *L*-fold cross-validation was found to be a useful tool for choosing an appropriate value for the tuning parameters. While the main interest of this paper was in wavelength selection rather than classification, cross-validation provided estimates of classification accuracies for various levels of model complexity. The goal was to choose a level of complexity sufficient to separate the groups of spectra yet simple enough for the wavelengths to be readily interpretable.

For the field-measured data, cross-validation showed that for both PDA and OSLASSO estimated validation classification accuracies > 80% were achievable for the chosen levels of model complexity. In this scenario, there were two grapevines varieties (Cabernet Sauvignon and Pinot Noir) and phylloxera-infested and uninfested vines for each variety. This level of accuracy is the same as that reported for conifer species discrimination by PDA [8]. Both procedures showed good separation between grapevine varieties, as well as between infested and uninfested Cabernet Sauvignon. Most of the misclassification occurred for Pinot Noir vines. Spectrally there is very little difference between the infested and uninfested Pinot Noir (Fig. 1(b)) compared with the Cabernet Sauvignon. We speculate that this may be due to the respective lengths of time the vines have been infested with phylloxera, the relative virulence of the phylloxera genetic strains or that when sampled the vines were at different phenological stages due to differences in climatology and/or soil type between vineyards.

The glasshouse experiment was devised in an attempt to control those factors influencing grapevine spectral response that were beyond our control in the field. There were four groups of Shiraz and Cabernet Sauvignon vines used in the experiment: H (control), P (phylloxera-infested), W (water-stressed) and N (nitrogen-deficient) groups (see Section II). The Shiraz and Cabernet Sauvignon vines were analyzed separately to characterize spectral differences due to stress and not varieties. Cross-validation showed that both PDA and OSLASSO performed poorly on the classification with estimated accuracies < 40% for validation samples. Tuning parameter selection was therefore based on estimated training classification errors of around 80%. The poorer performance may be due to the similarities in the mean spectral responses of the vines, with the difference only really becoming evident upon magnification (e.g. Fig. 1(c)). The number of spectra (approximately 24 spectra per group in the glasshouse compared with 36 in the field) may also have influenced the results of classification. The effects of sample size of the classification accuracy was not investigated in this study but could be considered in future research.

B. Wavelength selection

Wavelength selection was based on the magnitude of the normalized coefficients of the discriminant variables of interest. For the OSLASSO this is straightforward; wavelengths whose corresponding coefficient is nonzero are selected. For PDA this required the application of threshold to the coefficients; wavelengths with a coefficient value above the threshold were selected. In this way, PDA identified wavelength regions rather than individual wavelengths using OSLASSO. Generally there was high level of similarity between the approaches in terms of the broad spectral regions identified.

Throughout these investigations, wavelengths of a few spectral regions in which wavelengths were continually being selected. Moreover, these regions are known to correspond to spectral features related to plant physiology. For example there are: xanthophylls cycle pigments known to be spectrally active between 500-530 nm which are important for photo-

For Peer Review

protection; chlorophyll *a* and *b,* whose influence ranges from the maximum in the green peak around 550 nm, the chlorophyll well between 660-690 nm, the red-edge inflection point between 700-730 nm, and also the reported fluorescence feature around 760 nm [19]; and leaf water, with minor absorption features centered on 950, 1050, 1150 nm, and a major feature at 1450 nm.

Specific to the examples illustrated in Fig. 7, we observed for the Shiraz vines that some of the wavelengths selected that separate the N from the H group of vines occurred in the chlorophyll well. This suggests that chlorophyll absorption may be one of the distinguishing features between the nitrogen-deficient vines and control vines. This is supported by the finding reported [20] showing the nitrogen-deficient vines overall had lower total leaf chlorophyll content compared with other vines in the glasshouse experiment. Wavelengths in the water absorption regions were also selected but they play more of a dominant role in the separation of phylloxera-infested Cabernet Sauvignon from the control vines. Investigations have yet to confirm if leaf water content was significantly different between groups.

It was also observed that the selected wavelengths were in the location of the zero-crossings of the first- and higher-order derivative spectra. Derivative zero-crossings are known to correspond to absorption features in reflectance spectra [16]-[18]. Derivative operators, however, are also notorious for highlighting noise, particularly the higher-order derivatives. The PDA and OSLASSO procedure often selected wavelengths in noisy parts of the reflectance on the near-infrared plateau at wavelengths above 800 nm, which is also the location of numerous water absorption features. When the groups of data a very similar and it is difficult to identify "physically meaningful" changes in curvature to exploit, the procedures tend to use the noisy parts of the spectrum to separate the groups. The procedures' sensitivity to noise needs to further investigated.

Finally, bootstrap re-sampling of the spectra data was used to assess how repeatable the wavelength selection of the PDA and OSLASSO was. It was found that the wavelengths identified in Fig. 7 as the most important for the group discrimination were the ones most frequently selected. Furthermore there was once again a great deal of similarity in regions identified in the frequency histograms for PDA and the wavelengths selected in 10-nm binned samples in histogram for the OSLASSO.

VI. Conclusion

This paper has shown that the PDA and OSLASSO consistently identified similar spectral regions of interest. The advantage of the selection properties of OSLASSO over PDA is that the full spectrum need not be used. Many of the illustrations in this paper have focused on the results of OSLASSO. This is because, out of 1151 wavelength bands in the reflectance data, given between 20-40 observations per group, the procedure was able to consistently select 12 or so wavelengths to separate the groups of data. This paper demonstrated the use of the procedure as an exploratory tool in the analysis of grapevine stress. The application here was to high spectral resolution leaf-level spectroradiometer measurements, but the procedure may just as easily be applied to any other hyperspectral reflectance, in situ or remotely-sensed, for vegetation species discrimination or stress detection.

Future work may include quantifying the effects of noise and sample size on the classification accuracy and, indirectly, the choice of model complexity for interpretation. More work is needed in linking the wavelengths selected to plant physiology through leaf pigment and chemical analysis. Finally, the method needs to be applied to more grapevine varieties, under a range of different stresses before it can be claimed that the symptoms of phylloxera infestation can be distinguished from other stresses.

Acknowledgment

This research was supported by the Commonwealth Cooperative Research Centre Program and conducted through the CRC for Viticulture with support from Australia's grapegrowers and winemakers through their investment body the Grape and Wine Research and Development Corporation, with matching funds from the Federal Government.

The authors gratefully acknowledge the grape growers in northeastern Victoria, Australia, for the allowing us to conduct fieldwork on their vineyards.

References

[1] Renzullo, L., Held, A., Powell, K. and Blanchfield, A., "Remote sensing phylloxera infestation: current capabilities and future possibilities for early detection", *The Australian and New Zealand Grapegrower and Winemaker*, no. 32nd Annual Technical Issue, pp. 126-130, 2004.

[2] Curran, P. J., Kupiec, J. A. and Smith, G. M., "Remote sensing the biochemical composition of slash pine canopy", *IEEE Trans. Geosci. Remote Sensing*, vol. 35, no. 2, pp. 415-420, 1997.

[3] Blackburn, G. A., "Relationships between spectral refelctance and pigment concentrations in stacks of deciduous broadleaves", *Remote Sens. Environ.*, vol. 70, pp. 224-237, 1999.

[4] Curran, P. J., Dungan, J. L. and Peterson, D. L., "Estimating the foliar biochemical concentration of leaves with reflectance spectrometry: Testing the Kokaly and Clark methodologies", *Remote Sens. Environ.*, vol. 76, pp. 349-359, 2001.

[5] Sims, D. A. and Gamon, J. A., "Relationships between leaf pigment content and spectral reflectance across a wide range of species, leaf structure and development stages", *Remote Sens. Environ.*, vol. 81, pp. 337-354, 2002.

[6] Coops, N. C., M.-L. Smith, M. E. Martin and Ollinger, S. V., 'Prediction of Eucalypt Foliage Nitrogen Content from Satellite-derived Hyperspectral Data', *IEEE Trans. Geosci. Remote Sensing*, vol. 41, no. 6, pp. 1338-1346, 2003.

[7] Kiiveri, H. T., "Canonical variate analysis of high-dimensional spectral data", *Technometrics*, vol. 34, no. 3, pp. 321-331, 1992.

[8] Yu, B., Ostland, M., Gong, P. and Pu, R., "Penalized discriminant analysis of in situ hyperspectral data for species recognition", *IEEE Trans. Geosci. Remote Sensing*, vol. 37, no. 5, pp. 2569-2577, 1999.

[9] Burns, A. E. and Powell, K. S., "A novel approach for rapid screening of grapevine rootstocks for resistance to grape phylloxera", *Australian Journal of Grape and Wine Research* (submitted), 2005.

[10] Hastie, T., Tibshirani, R. and Buja, A., "Flexible discriminant analysis by optimal scoring", *Journal of the American Statistical Association*, vol. 89, no. 428, pp. 1255-1270, 1994.

For Peer Review

[11] Hastie, T., Buja, A. and Tibshirani, R., "Penalized discriminant analysis", *Annals of Statistics*, vol. 23, no. 1, pp. 73-102, 1995.
[12] Friedman, J. H., "Regularized discriminant analysis", *J. of the American Statistical Assoc.*, vol. 84, no. 405 pp. 165-175, 1989.
[13] Hastie, T. and Tibshirani, R., "Efficient quadratic regularization for expression arrays", *Biostatistics*, vol. 5, no. 3, pp. 329-340, 2004.
[14] Hoerl, A. E. and Kennard, R., "Ridge regression: biased estimation for nonorthogonal problems", *Technometrics*, vol. 12, pp. 55-67, 1970
[15] Tibshirani, R., "Regression shrinkage and selection via the Lasso", *Journal of the Royal Statistical Society, Series B*, vol. 58, no. 1, pp. 267-288, 1996.
[16] Tsai, F. and Philpot, W., "Derivative analysis of hyperspectral data", *Remote Sens. Environ*., vol. 66, pp. 41-51, 1998.
[17] Clark, R. N., Swayne, G. A., Livo, K. E., Kokaly, R. F., Sutley, S. J., Dalton, J. B., McDougal, R. R. and Gent, C. A., "Imaging spectroscopy: earth and planetary remote sensing with the USGS Tetracorder and expert systems", *J. Geophys. Res*., vol 108, no. E12, 5131, doi:10.1029/2002JE001847, pp. 5.1-5.44, 2003.
[18] Hsu, P.-H., "Spectral featured extraction of hyperspectral images using wavelet transform", PhD dissertation, Department of Surveying Engineering, National Cheng Kung University, Tainan, Taiwan, 2003.
[19] Zarco-Tejdada, P., Miller, J. R., Mohammed, G. H. and Noland, T. L., "Chlorophyll fluorescence effects on vegetation apparent reflectance: I. Leaf-level measurements and model simulation", *Remote Sens. Environ.*, vol. 75, pp. 582-595, 2000
[20] Renzullo, L. J., Blanchfield, A. L., Guillermin, R., Powell, K. S. and Held, A. A., "Comparison of Prospect and HPLC estimates of leaf chlorophyll contents in a grapevine stress study", *Int. J. Remote Sens.*, to be published.



Luigi J. Renzullo (M'05) received a B.Sc. in Mathematics and Computing in 1996, a PostGrad. Dip. in Applied Physics in 1997 and a Ph.D. in Remote Sensing Science in 2004 from Curtin University of Technology, Perth, Western Australia.

In 2000 he was employed as a Remote Sensing Analyst with CSIRO Mathematical and Information Sciences where he worked on the classification of sequences of Landsat TM and ETM+ imagery for the quantification of vegetation change as part of the Western Australian government's Land Monitor project. In 2003 he was appointed Postdoctoral Research Fellow with CSIRO Land and Water in Canberra, Australia, where he has since been working on the analysis of reflectance spectrometry as part of a CRC for Viticulture project on the early detection of grapevine phylloxera. His research interests include image processing and analysis, high-dimensional data mining and regression.

Dr. Renzullo is a Graduate Member of Australian Mathematical Society and a member of Statistical Society of Australia, Inc.



Annette L. Blanchfield received a B.App.Sc. in Applied Biology/Biotechnology in 1995 from the Royal Melbourne Institute of Technology, B.Sc (Hons) in 1996 and a MAg.Sc in 2000 from the University of Tasmania, Hobart, Australia.

In 2004 she was appointed Research Scientist with the Department of Primary Industries, Victoria, Australia, where she has since been working on the analysis of grapevine leaf pigments using HPLC as part of a CRC for Viticulture project on the early detection of grapevine phylloxera.



Kevin S. Powell received a B.Sc (Hons). in Combined Sciences (Earth Sciences/Biology) from the Staffordshire University, England in 1983, a MSc in Agronomy in 1986 from University of Nottingham, England and a Ph.D. in Insect Physiology in 1993 from University of Durham, England. He was appointed Lecturer in Entomology at the University of Technology, Papua New Guinea in 1996.

In 2004 he was appointed as Section Leader - Invertebrate Sciences with the Department of Primary Industries (Victoria) Australia, where he has been leading the Phylloxera Research program since 1998. His research interests include aphid physiology and early detection and management of invasive insect pests. He is Technical Adviser to the National Phylloxera Technical Reference Group.

Dr. Powell is a Member of the Royal Entomological Society (UK), Tropical Agriculture Association (UK), Australian Entomology Society and Australian Society for Viticulture and Oenology.

For Peer Review

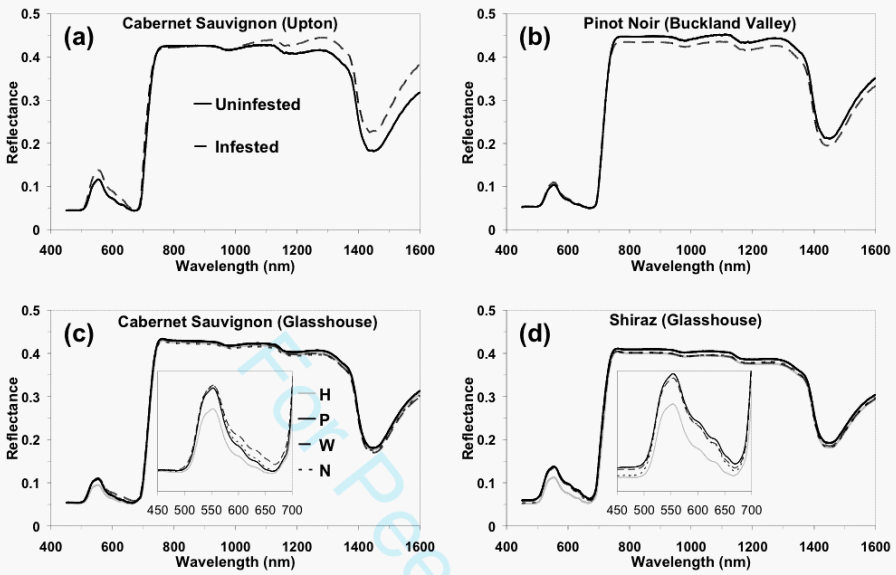


Fig. 1. Mean reflectance curves: field data for uninfested (solid lines) and infested (dashed lines) (a) Cabernet Sauvignon and (b) Pinot Noir vines; glasshouse data for the control "healthy" (H), phylloxera-infested (P), water stressed (W) and nitrogen deficient (N) (c) Cabernet Sauvignon and (d) Shiraz vines, respectively (boxes show an enlargement of the green-peak reflectances).

For Peer Review

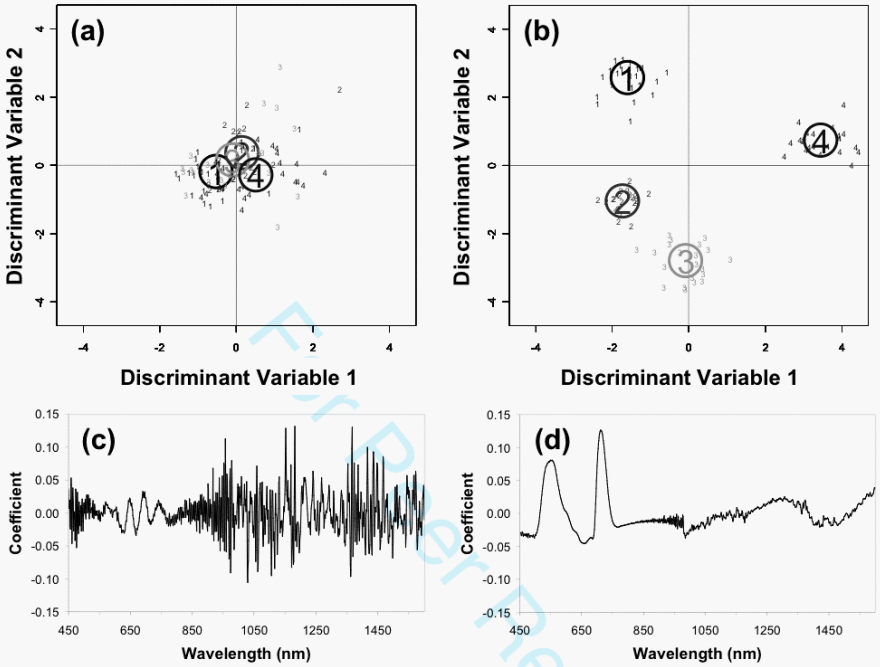


Fig. 2. The results of penalized discriminant analysis (PDA) applied to Shiraz glasshouse spectra for (a and c) high and (b and d) low levels of model complexity. Plots (a) and (b) illustrate the separation of the different groups of Shiraz vines: 1 = H, 2 = P, 3 = W and 4 = N; small numbers correspond to individual spectra, while the mean for each group is represented as a large number inside a circle. Plots (c) and (d) are the contours of the normalised coefficients of the first discriminant variable.

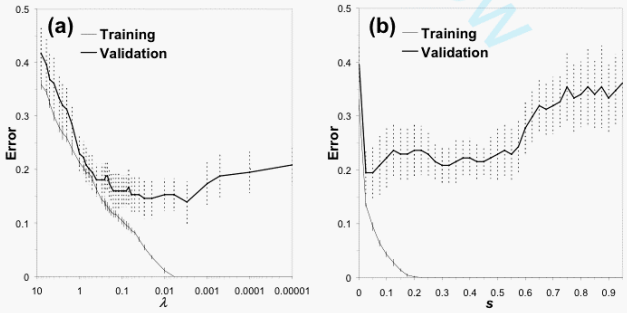


Fig. 3. Estimated training and validation errors from *L*-fold cross-validation of the field-measured reflectance spectra for (a) PDA and (b) OSLASSO procedures.

For Peer Review

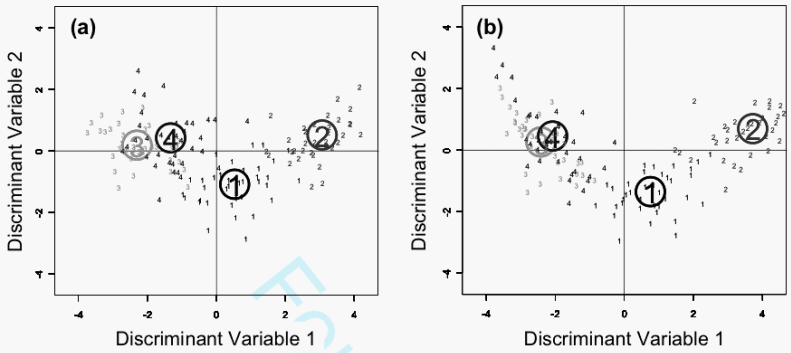


Fig. 4. Discriminant plots for optimal choice of tuning parameters for (a) PDA and (b) OSLASSO applied to the field-measured reflectance spectra of Cabernet Sauvignon (1 = uninfested and 2 = infested) and Pinot Noir (3 = uninfested and 4 = infested) vines. Training misclassification errors for both approaches are around 13% and over 90% of the between-group variation is explained by the first and second discriminant variables.

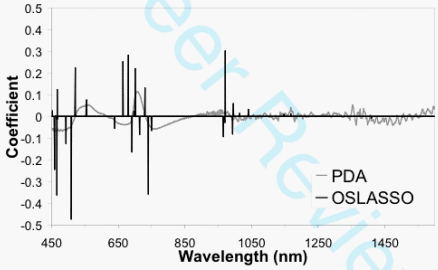


Fig. 5. Normalised coefficients of the first discriminant variable for optimal choice of tuning parameter resulting in the discriminant plots of Fig 4.

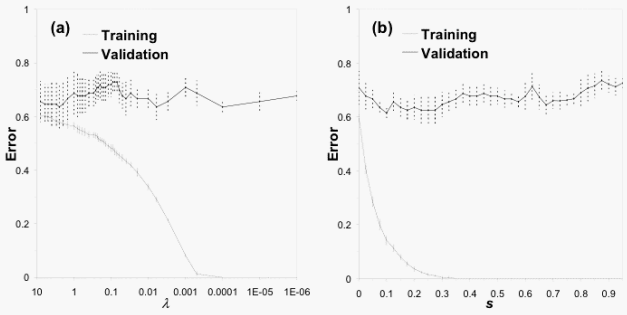


Fig. 6. Estimated training and validation errors from *L*-fold cross-validation of the glasshouse-measured reflectance spectra for Cabernet Sauvignon vines for (a) PDA and (b) OSLASSO.

For Peer Review

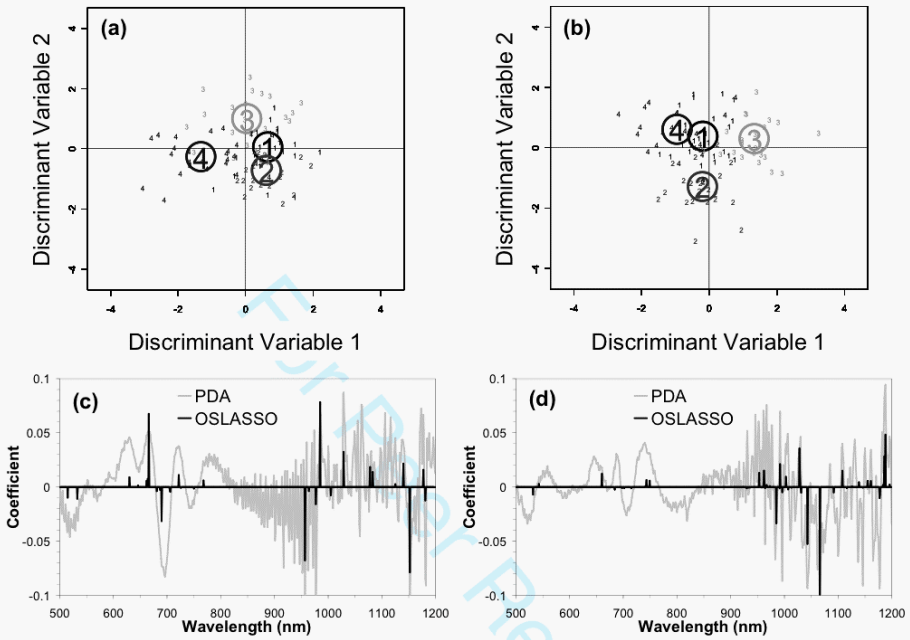


Fig. 7. Results of OSLASSO applied to glasshouse-measured reflectance data: first and second discriminant variables for (a) Shiraz and (b) Cabernet Sauvignon vines, where 1 = H, 2 = P, 3 = W, and 4 = N; the normalised coefficients of (c) the first discriminant variable the for Shiraz vines and (d) second discriminant variable for the Cabernet Sauvignon vines (the PDA coefficients for the same variable are displayed in grey for comparison).

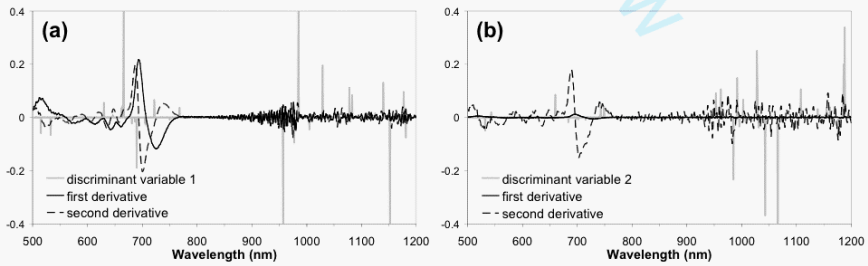


Fig. 8. First and second derivative spectra of the difference in mean spectra response between (a) N and H groups of Shiraz vines, and (b) P and H groups of Cabernet Sauvignon vines. OSLASSO discriminant variables 1 and 2 from Fig. 7 are displayed in grey. Note that the values have been scaled to aid comparisons.

For Peer Review

GENSTAT, 2005, GenStat product details. Available online at: http://www.vsn-intl.com/genstat/gsprod_details.htm (accessed 14 June 2005).

GUILLERMIN, R., 2004, Etude des effets de l'infestation du Phylloxéra sur l'espèce Vitis Vinifera par analyse statistique de paramètres optiques et chimiques dérivés du modèle PROSPECT de la feuille. Department of Civil Engineering and Topography, Strasbourg, Institut National des Sciences Appliquées de Strasbourg: 76.

JACQUEMOUD, S., 2004, New calibration of PROSPECT, unpublished report.

JACQUEMOUD, S. and BARET, F., 1990, PROSPECT: a model of leaf optical properties spectra. *Remote Sensing of Environment*, **34**, pp. 75–91.

JACQUEMOUD, S., BARET, F., ANDRIEU, B., DANSON, F.M. and JAGGARD, K., 1995, Extraction of vegetation biophysical parameters by inversion of the PROSPECT + SAIL models on sugar beet canopy reflectance data. Application to TM and AVIRIS Sensors. *Remote Sensing of Environment*, **52**, pp. 163–172.

MAIER, S.W., 2000, Modeling the radiative transfer in leaves in the 200 nm to 2.5 μm wavelength region taking into consideration chlorophyll fluorescence—the leaf model SLOPE. PhD thesis, Technische Universität München, Germany.

PRESS, W.H. and VETTERING, W.T., 1992, *Numerical Recipes in FORTRAN: The Art of Scientific Computing*, pp. 1–963 (Cambridge: Cambridge University Press).

RENZULLO, L., HELD, A., POWELL, K. and BLANCHFIELD, A., 2004, Remote sensing phylloxera infestation: current capabilities and future possibilities for early detection. *Australian and New Zealand Grapegrower and Winemaker, 32nd Annual Technical Issue*, No. 485a, pp. 126–130.

ZARCO-TEJADA, P.J., MILLER, J.R., MOHAMMED, G.H., NOLAND, T.L. and SAMPOSON, P.H., 2000, Chlorophyll fluorescence effects on vegetation apparent reflectance: II. Laboratory and airborne canopy-level measurements with hyperspectral data. *Remote Sensing of Environment*, **74**, pp. 596–608.

ZARCO-TEJADA, P.J., MILLER, J.R., MOHAMMED, G.H., NOLAND, T.L. and SAMPSON, P.H., 2002, Vegetation stress detection through chlorophyll a + b estimation and fluorescence effects on hyperspectral imagery. *Journal of Environmental Quality*, **31**, pp. 1437–1441.

phylloxera detection

Remote sensing phylloxera infestation: current capabilities and future possibilities for early detection



Luigi Renzullo*
Cooperative Research Centre for Viticulture
PO Box 154, Glen Osmond, South Australia 5064

CSIRO Land and Water
Clunies Ross Street, Acton, ACT, Australia

**Corresponding author*
email: Luigi.Renzullo@csiro.au
CSIRO Land and Water
GPO Box 1666, Canberra, ACT 2601

Alex Held
Cooperative Research Centre for Viticulture
CSIRO Office of Space Science and Applications
Clunies Ross Street, Acton, ACT, Australia

Kevin Powell
Cooperative Research Centre for Viticulture
Primary Industries Research Victoria (PIRVic)
Rutherglen Centre
Department of Primary Industries
Rutherglen, Victoria, Australia

Annette Blanchfield
Cooperative Research Centre for Viticulture
Primary Industries Research Victoria (PIRVic)

Introduction

Phylloxera (*Daktalosphaira vitifoliae* Fitch) is a root-feeding, aphid-like insect that is generally regarded as the world's most damaging grapevine pest. One of the most effective methods of containing the spread of phylloxera is the timely establishment of quarantine protocols and vineyard practices. To this end, there is considerable interest in Australia in methods for early detection (Herbert *et al.* 2003), and in particular the role of remotely-sensed observations for the task.

Remote sensing technologies have been used in the viticulture industry for mapping of sub-paddock variability in canopy-development and maturation. The derived information has been used to support selective harvesting, the quantification of missing vines, and broad regional assessment of grapegrowing areas. The advantage of this technology is that it can rapidly survey a much-greater area of vineyard than is feasible with on-ground methods. Moreover, it has been demonstrated that remotely-sensed observations, such as infrared photography, multispectral and hyperspectral imagery, can successfully identify weak spots in vine canopies that are a result of phylloxera infestation (Held 2001; Edwards, 2003). However, because visual symptoms of phylloxera-induced stress in the vines are similar to those due to other stresses,

FRENCH OAK COOPERAGE
PHILIPPE MORIN PTY. LTD.
The Fine-Grain French Oak Specialist.
Philippe Morin French Oak Cooperage imports the finest quality Fine-Grain French Oak available to the wine industry.
Berthomieu Tonnellerie
ARÔMES ET SAVEURS de France
Smooth, exquisitely elegant wines with perfumed aromas.
Contact Philippe Morin... Mobile 0438 816 934
Tel 08 8388 7597 Fax 08 8388 7497
Email philippe@frenchoak.com.au
www.frenchoak.com.au
Philippe Morin Identity & Design by Beanstalk 08 8361 7410 www.beanstalk.com.au

ADALONG PTY. LTD.
YOUR SOURCE OF ELASTOMER PRODUCTS FOR THE WINEMAKING INDUSTRY
- ***Silicon Bungs.*** The original and best. Three sizes plus fermentation and solid or recessed.
- ***Stainless steel hygienic fitting gaskets*** including BSM, CIP, Modified, Tri-Clover, DIN, SMS etc., etc.
- ***Butterfly valve seals,*** silicone, EPDM, Viton.
- ***Diaphragm*** valves & spares
- ***Carlson filter frame seals*** for 40x40 and 60x60 manway door seals.
- ***Flange gaskets***
- ***'O' rings***

5/150 Old Pittwater Road
Brookvale, NSW 2100
PHONE 02 9939 2177 FAX 02 9938 2582

it is still necessary for ground surveys to target identified areas for verification.

The challenge in this project has been to develop a mapping strategy for vineyards that is based solely on vine response to phylloxera infestation, and not the general symptoms of vine stress due to other factors. If remote sensing is to be used, it must be demonstrated that the data:

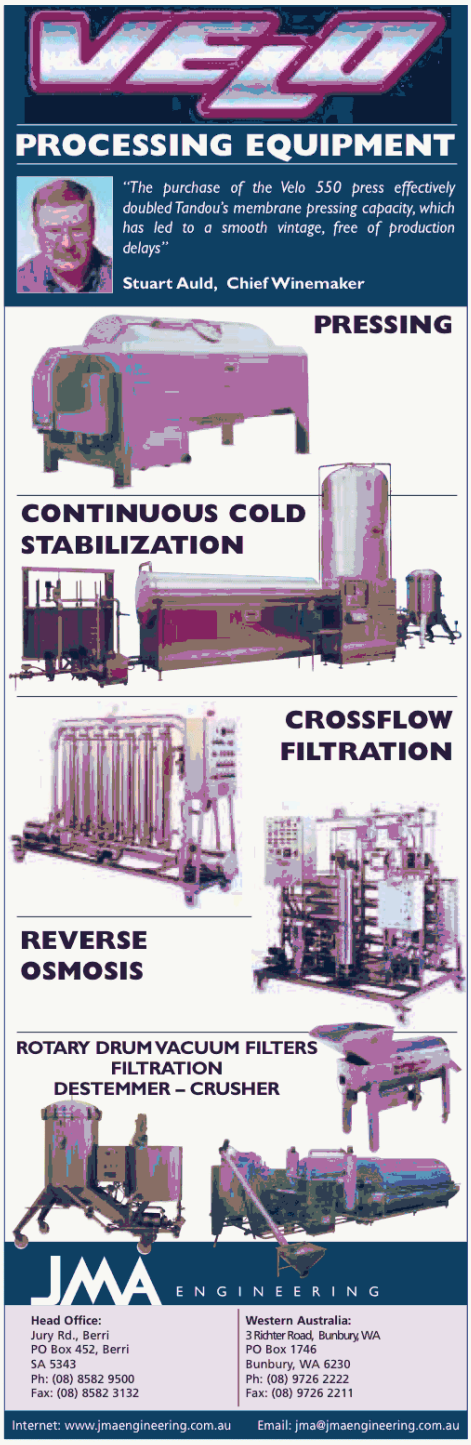
- can be used to distinguish the symptoms of phylloxera from those of other stresses, and:
- has the sensitivity to detect subtle changes in vine physiology that precede the visual symptoms that take at least two-to-three years to manifest.

This paper argues the use of field spectrometry as a fundamental technique to identify key spectral regions sensitive to phylloxera infestation, as a necessary precursor to airborne and spaceborne remote sensing. It is intended that the findings of the field spectrometry work will ultimately be used in the development of future remote sensing technologies for the early detection of phylloxera.

Remote sensing grapevine response to Phylloxera

Above-ground surveys aim to "detect" phylloxera infestation by observing grapevine responses to the pest as they are manifested in the foliage. Phylloxera damages roots (which results in the development of tuberosities and nodosities) thereby inhibiting a vine's ability to draw water and nutrients from the soil. This weakens the vine and renders it prone to secondary infection by soil-borne fungi (Granett *et al.* 1998). In its weakened state, a phylloxera-infested vine, compared to a healthy vine, will appear to have a reduced canopy size and its leaves become prematurely yellow. The yellowing of leaves (known as chlorosis) is due to reduced chlorophyll concentrations, in response to lower nutrient and water absorption by the roots, as the vine reallocates resources away from the leaves to mitigate the damage caused by phylloxera (Peterson and Johnson, 2000). ▸





phylloxera detection

Remotely-sensed multispectral and hyperspectral images have been used for phylloxera detection since the mid-nineties (Lobitz *et al.* 1997; Johnson, 1999; Held, 2001; Edwards, 2003). Images result from the multispectral or hyperspectral sensors (on satellite or airborne platforms) scanning back and forth along a flightpath over some location on the Earth's surface. Each pixel in an image is a spectrum of reflected solar radiation, measured for a number of colour-regions or "spectral bands". Figure 1a is a sample of such imagery, in this case acquired on 12 December 2003 with a four-band multispectral sensor on the QuickBird satellite which provides a 2.4m spatial resolution. The image shows ungrafted Pinot Noir vines in a recently identified phylloxera-infested vineyard in the Buckland Valley, Victoria. The figure, referred to as a false-colour composite, displays bands centred at 830, 560 and 485nm in the red, green and blue (RGB) parts of the visible spectrum, respectively.

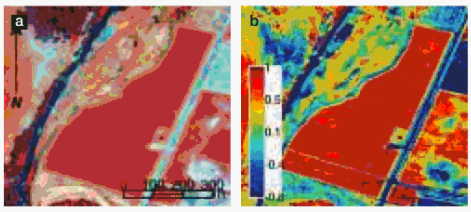


Fig. 1. QuickBird imagery of Pinot Noir vines in a new phylloxera-infested zone in the Buckland Valley, Victoria: (a) False-colour composite displaying the 830, 560 and 485nm bands in RGB; (b) NDVI image for the same scene highlighting differences in vigour in the form of grapevine canopy reflectances.

The normalised difference vegetation index (NDVI) combines red and near infrared (NIR) bands in a multispectral image in a way that highlight differences in canopy reflectances. The NDVI (Tucker, 1979) is calculated as:

$$NDVI = \frac{R830 - R660}{R830 + R660}$$

where *R*660 and *R*830 are reflectance values at 660 and 830nm respectively. Computing an NDVI value for each pixel in the image displayed in Figure 1a yields Figure 1b. A high value of the index indicates areas of high projected leaf area, whilst low (often negative) values indicate soil, water and non-vegetated areas.

Variations in canopy density are readily inferred using NDVI imagery. Vines of less vigour, for example, will have lower projected leaf area, and thus lower NDVI values, than the healthier vines; evident in Figure 1b as variations from red to yellow.

Figure 2a shows a false-colour composite of a hyperspectral (18-band) image acquired with the Compact Airborne Spectrographic Imager (CASI) for a vineyard in the Upton region, Victoria, in April 2001. Two blocks of Cabernet Sauvignon are displayed: the northern block is known to be infested with phylloxera (eg. the site highlighted by red polygon); the southern block has been surveyed and is considered free of phylloxera (eg. healthy vines highlighted by blue polygon), but appears to contain vines of low canopy density which we assume to be "weak" or stressed vines (eg. green polygon). NDVI imagery (Figure 2b, calculated using reflectances from CASI's 684 and 817nm bands) highlights the phylloxera-infested area in the northern block, and other weak spots in both blocks. Carter and Miller (1994) proposed the simple ratio (SR) index:

$$SR = \frac{R694}{R764}$$

for narrow-band sensors (such as CASI), for the early detection of plant stress. The index uses reflectances in a stress-sensitive band (694nm) and the reflectances in a band relatively insensitive to stress (764nm). Applying this index to the CASI imagery yields Figure 2c, where a high SR value is associated with higher vegetation stress than areas with lower SR values.

An examination of the derived NDVI and SR images reveals that the indices essentially highlight the same information (albeit inversely related). Both successfully highlight areas of vegetation stress, but neither managed to distinguish between phylloxera-infested vines and those for which the stressor (eg. dehydration or pathogen) is unknown. The physiological response of plants to any stress is often the same (Mohammed *et al.* 2000), and the similarity of spectral reflectances for affected areas (see Figure 2d) makes it difficult to identify key wavelength regions specific to any one stressor.

High spectral resolution reflectance spectrometry has been used to characterise the spectral response of vegetation to a variety of stressors (Carter, 1993; Gamon *et al.* 1997; Mohammed *et al.* 2000; Zarco-Tejada *et al.* 2003). Some preliminary results of investigations into grapevine spectral response to phylloxera using high spectral resolution data are presented in the next section.

Field spectrometry

A collaborative CRC for Viticulture team comprising scientists from CSIRO Division of

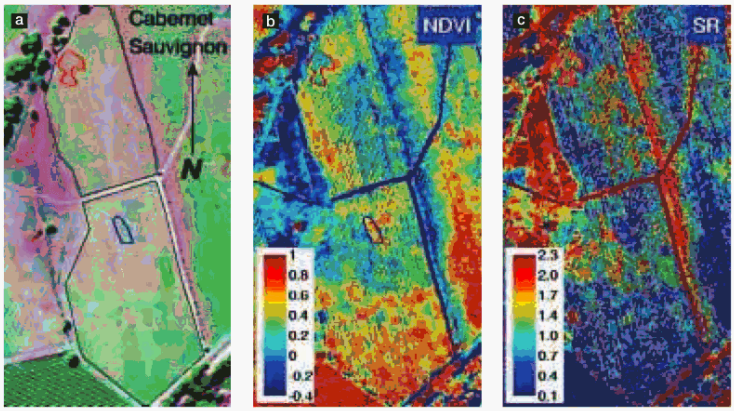


Fig. 2. CASI image for two Cabernet Sauvignon blocks in the Upton region, Victoria: (a) False-colour composite with 700, 817, 564nm bands displayed in RGB; (b) NDVI imagery calculated using 684 and 817nm bands; (c) SR index proposed by Carter and Miller (1994) using the 694 and 764nm bands; and (d) mean reflectance spectra for the pixels highlighted by red, blue and green polygons.

Land and Water, ACT, Department of Primary Industries, Victoria and the University of New England, NSW, have been conducting field campaigns over the 2003 and 2004 grapegrowing seasons at a number of vineyards throughout central and north-eastern Victoria. One aspect of their field work is the acquisition of high spectral resolution (1-nm sampling intervals between 350-2500nm), ground-based reflectance measurements of phylloxera-infested and "healthy" (ie. not phylloxera-infested) vines. The motivation for collecting this data is the belief that, combined with measurements of leaf chemistry, it will provide some additional insight into phylloxera detection by identifying specific spectral regions responsive to the infestation.

Reflectance measurements are acquired at the canopy and individual leaf levels with the hand-held Analytical Spectral Devices (ASD) FieldSpec-FR® spectroradiometer. Canopy reflectances (see Figure 3a) are useful as they closely approximate what would be observed by remote sensing systems. The quality of the data may be affected by atmospheric turbidity or cloud cover, and it is therefore not always possible to collect this data. Leaf reflectance measurements (see Figure 3b), however, can be made irrespective of the availability of direct sunlight by using the FieldSpec-FR spectroradiometer in conjunction with a Li-Cor Integrating Sphere. Using this system, a halogen lamp illuminates the interior of a highly-reflective spherical chamber, providing an isotropic diffuse-light environment. The light from the integrating sphere is reflected from the individual leaf, which is placed in a sample port, and is measured by the FieldSpec-FR spectroradiometer. The setup may be configured to also measure leaf transmittances, which will be useful for planned future work on canopy reflectance modelling.

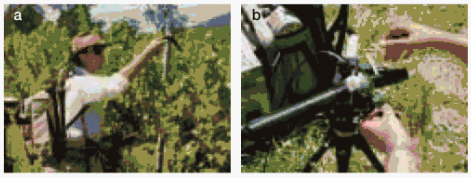


Fig. 3. Scientists using an ASD FieldSpec-FR spectroradiometer to measure grapevine reflectances at (a) the canopy-level and (b) the leaf level with the aid of a Li-Cor Integrating Sphere.

Figures 4-7 present some of the reflectance spectra acquired on a couple of the 2004 field campaigns. Spectra corresponding to vines that are infested by phylloxera are displayed in red, whereas spectra from uninfested vines are displayed in blue.

The effect of phylloxera root infestations on canopy reflectances is illustrated in Figure 4. The figure displays the canopy reflectance spectra of individual vines. In the reduced canopy density of an infested vine, there are fewer leaves contributing to the multiple scattering of NIR radiation that gives rise to the NIR plateau (740-900nm). Consequently, NIR canopy reflectances are less for infested vines than for uninfested vines.

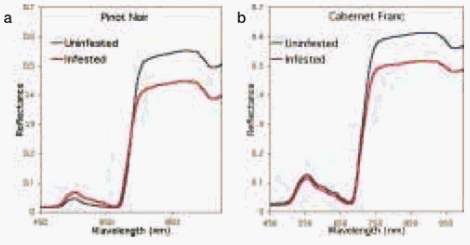


Fig. 4. Canopy reflectances of phylloxera-infested and uninfested, ungrafted *Vitis vinifera:* (a) Pinot Noir and (b) Cabernet Franc vines.

Leaf reflectance measurements were taken of large leaves from both uninfested and infested vines. For the data displayed in Figure 5, sample sizes ranged from 9-12 leaves. The *F*-statistic was employed to measure the statistical significance of the differences observed in the mean reflectance spectra of infested and uninfested samples. Difference with *F*-values (F-value; grey lines) less than the critical *F*-value (F-citical; dashed lines) for 95% level of significance are considered insignificant. No significant differences were observed between the mean reflectance curves early in the growing season (ie. November, Figures 5a and 5b). However, in January (Figures 5c and 5d), significant differences were observed over most of the spectral range, with the most significant difference occurring for wavelengths between 570-642nm and 718-728nm. Note that a peak in phylloxera populations was observed on vine roots at the sample site over the January-February period (Powell *et al.* 2003).

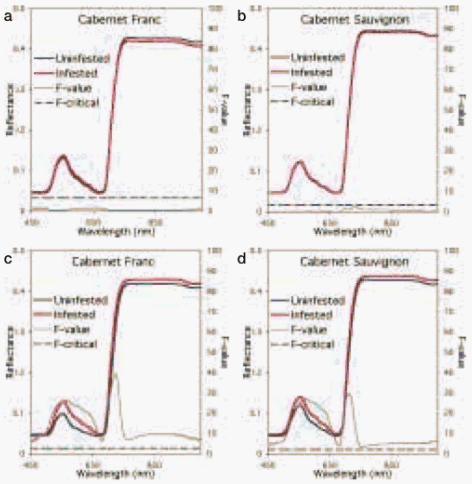


Fig. 5. Mean spectra illustrating the differences in leaf reflectances for uninfested (blue) and infested (red) Cabernet Franc and Cabernet Sauvignon vines. Data was acquired early in the growing season (a and b; November 2003) and mid-way (c and d; January 2004) at the Upton sampling site.

Penalised discriminant analysis (Hastie *et al.* 1995) was applied to reflectance spectra of leaf samples from infested and uninfested Pinot Noir, Cabernet Sauvignon and Cabernet Franc vines. The analysis highlighted the regions 558-567nm and 709-718nm as being most useful in discriminating between infested and uninfested spectra (see Table 1).

Higher leaf reflectances between 550-650nm (see Figures 5c and 5d) has been shown to be typical of a plant's response to stress (eg. Carter, 1993; Carter and Miller, 1994). The red edge, the transition from low to high reflectances between 700-740nm, is another much-studied spectral region, particularly in relation to early, or pre-visual, detection of plant stress. There are subtle variations in the shape of reflectance spectra along the red edge that relate to leaf chlorophyll content and/or fluorescence (Zarco-Tejada *et al.* 2003). The first derivative may be computed for high spectral resolution reflectance curves to better observe these subtle differences.

Table 1. Wavelengths identified using penalised discriminant analysis as being most useful for discriminating between infested and uninfested leaf reflectance spectra.

Variety	Wavelength (nm)
Pinot Noir	558, 718
Cabernet Sauvignon	567, 709
Cabernet Franc	564, 715

Figure 6 shows the derivative spectra of leaf reflectances modelled using the PROSPECT software (Jacquemoud and Baret, 1990), and two spectra measured in the field. The peak in the curves corresponds to the red edge inflection point (REIP). The figure demonstrates that the position of the REIP is related to leaf chlorophyll concentration: the lower the concentration, the more skewed the derivative spectra will be towards shorter wavelengths (known as a *blue* shift). Whilst the results shown here for the field spectra show a definite blue shift for the infested sample compared with the uninfested sample, the leaves showed no visual symptoms of chlorosis.

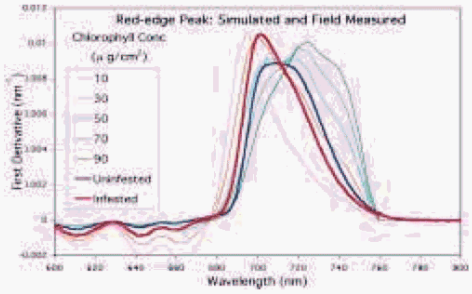


Fig. 6. Derivative curves illustrating the red-edge peak for some PROSPECT simulated reflectances and for field-measured reflectances of leaves from phylloxera-infested (red) and uninfested (blue) vines.

Finally, the expression of detectable spectral symptoms of phylloxera with leaf age is illustrated in Figure 7. As a healthy vine matures, its leaves will darken due to an increase in leaf pigment (eg. xanthophylls, carotene and chlorophyll) concentrations and leaf thickness (see Figure 7a). For an infested vine, however, there is little difference observed between the young and maturing leaves (Figure 7b) due to the vine's limited ability to draw sufficient water and nutrients.

Concluding remarks and future research

High spectral resolution data from reflectance spectrometry has the potential to identify wavelength regions sensitive to phylloxera infestation on a finer scale than is offered by current remote sensing systems. The results of the field spectrometry described in this paper are consistent with observations made by many researchers working in the area of plant stress, but also point to the utility of high spectral resolution spectroscopy (eg. red-edge analysis) to detect very subtle, often "pre-visual" differences in leaf chlorophyll and stress.

Clearly, phylloxera stress grapevines. But further work is required to determine if the spectral response of phylloxera-infested vines is discernible from that of vines stressed by other means. Also, the key to early detection is the identification of subtle differences in reflectance spectra due to leaf chemistry that are often early indicators of stress. High spectral resolution reflectance spectrometry, as described in this paper, will be invaluable to these investigations and may lead to the development of highly efficient operational techniques using airborne and spaceborne remote sensing systems.

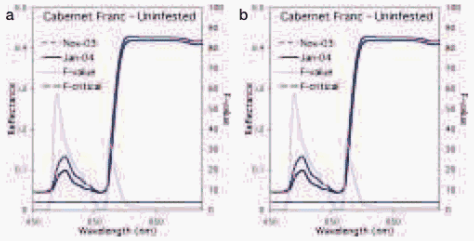


Fig. 7. Differences in the leaf reflectance spectra of infested (a) and uninfested (b) Cabernet Franc vines between November 2003 and January 2004.

Planned future work will involve integrating the reflectance measurements collected in the field with leaf chemistry data from high-performance liquid chromatography (HPLC) analysis. This will investigate how phylloxera infestation may affect leaf pigment concentrations, and how, in turn, this impacts spectral reflectances. Whilst the field spectrometry will continue to yield important insights, the task of identifying a spectral response specific to phylloxera infestations is better addressed in controlled glasshouse trials. Preparations are currently underway at the Department of Primary Industries (DPI), Rutherglen Centre, where two varieties of *Vitis vinifera* will be kept under controlled conditions. Leaf and canopy reflectance measurements will be made prior to phylloxera infestation and then again at regular intervals until chlorosis is visually evident. The temporal evolution of the reflectance curves may provide insight into how early the infestation can be detected. Furthermore, the controlled conditions will facilitate comparisons of the reflectance spectra for the different stressors (phylloxera, dehydration and low nutrients). Research updates will be provided through annual phylloxera-management workshops.

Acknowledgements

This research was supported by the Commonwealth Cooperative Research Centre Program and conducted through the CRC for Viticulture with support from Australia's grapegrowers and winemakers through their investment body the Grape and Wine Research and Development Corporation, with matching funds from the Federal Government. The authors would also like to acknowledge the contributions to the work made by Guy Byrne, Paul Daniel, Alan Marks, and Dr Catherine Ticehurst from CSIRO, Canberra, and Max Daniel, Carolyn Trethowan, and Sarah Brown from DPI, Rutherglen. Finally, we gratefully acknowledge the growers in the Upton, King Valley, Nagambie and Buckland Valley regions for allowing us to conduct this fieldwork on their vineyards.

References

Carter, G. A. (1993) Responses of leaf spectral reflectance to plant stress. American Journal of Botany. 80(3):239-243.
Carter, G. A. and Miller, R. L. (1994) Early detection of plant stress by digital imaging within narrow stress-sensitive wavebands. Remote Sensing of Environment. 50:295-302.
Edwards, J. (2003) Identification of Phylloxera, the Grapevine Pest, using High Resolution Infrared Aerial Imagery. MSc thesis, Adelaide University, Australia, pp.56.
Gamon, J. A., Serrano, L., and Surfus, J. S. (1997) The photochemical reflectance index: an optical indicator of photosynthetic radiation use efficiency across species, functional types, and nutrient levels. Oecologia, 112: 492-501
Granett, J. Omer, A. D., Pessereau, P., and Walker, M. A. (1998) Fungal infections of grapevine roots in phylloxera-infested vineyards. Vitis 37(1):39-42.
Hastie, T., Buja, A. and Tibshirani, R. (1995) Penalised discriminant analysis, Annals of Statistics. 23(1):73-102.
Held, A. (2001) Grape 'Health' Monitoring Using Imaging Spectroscopy: Results of a Pilot Study. CSIRO Land and Water, Ball AIMS, and DPI Internal Report (available on request).
Herbert, K., Powell, K. Hoffman, A., Parsons, Y. Ophel-Keller, K., and van Heeswijck, R. (2003) Early detection of phylloxera - present and future directions. The Australian & New Zealand Grapegrower & Winemaker. 473a:93-96.
Jacquemoud, S. and Baret, F. (1990) PROSPECT: A model of leaf optical properties Spectra, Remote Sensing of Environment, 34:75-91.
Johnson, L. F. (1999) Response of Grape Leaf Spectra to Phylloxera Infestation. NASA Report #CR-208765, NASA Center for AeroSpace Information, Hanover, MD, 21076-1320.
Lobitz, B., Johnson, L., Armstrong, R., Hlavka, C., and Bell, C. (1997) Grapevine Remote Sensing Analysis of Phylloxera Early Stress (GRAPES): Remote sensing Analysis Summary. NASA Technical Memorandum No. 112218.
Mohammed, G. H., Noland, T. L., Irving, D., Sampson, P. H., Zarco-Tejada, P. J., and Miller, J. R. (2000) Natural and stress-induced effects on leaf spectral reflectance in Ontario species. Forest Research Report No. 156. Ministry of Natural Resources, Ontario, Canada.
Peterson, D. L. and Johnson, L. F. (2000) The application of earth science findings to the practical problem of growing winegrapes. Geographic Information Sciences. 6(2):181-187.
Powell, K. S., Slattery, W. J., Deretic, J., Herbert, K., and Hetherington, S. (2003) Influence of soil type and climate on the population dynamics of grapevine phylloxera in Australia. Acta Horticulturae. 617:33-37.
Tucker, C. J. (1979) Red and photographic infrared linear combinations for monitoring vegetation. Remote Sensing of Environment. 8:127-150.
Zarco-Tejada, P. J., Pushnik, J. C., Dobrowski, S., and Ustin, S. L. (2003) Steady-state chlorophyll a fluorescence detection from canopy derivative reflectance and double-peaked red-edge effects. Remote Sensing of Environment. 84:283-294.

news

Mixed fortunes in record vintage

The Winemakers' Federation of Australia (WFA) announced a record vintage for the Australian wine industry in 2004, with an estimated crush of 1.86 million tonnes - 40% more than the drought-affected 2003 vintage and 23% more than the previous record vintage of 1.51 million tonnes in 2002.

Increased crop levels were recorded across almost all varieties, with bearing areas up 5% on 2003 and above-average yields in virtually all parts of Australia.

WFA chief executive, Stephen Strachan, said that good winter rainfalls and favourable weather conditions during spring and summer had delivered a disease-free vintage of 'above average' to 'outstanding' quality across all regions.

"Red winegrape production has increased by 38% to 1.07 million tonnes, surpassing 1 million tonnes for the first time, whilst white winegrape production has increased by 43% to 794,000 tonnes," he said.

Shiraz production is up 43% to 442,000 tonnes, representing around one quarter of total winegrape production, with Cabernet Sauvignon production up 41% to 317,000 tonnes. Chardonnay production is up 41% to 329,000 tonnes, accounting for 18% of total winegrape production.

"Although production of multipurpose winegrapes (Sultana and Muscat Gordo Blanco) has increased by 52% to 122,000 tonnes, the share of these varieties in the national crush has declined from 30% in 1994 to just 7% in 2004, reflecting the consumer demand for varietal wine," Strachan said.

Commenting on the implications of the vintage, Strachan said that the increased intake of white winegrapes would assist in alleviating the shortage of some premium white varieties, especially Chardonnay, and that a more balanced position was expected for most regions.

"The substantial increase in red winegrapes will provide both a challenge and opportunity for the industry, particularly in our export markets," he said.

"The aggravated supply position relates primarily to cool-climate production with the intake of warm-climate red winegrapes considered to be more balanced with domestic and export demand for branded products at 'popular premium' price points."

"Through aggressive and successful export growth the wine industry has responded to an increase in production of 180% since 1994. The increased intake in this vintage, particularly of reds, increases the pressure to maintain export growth rates and move stock before the next vintage."

32nd Annual Technical Issue

Correction

The article *"Remote sensing phylloxera infestation: current capabilities and future possibilities for early detection,"* by Luigi Renzullo, Alex Held, Kevin Powell and Annette Blanchfield, *(Australian & New Zealand Grapegrower & Winemaker, Annual Technical Issue, page 126-130),* duplicated Figure 7b, on page 130. The correct version of Figures 7a and 7b showing the expression of detectable spectral symptoms of phylloxera with leaf age appears below.

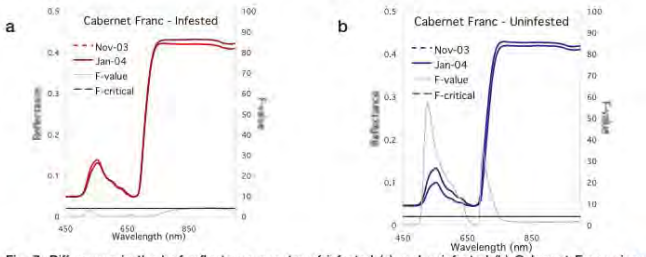


Fig. 7. Differences in the leaf reflectance spectra of infested (a) and uninfested (b) Cabernet Franc vines between November 2003 and January 2004.

TASTERS
FROM $1.50
Australias best prices on printed Winetasters
Barossa
Small or large quantities
Fast turnaround time
Other glasses available
Phone for price comparison
KINGFISHER GLASS PRINT
45 - 47 Raglan Avenue
EDWARDSTOWN
South Australia 5039
Telephone 08 8297 1099
Facsimile 08 8293 4777
email: sales@kingfisherglass.com.au
web: www.kingfisherglass.com.au

Characterising the development of grape phylloxera infestation with multi-temporal near-infrared aerial photography



Paul Frazier
Centre for Spatial Sciences, Ecosystem Management
University of New England, Armidale, New South Wales 2351
pfrazier@pobox.une.edu.au

John Whiting
Primary Industries Research Victoria (PIRVic)
Tatura Centre
Department of Primary Industries, Private Bag, 1 Ferguson Road
Tatura, Victoria 3616

Kevin Powell
Primary Industries Research Victoria (PIRVic)
Rutherglen Centre
Department of Primary Industries, RMB 1145
Chiltern Valley Road
Rutherglen, Victoria 3685

David Lamb
Centre for Spatial Sciences
School of Biological, Biomedical & Molecular Sciences
University of New England, Armidale, NSW, 2351

Introduction

Grape phylloxera (*Daktulosphaira vitifoliae*) is a major threat to the Australian grape and wine industry. The phylloxera aphid feeds on the vine root system causing extensive damage which results in reduced vine vigour and can lead to vine death. Apart from replanting with phylloxera-resistant rootstocks and adhering to quarantine protocols there are no other effective control options at present. Phylloxera is able to spread from an infested site by crawling and being blown in the wind for short distances. However, transport of vine material and soil on vineyard machinery by people can spread phylloxera within and between vineyards and grapegrowing regions. A program of early detection and monitoring the rate at which phylloxera spreads over time is vital for confining this pest to designated quarantine zones.

This paper describes the development of a phylloxera infestation in a vineyard in the King Valley region between 1996 and 2001. A six-year sequence of high-resolution colour infrared aerial photographs provided a unique insight into the spread of the pest throughout an infested vineyard.

Study area

This study was undertaken on a vineyard set in the King Valley region of north-eastern Victoria. The 30ha drip-irrigated vineyard consisted of 12 blocks of winegrape varieties including: Riesling, Shiraz, Merlot, Chardonnay, Cabernet Sauvignon, Cabernet Franc, Pinot Noir and Pinot Gris. 78% of the vineyard was established with ungrafted vines with the remainder on rootstocks. The vineyard manager first noticed phylloxera in 1995 in a single 4ha block in the north-east of the vineyard. Following this initial detection a program of aerial photographic survey was undertaken from 1996 to 2001 inclusive (Buchanan *et al.* 1997, Powell 2000). Phylloxera damage has resulted in ungrafted sections of the vineyard being replanted with phylloxera-resistant rootstocks.

Materials and methods

Aerial photography

A series of colour infrared aerial photographs captured annually from 1996 to 2001 was used to detect maximum growth differences between uninfested and infested vines (see Table 1).

Table 1. Details of colour infrared aerial photography.

Date stamp	Time	Approximate scale	Comments
27/3/96	09:24:10	1:11300	Over-exposed print with red colour saturation. Significant shadow falling to the south. Smoke haze present.
11/4/97	10:39:47	1:11700	Clear print showing range of colours. Significant shadow falling to the south.
27/3/98	8:38:17	1:11000	Clear print showing range of colours. Significant shadow falling to the south west.
5/5/99	12:47:37	1:11300	Clear print showing range of colours. Significant shadow falling to the south south east.
22/3/00	09:41:45	1:11000	Over exposed print with red colour saturation, significant shadow falling to the south west.
20/3/01	14:07:59	1:8300	Clear print showing range of colours. Flown under a cover of high cloud, resulting in higher resolution and less shadow. South-west corner of vineyard is cut-off.

Each photograph was scanned at 300 dots per inch (DPI) and converted into a TIFF image using an A3 flat-bed scanner. Scanned colour infrared photographs produce digital images that simulate multi-spectral images with green, red and near-infrared bands. However, because of the process of photographic development, the photosensitive emulsions and filter combination used for the actual colour infrared photography, these data have significant differences from images from digital multi-spectral systems.

To facilitate analysis each image was registered to the 1999 image so that all images overlayed each other with a maximum error of three metres.

Mapping

Phylloxera attacks grapevine roots resulting in decreased vine vigour and eventual plant death. Colour infrared photographs generally show areas of reduced grapevine vigour as regions of dull red-brown amongst the bright red-coloured healthy vines (see Figure 1). This is attributable to a decrease in near-infrared reflectance due to leaf desiccation (and associated loss of intercellular water) and leaf cell collapse as well as a decrease in ▸

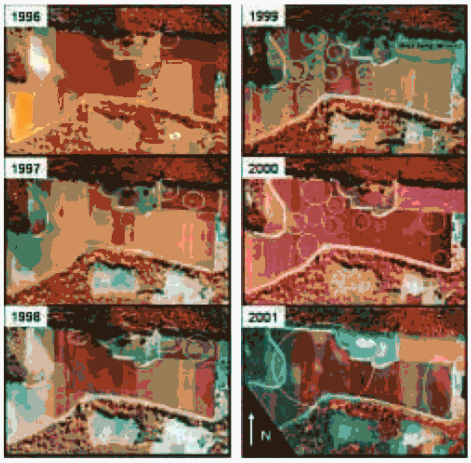


Fig. 1. Colour infrared photography from 1996 to 2001 documenting reduced vine growth due to the spread of phylloxera across the vineyard. White ellipses highlight the main areas of phylloxera infestation.

the green component of the reflected radiation via a reduction in leaf-chlorophyll content and leaf biomass. However, the nature of the upward reflected light that comes from a vineyard is also influenced by:

- vine maturity (generally linked to canopy density and size)
- grapevine variety (differences in chlorophyll content, canopy density and size)
- vine stress (from a range of causes such as shallow soil, weed competition, waterlogged areas, etc.)
- phenological development (again linked to canopy density and size)
- solar illumination conditions (azimuth and elevation are determined by time of day and year)
- covercrop type and density as observed between vine rows (this may also include enhanced weed growth in the vicinity of phylloxera-stressed vines due to successful root competition);

as well as even less-controlled variations in photographic print quality caused by the development process. Consequently, the identification of phylloxera-infested areas in a vineyard based on aerial infrared photography is complex, may be counter-intuitive and requires considerable "hands-on" experience in image interpretation.

As a consequence of the complex and hitherto insurmountable requirements of any automated process of image characterisation, areas of reduced vine growth associated with phylloxera were investigated in this sequence of imagery using a combination of pattern, colour and shape image interpretation elements (Jensen 2000) along with temporal variation between the photographs. On colour infrared photographs healthy vineyards are characterised by regularly spaced linear patterns of bright red-coloured vines and darker inter-row spaces that are a combination of shadow, covercrop and soil reflectance. Where phylloxera has reduced vine vigour the bright red of the vines is reduced to a relatively dull red colour (see Figure 1). Poor vine growth can also reduce shadow areas in the inter-row spaces and increase sunlight incident in the inter-row regions. Depending upon the vegetative nature of the covercrop this can lead to increased red colour or brighter brown colour in the inter-row spaces (see Table 2, Figure 1). The net result of reduced vine vigour on the image is to reduce the contrast between the rows and inter-rows and produce regions of more uniform red-pink or brown colour. In addition to these changes the pattern and colour of the phylloxera-infested areas show an often elliptical shape that does not conform to the linear row pattern (Figure 1).

Table 2. Expression of grapevine phylloxera on each of the aerial photographs.

Year	Expression of phylloxera
1996	Relatively dull pink among bright red vines and shadowed inter-row spaces
1997	Relatively dull pink-brown among bright red vines and shadowed inter-row spaces
1998	Brown among bright red vines and shadowed inter-row spaces
1999	Red surrounded by a ring of brown-straw colour among duller red vines and shadowed inter-row spaces
2000	Relatively uniform pink among bright red vines and shadowed inter-row spaces
2001	Brown light-pink among bright red vines and shadowed inter-row spaces

Results

Grapevine phylloxera was shown by survey to have spread throughout most of the ungrafted vine blocks in the six-year period from 1996 to 2001 (Figure 1). On the 1996 photograph areas of visibly-reduced vine vigour attributed to phylloxera had an area of 0.03ha and were confined to a single block in the north of the vineyard (Figure 1). By 2001 areas of substantially-reduced vine vigour totalled 1.88ha (Figure 2) and were spread across the entire vineyard (Figure 1). The area mapped as reduced vine vigour on the 2001 photograph did not include the removal of the 4ha block in two sections after the 1998 and 1999 harvests that was the site of original infection (Figure 1), nor a 0.6ha block removed after the 2000 harvest.

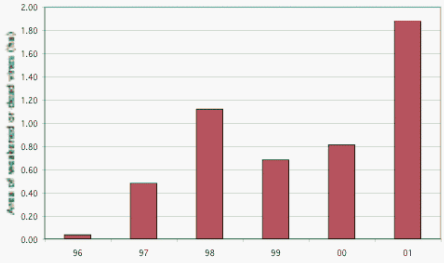


Fig. 2. Temporal change in the area of substantially-reduced vine growth.

The temporal pattern of phylloxera-spread showed that existing sites of infestation grew outwardly each year and new nuclei of infection were established throughout the vineyard. Established sites of infestation increased monotonically in each subsequent year with the area of decreased vine vigour growing radially from the infected area of the previous year. New sites of infestation were visible on each of the annual photographs increasing from three identified sites of infestation in 1996 to more than 50 sites in 2001.

Discussion

High-resolution colour infrared photography proved to be a useful tool that permitted the detection and delineation of phylloxera-infested vines across a vineyard. Areas of low vine vigour were detectable primarily as areas of vines showing reduced NIR reflectance and hence less red on the photograph. However, alteration to the distinctive vine-row pattern as covercrop became dominant under dead or dying vines, was also an important key for recognising areas of infestation. Because of the complexity of the interaction between incident visible and near-infrared light and vineyard land cover, including vines in various growth stages and inter-row covercrops also in various growth stages, it is unlikely that spectral information alone will allow for accurate detection and mapping of phylloxera infestations. ▸

It is important to note that the reduced vine vigour similar to that caused by phylloxera may also be caused by other factors such as: soil variation; faulty irrigation systems; vine diseases; weed infestations and other pests (Herbert *et al.* 2003). Broad band multi-spectral data, such as those provided by aerial photographs, or higher spectral resolution airborne digital-imaging systems (Hall *et al.* 2002, Lamb *et al.* 2001) and high-resolution satellite systems (eg. Quickbird Digitalglobe 2004)) are capable of detecting regions of reduced vine vigour within a vineyard block. However, attributing the reason for reduced vigour to a specific cause, such as phylloxera, will require additional information ostensibly through field verification. Nevertheless, data from these systems is useful for identifying weak regions in a vineyard and directing field survey strategies, saving survey time and costs.

Acknowledgement

Funds for the aerial photography were provided by the Department of Primary Industries, Victoria, and the aerial photography was undertaken by the Department of Environment and Heritage, South Australia.

References

Buchanan, G., Corrie, A., Whiting, J. and Brown, D. (1997) Management of grape phylloxera in Australia. Final report to Horticultural Research and Development Corporation, Phylloxera Board of South Australia and Grape and Wine Research and Development Corporation.

Digitalglobe (2004) http://www.digitalglobe.com/

Hall, A., Lamb, D., Holzapfel, B. and Louis, J. (2002) Optical remote sensing applications in viticulture - a review. Australian Journal of Grape and Wine Research. 8:36-47.

Herbert, K., Powell, K., Hoffman, A., Parsons, Y., Ophel-Keller, K and van Heeswijck, R. (2003) Early detection of phylloxera - present and future directions. *The Australian & New Zealand Grapegrower & Winemaker*. 473a:93-96.

Jensen (2000) Remote Sensing of the Environment. Prentice Hall, Upper Saddle River, New Jersey.

Lamb, D.W., Hall, A. and Louis J. (2001) Airborne remote sensing of vines for canopy variability and productivity. The Australian Grapegrower & Winemaker. 449a:89-92.

Powell, K.S. (2000) Management of grapevine phylloxera in South-east Australia. Phase 1 and 2. Report to Grape and Wine Research and Development Corporation.

Paul Frazier (BEd, MAppSci, PhD) is a senior lecturer in remote sensing and GIS at the University of New England. Since 1989 he has been using remotely sensed data to map and monitor natural resources. In the last two years he has focused on the application of high-resolution remote sensing to improve vineyard management.

John Whiting (BSc) is a senior viticulturist with the Department of Primary Industries - Victoria. He has over 30 years experience with viticultural research and extension and has been conducting aerial surveys of phylloxera-infested vineyards since the mid 1990s.

Kevin Powell (BSc (Hons), MSc, PhD) leads the Phylloxera research program based at DPI-Rutherglen which includes projects focusing on early detection, rootstock management risk analysis, phylloxera physiology and population monitoring.

David Lamb (BSc, PhD (NE)) has established major research projects in precision viticulture, including airborne and proximal remote sensing, and also leads research projects investigating the chemical fingerprinting of phylloxera in grapevines and optical fibre sensing of grape quality. He is presently convenor of Physics and Electronics in the School of Biological, Biomedical & Molecular Sciences. ■

maselli misure

PROCESS ANALYZERS

MULTIPARAMETRIC STATION SM-03

The Multiparametric SM station is a modular system and can be supplied with one, two, three or four functions, as follows:

Station SM-01: Measurement of sugar content

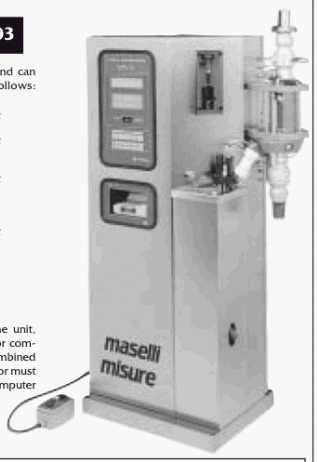
Station SM-02: Measurement of sugar content
Measurement of pH

Station SM-03: Measurement of sugar content
Measurement of pH
Measurement of total acidity

Station SM-05: Measurement of sugar content
Measurement of pH
Measurement of total acidity
Colour determination unit

Temperature measurement for all stations

It is possible to expand the station at a later time. The unit, whichever paramaters are chosen, can be manually fed or completed with the must transferrer. The SM-03 can be combined with other types of transferrers for the sampling of grapes or must (documentation on request). Industry standard RS232 computer interface.

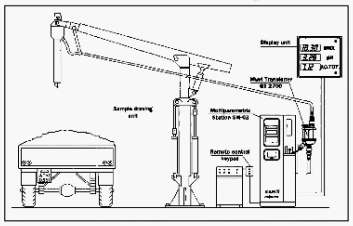


GRAPE ANALYSIS CENTRE

The Multiparametric Station SM-03 is the heart of the Maselli Misure modular analysis system for the testing of grape quality at the point of consignment.

The complete Analysis Centre is made up of the following units:

- **Sample drawing unit**
- **Must transferrer GT2700 with remote control keypad**
- **Multiparametric Station SM-03**
- **Display unit**



We Also Have Lab Analyzers – To Enquire Further, Please Call

PROCESS ANALYSIS SERVICES

ABN 13 613 545 130

PO BOX 1893, GRIFFITH, NSW 2680

TELEPHONE (02) 6964 1894 ● FAX (02) 6964 1946

● Mobile 0427 641 894

Email: gdp895@ozemail.com.au

Appendix 2: Intellectual Property

No new IP has been identified at this stage.

Appendix 3: References

ASD (2005) FieldSpec® Pro product specifications. Available on line at: http://www.asdi.com/products_specifications-FSP.asp (accessed 11 August 2005).

Blanchfield., A.L., S.A. Robinson, L.J. Renzullo and Powell. K.S. (2006). Phylloxera-infested grapevines have reduced chlorophyll and increased photoprotective pigment content - Can leaf pigment composition aid pest detection? *Functional Plant Biology*, **33**, 1-9.

Burns, A. E. and Powell, K. S. (2006) A novel approach for rapid screening of grapevine rootstocks for resistance to grape phylloxera. *Australian Journal of Grape and Wine Research*, submitted.

Carter, G. A. (1993) Responses of leaf spectral reflectances to plant stress. *American Journal of Botany*, **80**, 239-243.

Charlton, A.J., Farrington, W.H.H. and Brereton, P. (2002) Application of ^{1}H NMR and multivariate statistics for screening complex mixtures: quality control and authenticity of instant coffee. *J. Agric. Food Chem.*, **50**, 3098 - 3103.

Chaumont, M., Osorio, M.L., Chaves, M.M., Vanacker, H., Morot-Gaudry, J.-F. and Foyer, C.H. (1997) The absence of photoinhibition during the mid-morning depression of photosynthesis in *Vitis vinifera* grown in semi-arid and temperate climates. *Journal of Plant Physiology*, **150**, 743-751.

Clark, R. N., Swayne, G. A., Livo, K. E., Kokaly, R. F., Sutley, S. J., Dalton, J. B., McDougal, R. R. and Gent, C. A. (2003) Imaging spectroscopy: earth and planetary remote sensing with the USGS Tetracorder and expert systems. *J. Geophys. Res.*, **108** (E12, 5131), doi:10.1029/2002JE001847, pp. 5.1-5.44.

Corrie, A.M. Van Heeswijck, R., and Hoffmann, A.A. (2003) Evidence for host associated clones of grape phylloxera *Daktulosphaira vitifoliae* (Hemiptera: Phylloxeridae) in Australia. *Bulletin of Entomological Research*, **93**, 193-201.

de Benedictis J.A. and Granett J. (1993) Laboratory evaluation of grape roots as hosts of Californian grape phylloxera biotypes. *American Journal of Enology and Viticulture*, **44**, 285-291.

Duarte, I., Barros, A., Belton, P.S., Righelato, R., Spraul, M., Humpfer, E., Gil, A.M. (2002) High-resolution nuclear magnetic resonance spectroscopy and multivariate analysis for the characterization of beer. *J. Agric. Food Chem.*, **50**, 2475-2481.

Dunn J.L., Turnbull J.D. and Robinson S.A. (2004) Comparison of solvent regimes for the extraction of photosynthetic pigments from leaves of higher plants. *Functional Plant Biology*, **31**, 195-202.

Edwards, J. (2003) *Identification of Phylloxera, the Grapevine Pest, using High Resolution Infrared Aerial Imagery.* MSc thesis, University of Adelaide, South Australia, p. 56.

Edwards, J., Lewis M., Powell K.S., P. Hackworth and D. Lamb (2004). Identification of phylloxera from high resolution infra-red imagery: a comparative study between airborne imagery types. *The Australian and New Zealand Grapegrower and Winemaker*, (September), 51-54.

Efron, B. and Tibshirani, R. (1993) *An Introduction to the Bootstrap.* Chapman and Hall, London.

Frasier, P., Whiting., J. K.S. Powell and D. Lamb (2004) Characterising the development of grape phylloxera infestation with multi-temporal near infra read aerial photography. *The Australian and New Zealand Grapegrower and Winemaker* (32nd Annual Technical Issue), 133-136.

Gamon J.A., Serrano, L. and Surfus, J.S. (1997) The photochemical reflectance index: an optical indicator of photosynthetic radiation use efficiency across species, functional types, and nutrient levels. *Oecologia*, **112**, 492-501.

GenStat (2005) GenStat product details. Available online at: http://www.vsn-intl.com/genstat/gsprod_details.htm (accessed 11 August 2005).

Gilmore A.M. and Yamamoto H.Y. (1991) Resolution of lutein and zeaxanthin using a non-endcapped, lightly carbon-loaded C_{18} high-performance liquid chromatographic column. *Journal of Chromatography*, **543**, 137-145.

Gitelson, A. A., Gritz, Y. and Merzlyak, M.N. (2003) Relationships between leaf chlorophyll content and spectral reflectance and algorithms for non-destructive chlorophyll assessment in higher plant leaves. *Journal of Plant Physiology*, **160**, 271-282.

Hastie, T. Buja, A. and Tibshirani, R. (1995) Penalized discriminant analysis. *Annals of Statistics*, **23**, 73-102

Held, A. (2001) *Grape "Health" Monitoring Using Imaging Spectroscopy: Results of a Pilot Study.* CSIRO Land and Water, Ball AIMS, and DPI Internal Report (available on request).

Herbert, K.S., Powell., K.S., Hoffmann, A., Parson, Y., Ophel-Keller, K. and van Heeswijck, R. (2003) Early detection of phylloxera-present and future directions. *The Australian and New Zealand Grapegrower and Winemaker.* 31st Annual Technical Issue. **473a**, 93-96.

Hoerl, A. E. and Kennard, R. (1970) Ridge regression: biased estimation for nonorthogonal problems. *Technometrics*, 55-67.

Hsu, P.-H. (2003) *Spectral featured extraction of hyperspectral images using wavelet transform.* PhD dissertation, Department of Surveying Engineering, National Cheng Kung University, Tainan, Taiwan, p. 146.

Jacquemoud, S. and Baret, F. (1990) PROSPECT: A model of leaf optical properties spectra. *Remote Sensing of Environment*, **34**, 75–91.

Kellow., A.V. (2001) *A study of the interaction between susceptible and resistant grapevines and phylloxera.* PhD Thesis, University of Adelaide, South Australia.

Kourkoutas, Y.; Komaitis, M.; Koutinas, A. A. and Kanellaki, M. (2001) Wine Production Using Yeast Immobilized on Apple Pieces at Low and Room Temperatures. *Journal of Agricultural and Food Chemistry*, **49**, 1417-1425.

Koussa, T. and Cherrad, M. (2000) Levels and composition of fatty acids in buds and internodes of *Vitis vinifera* L cv. Merlot and their relationship with abscisic acid and water content. *Vitis*, **39**, 93-98.

Koussa, T., Dubos, B. and Cherrad, M. (2002) Water, fatty acids and abscisic acid contents of grapevine leaves (*Vitis vinifera*, cv. Cabernet Sauvignon) infected by *Eutypa lata. Vitis*, **41**, 143-146.

Lindon, J. C., Nicholson, J. K., Holmes, E. and Everett, J. R. (2000) Metabonomics: Metabolic processes studied by NMR spectroscopy of biofluids. *Concepts in Magnetic Resonance*, **12**, 289 - 320.

Lobitz, B., Johnson, L., Armstrong, R., Hlavka, C. and Bell, C. (1997) Grapevine Remote Sensing Analysis of Phylloxera Early Stress (GRAPES): Remote sensing analysis summary. *NASA Technical Memorandum* No. 112218, December 1997.

Lovisolo, C., Schubert, A. and Restagno, M. (1996) Photosynthesis of grapevine leaves of different age at high and low light intensity. *Acta Horticulturae*, **427**: 171-175.

Mallouchos, A., Skandamis, P., Loukatos, P.,Komaitis, M., Koutinas, A.A. and Kanellaki, M. (2003) Volatile Compounds of Wines Produced by Cells Immobilized on Grape Skins. *J. Agric. Food Chem.*, **51**, 3060-3066.

Penuelas, J. and Filella, I. (1998) Visible and near-infrared reflectance techniques for diagnosing plant physiological status. *Trends in Plant Science*, **3**: 151-156.

Peterson, D. L. and Johnson, L. F. (2000) The application of earth science findings to the practical problems of growing winegrapes. *Geographic Information Sciences*, **6**, 181-187.

Poni, S., Intrieri, C. and Silvestroni, O. (1994) Interactions of leaf age, fruiting, and exogenous cytokinins in Sangiovese grapevines under non-irrigated conditions. II. Chlorophyll and nitrogen content. *American Journal of Enology and Viticulture*, **45**, 278-284.

Powell, K., Brown, D., Dunstone, R., Hetherington, S. and Corrie, A. (2000) Population dynamics of phylloxera in Australian vineyards and implications for management. In: *Proceedings of International Symposium, Grapevine Phylloxera Management* (Eds: Powell, K.S. and Whiting, J.), Melbourne. DNRE, 7-19.

Powell, 2003 *Targeted Phylloxera Management Options.* GWRDC Final Project report, September 2003, p 135.

Powell, 2006 *Sustainable Phylloxera Management.* GWRDC Final Project report, in. preparation.

Powell and Herbert, 2005 *Early detection and alternative management of phylloxera in ungrafted vineyards.* CRCV Final Report, pp 118.

Renzullo, L. J. (2004) *Radiometric processing of multitemporal sequences of satellite imagery for surface reflectance retrievals in change detection studies.* PhD dissertation, Department of Applied Physics, Curtin University of Technology, Perth, Western Australia, p. 274.

Renzullo, L., Held, A., Powell, K. and Blanchfield, A. (2004) Remote sensing phylloxera infestation: current capabilities and future possibilities for early detection. *The Australian and New Zealand Grapegrower and Winemaker* (32nd Annual Technical Issue), 126-130.

Renzullo, L. J., Blanchfield, A. L., Guillermin, R., Powell, K. S. and Held, A. A. (2006) Comparison of PROSPECT and HPLC estimates of leaf chlorophyll contents in a grapevine stress study. *International Journal of Remote Sensing*, 27 (4), 817-823.

Renzullo, L. J., Blanchfield, A. L. and Powell, K. S. (2005) A method of wavelength selection and spectral discrimination of hyperspectral reflectance spectrometry. *IEEE Transactions on Geoscience and Remote Sensing,* submitted.

Richardson, A. D., Duigan, S.P. and Berlyn, G.P. (2002) An evaluation of noninvasive methods to estimate foliar chlorophyll content. *New Phytologist*, **153**: 185-194.

Ryan, F.J., Omer, A.D., Aung, L.H. and Granett, J. (2000) Effects of infestation by grape phylloxera on sugars, free amino acids, and starch of grapevine roots. *Vitis*, **39**, 175-176.

Schaefer, H. (1972) Metabolic differences between phylloxera-infected and healthy grape leaves. *Phytopathologische Zeitschrift*, **75**, 285-314.

Schaefer, H. (1985) Metabolic differences between phylloxera root galls and healthy grapevine roots. *Wein-Wissenschaft*, **40**, 219-27.

Sims, D. A. and Gamon, J.A. (2002) Relationships between leaf pigment content and spectral reflectance across a wide range of species, leaf structures and developmental stages. *Remote Sensing of Environment*, **81**, 337-354.

Sobolev, A.P., Brosio, E., Gianferri, R. and Segre A.L. (2005) Metabolic profile of lettuce leaves by high-field NMR spectra. *Magn. Reson. Chem.*, **43**, 625-638.

Suzuki, Y. and Shioi, Y. (2004) Changes in chlorophyll and carotenoid contents in radish (*Raphanus sativus*) cotyledons show different time courses during senescence. *Physiologia Plantarum*, **122**, 291-296.

Tibshirani, R. (1996) Regression shrinkage and selection via the Lasso. *Journal of the Royal Statistical Society, Series B*, **58**, 267-288.

Tsai, F. and Philpot, W. (1998) Derivative analysis of hyperspectral data. *Remote Sensing of Environment*, vol. 66, pp. 41-51.

Tucker, D.J., Powell, K.S., Lamb, D.W., Murison, R.D., Blanchfield, A.L. and Brereton, I.M. (2006) Detection of phylloxera infestation in grapevines by NMR. *Acta Horticulturae*, in preparation.

Warick, R. P. and Hildebrandt, A. C. (1966) Free amino acid contents of stem and phylloxera gall tissue cultures of grape. *Plant Physiology*, **41**, 573-8.

Young, A. and Britton G. (1990) Carotenoids and stress. in *Stress responses in plants: adaptation and acclimation mechanisms.* Alscher, R.G. and Cumming J.R. (eds), Wiley-Liss, Inc., New York, pp. 87-112.

Zarco-Tejada, P., Miller, J. R., Mohammed, G. H. and Noland, T. L. (2000) Chlorophyll fluorescence effects on vegetation apparent reflectance: I. Leaf-level measurements and model simulation. *Remote Sensing of Environment,* **75**, 582-595.

Zarco-Tejada, P. J., Miller, J. R., Mohammed, G. H., Noland, T. L., Sampson, P. H. (2002) Vegetation stress detection through chlorophyll a + b estimation and fluorescence effects on hyperspectral imagery. *J. Environ. Qual.,* **31**, 1433-1441.

Zarco-Tejada, P. J., Pushnik, J. C., Dobrowski, S. and Ustin, S. L. (2003) Steady-state chlorophyll a fluorescence detection from canopy derivative reflectance and double-peaked red-edge effects. *Remote Sensing of Environment,* **84**, 283-294.

Appendix 4: Staff

Kevin Powell (Victoria Department of Primary Industries)

David Lamb (University of New England)

Damien Barret (CSIRO Land & Water)

Annette Blanchfield (Victoria Department of Primary Industries)

Alex Held (CSIRO Land & Water)

Luigi Renzullo (CSIRO Land & Water)

David Tucker (University of New England)

Ian Brereton (University of Queensland)

Robert Murison (University of New England)

Sharon Robinson (University of Wollongong)

Sarah Brown (Victoria Department of Primary Industries)

Appendix 5: Sampling strategy for leaves used for reflectance spectra and HPLC in the field trial.

Vineyard Location	Grapevine Variety	Date of Sampling	Number of Samples	
			Phylloxera Infested	Phylloxera Free
Buckland Valley	Pinot Noir	January 04 March 04 January 05 March 05	6 (6 vines x 1 leaf) 6 (6 vines x 1 leaf) 36 (12 vines x 3 leaves; identical) 36 (12 vines x 3 leaves; identical) (HPLC only)	6 (6 vines x 1 leaf) 6 (6 vines x 1 leaf) 36 (12 vines x 3 leaves; identical) 36 (12 vines x 3 leaves; identical) (HPLC only)
King Valley	Riesling	January 03 March 03 November 03 January 04 March 04	24 (8 vines x 3 leaves; S,M,L) 24 (8 vines x 3 leaves; S,M,L) 16 (8 vines x 3 or 1 leaf; S,M,L or L) 24 (24 vines x 1 leaf) 24 (24 vines x 1 leaf)	NA
	Sauvignon Blanc	January 03 March 03 November 03 January 04 March 04	12 (4 vines x 3 leaves; S,M,L) 12 (4 vines x 3 leaves; S,M,L) 4 (4 vines x 1 leaf) 12 (12 vines x 1 leaf)	NA
Mitchelton	Semillon	January 03 March 03 November 03 January 04 March 04	12 (4 vines x 3 leaf; S,M,L) 12 (4 vines x 3 leaf; S,M,L) 4 (4 vines x 1 leaf) 36 (36 vines x 1 leaf) 12 (12 vines x 1 leaf)	NA
	Shiraz	January 03 March 03 November 03 January 04 March 04	9 (3 vines x 3 leaves; S,M,L) 9 (3 vines x 3 leaves; S,M,L) 9 (3 vines x 3 leaves; S,M,L) 9 (9 vines x 1 leaf) 9 (9 vines x 1 leaf)	NA
Upton	Cabernet Sauvignon	January 03 March 03 November 03 January 04 March 04 January 05	12 (4 vines x 3 leaves; S,M,L) 12 (4 vines x 3 leaves; S,M,L) 12 (4 vines x 3 leaves; S,M,L) 12 (12 vines x 1 leaf) 12 (12 vines x 1 leaf) 36 (12 vines x 3 leaves)	12 (4 vines x 3 leaves; S,M,L) 12 (4 vines x 3 leaves; S,M,L) 4 (4 vines x 1 leaf) 12 (12 vines x 1 leaf) 12 (12 vines x 1 leaf) 36 (12 vines x 3 leaves)
	Cabernet Franc	January 03 March 03 November 03 January 04 March 04	12 (4 vines x 3 leaves; S,M,L) 4(2 vines x 2 leaves; S,L) 6 (6 vines x 1 leaf) 6 (6 vines x 1 leaf) 6 (6 vines x 1 leaf)	12 (4 vines x 3 leaves; S,M,L) 4 (2 vines x 2 leaves; S,L) 6 (6 vines x 1 leaf) 6 (6 vines x 1 leaf) 6 (6 vines x 1 leaf)
	Merlot	March 04	6 (6 vines x 1 leaf)	6 (6 vines x 1 leaf)

Appendix 6: Budget reconciliation

GRAPE & WINE RESEARCH & DEVELOPMENT CORPORATION

Statement of Receipts and Expenditure - **FORM B**

Reconciliation Funding for 2005/06

Trust Fund :	RESEARCH TRUST FUND	FUNDING	$
Project No :		Salaries	
Grantee :		Travel	
Title of Project :		Operating	
		Capital	
		Total Funding	

EXPENDITURE										
	Salaries		Travel		Operating		Capital		Total	
	$	¢	$	¢	$	¢	$	¢	$	¢
A Uncommitted (c/f 1 July)										
B Outstanding Commitments (c/f 1 July)										
C Refunds of funding										
D Cash Received From Trust Fund										
E Approved transfers (from Form C)										
F Cash available (A+B-C+D±E)										
G Expenditure										
H Outstanding Commitments (30 June)										
I Total funds Committed (G-H)										
J Uncommitted (30 June) (F-I)										
K Other income (Paid to Trust Funds)										

Note : *Row B should be the same as Row H from the previous year and Row A the same as Row J from the previous year.*

I hereby certify that this statement of expenditure is correct.

…….	…….	…….
Signature	Printed Name	Date